Anaerobic Amino Acid Production in Saccharomyces cerevisiae: A Thermodynamics Approach

Cueto Rojas, Hugo

DOI
10.4233/uuid:a565936a-b081-4581-9eb0-8c66bff307a8

Publication date
2016

Document Version
Final published version

Citation (APA)
Cueto Rojas, H. (2016). *Anaerobic Amino Acid Production in Saccharomyces cerevisiae: A Thermodynamics Approach*. [Dissertation (TU Delft), Delft University of Technology]. https://doi.org/10.4233/uuid:a565936a-b081-4581-9eb0-8c66bff307a8

Important note
To cite this publication, please use the final published version (if applicable).
Please check the document version above.

Anaerobic Amino Acid Production in *Saccharomyces cerevisiae*: A Thermodynamics Approach

Proefschrift

ter verkrijging van de graad van doctor
aan de Technische Universiteit Delft,
op gezag van de Rector Magnificus prof. ir. K.Ch.A.M. Luyben,
voorzitter van het College voor Promoties
in het openbaar te verdedigen op
woensdag 22 Juni 2016 om 12:30 uur

door

Hugo Federico CUETO ROJAS

ingenieur Biochemical Engineering
geboren te Teziutlan, Mexico

This dissertation has been approved by the

Promotor: Prof. dr. ir. J.J. Heijnen
Copromotor: Dr. S.A. Wahl

Composition of the doctoral committee:

Rector Magnificus,	chairperson
Prof. dr. ir. J.J. Heijnen,	promotor
Dr. ir. S.A. Wahl,	copromotor

Independent members:

Prof. dr. H. Noorman,	TNW, TU Delft
Prof. dr. M. Oldiges,	Forschungszentrum Jülich
Prof. dr. H.V. Westerhoff,	U-Manchester/U-Amsterdam
Prof. dr. G.J. Witkamp,	TNW, TU Delft
Dr. ir. A.J.A. van Maris,	TNW, TU Delft

Reserve member:

Prof. dr. U. Hanefeld,	TNW, TU Delft

The research presented in this thesis was performed at the Cell Systems Engineering section, Department of Biotechnology, Faculty of Applied Sciences, Delft University of Technology (The Netherlands).

This project was carried out within the research programme of BE-BASIC Foundation. The author acknowledges CONACyT for the grant given (DOC 258960 212059).

ISBN: 978-94-6299-363-1

Cover designed by Shokar@linkedin.com, back cover illustration by Víctor Hugo Cueto Cárdenas "The survival machine", 2016.

Printing: Ridderprint BV, the Netherlands

AAN MIJNE OUDERS EN OPA

Cum essem parvulus, loquebar ut parvulus,
sapiebam ut parvulus, cogitabam ut parvulus;
quando factus sum vir, evacuavi, quæ erant parvuli.

When I was a child, I used to speak like a child,
think like a child, reason like a child;
when I became a man, I did away with childish things

Saint Paul of Tarsus (1 Cor 13:11)

Table of contents

Preface

First of all, I would like to start sharing with you the propositions that didn't qualify to become one of the 10 requested by the graduate school at TU Delft, because probably you are wondering "*if every Ph.D. student should write 27 propositions, where can I find the other 17 that you wrote?*" My proposition #1 encourages other Ph.D. candidates to reflect about their work beyond what it is required by the norm. In my opinion, the Ph.D. propositions are an excellent exercise to develop philosophical skills. Together with Peter Verheijen, I set myself the goal of writing 27 propositions for this thesis; on a lucky strike and after finding the proper inspiration I ended up with 31. Therefore, I decided to include the remaining 21 in this preface in order to share them with those who dared to read this section.

The first four from this second set of propositions were written during one of the most obscure stages of my project; at that time I had no publications, no foreseeable results and a bunch of emotional issues over my shoulders. Thus, they reflect the dark way in which I used to motivate myself to keep working until achieving whatever *Pyrrhic victory*; in some other cases I wrote propositions to try to let out my feelings as a sort of self-healing activity.

1. *If you don't know the end port, any wind will be unfavorable (Seneca).*
2. *A single Pyrrhic victory tastes better than 1000 undeserved victories.*
3. *The best way to construct meaningful learning is by means of a traumatic experience.*
4. *To achieve success, a team requires a solid strategy, discipline and cooperation. Teams that lack those elements will be subjected to high chances of failure, even if only outstanding people compose them.*

Moreover, some of my propositions were not totally related to the thesis but they were inspired on ideas that came to me during the development of this work.

5. *In science, educated guesses are useful; assumptions are not. (Thanks papa)*
6. *Theoretical thermodynamic descriptions of cellular processes should be enough driving force for doing research about a particular topic in Life Sciences.*
7. *S. cerevisiae is an extremely efficient and robust survival machine (according to the definition of survival machine from Richard Dawkins, in The selfish gene, 1976).*

Next to the previous propositions, I wrote a couple of propositions derived from this thesis. Some of them were good enough to be part of the 10 required propositions, however, they were less appealing to me than the ones that you found together with the thesis.

8. *Ammonium is required to a minimal level of at least 3 mmol/L_{IC} in Saccharomyces cerevisiae (wild type) to keep active the N-central metabolism, regardless of the N-source (this thesis).*
9. *Opposed to hypothesis of Soupene et al., 2001 (Soupene et al., 2001), intracellular ammonium measurements suggest that NH_4^+ is the transported species by Mep-proteins in Saccharomyces cerevisiae (this thesis).*
10. *Saccharomyces cerevisiae cells defective on Mep-transporters use NH_3-diffusion as main NH_X-uptake mechanism (this thesis).*
11. *Opposed to the hypothesis of Hess et al. (2006), intracellular ammonium measurements suggest that unspecific NH_4^+ uptake through K^+ channels is not the NH_X-uptake mechanism in Saccharomyces cerevisiae cells defective on Mep-transporters (this thesis).*
12. *In agreement with the hypothesis of Hess et al. (2006), high-ammonium low-potassium conditions lead to ammonium toxicity and amino acid excretion in Saccharomyces cerevisiae (this thesis).*

13. *In agreement with Wood et al. (2006), intracellular ammonium measurements show that ammonium is mainly compartmentalized in the vacuole of Saccharomyces cerevisiae (this thesis).*
14. *Ammonium storage in the vacuole buffers any potential ammonium depletion in the cytosol, allowing Saccharomyces cerevisiae to survive long starvation periods (this thesis).*
15. *Deletion of Mep-transporters in Saccharomyces cerevisiae leads to severe N-limitation (this thesis).*

Please check the following references:

Hess, D. C., Lu, W., Rabinowitz, J. D., Botstein, D., 2006. Ammonium toxicity and potassium limitation in yeast. PLoS Biol. 4**,** e351.

Soupene, E., Ramirez, R. M., Kustu, S., 2001. Evidence that Fungal MEP Proteins Mediate Diffusion of the Uncharged Species NH_3 across the Cytoplasmic Membrane. Mol. Cell. Biol. 21**,** 5733-5741.

Wood, C. C., Poree, F., Dreyer, I., Koehler, G. J., Udvardi, M. K., 2006. Mechanisms of ammonium transport, accumulation, and retention in ooyctes and yeast cells expressing *Arabidopsis AtAMT1;1.* FEBS Lett. 580**,** 3931-6.

Additionally, with some other propositions I tried to create awareness (in a diplomatic way) that negotiations and so-called politics in the scientific community must not be turbid or obscure; they should be transparent for the benefit of science itself. Nevertheless, I must say that Camilo Suárez Méndez was more successful than me in achieving that goal (see his thesis *Dynamics of storage carbohydrate metabolism in S. cerevisiae: A quantitative analysis*). Still, I came up with a couple of those propositions and my second set of propositions was left with proposition #16.

16. *A good scientist should know how to do business and politics.*

Finally, I wrote a couple of propositions reflecting my strong republican background. Personally, I believe in the principles of *liberté*, *égalité et fraternité*; which led to the foundation of modern democracies. All men were created equal -or "*all men are equally evolved*" for those of you who hate the word "create"- without exemptions, and I strongly oppose to believe that a particular human

being is better than others or has any especial (divine) right over the rest of us: politically, scientifically or morally. Furthermore, these propositions are the perfect excuse to start discussions about the democratization of science; every man or woman is capable of doing science and finding the truth using the scientific method. Nobody, whatever his or her background and "*qualifications*", possesses the truth. The truth is a common good for the human kind, by no means should we make it a private resource, and it is high time for us to revise how we teach, communicate and do science.

17. *The second match Kasparov vs Carlsen (Reykjavik rapid tournament, 2004) finished in draw before officially starting due to two crucial factors: i) Kasparov underestimated Carlsen due to his young age and ii) Carlsen was intimidated by Kasparov's renown.*
18. *Orwellian principles of mass control are widely used in many modern societies.*
19. *As proposed by Daniel Dennet religion is an important human invention from which we need to learn more.*
20. *Sadly, many people misuse the concepts of evolution in the form of social Darwinism to explain (and even justify) the European conquest of the Americas.*

    N.B. To my dismay, it was easy for me to find highly educated European citizens asserting that "*native Americans were less [sic] evolved than Europeans in the XVI century*" or that "*European conquerors [sic] saved native Americans from themselves, because they were killing each other at that time due to its sanguinary religion*" - I'm wondering if those people ever heard about the European reformation wars. The theory of evolution by natural selection is in my opinion one of the most beautiful scientific theories, and it is extremely sad to see that some people misuse the concept of **evolution** to justify their ignorance and bigotry.

21. The foundational principles of all constitutional monarchies are as inconsistent as the concepts that support intelligent design.

Following that line of thought, these days I have been reflecting about the situations that led me to pursue a Ph.D. degree. I could come up with many reasons, for instance that I like science, or that my curiosity led me naturally to become a "scientist". But I guess there is a more powerful reason beyond those: I owe my life to science, not in a romantic kind of way but in a literal sense. I was born by a Cesarean section and the first years of my life were marked with diseases that required the use of antibiotics. Thus, without the medical advances of the XX century my mother, brother, and I wouldn't be here with you today.

My first memories go back to my mother explaining how I used to be "*[sic] inside her*" and how I "*[sic] came out of her*" after an operation, while she spoke she used to show me the scar left by the C-section. Probably she is to blame for my admiration towards the big scientists of old (van Leeuwenhoek, Pasteur, Marie Curie, Darwin, *etc*.) and appreciation for all natural sciences. In those early years, I developed an especial fascination for life, which made prone to study biology and, as a hobby, medical sciences, in the later case also due to the influence of my uncle Heriberto. While I was discovering the world, I also became familiar with the scary concept of death, the inexorable end of the spark that inhabits in all living-beings. Little I knew at the time that life exists due to its coupling to the highly favorable (in thermodynamic terms) process of death.

Over the years, my father was also a key figure that encouraged the choices that led me to this point in my life by saying that I was similar to those whom I admired because: "*we can become whatever person we want to be with hard work and effort*", so him and his Marxists ideas are also to blame for this. Now, with this background it is easy for you to imagine how in my case everything started with a boy observing ants outside his house, accompanied by his scale models of dinosaurs. Those little ants made me become curious about biological processes and I started asking questions that began with: *Why? How? What? Which?* [...] Nowadays, I recognize that my goal of

pursuing a scientific degree has a direct correlation with the positive influence of many science communicators -and I include in this group some family members. My early contact with science made me passionate about it, and probably my ultimate life goal is to return the favor to society by communicating science. To achieve that goal, in some point in my life I figured out that I needed a Ph.D. degree in order to be recognized by society as a *serious* or *professional* science communicator.

Then, I became aware that pursuing a Ph.D., the process by which you get the right to be called "*Doctor*", is a social ritual. In my humble opinion, that social ritual is sometimes useless, take as an example the life of the great *Antonie van Leeuwenhoek*, a cloth merchant from Delft that became one of the best scientists and science communicators of his time without a Ph.D. degree, his fame was almost as big as Newton's. But, I'm not as radical as you may think and by no means I consider myself as special as my hero *van Leeuwenhoek*; I believe in the importance of social rituals, therefore I decided to go through the process in order to show my willingness to play by the book.

I also realized that the process of getting a Ph.D. is the same in every part of the world, Mexico, USA, Europe, etc., the difference is probably the amount of money available in each region, that statement is not precisely a compliment or justification. Nevertheless, be aware that I decided to study my Ph.D. in Europe because I was pursuing the high values of honesty, transparency and equality (But…). Sharing experiences with other colleagues in this side of the world showed me that the system consistently generates from time to time tyrannical figures everywhere; people that believe they have the *divine* right to be consistently correct regardless of the scientific method or the ethical norms in modern research. I don't mean to pinpoint anyone, dear reader please forgive me for that, and try hard to understand that I'm not in an easy position at this point.

In my case I was lucky to have Sef Heijnen as Promotor, I learnt important lessons from Aljoscha Wahl, and certainly I applaud the efforts made by TU Delft to improve their policies for resolving conflicts and avoiding scientific fraud -we hope this administrative

change leads to a culture change, and it is adopted by other universities around the globe. But many other colleagues of mine were and are not as lucky as I was; social gatherings among us Ph.D. students consistently showed me people suffering from depression, addictions (coffee, tobacco, alcohol, etc.), low self-esteem, high levels of frustration, etc., at some point I asked myself: When will we look down at those building up scientific knowledge and acknowledge, as society, that such living and working conditions are neither normal nor correct?

I decided to dedicate this section of my thesis to call for help, in the name of those who are not speaking right now: my brothers and sisters Ph.D. students of the world. If we are supposed to secure the conquests derived from the Enlightenment and modern scientific progress, we need to train new generations of people ready to pursue truth through the scientific method. But first, we need to revise the current conditions in which modern scientists work and live. Remembering how I started, I realize that many children who may become acquainted with the misfortunes of many Ph.D. students and scientists will not dare to pursue a scientific career, just because of those horror stories that my colleagues shared with me.

It is not right that our colleagues live under the pressure of a system that treats scientific truth as good of exchange to sell by the rules of the free market; it is a terrible idea to produce papers, do experiments, give the "proper" format to articles and be charged for consulting our own results; it is undeniably wrong to lobby in order to get our work published; it is morally intolerable to compromise authorships in the name of "political agreements"; it is unacceptable that editors reject works on the grounds of being competitors with the lab that produced such work; it is unfair to review with less rigor those papers coming from a "well-known" lab in comparison to the rigor applied to "unknown" labs; it is necessary to generate conditions for gender equality in academia; it is impossible to become scientists if we don't accept that we all are error-prone (*errare humanum est*) and that we need to learn from our mistakes.

As far as I'm concerned, this is a warning from someone who sees that his fellow countrymen prefer to become football players,

celebrities in social networks or reality-show stars instead of engineers, medical practitioners or scientists. Unfortunately, this pattern is not endemic of my beloved Mexico, if we continue on this path, the future of the human kind will not be as bright as it was envisioned by the giants that lend me their shoulders to step over them.

After sharing these thoughts with you, I'll leave you to continue reading this work and I hope, dear reader, that you enjoy this thesis. And if we are lucky enough to cross our paths in the future, we could talk about the content of this book, its propositions or whatever other topic that you wish to share with me to make my existence richer than it is today.

Sincerely yours,

Hugo Federico Cueto Rojas
February 19th, 2016. Teziutlán, Puebla, México.

SUMMARY

/

SAMENVATTING

Summary

In the present work, we studied amino acid metabolism and NH_4^+-transport in *Saccharomyces cerevisiae* from a Thermodynamic perspective. We proposed a thermodynamics-based feasibility assessment of substrate-to-product reactions for anaerobic product formation (**Chapter 2**). As discussed previously, our main hypothesis is that any substrate/product couple, which generates enough free energy for ATP or pmf production at full process conditions, is feasible under anaerobic conditions. Many products from the DOE list (Werpy and Petersen, 2004) (21 out of 30) have the potential to be produced anaerobically using glucose as substrate. Additionally, our calculations suggest that non-conventional substrates (CO and H_2) are also relevant for anaerobic process development.

Furthermore, the value of our method relies on the fact that a minimum of information is necessary in order to obtain important process parameters that allow performing technical and economical feasibility assessments at early stages of a project. We foresee that the key future challenge for synthetic biology will be to build pathways that can convert the Gibbs free energy available into biologically useful energy; and we strongly believe that Synthetic Biology will be a determinant tool to achieve this goal.

Next to this, a new experimental protocol to measure intracellular ammonium was presented (**Chapter 3**), a valuable tool for metabolomics and thermodynamic pathway analysis of amino acid production pathways and NH_4^+-transport processes. The validation experiments of the method demonstrated that metabolomics approaches to monitor the N-metabolism require improved quenching and sample processing protocols due to metabolite instability. In comparison with results obtained by Canelas *et al.* (2009), we were able to observe degradation of amino acids into keto acids and pyroglutamic acid, showing that the widely used ethanol boiling method degrades some key metabolites. Therefore, buffered cold chloroform-methanol extraction should be preferred over ethanol boiling for metabolite extraction when studying N-metabolism and tricarboxylic acid cycle intermediates.

Moreover, the experimental measurements of intracellular ammonium indicate that in aerobic N-limited conditions more than 95% of the ammonium is found in the intracellular space, regardless of the N-source (**Chapter 4**). Accumulation of intracellular ammonium is in agreement with previous hypotheses that suggested an electrochemical driven ammonium uptake mechanism; surprisingly, we found evidence of a potential futile cycle between the processes of NH_3 excretion and NH_4^+ uptake under N-limiting conditions (**Chapter 4**).

Furthermore, one of the most important findings from this work is the fact that not only C-metabolism is highly compartmentalized, but also N-metabolism (**Chapters 4** and **5**). Our experimental results suggest that vacuoles play an important role in N-limitation. Particularly, our calculations showed that intracellular ammonium is mainly compartmentalized in the vacuole (>90% of all ammonium). Compartmentalization is an important biological phenomenon that needs to be taken into account when performing thermodynamic and kinetic modeling as the common assumption of homogeneity is namely not always justified. For instance, based on our thermodynamic pathway analysis, we found strong indications that key metabolites, other than ammonium, are compartmentalized. If then whole cell amounts are considered reactions such as NADH-dependent glutamate dehydrogenase (*gdh2*), do not comply with the second law of thermodynamics. Additionally, our measurements indicate that in *Saccharomyces cerevisiae* it is incorrect to assume thermodynamic equilibrium in many of the N-central metabolism reactions, which apparently require large thermodynamic driving forces to function properly.

In contrast to existing hypotheses of alternative transport mechanisms of ammonium in yeast in absence of Mep-proteins, such as unspecific transport through K^+ channels (Hess *et al.*, 2006) or uptake of NH_3 through Mep proteins (Soupene *et al.*, 2001), it was demonstrated that the uptake mechanism of NH_X was NH_3-diffusion in the strain IMZ351 (*mep1*Δ, *mep2*Δ, *mep3*Δ) (**Chapter 5**). However, we found that energy efficiency improvement strategies have to take into account cellular stress responses mechanisms. Similarly to

Milne *et al.* (2015), we did not observe the expected biomass yield improvement associated with ATP-independent NH_4^+-assimilation. Our current hypothesis is that certain stress response pathways are activated, which overall led to observed lower N-content and concomitant accumulation of storage carbohydrates (*i.e.* trehalose and glycogen). In industrially relevant conditions (C-limitation, high residual N), it is expected that this strain will not show those detrimental effects due to the large concentration of NH_X in the extracellular space, opposed to the observed results in N-limiting conditions.

Samenvatting

In het huidige onderzoek, bestudeerden wij het aminozuur metabolisme en NH_4^+-transport in *Saccharomyces cerevisiae* vanuit een thermodynamisch perspectief. Wij gaven een voorstel voor een op thermodynamica gebaseerde haalbaarheidsevaluatie van substraat-tot-product reacties voor anaerobe product vorming (**hoofdstuk 2**). Zoals eerder besproken, is onze hypothese dat het gebruikte substraat-product koppel met voldoende vrije energie voor ATP of pmf productie bij volle procesomstandigheden, haalbaar onder anaërobe omstandigheden. Veel producten uit de DOE lijst (Werpy en Peterson, 2004) (21 van 30) hebben het potentieel anaëroob geproduceerd te kunnen worden met glucose als substraat. Bovendien suggereren onze berekeningen dat niet-conventionele substraten (CO en H_2) ook relevant zijn voor anaerobe procesontwikkeling.

Daarenboven, berust de waarde van onze werkwijze op het feit dat een minimum aan informatie nodig is voor belangrijke procesparameters die toelaten dat het uitvoeren van technische en economische haalbaarheidsstudies in een vroeg stadium van een project mogelijk is. Wij verwachten dat de belangrijkste uitdaging voor de toekomst van synthetische biologie zal zijn om routes te construeren die de beschikbare Gibbs vrije energie kan omzetten in biologisch bruikbare energie. Wij zijn ervan overtuigd dat de synthetische biologie een beslissend instrument zal zijn om dit doel te bereiken.

Daarnaast, een nieuw experimenteel protocol om intracellulaire ammonium meten werd gepresenteerd (**hoofdstuk 3**), een waardevol gereedschap voor metabolomics en thermodynamische reactieroute-analyse van aminozuur productiepaden en NH_4^+ -transport processen. De validatie experimenten voor de methode toonde aan dat metabolomics benaderingen tot het observeren van N-metabolisme verbeterde quenching en monsterverwerking protocollen vereisen als gevolg van metaboliet instabiliteit. In vergelijking met de resultaten die Canelas *et al.* (2009), konden we afbraak van aminozuren in ketozuren en pyroglutaminezuur

observeren, waaruit blijkt dat de gebruikte ethylalcohol kookmethode een aantal belangrijke metabolieten degradeert. Daarom geniet gebufferde koud chloroform-methanol-extractie de voorkeur boven het koken met ethanol voor metaboliet extractie bij het bestuderen van N-metabolisme en tricarbonzuur cyclus tussenproducten.

Bovendien, de experimentele metingen van intracellulaire ammonium geven aan dat bij aërobe N-limiterende condities meer dan 95% van de ammonium zich in de intracellulaire ruimte bevindt, ongeacht de stikstofbron (**Hoofdstuk 4).** Accumulatie van intracellulaire ammonium is in overeenstemming met eerdere hypotheses die een elektrochemische gedreven ammonium opname mechanisme voorstelden. Verrassend genoeg, vonden wij het bewijs van een mogelijke futiele cyclus tussen de processen van NH_3 excretie en NH_4^+ opname onder N-limiterende omstandigheden (**hoofdstuk 4**).

Voorts is een van de belangrijkste resultaten van dit werk dat niet alleen het C-metabolisme sterk gecompartimenteerd is, maar ook het N-metabolisme (**hoofdstukken 4 en 5**). Onze experimentele resultaten suggereren dat vacuolen een belangrijke rol spelen bij N-limitatie. In het bijzonder, tonen onze berekeningen aan dat intracellulaire ammonium vooral in compartimenten in de vacuole (> 90% van alle ammonium) aanwezig is. Compartimentering is een belangrijk biologisch verschijnsel waarmee rekening moet worden gehouden bij het uitvoeren van thermodynamische en kinetische modellering vanwege de grote fouten geïntroduceerd in het model als een homogene intracellulaire ruimte wordt verondersteld. Bijvoorbeeld, op basis van onze thermodynamische pathway-analyse, vonden we sterke aanwijzingen dat de belangrijkste metabolieten, naast ammonium, zich in compartimenten bevinden. Als de totale cel bedrage wordt beschouwd, reacties, zoals NADH-afhankelijke glutamaat dehydrogenase (*gdh2*), voldoen dan niet aan de tweede wet van de thermodynamica. Bovendien, geven onze metingen aan dat in *Saccharomyces cerevisiae* het onjuist is thermodynamisch evenwicht aan te nemen in veel van de N-centrale metabolisme reacties, die blijkbaar grote thermodynamische drijvende krachten vereisen om goed te functioneren.

In tegenstelling tot bestaande hypotheses van alternatieve transportmechanismen van ammonium in gist zonder Mep-eiwitten, zoals niet-specifieke transport door K^+ kanalen (Hess et al., 2006) of opname van NH_3 tot Mep eiwitten (Soupene et al., 2001) werd hier aangetoond dat het opname mechanisme van NH_X de NH_3-diffusie is in de stam IMZ351 (mep1Δ, mep2Δ, mep3Δ) (**hoofdstuk 5**). Echter, we vonden dat de verbetering van energie-efficiëntie strategieën rekening moeten houden met cellulaire stress respons mechanismen. Evenals Milne et al. (2015), hebben we niet het verwachte biomassa rendementsverbetering geobserveerd in verband met de ATP-onafhankelijke NH_4^+-assimilatie. Onze huidige hypothese is dat bepaalde stress respons trajecten worden geactiveerd, die over het algemeen leiden tot een waargenomen lager N-gehalte en gelijktijdige accumulatie van opslag koolhydraten (*dwz* trehalose en glycogeen). In industrieel relevante omstandigheden (C-beperking, hoge overblijvende N), wordt verwacht dat deze stam niet de nadelige effecten vertonen als gevolg van de hoge concentratie van NH_X in de extracellulaire ruimte, in tegenstelling tot de waargenomen resultaten in N-limiterende omstandigheden.

CHAPTER

1

General introduction

My work, which I've done for a long time, was not pursued in order to gain the praise I now enjoy, but chiefly from a craving after knowledge, which I notice resides in me more than in most men. And therewithal, whenever I found something remarkable, I have thought it my duty to put down my discovery on paper, so that all ingenious people might be informed thereof.

Antonie van Leeuwenhoek (27 Jun 1716), Letter to the University of Louvain. As cited by Charles-Edward Amory Winslow in *The Conquest of Epidemic Disease: A Chapter in the History of Ideas* (), 156

Bio-based production of chemicals: Why anaerobic?

In recent years, metabolic engineering has been successfully applied to develop and improve production strains for relevant bio-based processes (Choi *et al.*, 2015; Shin *et al.*, 2013). Most of these processes are designed to be carried out under aerobic fed-batch conditions, for instance the production of amino acids (L-glutamate and L-lysine), antibiotics, biofuels (except ethanol), synthesis intermediates (isoprene), and drug products (artemisinin) (Nielsen, 2001). Despite of their popularity, aerobic processes have several drawbacks for large-scale applications compared to anaerobic conversions, namely:

(a) High mechanical energy-input related to oxygen transfer and liquid mixing;

(b) Oxygen transfer limitations inherent to the low solubility of oxygen in water, leading to low productivities;

(c) Carbon losses into CO_2 due to complete oxidation of the C-source, usually glucose, leading to lower yields;

(d) High heat generation due to complete substrate oxidation;

(e) Foaming, which correlates with high biomass concentration and aeration rates.

Therefore, anaerobic substrate-to-product conversions are more desirable for the large-scale bio-based production of chemicals. Some of the most important bio-based chemicals are amino acids (Straathof, 2014). These nitrogenous organic compounds are used mainly in the food and feed industry, some times in quantities of Mtons a year, and the market for them is both prosperous and expanding. Particularly L-glutamic acid and L-lysine are the most relevant amino acids (industrially speaking) and several companies produce them on a large-scale, predominantly using the strictly aerobic bacterium *Corynebacterium glutamicum* as microbial cell factory (Straathof, 2014).

Amino acids have recently also been recognized as important building blocks (Choi *et al.*, 2015) for the synthesis of new polymers and fibers (Qian *et al.*, 2009; Qian *et al.*, 2011). For instance, L-lysine can be decarboxylated into cadaverine, which can be used to produce polyamides (Qian *et al.*, 2011). L-valine and L-alanine playing important roles in the pharmaceutical industry, especially as drug

precursors, for instance in the production of new generation antibiotics and antivirals (Clardy *et al.*, 2006; Oldiges *et al.*, 2014); furthermore, they also play an important role as raw materials for the cosmetics industry (Oldiges *et al.*, 2014). Because of the wide range of new and traditional applications, it is expected that the amino acid market will expand even more in the context of the emerging bio-based economy. Sustainable production routes will therefore become increasingly important.

C. glutamicum is generally considered a good amino acid production host due to its high product excretion capacity. Nevertheless, anaerobic amino acid production is not feasible with this organism, limiting the achievable product yield and economy of the process. Therefore, other production hosts need to be considered as potential microbial cell factories, and modified using metabolic engineering tools. *S. cerevisiae* is a well-known industrial workhorse used for the production of first and second-generation bio-ethanol (Nielsen *et al.*, 2013). Due to its high glycolytic flux and biological robustness, yeast is one of the most promising organisms for anaerobic production processes (Choi *et al.*, 2015; Hong and Nielsen, 2012; Nielsen *et al.*, 2013). Moreover, genome, transcriptome, and metabolome methods are extensively available for use in the development of rational strain improvement strategies for the production of fine chemicals (Hong and Nielsen, 2012).

Reprograming *Saccharomyces cerevisiae* ***metabolism for the anaerobic production of L- amino acids***

Pathway engineering considerations

In this work, we focus on the putative anaerobic production of amino acids. In order to reprogram yeast metabolism and achieve efficient amino acid synthesis under anaerobic conditions, we propose to implement thermodynamically inspired metabolic strategies to address the following challenges:

i) Balanced redox product pathways in all cellular compartments;

ii) Free energy conservation, where possible, as ATP or pmf production;
iii) Engineering of energy efficient transport processes;
iv) Preventing of unwanted amino acid compartmentalization;
v) Development of energy efficient nitrogen uptake and assimilation;
vi) Elimination of the native fermentative pathway (ethanol formation).

A useful example to illustrate these aspects is the anaerobic production of L-alanine in yeast. The theoretical maximum yield for alanine in anaerobic *S. cerevisiae* would not be higher than 2 $mol_{alanine}/mol_{glucose}$ using glucose and ammonium as substrates (1.1), based on the theoretical product reaction.

$$\begin{aligned} &Glc_{(aq)} + 2\times NH^{+}_{4(aq)} \longrightarrow 2\times Alanine_{4(aq)} + 2\times H_2O_{(aq)} + 2\times H^{+}_{(aq)} \\ &\Delta_{cat}G^{0'} = -213.6\frac{kJ}{mol_{Glc}} \end{aligned} \qquad (1.1)$$

On the other hand, if it is assumed that the metabolic energy for biomass formation comes from this product reaction, the amount of product required for the synthesis of 1 C-mol of biomass (1.2) can be estimated according to Heijnen *et al.* (Heijnen, 1999; Heijnen *et al.*, 1992).

$$\begin{aligned} 1.28\times Glc_{(aq)} + 2.41\times NH^{+}_{4(aq)} \longrightarrow\ & 2.21\times Alanine_{(aq)} + 2.66\times H_2O_{(aq)} \\ & +1\times C\text{-}mol\ Biomass_{(aq)} \\ & +0.05\times CO_{2(g)} + 2.41\times H^{+}_{(aq)} \end{aligned} \qquad (1.2)$$

To achieve anaerobic L-alanine production in *S. cerevisiae*, two strategies can be considered: (a) Alanine formation from pyruvate via transamination, requiring a change of the glutamate dehydrogenase cofactor requirement from NADPH (Garcia-Campusano *et al.*, 2009) to NADH by expressing a heterologous NADH-dependent glutamate dehydrogenase; or (b) direct reductive amination of pyruvate by a NADH-dependent alanine dehydrogenase. Both strategies will

ensure a redox-neutral alanine production pathway (figure 1.1), leading to (1.3).

$$Glc_{(aq)in} + 2\times NH^{+}_{4(aq)in} + 2\times ADP_{(aq)in} + 2\times Pi_{(aq)in} \longrightarrow 2\times Alanine_{4(aq)in} + 2\times ATP_{(aq)in} \quad (1.3)$$

Note that from 214 kJ (equation 1.1), 2 ATP are synthesized, which implies that there is about 50% of free energy conservation efficiency.

A key item to take into account when designing a pathway for alanine production is the uptake of the N-source. NH_3 could be transported via passive diffusion over cell membranes, with an estimated diffusion coefficient of 48×10^{-3} cm/s in synthetic membranes (Antonenko *et al.*, 1997). On the other hand, NH_4^+ is transported via a protein-mediated uniport mechanism (Ullmann *et al.*, 2012; Winkler, 2006). Different proteins are reported to be involved in NH_4^+ transport; in particular, in *S. cerevisiae* Mep (**Me**thylammonium and ammonium **p**ermeases) proteins are responsible for ammonium transport (Marini *et al.*, 1997).

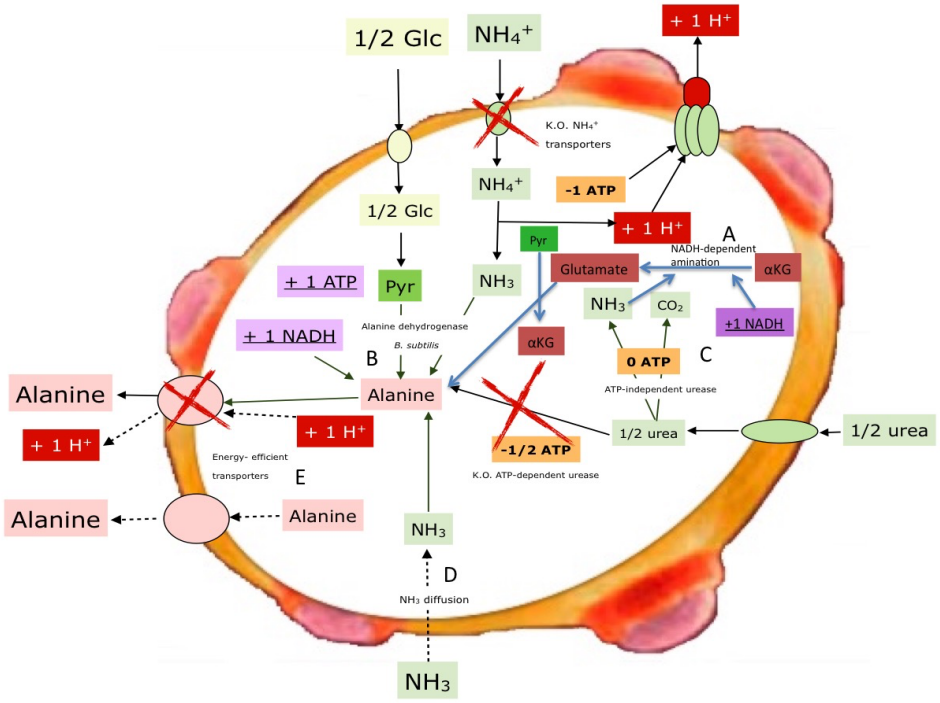

Figure 1.1 Potential pathways for anaerobic alanine production. A)

Naturally occurring transamination of pyruvate into alanine, coupled to NADH-dependent glutamate synthesis. B) Alanine synthesis via direct reductive amination. As both routes need to be associated with ATP-independent ammonium assimilation, two strategies are proposed C) expression of ATP-independent urease (Milne et al., 2015) and D) NH_3-uptake instead of NH_4^+-uniport. Besides the product pathway, E) energy efficient transporters need to be expressed to export the product to the extracellular space.

From an energetic point of view, nitrogen transport and NADPH-dependent assimilation are costly processes; Mep-mediated NH_4^+-uptake in *S. cerevisiae* requires, per mole NH_4^+ taken up, the export of one mole H^+ through the cytosolic H^+-ATPase *Pma1* (Magasanik, 2003) at the cost of one mole ATP per mole H^+. This leads to no net ATP gain from alanine production from glucose and ammonium. Two potential solutions to overcome the energetic costs of nitrogen uptake and assimilation are proposed: (a) Change the type transport mechanism of nitrogen from NH_4^+-uptake to NH_3-diffusion, avoiding ATP expenditure; or (b) express an ATP-independent urease to assimilate urea (instead of the native ATP-dependent urea amidolyase), relying on ATP-free urea transport (Milne *et al.*, 2015).

Although, the transporters (Kleiner, 1981; Marini *et al.*, 1997; Ullmann *et al.*, 2012; Winkler, 2006) and main mechanisms by which ammonium is assimilated in yeast cells (Ljungdahl and Daignan-Fornier, 2012; Magasanik, 2003) have been known and documented for many years, one of the key challenges when studying *in vivo* Nitrogen metabolism and ammonium transport and sensing in different biological systems, but particularly in yeast, is the intracellular ammonium concentration.

Most research on ammonium transport and metabolism relies on analogous molecules, such as methylamine, instead of ammonium (Kleiner, 1981; Roon *et al.*, 1975; Van Nuland *et al.*, 2006). Other studies measured only the extracellular ammonium concentration and correlated it with intracellular observations, or simply estimated the intracellular ammonium concentration based on assumptions such as the thermodynamic equilibrium of the reaction glutamate

dehydrogenase (Kim *et al.*, 2012; Wang *et al.*, 2011). However, little is known about the energy status of the N-assimilating reactions; furthermore, the molecular mechanisms behind nitrogen sensing and control of the N-metabolism are still not fully understood (Conrad *et al.*, 2014; Ljungdahl and Daignan-Fornier, 2012).

In order to test the different free energy conservation strategies for anaerobic amino acid production in yeast, a detailed strain characterization using *in vivo* metabolic profiling to perform thermodynamic analysis of the product pathway and transport steps is required. Heterologous genes in *S. cerevisiae* are typically expressed in the cytosol; thus, the cytosolic concentrations of key metabolites need to be monitored.

Scope and outline of this thesis

The aim of this project is to answer the following research questions:

1. Is anaerobic amino acid production feasible in *S. cerevisiae*? That is, is there a sufficient thermodynamic driving force to generate ATP?
2. What is the transport mechanism of ammonium/ammonia (NH_X) when the genes encoding for Mep-transporters are knocked out, as proposed in our metabolic engineering strategy? In order to test the different hypothesis available in literature, an accurate measurement of intracellular ammonium is required.
3. What are the intracellular/cytosolic concentrations in *S. cerevisiae* of key metabolites of amino acid metabolism? In particular, what is the intracellular/cytosolic concentration of ammonium?
4. What are the thermodynamic driving forces in the central N-metabolism of *S. cerevisiae*?
5. What is the physiological effect of implementing the free energy conservation strategies proposed for anaerobic amino acid production in *S. cerevisiae*?

Chapter 2 focuses on question 1 by introducing a general thermodynamics-based approach to assess the theoretical product

reaction, taking into account process conditions and the minimal amount of Gibbs free energy needed to obtain a feasible anaerobic process.

Chapter 3 addresses research questions 2 and 3 by extending metabolomics approaches to intracellular NH_4^+ quantification, a metabolite that is not often measured but is key for NH_4^+-transport and the thermodynamic pathway analysis of N-central metabolism in yeast. A newly validated method for the quantification of intracellular ammonium is presented. The chapter also presents an evaluation of the performance of two methods of metabolite extraction that are widely used in metabolic profiling of *S. cerevisiae*. The methods were compared in order to assess key items such as amino acid stability and the production of keto acids (pyruvate and αKG) and pyroglutamic acid due to amino acid degradation during sample processing.

Research question 4 is addressed in **Chapter 4**, which presents an analysis of the thermodynamic driving forces in the central N-metabolism, using different entry points to N-metabolism to characterize these driving forces. The chapter also addresses membrane transport, futile cycling and compartmentalization of ammonium (key substrate for amino acid production), and the molecular regulation of the N-metabolism, all in relation to different N-sources (ammonium, urea, and glutamic acid).

Finally, **Chapter 5** focuses on research questions 4 and 5, where Mep-genes are knocked-out to achieve NH_3-diffusion as a strategy for ATP saving in *S. cerevisiae*. A thorough comparison of two strains of *S. cerevisiae* (reference and Mep-deficient strains) is carried out to determine the uptake mechanism of ammonium/ammonia (NH_X) in the absence of Mep-proteins, and the energy consequences and physiological effects of the deletion of Mep-genes under aerobic N-limiting conditions.

References

Antonenko, Y. N., Pohl, P., Denisov, G. A., 1997. Permeation of ammonia across bilayer lipid membranes studied by ammonium ion selective microelectrodes. Biophys. J. 72**,** 2187-95.

Choi, S., Song, C. W., Shin, J. H., Lee, S. Y., 2015. Biorefineries for the production of top building block chemicals and their derivatives. Metab. Eng. 28**,** 223-39.

Clardy, J., Fischbach, M. A., Walsh, C. T., 2006. New antibiotics from bacterial natural products. Nat. Biotechnol. 24**,** 1541-50.

Conrad, M., Schothorst, J., Kankipati, H. N., Van Zeebroeck, G., Rubio-Texeira, M., Thevelein, J. M., 2014. Nutrient sensing and signaling in the yeast *Saccharomyces cerevisiae*. FEMS Microbiol. Rev. 38**,** 254-99.

Garcia-Campusano, F., Anaya, V. H., Robledo-Arratia, L., Quezada, H., Hernandez, H., Riego, L., Gonzalez, A., 2009. ALT1-encoded alanine aminotransferase plays a central role in the metabolism of alanine in Saccharomyces cerevisiae. Can. J. Microbiol. 55**,** 368-74.

Heijnen, J. J., 1999. Bioenergetics of microbial growth. In: Flickinger, M. C., and Drew, S.W., (Ed.), Encyclopedia of bioprocess technology: Fermentation, biocatalysis, and bioseperation. John Wiley & Sons, pp. 267-291.

Heijnen, J. J., Vanloosdrecht, M. C. M., Tijhuis, L., 1992. A Black-Box Mathematical-Model to Calculate Autotrophic and Heterotrophic Biomass Yields Based on Gibbs Energy-Dissipation. Biotechnology and Bioengineering. 40**,** 1139-1154.

Hong, K. K., Nielsen, J., 2012. Metabolic engineering of *Saccharomyces cerevisiae*: a key cell factory platform for future biorefineries. Cell. Mol. Life Sci. 69**,** 2671-90.

Kim, M., Zhang, Z., Okano, H., Yan, D., Groisman, A., Hwa, T., 2012. Need-based activation of ammonium uptake in Escherichia coli. Mol. Syst. Biol. 8**,** 616.

Kleiner, D., 1981. The transport of NH_3 and HN_4^+ across biological membranes. Biochimica et Biophysica Acta (BBA) - Reviews on Bioenergetics. 639**,** 41-52.

Ljungdahl, P. O., Daignan-Fornier, B., 2012. Regulation of amino acid, nucleotide, and phosphate metabolism in Saccharomyces cerevisiae. Genetics. 190**,** 885-929.

Magasanik, B., 2003. Ammonia Assimilation by *Saccharomyces cerevisiae*. Eukaryot. Cell. 2**,** 827-829.

Marini, A. M., Soussi-Boudekou, S., Vissers, S., Andre, B., 1997. A family of ammonium transporters in *Saccharomyces cerevisiae*. Mol. Cell. Biol. 17**,** 4282-93.

Milne, N., Luttik, M. A., Cueto Rojas, H. F., Wahl, A., van Maris, A. J., Pronk, J. T., Daran, J. M., 2015. Functional expression of a heterologous nickel-dependent, ATP-independent urease in *Saccharomyces cerevisiae*. Metab. Eng. 30**,** 130-140.

Nielsen, J., 2001. Metabolic engineering. Appl. Microbiol. Biotechnol. 55**,** 263-83.

Nielsen, J., Larsson, C., van Maris, A., Pronk, J., 2013. Metabolic engineering of yeast for production of fuels and chemicals. Curr. Opin. Biotechnol. 24**,** 398-404.

Oldiges, M., Eikmanns, B. J., Blombach, B., 2014. Application of metabolic engineering for the biotechnological production of L-valine. Appl. Microbiol. Biotechnol. 98**,** 5859-70.

Qian, Z. G., Xia, X. X., Lee, S. Y., 2009. Metabolic engineering of *Escherichia coli* for the production of putrescine: a four carbon diamine. Biotechnol. Bioeng. 104**,** 651-62.

Qian, Z. G., Xia, X. X., Lee, S. Y., 2011. Metabolic engineering of *Escherichia coli* for the production of cadaverine: a five carbon diamine. Biotechnol. Bioeng. 108**,** 93-103.

Roon, R. J., Even, H. L., Dunlop, P., Larimore, F. L., 1975. Methylamine and ammonia transport in Saccharomyces cerevisiae. J. Bacteriol. 122**,** 502-9.

Shin, J. H., Kim, H. U., Kim, D. I., Lee, S. Y., 2013. Production of bulk chemicals via novel metabolic pathways in microorganisms. Biotechnol. Adv. 31**,** 925-35.

Straathof, A. J., 2014. Transformation of biomass into commodity chemicals using enzymes or cells. Chem. Rev. 114**,** 1871-908.

Ullmann, R. T., Andrade, S. L., Ullmann, G. M., 2012. Thermodynamics of transport through the ammonium transporter *Amt-1* investigated with free energy calculations. J. Phys. Chem. B. 116**,** 9690-703.

Van Nuland, A., Vandormael, P., Donaton, M., Alenquer, M., Lourenco, A., Quintino, E., Versele, M., Thevelein, J. M., 2006. Ammonium permease-based sensing mechanism for rapid ammonium activation of the protein kinase A pathway in yeast. Mol. Microbiol. 59**,** 1485-505.

Wang, L., Lai, L., Ouyang, Q., Tang, C., 2011. Flux balance analysis of ammonia assimilation network in E. coli predicts preferred regulation point. PloS one. 6**,** e16362.

Winkler, F. K., 2006. Amt/MEP/Rh proteins conduct ammonia. Pflugers Archiv : European journal of physiology. 451**,** 701-7.

CHAPTER

2

Thermodynamics-based design of microbial cell factories for anaerobic product formation

"Thermodynamic tables are mines of information. They allow scientists to speculate on combinations of suitable electron donors and acceptors, and propose unexpected ways that microorganisms might make a living."

J. Gijs Kuenen. (2008) Nature Reviews Microbiology **6**, 320-326

Abstract

The field of metabolic engineering has delivered new microbial cell factories and processes for the production of different compounds including biofuels, (di)carboxylic acids, alcohols, and amino acids. Most of these processes are aerobic, with few exceptions (e.g., alcoholic fermentation), and attention is focused on assembling a high-flux product pathway with a production limit usually set by the oxygen transfer rate. By contrast, anaerobic product synthesis offers significant benefits compared to aerobic systems: higher yields, less heat generation, reduced biomass production, and lower mechanical energy input, which can significantly reduce production costs. Using simple thermodynamic calculations, we demonstrate that many products can theoretically be produced under anaerobic conditions using several conventional and non-conventional substrates.

Keywords

Thermodynamics; anaerobic product formation; microbial cell factories; bioprocess design

This Chapter is published as: Cueto-Rojas H.F., van Maris A. J. A., Wahl S. A., Heijnen J. J., 2015. Thermodynamics-based design of microbial cell factories for anaerobic product formation, Trends in Biotechnology 33(9) 534-546.
doi: 10.1016/j.tibtech.2015.06.010

Glossary

γ Value. The degree of reduction of a molecule, describes the electron content of a chemical compound based on the biological frame of reference where water, CO_2, protons, NH_4^+, and SO_4^{-2} have a $\gamma = 0$.

$\Delta_e G^{0'}_P$ or $\Delta_e G^{0'}_S$. Gibbs free energy content per electron of a product or substrate, respectively (kJ/mol e^-); derived from half-redox reaction using the biological frame of reference; where H_2O, CO_2, H^+, NH_4^+, and SO_4^{-2} have a $\Delta_f G = 0$ kJ/mol under standard conditions.

$\Delta_f G^{0'}$ and $\Delta_f H^{0'}$. Standard Gibbs free energy and enthalpy of formation (kJ/mol), that relate to a frame of reference where all elements have $\Delta_f G = 0$ kJ/mol and $\Delta_f H = 0$ kJ/mol under standard conditions: pH = 7, T = 298 K, partial pressure of 1bar for all gaseous compounds, and concentrations of 1 mol/L for all dissolved compounds.

$\Delta_{fb} G^{0'}$. Gibbs free energy of formation under the biological frame of reference, where H_2O, CO_2, H^+, NH_4^+, and SO_4^{-2} have a $\Delta_f G = 0$ kJ/mol under standard conditions (kJ/mol).

$\Delta_r G^{0'}$, $\Delta_r H^{0'}$, $\Delta_r S^{0'}$. Gibbs free energy, enthalpy, and entropy of the product reaction (kJ/molProduct). Calculated from the reaction stoichiometry and $\Delta_f G^{0'}$, $\Delta_f H^{0'}$, and $\Delta S^{0'}$ values of all compounds involved in the product reaction under standard conditions.

Anaerobic production of bio-based chemicals

In the past years, the use of renewable sources for production of chemicals has gained significant notoriety (Choi *et al.*, 2015; Rabinovitch-Deere *et al.*, 2013; Zhang *et al.*, 2012), particularly since the US Department of Energy (DOE) published a list of chemicals that are relevant for the transition to a bio-based economy (table 2.1) (Bozell and Petersen, 2010; Werpy and Petersen, 2004). Design of cost-effective processes demands maximisation of product titer, production rate and yield, and minimisation of waste streams and both fixed and variable costs (Porro *et al.*, 2014). These imperatives encourage the development of anaerobic processes, as opposed to aerobic cultivations. Most notably, energy requirements for mixing, aeration and heat removal are significantly reduced using anaerobic methods and the production rate, titer and yield are increased.

This review highlights a general approach to assessing the feasibility of anaerobic substrate-to-product conversions based on basic thermodynamic calculations. The proposed thermodynamic analysis requires minimum input data, and allows for a quick and simple feasibility check of the anaerobic process taking into account different substrates and full-scale process conditions. Special attention is given to the DOE list of key compounds and some relevant amino acids (table 2.1).

Choosing the right substrate

The choice of a suitable substrate for production of bio-based chemicals under anaerobic conditions is a critical first step, as it will determine important features of the process, especially if the substrate is not glucose, which is widely used. Depending on the type of biorefinery, different feedstocks could be used as fermentation substrates (Kamm *et al.*, 2005):

a) First-generation substrates: Carbohydrates and lipids can be obtained from crops, such as sugar cane, palm trees, corn and others. These feedstocks are advantageous to the fermentation process, because high substrate concentrations are possible. This facilitates a minimal water requirement, allowing the achievement of higher

product concentrations. The disadvantage of these feedstocks, which is widely discussed, is competition with land for food production (Ekman *et al.*, 2013; Viikari *et al.*, 2012).

Table 2.1. Key compounds that can be produced from biomass (Bozell and Petersen, 2010; de Jong, 2012; Werpy and Petersen, 2004).

Compound	Chemical formula (γ)	$\Delta_e G^{0'}$ (kJ/mol)	Potential uses of derivatives
Carbon monoxide	CO (2)	49.7188 ± 0.4330	Fuels, synthesis precursors and others
3-Hydroxypropionic acid	$C_3H_6O_3$ (12)	32.5994 ± 0.2165	Fibres, absorbent polymers
Propionic acid	$C_3H_6O_2$ (14)	27.8648 ± 0.2585	Building block
3-Hydroxybutyrolactone	$C_4H_6O_3$ (16)	37.2073 ± 0.2706	Pharmaceuticals, solvents and fibres
Fumaric acid	$C_4H_4O_4$ (12)	35.4060 ± 0.3805	Solvents, fibres and water-soluble polymers
Succinic acid	$C_4H_6O_4$ (14)	29.9962 ± 0.5533	Solvents, fibres and water-soluble polymers
Arabitol	$C_5H_{12}O_5$ (22)	39.9152 ± 0.6223	Sweeteners, new polymers and antifreeze fluids
Furfural	$C_5H_4O_2$ (20)	41.1388 ± 0.4138	Building block
Itaconic acid	$C_5H_6O_4$ (18)	34.8205 ± 0.2992	Solvents, copolymers
Levulinic acid	$C_5H_8O_3$ (22)	30.9370 ± 0.2756	Fuels, solvents, catalysts, polymers
Xylitol	$C_5H_{12}O_5$ (22)	39.8023 ± 0.3036	Sweeteners, new polymers and antifreeze fluids
Xylonic acid	$C_5H_{10}O_6$ (18)	41.6261 ± 0.1964	Building block
2,5-Furan dicarboxylic acid (FDCA)	$C_6H_4O_5$ (18)	29.7816 ± 0.3368	PET analogs, new polyesters, polyamides and nylons
Glucaric acid	$C_6H_9O_8$ (18)	42.8509 ± 0.2640	Solvents and nylons
Gluconic acid	$C_6H_{12}O_7$ (22)	40.4469 ± 0.2114	Building block

Compound	Chemical formula (γ)	$\Delta_e G^{0'}$ (kJ/mol)	Potential uses of derivatives
Levoglucosan	$C_6H_{10}O_5$ (24)	37.8972 ± 0.2526	Building block
Lysine	$C_6H_{14}N_2O_2$ (28)	31.1489 ± 0.3209	Feed and food, building block
Alanine*	$C_3H_7NO_2$ (12)	32.0038 ± 0.3775	Feed and food
Valine*	$C_5H_{11}NO_2$ (24)	29.7322 ± 0.3493	Feed and food

*Included as interesting additional products and analysed in more detail in the examples found in the text boxes.

b) Second-generation substrates. Usually, these substrates are rich in C6 and C5 sugars, and lignocellulosic molecules (Kamm, 2014). The advantage of these substrates is that they reduce competition with food crops. Their main disadvantage is that they require expensive pretreatment processes to obtain fermentable C_6 and C_5 sugars diluted in aqueous solutions, which leads to low product titers, and high downstream processing costs. In addition, pretreatment processing produces a wide variety of molecules including toxic compounds, such as furfural (Nielsen *et al.*, 2013; Straathof, 2014).

c) Third-generation (water free) substrates. Other potential (non-conventional) substrates are biogas, synthesis gas (H_2/CO) obtained from biomass (Straathof, 2014), ethanol, methanol, or glycerol waste from biodiesel and ethanol production. Ethanol might be an attractive non-conventional substrate as it is cheap and can be obtained from second-generation substrates. The advantage of these substrates is that they do not contain water, which increases product titers and decreases downstream processing costs. On the other hand, these substrates will impose important challenges, for instance gaseous substrates will require efficient gas-to-liquid mass transfer (Hu *et al.*, 2013).

Thermodynamic analysis of anaerobic product reactions under standard conditions

For each substrate and product, $\Delta_f G^{0'}$ (Alberty, 2003; Kleerebezem and Van Loosdrecht, 2010; Noor *et al.*, 2012) and $\Delta_f H^{0'}$ (Haynes, 2015; Kleerebezem and Van Loosdrecht, 2010) (see glossary) can be obtained from databases (Alberty *et al.*, 2011; Noor *et al.*, 2012) (see http://webbook.nist.gov) or from calculations using methods reported in literature (Mavrovouniotis, 1990; Noor *et al.*, 2013) e.g. group contribution group contribution (Mavrovouniotis, 1990). For a complete list with the standard thermodynamic properties of relevant substrates and products see Supplementary Table S2.1.

Given that water, carbon dioxide, protons, N-source (NH_4^+ in most cases) and sulfate (SO_4^{-2}) are found universally in anaerobic substrate-to-product reactions, it is useful to employ a different frame of reference, this frame of reference will be called the anaerobic biological reference, indicated by the subscript *fb* (Kleerebezem and Van Loosdrecht, 2010). $\Delta_{fb}G^{0'}$ (see glossary) for each organic compound (substrate or product) is calculated by setting up a redox half reaction as shown in (1), using 1 mole of compound and the reference components and elements discussed previously.

$$-1 \times \text{Compound} + \upsilon_{CO_{2(g)}} \times CO_{2(g)} + \upsilon_{H_2O_{(l)}} \times H_2O_{(l)} + \upsilon_{H^+_{(aq)}} \times H^+_{(aq)} + \upsilon_{NH^+_{4(aq)}} \times NH^+_{4(aq)} + \upsilon_{SO^{-2}_{4(aq)}} \times SO^{-2}_{4(aq)} + \gamma \times \text{electron}^{-1} = 0 \quad (1)$$

In equation (1) the six unknown stoichiometric coefficients are calculated by setting up the five elements (C,H,O,N,S) and charge balances. Note that the stoichiometric coefficient of electrons is, by definition, equal to γ (Heijnen, 1999) (see glossary). $\Delta_{fb}G^{0'}$ is now defined as the opposite of the Gibbs free energy of the redox half reaction (1), calculated from the standard Gibbs free energy of formation of each component as shown in (2).

$$\Delta_{fb}G^{0'}_{compound} = \Delta_f G^{0'}_{compound} - (\upsilon_{CO_{2(g)}} \times \Delta_f G^{0'}_{CO_{2(g)}} + \upsilon_{H_2O_{(l)}} \times \Delta_f G^{0'}_{H_2O_{(l)}} + \upsilon_{H^+_{(aq)}} \times \Delta_f G^{0'}_{H^+_{(aq)}} + \upsilon_{NH^+_{4(aq)}} \times \Delta_f G^{0'}_{NH^+_{4(aq)}} + \upsilon_{SO^{-2}_{4(aq)}} \times \Delta_f G^{0'}_{SO^{-2}_{4(aq)}} + \gamma \times \Delta_f G^{0'}_{electron^-}) \quad (2)$$

Because of this definition, the values of $\Delta_{fb}G^{0'}$ for CO_2, H_2O, H^+, NH_4^+, SO_4^{2-} and electrons become zero. Under anaerobic conditions, no external electron acceptors are present, and consequently all

electrons from the substrate will be found in the product. Because of this link, as shown in (3), it is useful to define $\Delta_e G^{0'}_{Compound}$ (see glossary) (Heijnen, 1994).

$$\Delta_e G^{0'}_{compound} = \frac{\Delta_{fb} G^{0'}_{compound}}{\gamma_{compound}} \tag{3}$$

Note that $\Delta_e G^{0'}$ is related to the redox potential using Faraday's Constant. γ- and $\Delta_e G^{0'}$ values for the DOE list of products were calculated (table 2.1).

Using the approach of the redox half reaction, $\Delta_e H^{0'}_{Compound}$ and $\Delta_e S^{0'}_{Compound}$ can be calculated alongside $\Delta_e G^{0'}$ for any organic compound. For anaerobic products, we can define the reaction for 1 mole of product as equation (4).

$$\begin{aligned} &-\frac{\gamma_P}{\gamma_S} \times \text{Substrate} + \omega_{CO_{2(g)}} \times CO_{2(g)} + \omega_{H_2O_{(l)}} \times H_2O_{(l)} + \omega_{H^+_{(aq)}} \times H^+_{(aq)} \\ &\quad + \omega_{NH^+_{4(aq)}} \times NH^+_{4(aq)} + \omega_{SO^{-2}_{4(aq)}} \times SO^{-2}_{4(aq)} + 1 \times \mathbf{Product} = 0 \end{aligned} \tag{4}$$

The substrate stoichiometric coefficient γ_P/γ_S, in mol_S/mol_P comes from the degree of reduction balance due to the absence of O_2 or any other external electron acceptor; this number is the inverse of the theoretical molar yield in mol_P/mol_S (Dugar and Stephanopoulos, 2011), $\Delta_r G^{0'}$ (see glossary) is obtained using (5), which can be simplified to (6), for 1 mole of product.

$$\Delta_r G^{0'} = (+1) \times \gamma_P \times \Delta_e G^{0'}_P - \frac{\gamma_P}{\gamma_S} \times \gamma_S \times \Delta_e G^{0'}_S \tag{5}$$

$$-\Delta_r G^{0'} = \gamma_P \times \left(\Delta_e G^{0'}_S - \Delta_e G^{0'}_P \right) \tag{6}$$

This result shows that by comparing $\Delta_e G^{0'}$ values of substrate and product, it is immediately apparent whether the combination can produce Gibbs free energy under standard anaerobic conditions; the term "production of Gibbs free energy" refers to the Gibbs free energy of reaction in thermodynamically favorable reactions. Additionally, the different compounds can be classified according to their standard $\Delta_e G^{0'}$ values (figure 2.1).

In anaerobic processes, the product pathway must provide the energy for synthesis of ATP. Suitable substrates must therefore have higher energy content than the products (von Stockar, 2010) in order to

produce sufficient Gibbs free energy to sustain the anabolic activity of the cell. It is clear that, under standard anaerobic conditions, energy production from any substrate to any product is only possible when $\Delta_e G_S - \Delta_e G_P > 0$.

When $\Delta_e G_P > \Delta_e G_S$, useful biological energy cannot be produced anaerobically from product formation (at process conditions), and the transformation of substrate-to-product requires an aerobic process. This is essential strategic information for the early stages of process development.

For example, glycerol ($\Delta_e G^{0'} = 38.6396 \pm 0.1856\ kJ/e\text{-}mol$) can, in principle, be used as substrate for anaerobic production of all compounds exhibiting lower energy content per electron (see figure 2.1). The potential use of glycerol as substrate in anaerobic processes has already been discussed in literature (Richter and Gescher, 2014; Yazdani and Gonzalez, 2007), but not from a thermodynamic point of view. Interestingly, ethanol is not only a product, but also a suitable anaerobic substrate for some compounds, e.g. fatty acids and alkanes; for most compounds, however, aerobic conditions are needed if ethanol is considered as substrate.

Another interesting example is the use of synthesis gas, a non-conventional substrate. H_2 and CO are two of the most energy-rich compounds per electron (figure 2.1). They could be used as substrates to produce nearly all compounds found in the DOE list anaerobically. Anaerobic syngas fermentation is now given more prominence (Hu *et al.*, 2013; Kopke *et al.*, 2010; Mohammadi *et al.*, 2012) (see also http://www.lanzatech.com). Furthermore, note that for highly oxidised organic products CO_2 will be required as additional substrate in the product reaction depending on the degree of reduction of the used organic substrate, e.g. succinate production using glucose as substrate (Taymaz-Nikerel *et al.*, 2013; Thakker *et al.*, 2012), in this case CO_2 is required because C-atoms in succinate are more oxidized (3.5 e-mol/Cmol) compared to C-atoms in glucose (4e-mol/Cmol) (see also http://www.reverdia.com and http://www.succinity.com). Other interesting examples of the use of CO_2 as substrate are described elsewhere in literature (Guadalupe-

Medina *et al.*, 2013; Hu *et al.*, 2013; Taymaz-Nikerel *et al.*, 2013; Zelle *et al.*, 2010).

Effect of full-scale process conditions on Gibbs free energy produced

a) Effect of concentration of products and substrates. The values calculated for $-\Delta_r G^{0'}$ apply to standard conditions. The impact of concentrations different from those under standard conditions can be calculated as (7) (Jol *et al.*, 2010).

$$-\Delta_r G = -\left\{\Delta_r G^{0'} + R \times T \times \ln\left(Q_r\right)\right\} \quad (7)$$

With $-\Delta_r G$ representing the Gibbs free energy produced per mole of product under defined process conditions. In equation (7), $-\Delta_r G^{0'}$ is the Gibbs free energy of the reaction under standard conditions and pH=7, R the ideal gas constant, T the temperature in K, and Q_r the reaction quotient.

Depending on the stoichiometry (mol_S/mol_P), low limiting substrate concentration (of about 10^{-3} mol/L) and a high product concentration (of about 1 mol/L) can reduce the available thermodynamic energy by up to 20 $kJ/mol_{Product}$ (see appendix 2.1). Some of the reactions considered feasible under standard conditions could become unfeasible under full-scale process conditions.

b) Effect of temperature on $-\Delta_r G$. In addition to concentrations of products and substrates, the value for $-\Delta_r G$ is affected by temperature. Assuming that $-\Delta_r H$ (see glossary) and $-\Delta_r S$ (see glossary) do not change significantly between 273.15 K (0 ºC) and 373.15 K (100 ºC), the effect of temperature on the Gibbs free energy produced per mole product ($-\Delta_r G$) can be calculated from equation (8).

$$-\Delta_r G = -\Delta_r H + T \times \Delta_r S \quad (8)$$

For biologically relevant temperatures, it is possible to neglect the influence of temperature over ΔH. Therefore, the Gibbs free energy produced changes with T due to the term $T\Delta_r S$. In most of the cases, this occurs because $-\Delta_r S<0$ and $-\Delta_r H>0$, indicating that entropy and heat are produced. However, this is not always the pattern. For instance, when one or more of the substrates is a gas and all the

products are dissolved in water, the Gibbs free energy produced decreases with increasing temperature. The effect of temperature is case-specific and can be very significant (see appendix 2.2).

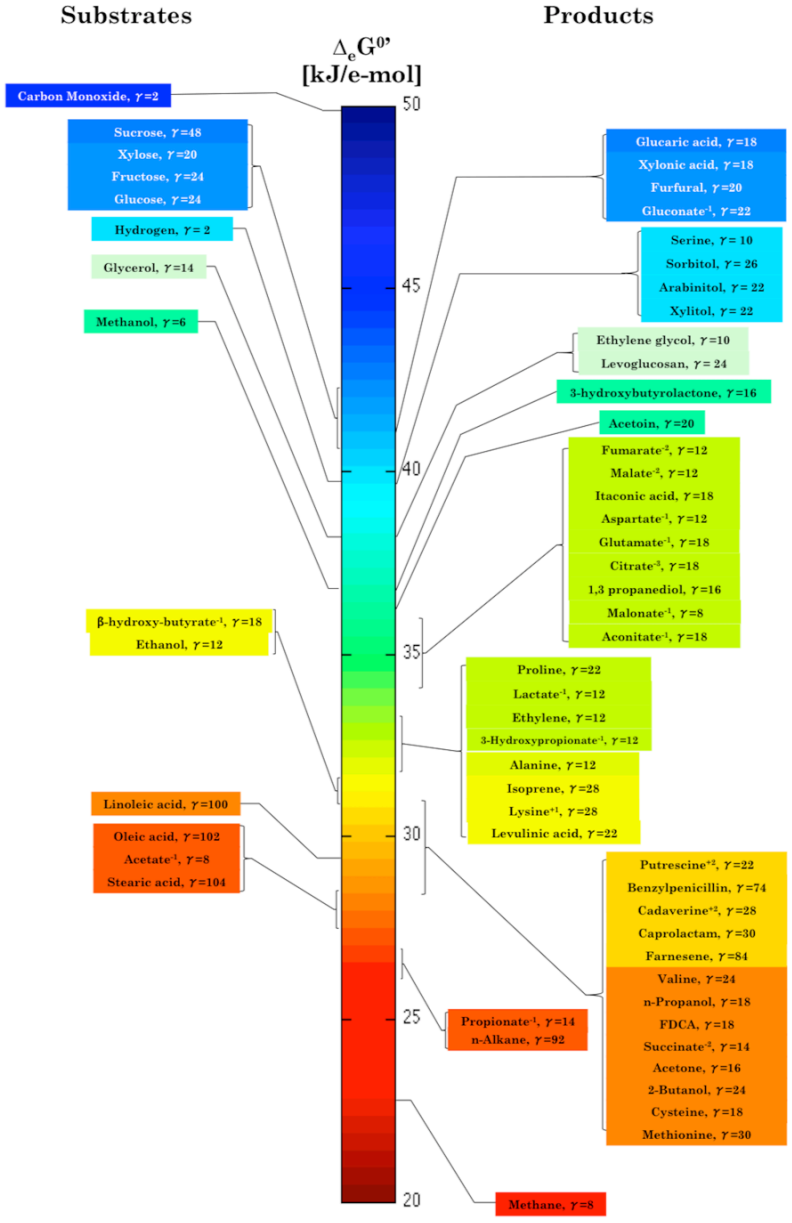

Figure 2.1. Gibbs free energy content per electron ($\Delta_e G^{0'}$), as well as degree of reduction (γ) for selected chemicals; the color code is based on the $\Delta_e G^{0'}$ values. Organic compounds with high $\Delta_e G^{0'}$ are closer to the

top and are better substrates than the organic compounds closer to the bottom, which are considered as potential products under anaerobic conditions.

c) Effects of pH, dissociation and solubility limits on $-\Delta_r G$. The substrate-to-product conversion can include protons, weak dissociable acids and compounds with limited solubility. The later reduces the product concentration in the liquid phase and contributes to a higher $-\Delta_r G$ value (see appendix 2.2).
When protons are involved in the substrate-to-product reaction, e.g. in production of carboxylic acids, $-\Delta_r G$ is strongly affected by pH. Anaerobic production of succinic and fumaric acids from glucose was analyzed thermodynamically in Taymaz-Nikerel *et al.* (2013) . At low pH (around 2-3) the Gibbs free energy produced decreases by around 100 kJ per mol of product. For succinic acid, anaerobic production at low pH is still possible, but fumaric acid production at low pH must be carried out aerobically (Taymaz-Nikerel *et al.*, 2013).

Converting free energy into useful biological energy

Under anaerobic conditions, microorganisms must obtain biological energy from the substrate-to-product conversion. This means that the amount of Gibbs free energy from the substrate-to-product reaction ($-\Delta_r G$) under process conditions must be large enough to provide biological energy in the form of ATP or membrane potential (sodium or proton motive force) (Schoepp-Cothenet *et al.*, 2013) and thermodynamic driving force (TDF) for the product pathway. This biological energy can be used for biomass production, maintenance (von Stockar, 2014), and product excretion (Taymaz-Nikerel *et al.*, 2013) (figure 2.2a). Here, we will focus on three of the aforementioned items: i) ATP and/or proton (or sodium) motive force generation, ii) thermodynamic driving force and iii) product excretion. Therefore, it is necessary to analyze the amount of energy that needs to be produced by any anaerobically feasible product pathway.

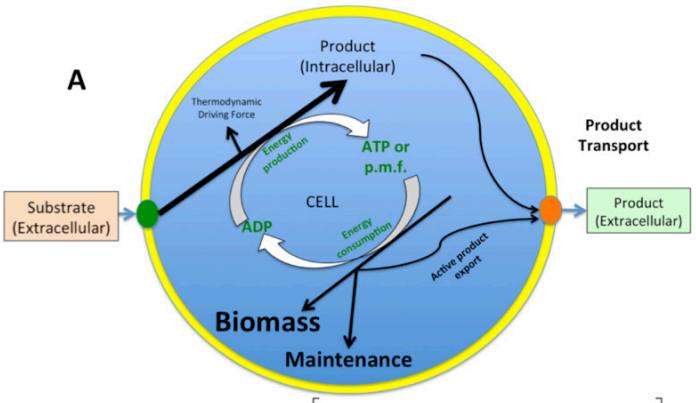

$$-\Delta_r G \geq TDF + \textbf{Transport energy} + \left[1ATP(\Delta_r G \approx 46.2kJ) \quad or \quad pmf(\approx 15kJ) \right]$$

B Transport mechanism		pH_{out}	Out/in ratio*	ATP cost**	ΔG cost*** kJ/$mol_{Product}$
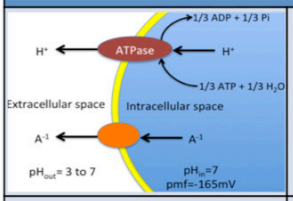	Uniport A^{-1}	3	6×10^{-2}	-1/3	15.4
		7	6×10^{2}	-1/3	15.4
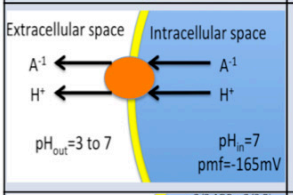	Symport $A^{-1} + H^+$	3	1×10^{-4}	0	0
		7	1	0	0
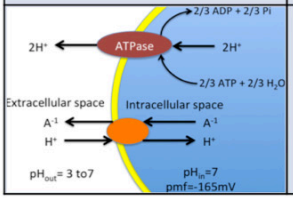	Antiport $A^{-1} + H^+$	3	37.96	-2/3	30.8
		7	3.8×10^{5}	-2/3	30.8

*Ratios are calculated assuming pH_{in}=7 and pmf=-165mV, T=298K.
** It is assumed that an ATPase stoichiometry of 3 H^+ excreted per mole ATP.
*** Calculated assuming $-\Delta_r G$ = 46.2 kJ/mol

Figure 2.2. (A) Sketch of energy production and consumption in biological systems under anaerobic conditions. The energy produced by the product pathway ($-\Delta_r G$) should be large enough to provide energy for ATP or pmf generation and dissipation of energy as thermodynamic driving force (TDF). The biological useful energy (ATP or pmf) can be invested in growth, maintenance or active product excretion (transport energy). (B) Equilibrium out/in ratios and ATP requirements for

carboxylic acid removal for different transport mechanisms, efficient excretion systems that keep high out/in ratios (antiport system in this example) require significant energy investments. We strongly recommend the reader to check van Maris *et al.* (2004a) for a detailed explanation about thermodynamic calculations of transport processes.

In addition, $-\Delta_r G$ can be used to predict interesting parameters such as biomass yield and maximum growth rate of the potential microbial cell factory. These calculations are out of the scope of the present review, however the reader is encouraged to check relevant publications on the topic (Heijnen, 1999; Heijnen *et al.*, 1992; Kleerebezem and Van Loosdrecht, 2010; Liu *et al.*, 2007; McCarty, 2007; von Stockar *et al.*, 2006).

i) ATP and pmf generation

ATP is the universal energy carrier in living organisms (Thauer *et al.*, 1977). The energy content of ATP can be described by ATP hydrolysis (9).

$$ATP_{(aq)} + H_2O_{(l)} \longrightarrow ADP_{(aq)} + H^+_{(aq)} + Pi_{(aq)} \quad (9)$$

The Gibbs free energy in this reaction is called energy of phosphorylation ($-\Delta_P G$), with a value of 30.5 kJ/mol under standard conditions ($-\Delta_P G^{0'}$). Under physiological conditions in anaerobic microorganisms, $-\Delta_P G$ varies from 43.3 kJ/mol in *Methanococcus voltae* (Jin, 2012) to about 50 or 53 kJ/mol in *Paracoccus denitrificans* (Jin, 2012); the energy of phosphorylation is organism specific and many factors affect its value (ionic strength, pH, pMg, etc.), an average value of 46.2 kJ/mol is assumed based on the different values reported in literature (Jin, 2012; Tran and Unden, 1998), which is closer to $-\Delta_P G$ in *Escherichia coli* growing on glucose under anaerobic conditions (Tran and Unden, 1998).

Examples of fermentative processes and their ATP efficiency are summarised in table 2.2. Microorganisms can produce ATP by means of substrate level phosphorylation (Thauer *et al.*, 1977) or proton (or sodium) motive force (Jin, 2012; Thauer *et al.*, 1977). Differences in the transmembrane electrochemical potential of protons (H^+) is reported to be between 11.6 kJ/mol H^+ (-120 mV) and 19.3 kJ/ mol H^+ (-200 mV) (Tikhonov, 2012), with an average of 15 kJ/mol H^+ (-165

mV). Anaerobic substrate-to-product reactions should therefore provide at least enough energy to generate the pmf energy quantum; different strategies can be used to increase conservation of free energy as useful biological energy, as discussed in literature (de Kok *et al.*, 2012; de Kok *et al.*, 2011; Kozak *et al.*, 2014).

ii) Thermodynamic Driving Force for the product pathway

To achieve reasonable reaction rates, part of the Gibbs free energy available must be used in irreversible reactions (Bar-Even *et al.*, 2012), which is defined as thermodynamic driving force (TDF). This free energy dissipation must be considered in the thermodynamic analysis, in a pathway-specific manner and can also be exploited to design functional anaerobic cell factories, as exemplified in Shen *et al.* (2011).

The value can be estimated based on the difference between $-\Delta_r G$ and the energy equivalent of ATP and pmf produced; It has been shown that ¼ of the reactions in central metabolism (in *Saccharomyces cerevisiae*) are far from equilibrium (Canelas *et al.*, 2011); the loss of Gibbs free energy incurred in the form of irreversible reactions accounts for the so-called TDF. This observation allows the assumption that in substrate-to-product pathways, ¼ of the reactions contribute to TDF. A rule-of-thumb to estimate TDF, if the pathway length is known, is given in (10).

$$\mathrm{TDF} = \frac{1}{4} \times \mathrm{n} \times \left[20\mathrm{kJ} \right] \tag{10}$$

Where *n* is the number of reactions in the pathway; ¼ is the fraction of irreversible reactions in the pathway; and 20kJ is the typical energy requirement for a far from equilibrium reaction (Canelas *et al.*, 2011). For a typical pathway of 12 reactions, e.g. glucose to ethanol, the TDF requirements are estimated as 60 kJ per mole of product. This first estimate gives a good indication about possible Gibbs free energy losses in the pathway, but TDF is pathway and organism-specific. Different experimental observations point at the fact that in average 45% of the Gibbs free energy of the catabolic pathway is required as TDF (table 2.2).

A first estimate of the minimum amount of Gibbs free energy necessary for a feasible anaerobic substrate-to-product conversion, which yields useful biological energy, can be obtained using the TDF concept. For organisms that use pmf-driven ATP synthesis, the minimum amount of Gibbs free energy required will be around 27 kJ/mol$_P$; from which 15 kJ/mol (in average (Tikhonov, 2012)) will be used for pmf generation and the rest will be dissipated as TDF . On the other hand, for organisms that use substrate-level phosphorylation, the minimum will be close to 84 kJ/mol$_P$; 46.2 kJ/mol (in average (Jin, 2012; Tran and Unden, 1998)) will be used to generate ATP and the rest will be dissipated in the product pathway as TDF. We can hypothesize that any substrate-to-product reaction that yields more Gibbs free energy (per mole product) than these minimal thermodynamic limits has high probability of resulting in a viable anaerobic bioprocess, where substrate-to product-conversion generates useful biological energy in the form of ATP or pmf. Thermodynamically feasible product-reactions that yield $-\Delta_r G$ amounts below the proposed limits are unlikely to be anaerobically feasible or unattractive for industrial applications as the growth rate of these organisms will be slow (LaRowe *et al.*, 2012).

Similar energy thresholds have been reported in literature for a wide range of organisms. The minimum amount of Gibbs free energy necessary for biologically active cells ranges between values as high as 187.2 kJ/mol for *Desulfovibrio* sp SHV and as low as 9.4 kJ/mol for *Methanogenium marinum* (Jin, 2012).

The reader must note that there are highly efficient organisms that harvest small amounts of $-\Delta_r G$, at even lower limits than those proposed hitherto. Nevertheless, these organisms often display a slow growth rate, as discussed in LaRowe *et al.* (2012), and the metabolic rates achieved are not interesting from an industrial point of view. Therefore, the proposed limits in this study are not absolute limits for life, but limits for industrially relevant microorganisms.

iii) Product transport

A frequently neglected factor in metabolic engineering projects is product excretion. This is probably related to the inherent challenges of studying transmembrane proteins, and the consequent lack of

knowledge of transport mechanisms related to a particular product. The transport mechanism for the end product of a catabolic reaction is critical for the functional design of an anaerobic cell factory, as exemplified in (van Maris *et al.*, 2004a; van Maris *et al.*, 2004b).
Ideally, the removal of the end product of any anaerobic fermentation should not cost ATP, and maintain an out/in concentration ratio as high as possible. However, these requirements conflict; high out/in product concentration ratios cost energy, and for organic acids and negatively charged products there is also an energy cost in removing the H^+ produced. In the case of a carboxylic acid, it is possible to deduce the most energetically suitable transporter if different mechanisms are employed (figure 2.2b).
Assuming thermodynamic equilibrium, it is possible to calculate the achievable out/in ratio for monocarboxylic acids under equilibrium conditions as a function of extracellular pH (see appendix 2.1). It is clear that some of the mechanisms have an ATP requirement due to high out/in ratio and maintenance of pH homeostasis inside the cell (figure 2.2b). Thus, the Gibbs free energy of the anaerobic substrate-to-product conversion should be large enough to yield a positive net amount of ATP, including the ATP cost of product excretion. On the other hand, products that can diffuse through the cell membrane, such as alcohols, alkenes and other small molecules do not require energy for transport.

Applying thermodynamic pathway analysis in strain design

Recently, some stoichiometric models covering the full genome have been used to design microbial cell factories (Kim *et al.*, 2015; King *et al.*, 2015). In this case thermodynamic constraints have played an important role narrowing the amount of feasible pathways (Boghigian *et al.*, 2010; Campodonico *et al.*, 2014; Henry *et al.*, 2007; Shin *et al.*, 2013). Although this approach is extremely useful, the main limitations are the relatively little thermodynamic information available for most pathway intermediates and the amount of known biochemical pathways (Basler *et al.*, 2012; Shin *et al.*, 2013). In this sense, we strongly believe that before using such tools (or performing

any genetic modification), it is first necessary to do a basic feasibility study as proposed in this review and, if the feasibility study is not favorable for the combination substrate/product, other options must be considered such as using a different substrate or using an external electron acceptor; in case of a favorable assessment, then it is relevant to perform *in silico* studies to find the optimal pathway and later perform genetic modifications towards generating a functional anaerobic cell factory.

Concluding remarks

Albert Einstein wrote: "Thermodynamics is the only physical theory of universal content, (…) that will never be overthrown" (Einstein and Schilpp, 1949). In this review, it has been shown how thermodynamic analysis can be applied to study the feasibility of anaerobic product formation as a first step in microbial cell factory design. This is relevant to industry because anaerobic processes guarantee better economic and sustainability performance than widely used aerobic processes. The analysis suggested is easy to perform and is recommended before any detailed analysis using stoichiometric models. Furthermore, this analytical method makes use of the $-\Delta_e G$ concept, which allows a unique measure of substrate energy levels compared to product.

Thus, a first step towards a successful anaerobic metabolic engineering strategy is to a) find a feasible substrate/product couple, which generates enough Gibbs free energy, b) analyse $-\Delta_r G$ under desired full-scale process conditions, and check whether it is higher than the proposed minimum amount of Gibbs free energy needed to generate ATP or pmf. Finally, it is recommended to carry out a c) product excretion feasibility assessment using different assumptions on transport mechanisms in order to determine the optimal transporter and its energy demand for the product in question, this energy demand should be met by the Gibbs free energy of the substrate-to-product reaction.

Any bioprocess that fulfills these first three requirements is feasible under anaerobic conditions, and a microorganism that carries out the substrate-to-product reaction could be found in nature or designed using synthetic biology tools and stoichiometric models. If these

requirements are not fulfilled, a different substrate with higher energy values will be required, or an external electron acceptor, preferably O_2 should be used to achieve the required energy production. These early-stage calculations determine whether the desired anaerobic process is possible. Potential substrates and products and their $-\Delta_r G^{0'}$ values can be calculated (Figure I, in appendix 2.1).

Following this approach, 21 out of the 30 compounds listed in the DOE list (table 2.1) could be produced from glucose under anaerobic conditions (figure I in appendix 2.1). With the exception of carbon monoxide, the remaining compounds on the list (serine, arabinitol, furfural, xylitol, xylonic acid, glucaric acid, gluconic acid and sorbitol) could be produced under anaerobic conditions using alternative (non-conventional) substrates, such as H_2 or CO. Using the biochemical information available at the time, it was found that five out of the 30 compounds on the DOE list had the potential for anaerobic production from glucose (Werpy and Petersen, 2004). These were glycerol, lactic acid, propionic acid, acetoin and succinic acid. Our assessment using thermodynamic calculations indicates that, from a thermodynamic point of view, the majority of the products on this list can be obtained from anaerobic substrate-to-product conversions. Therefore, the take-home message is to start with a thermodynamics-based evaluation of the anaerobic substrate-to product-conversion, before performing stoichiometric calculations or using molecular biology tools. An important future challenge for synthetic biology will be to build pathways that can convert the Gibbs free energy available into biologically useful energy in the form of ATP or pmf.

Acknowledgements

We thank Leonor Guedes da Silva for her valuable help reviewing this manuscript. This project is funded by the BE-BASIC Foundation. The author HFCR thanks CONACyT for the support granted.

Table 2.2. Energy conservation of selected anaerobic microorganisms

Microorganism	Anaerobic reaction	$-\Delta_r G'$ (kJ/mol_P)	$-\Delta_r G$ (kJ/mol_P)	$-\Delta_p G$ (kJ/mol_P)	ATP prod. ($mol//mol_P$)	Energy conserved as ATP (kJ/mol)	TDF (kJ/mol)	Pathway length	%used as TDF	Ref.
S. cerevisiae[a]	0.5 Glucose → 1 Ethanol + 1 $CO_{2(g)}$	112.7	*ca.* 116.2	50	1 (SLP)	50	66.2	12	57%	(Canelas *et al.*, 2009; Canelas *et al.*, 2008; Madigan *et al.*, 2012)
Z. mobilis[b]	0.5 Glucose → 1 Ethanol + 1 $CO_{2(g)}$	112.7	*ca.* 116.2	46.2	0.5 (SLP)	23.1	93.1	13	80.10%	(Madigan *et al.*, 2012)
Lactococcus lactis	0.5 Glucose → 1 Lactate$^-$ + 1 H^+	97.9	85	46.2	1 (SLP)	46.2	38.8	11	45.60%	(Jin and Bethke, 2007; Madigan *et al.*, 2012)
Lactococcus lactis (GMO)[c]	0.5 Glucose + 1 NH_4^+ → 1 Alanine + 1 H^+ + 1 H_2O	107.8	*ca.* 99.3	46.2	1 (SLP)	46.2	53.1	11	53.50%	(Hols *et al.*, 1999; Madigan *et al.*, 2012)
Acetobacterium[d]	0.57 Glycerol + 0.29 $CO_{2(g)}$ → 1 Acetate$^-$ + 1 H^+ + 0.29 H_2O	85.3	*ca.* 81.9	46.2	1.14 (SLP)	52.8	29.1	N.A.	35.50%	(Madigan *et al.*, 2012)
Propionigenium modestum[e]	1 Succinate^{2-} + 1 H^+ → 1 Propionate$^-$ + 1 $CO_{2(g)}$	25.5	*ca.* 25.7	46.2	0.25 (ETC)	11.6	14.1	1	54.90%	(Madigan *et al.*, 2012)
Oxalobacter vibrioformis[f]	1 Oxalate$^-$ + 1 H^+ → 1 Formate$^-$ + 1 $CO_{2(g)}$	31.5	*ca.* 24.0	46.2	0.25 (ETC)	11.55	8.45	1	42%	(Madigan *et al.*, 2012)

Microorganism	Anaerobic reaction	$-\Delta_r G^{0'}$ (kJ/mol$_P$)	$-\Delta_r G$ (kJ/mol$_P$)	$-\Delta_r G$ (kJ/mol$_P$)	ATP prod. (mol//mol$_P$)	Energy conserved as ATP (kJ/mol)	TDF (kJ/mol)	Pathway length	%used as TDF	Ref.
Methanosaeta	1 Acetate$^-$ + 1 H^+ → 1 $CH_{4(g)}$ + 1 $CO_{2(g)}$	35.8	17	46.2	0.25 (ETC)	11.6	5.4	10	32%	(Jin, 2012)
Acetobacter woodii	$4H_{2(g)}$ + $2CO_{2(g)}$ → 1 Acetate$^-$ + 1 H^+ + 2 H_2O	95	40	46.2	0.125 (ETC)	23.1	16.9	10	42%	(Poehlein *et al.*, 2012)
Methanobacteriales, Methanococcales, Methanopyrales, Methanomicrobiales	$4H_{2(g)}$ + $CO_{2(g)}$ → 1 $CH_{4(g)}$ + 2 H_2O	131	40	46.2	0.125 (ETC)	23.1	16.9	7	42%	(Buckel and Thauer, 2013)
Syntrophomonas	0.5 Butyrate$^-$ + 0.5 H_2O → 1 Acetate$^-$ + 0.5 H^+ + 1 $H_{2(g)}$	-24.1	From 6.4 to 9	46.2	0.13 (ETC)	5.8	From 0.6 to 3.2	8	From 9% to 36%	(Jackson and McInerney, 2002; Madigan *et al.*, 2012)
Homoacetogenic bacteria[g] *e.g. Clostridium thermoaceticum*	0.33 Glucose → 1 Acetate$^-$ + 1 H^+	103.6	*ca.* 102.1	46.2	1.33(SLP)	61.6	40.5	21	39.70%	(Muller, 2003)
Clostridium carboxydovorans[h]	$3H_2O$ + $6CO_{(g)}$ → 1 Ethanol + 4 $CO_{2(g)}$	224.6	*ca.* 250.6	46.2	0.39 to 0.52	From 108.1 to 144.1	From 142.5 to 106.5	12	From 56.9% to 42.5%	(Perez *et al.*, 2013)

Microorganism	Anaerobic reaction	$-\Delta_r G'^{\circ}$ (kJ/mol$_{EP}$)	$-\Delta_r G$ (kJ/mol$_{EP}$)	$-\Delta_d G$ (kJ/mol$_{EP}$)	ATP prod. (mol/mol$_{EP}$)	Energy conserved as ATP (kJ/mol)	TDF (kJ/mol)	Pathway length	%used as TDF	Ref.
Clostridium kluyverii	5 Ethanol + 3 Acetate$^-$ → 4 Butyrate$^-$ + 3 H_2O + 1 H^+ + 2 $H_{2(g)}$	145	77	46.2	1 ATP per reaction	46.2	30.8	N.A.	40%	(Buckel and Thauer, 2013)

N.A. = Data not available

SLP = Substrate-level phosphorylation

ETC= Electron transport chain

[a] Calculated using unpublished experimental data from anaerobic glucose limited chemostat at D=0.1h^{-1}: $C_{glucose}$ = 6.55x10^{-4} mol/L, $C_{ethanol}$ = 0.247 mol/L, P_{CO2} = 0.0261 bar,.

[b] Calculated similarly to *S. cerevisiae*.

[c] Calculated using data from Hols *et al.* (1999) (99.5% conversion of 100 mmol/L glucose): $C_{glucose}$ = 5x10^{-4} mol/L, $C_{Alanine}$ = 0.199 mol/L, $C_{Ammonium}$ = 0.1 mol/L, pH = 7.5 (constant).

[d] Calculated using data from Emde and Schink (1987): $C_{glycerol}$ = 2x10^{-4} mol/L (lower limit presented by these authors), P_{CO2} = 0.2 bar, $C_{Acetate}$ = 0.016 mol/L, pH = 7.2 (constant).

[e] Calculated using data from Schink and Pfennig (1982): $C_{Succinate}$ = 5x10^{-3} mol/L (lower limit presented by these authors), P_{CO2} = 0.2 bar, $C_{Propionate}$ = 14.5x10^{-3} mol/L, pH = 7.2 (Initial, final pH not reported).

[f] Calculated using data from Dehning and Schink (1989) (95% conversion of 40 mmol/l Oxalate): $C_{Oxalate}$ = 2x10^{-3} mol/L, P_{CO2} = 0.1 bar, $C_{Propionate}$ = 38x10^{-3} mol/L, pH = 8 (Approx. final pH).

[g] Calculated using the following process conditions (Shah *et al.*, 1997) (end of batch phase): T = 60 ºC, $C_{acetate}$ = 0.525 mol/L, $C_{glucose}$= 0.026 mol/L, pH = 7.

[h] Calculated using the following process conditions (end of batch phase): T = 37 ºC, P_{CO} = 2 bar, P_{CO2} = 0.5 bar, $C_{ethanol}$ = 0.043 mol/L (2 g/L), pH (final) = 4.72 (Hurst and Lewis, 2010).

References

Alberty, R. A., 2003. Thermodynamics of Biochemical Reactions. Wiley-Interscience, Hoboken, New Jersey.

Alberty, R. A., Cornish-Bowden, A., Goldberg, R. N., Hammes, G. G., Tipton, K., Westerhoff, H. V., 2011. Recommendations for terminology and databases for biochemical thermodynamics. Biophys. Chem. 155**,** 89-103.

Bar-Even, A., Flamholz, A., Noor, E., Milo, R., 2012. Rethinking glycolysis: on the biochemical logic of metabolic pathways. Nat. Chem. Biol. 8**,** 509-17.

Basler, G., Grimbs, S., Nikoloski, Z., 2012. Optimizing metabolic pathways by screening for feasible synthetic reactions. BioSyst. 109**,** 186-91.

Boghigian, B. A., Shi, H., Lee, K., Pfeifer, B. A., 2010. Utilizing elementary mode analysis, pathway thermodynamics, and a genetic algorithm for metabolic flux determination and optimal metabolic network design. BMC Syst Biol. 4**,** 49.

Bozell, J. J., Petersen, G. R., 2010. Technology development for the production of biobased products from biorefinery carbohydrates—the US Department of Energy's "Top 10" revisited. Green Chemistry. 12**,** 539.

Buckel, W., Thauer, R. K., 2013. Energy conservation via electron bifurcating ferredoxin reduction and proton/Na(+) translocating ferredoxin oxidation. Biochim. Biophys. Acta. 1827**,** 94-113.

Campodonico, M. A., Andrews, B. A., Asenjo, J. A., Palsson, B. O., Feist, A. M., 2014. Generation of an atlas for commodity chemical production in *Escherichia coli* and a novel pathway prediction algorithm, GEM-Path. Metab. Eng. 25**,** 140-58.

Canelas, A. B., Ras, C., ten Pierick, A., van Gulik, W. M., Heijnen, J. J., 2011. An *in vivo* data-driven framework for classification and quantification of enzyme kinetics and determination of apparent thermodynamic data. Metab. Eng. 13**,** 294-306.

Canelas, A. B., ten Pierick, A., Ras, C., Seifar, R. M., van Dam, J. C., van Gulik, W. M., Heijnen, J. J., 2009. Quantitative evaluation of intracellular metabolite extraction techniques for yeast metabolomics. Anal. Chem. 81**,** 7379-89.

Canelas, A. B., van Gulik, W. M., Heijnen, J. J., 2008. Determination of the cytosolic free NAD/NADH ratio in *Saccharomyces*

cerevisiae under steady-state and highly dynamic conditions. Biotechnol. Bioeng. 100**,** 734-43.

Choi, S., Song, C. W., Shin, J. H., Lee, S. Y., 2015. Biorefineries for the production of top building block chemicals and their derivatives. Metab. Eng. 28**,** 223-39.

de Jong, E., Higson, A., Walsh, P., and Wellisch, M., Bio-based Chemicals. Value Added Products from Bioferineries. IEA Bioenergy, 2012.

de Kok, S., Kozak, B. U., Pronk, J. T., van Maris, A. J., 2012. Energy coupling in *Saccharomyces cerevisiae*: selected opportunities for metabolic engineering. FEMS Yeast Res. 12**,** 387-97.

de Kok, S., Yilmaz, D., Suir, E., Pronk, J. T., Daran, J. M., van Maris, A. J., 2011. Increasing free-energy (ATP) conservation in maltose-grown *Saccharomyces cerevisiae* by expression of a heterologous maltose phosphorylase. Metab. Eng. 13**,** 518-26.

Dehning, I., Schink, B., 1989. Two new species of anaerobic oxalate-fermenting bacteria, *Oxalobacter vibrioformis* sp. nov. and *Clostridium oxalicum* sp. nov., from sediment samples. Arch. Microbiol. 153**,** 79-84.

Dugar, D., Stephanopoulos, G., 2011. Relative potential of biosynthetic pathways for biofuels and bio-based products. Nat. Biotechnol. 29**,** 1074-8.

Einstein, A., Schilpp, P. A., 1949. Autobiographical notes. Open Court Publishing Company, Evanston, Ill.

Ekman, A., Wallberg, O., Joelsson, E., Börjesson, P., 2013. Possibilities for sustainable biorefineries based on agricultural residues – A case study of potential straw-based ethanol production in Sweden. Applied Energy. 102**,** 299-308.

Emde, R., Schink, B., 1987. Fermentation of Triacetin and Glycerol by *Acetobacterium* Sp - No Energy Is Conserved by Acetate Excretion. Arch. Microbiol. 149**,** 142-148.

Guadalupe-Medina, V., Wisselink, H. W., Luttik, M. A., de Hulster, E., Daran, J. M., Pronk, J. T., van Maris, A. J., 2013. Carbon dioxide fixation by Calvin-Cycle enzymes improves ethanol yield in yeast. Biotechnol Biofuels. 6**,** 125.

Hasegawa, S., Suda, M., Uematsu, K., Natsuma, Y., Hiraga, K., Jojima, T., Inui, M., Yukawa, H., 2013. Engineering of *Corynebacterium glutamicum* for high-yield L-valine production under oxygen deprivation conditions. Appl. Environ. Microbiol. 79**,** 1250-7.

Haynes, W. M., 2015. CRC Handbook of Chemistry and Physics. CRC Press/Taylor and Francis, Boca Raton, FL.

Heijnen, J. J., 1999. Bioenergetics of microbial growth. In: Flickinger, M. C., and Drew, S.W., (Ed.), Encyclopedia of bioprocess technology: Fermentation, biocatalysis, and bioseperation. John Wiley & Sons, pp. 267-291.

Heijnen, J. J., 2010. Impact of thermodynamic principles in systems biology. Advances in biochemical engineering/biotechnology. 121**,** 139-62.

Heijnen, J. J., Vanloosdrecht, M. C. M., Tijhuis, L., 1992. A Black-Box Mathematical-Model to Calculate Autotrophic and Heterotrophic Biomass Yields Based on Gibbs Energy-Dissipation. Biotechnology and Bioengineering. 40**,** 1139-1154.

Heijnen, S. J., 1994. Thermodynamics of Microbial-Growth and Its Implications for Process Design. Trends Biotechnol. 12**,** 483-492.

Henry, C. S., Broadbelt, L. J., Hatzimanikatis, V., 2007. Thermodynamics-based metabolic flux analysis. Biophys. J. 92**,** 1792-805.

Hols, P., Kleerebezem, M., Schanck, A. N., Ferain, T., Hugenholtz, J., Delcour, J., de Vos, W. M., 1999. Conversion of *Lactococcus lactis* from homolactic to homoalanine fermentation through metabolic engineering. Nat. Biotechnol. 17**,** 588-592.

Hu, P., Rismani-Yazdi, H., Stephanopoulos, G., 2013. Anaerobic CO2 fixation by the acetogenic bacterium *Moorella thermoacetica*. AICHE J. 59**,** 3176-3183.

Hurst, K. M., Lewis, R. S., 2010. Carbon monoxide partial pressure effects on the metabolic process of syngas fermentation. Biochem. Eng. J. 48**,** 159-165.

Jackson, B. E., McInerney, M. J., 2002. Anaerobic microbial metabolism can proceed close to thermodynamic limits. Nature. 415**,** 454-456.

Jin, Q., 2012. Energy conservation of anaerobic respiration. Am. J. Sci. 312**,** 573-628.

Jin, Q., Bethke, C. M., 2007. The thermodynamics and kinetics of microbial metabolism. Am. J. Sci. 307**,** 643-677.

Jol, S. J., Kummel, A., Hatzimanikatis, V., Beard, D. A., Heinemann, M., 2010. Thermodynamic calculations for biochemical transport and reaction processes in metabolic networks. Biophys. J. 99**,** 3139-44.

Kamm, B., 2014. Biorefineries – their scenarios and challenges. Pure Appl. Chem. 86.

Kamm, B., Kamm, M., Gruber, P. R., Kromus, S., 2005. Biorefinery Systems- An Overview. In: Kamm, B., Gruber, P. R., Kamm,

M., Eds.), Biorefineries- Industrial Processes and Products: Status Quo and Future Directions vol. 1. Wiley-VCH Verlag GmbH, Weinheim, Germany.

Kim, B., Kim, W. J., Kim, D. I., Lee, S. Y., 2015. Applications of genome-scale metabolic network model in metabolic engineering. J. Ind. Microbiol. Biotechnol. 42**,** 339-48.

King, Z. A., Feist, A. M., 2013. Optimizing Cofactor Specificity of Oxidoreductase Enzymes for the Generation of Microbial Production Strains—OptSwap. Industrial Biotechnology. 9**,** 236-246.

King, Z. A., Lloyd, C. J., Feist, A. M., Palsson, B. O., 2015. Next-generation genome-scale models for metabolic engineering. Curr. Opin. Biotechnol. 35C**,** 23-29.

Kleerebezem, R., Van Loosdrecht, M. C. M., 2010. A Generalized Method for Thermodynamic State Analysis of Environmental Systems. Critical Reviews in Environmental Science and Technology. 40**,** 1-54.

Kopke, M., Held, C., Hujer, S., Liesegang, H., Wiezer, A., Wollherr, A., Ehrenreich, A., Liebl, W., Gottschalk, G., Durre, P., 2010. *Clostridium ljungdahlii* represents a microbial production platform based on syngas. Proceedings of the National Academy of Sciences of the United States of America. 107**,** 13087-92.

Kozak, B. U., van Rossum, H. M., Benjamin, K. R., Wu, L., Daran, J. M., Pronk, J. T., van Maris, A. J., 2014. Replacement of the Saccharomyces cerevisiae acetyl-CoA synthetases by alternative pathways for cytosolic acetyl-CoA synthesis. Metab. Eng. 21**,** 46-59.

LaRowe, D. E., Dale, A. W., Amend, J. P., Van Cappellen, P., 2012. Thermodynamic limitations on microbially catalyzed reaction rates. Geochim. Cosmochim. Acta. 90**,** 96-109.

Liu, J. S., Vojinović, V., Patiño, R., Maskow, T., von Stockar, U., 2007. A comparison of various Gibbs energy dissipation correlations for predicting microbial growth yields. Thermochimica Acta. 458**,** 38-46.

Madigan, M. T., Martinko, J. M., Stahl, D. A., Clark, D. P., 2012. Catabolism of organic compounds. In: Madigan, M. T., Martinko, J. M., Stahl, D. A., Clark, D. P., Eds.), Brock: Biology of Microorganisms. Pearson, pp. 373 - 406.

Mavrovouniotis, M. L., 1990. Group contributions for estimating standard gibbs energies of formation of biochemical

compounds in aqueous solution. Biotechnol. Bioeng. 36**,** 1070-82.

McCarty, P. L., 2007. Thermodynamic electron equivalents model for bacterial yield prediction: modifications and comparative evaluations. Biotechnol. Bioeng. 97**,** 377-88.

Mohammadi, M., Younesi, H., Najafpour, G., Mohamed, A. R., 2012. Sustainable ethanol fermentation from synthesis gas by *Clostridium ljungdahlii* in a continuous stirred tank bioreactor. Journal of Chemical Technology & Biotechnology. 87**,** 837-843.

Muller, V., 2003. Energy Conservation in Acetogenic Bacteria. Appl. Environ. Microbiol. 69**,** 6345-6353.

Nielsen, J., Larsson, C., van Maris, A., Pronk, J., 2013. Metabolic engineering of yeast for production of fuels and chemicals. Curr. Opin. Biotechnol. 24**,** 398-404.

Noor, E., Bar-Even, A., Flamholz, A., Lubling, Y., Davidi, D., Milo, R., 2012. An integrated open framework for thermodynamics of reactions that combines accuracy and coverage. Bioinformatics. 28**,** 2037-2044.

Noor, E., Haraldsdottir, H. S., Milo, R., Fleming, R. M., 2013. Consistent estimation of Gibbs energy using component contributions. PLoS Comput Biol. 9**,** e1003098.

Oldiges, M., Eikmanns, B. J., Blombach, B., 2014. Application of metabolic engineering for the biotechnological production of L-valine. Appl. Microbiol. Biotechnol. 98**,** 5859-70.

Perez, J. M., Richter, H., Loftus, S. E., Angenent, L. T., 2013. Biocatalytic reduction of short-chain carboxylic acids into their corresponding alcohols with syngas fermentation. Biotechnology and Bioengineering. 110**,** 1066-1077.

Poehlein, A., Schmidt, S., Kaster, A. K., Goenrich, M., Vollmers, J., Thurmer, A., Bertsch, J., Schuchmann, K., Voigt, B., Hecker, M., Daniel, R., Thauer, R. K., Gottschalk, G., Muller, V., 2012. An ancient pathway combining carbon dioxide fixation with the generation and utilization of a sodium ion gradient for ATP synthesis. PloS one. 7**,** e33439.

Porro, D., Branduardi, P., Sauer, M., Mattanovich, D., 2014. Old obstacles and new horizons for microbial chemical production. Curr. Opin. Biotechnol. 30**,** 101-6.

Rabinovitch-Deere, C. A., Oliver, J. W., Rodriguez, G. M., Atsumi, S., 2013. Synthetic biology and metabolic engineering approaches to produce biofuels. Chem. Rev. 113**,** 4611-32.

Richter, K., Gescher, J., 2014. Accelerated glycerol fermentation in *Escherichia coli* using methanogenic formate consumption. Bioresour. Technol. 162**,** 389-91.

Ruhrmann, J., Sprenger, G. A., Kramer, R., 1994. Mechanism of alanine excretion in recombinant strains of *Zymomonas mobilis*. Biochim. Biophys. Acta. 1196**,** 14-20.

Schink, B., Pfennig, N., 1982. *Propionigenium modestum* gen. nov. sp. nov. a new strictly anaerobic, nonsporing bacterium growing on succinate. Arch. Microbiol. 133**,** 209-216.

Schoepp-Cothenet, B., van Lis, R., Atteia, A., Baymann, F., Capowiez, L., Ducluzeau, A. L., Duval, S., ten Brink, F., Russell, M. J., Nitschke, W., 2013. On the universal core of bioenergetics. Biochim. Biophys. Acta. 1827**,** 79-93.

Shah, M. M., Akanbi, F., Cheryan, M., 1997. Potassium acetate by fermentation with *Clostridium thermoaceticum*. Appl. Biochem. Biotechnol. 63-65**,** 423-33.

Shen, C. R., Lan, E. I., Dekishima, Y., Baez, A., Cho, K. M., Liao, J. C., 2011. Driving forces enable high-titer anaerobic 1-butanol synthesis in *Escherichia coli*. Appl. Environ. Microbiol. 77**,** 2905-15.

Shin, J. H., Kim, H. U., Kim, D. I., Lee, S. Y., 2013. Production of bulk chemicals via novel metabolic pathways in microorganisms. Biotechnol. Adv. 31**,** 925-35.

Straathof, A. J., 2014. Transformation of biomass into commodity chemicals using enzymes or cells. Chem. Rev. 114**,** 1871-908.

Taymaz-Nikerel, H., Jamalzadeh, E., Espah Borujeni, A., Verheijen, P. J. T., van Gulik, W. M., Heijnen, J. J., 2013. A Thermodynamic Analysis of Dicarboxylic Acid Production in Microorganisms. In: von Stockar, U., van der Wielen, L. A. M., Prausnitz, J. M., Eds.), Thermodynamics in Biochemical Engineering.

Thakker, C., Martinez, I., San, K. Y., Bennett, G. N., 2012. Succinate production in *Escherichia coli*. Biotechnology journal. 7**,** 213-24.

Thauer, R. K., Jungermann, K., Decker, K., 1977. Energy conservation in chemotrophic anaerobic bacteria. Bacteriol Rev. 41**,** 100-80.

Tikhonov, A. N., 2012. Energetic and regulatory role of proton potential in chloroplasts. Biochemistry (Mosc). 77**,** 956-74.

Tran, Q. H., Unden, G., 1998. Changes in the proton potential and the cellular energetics of *Escherichia coli* during growth by

aerobic and anaerobic respiration or by fermentation. Eur. J. Biochem. 251, 538-543.

Uhlenbusch, I., Sahm, H., Sprenger, G. A., 1991. Expression of an L-alanine dehydrogenase gene in *Zymomonas mobilis* and excretion of L-alanine. Appl. Environ. Microbiol. 57, 1360-6.

van Maris, A. J., Konings, W. N., van Dijken, J. P., Pronk, J. T., 2004a. Microbial export of lactic and 3-hydroxypropanoic acid: implications for industrial fermentation processes. Metab. Eng. 6, 245-55.

van Maris, A. J. A., Winkler, A. A., Porro, D., van Dijken, J. P., Pronk, J. T., 2004b. Homofermentative Lactate Production Cannot Sustain Anaerobic Growth of Engineered *Saccharomyces cerevisiae*: Possible Consequence of Energy-Dependent Lactate Export. Appl. Environ. Microbiol. 70, 2898-2905.

Viikari, L., Vehmaanperä, J., Koivula, A., 2012. Lignocellulosic ethanol: From science to industry. Biomass Bioenergy. 46, 13-24.

von Stockar, U., 2010. Biothermodynamics of live cells: a tool for biotechnology and biochemical engineering. J. Non-Equilib. Thermodyn. 35.

von Stockar, U., 2014. Optimal energy dissipation in growing microorganisms and rectification columns. J. Non-Equilib. Thermodyn. 39.

von Stockar, U., Maskow, T., Liu, J., Marison, I. W., Patino, R., 2006. Thermodynamics of microbial growth and metabolism: an analysis of the current situation. J. Biotechnol. 121, 517-33.

Werpy, T., Petersen, G., Top Value Added Chemicals From Biomass. Vol. I: Results of screening for potential candidates from sugars and synthesis gas. National Renewable Energy Laboratory, 2004.

Yazdani, S. S., Gonzalez, R., 2007. Anaerobic fermentation of glycerol: a path to economic viability for the biofuels industry. Curr. Opin. Biotechnol. 18, 213-9.

Zelle, R. M., Trueheart, J., Harrison, J. C., Pronk, J. T., van Maris, A. J., 2010. Phosphoenolpyruvate carboxykinase as the sole anaplerotic enzyme in *Saccharomyces cerevisiae*. Appl. Environ. Microbiol. 76, 5383-9.

Zhang, J., Babtie, A., Stephanopoulos, G., 2012. Metabolic engineering: enabling technology of a bio-based economy. Current Opinion in Chemical Engineering. 1, 355-362.

Zhang, X., Jantama, K., Moore, J. C., Shanmugam, K. T., Ingram, L. O., 2007. Production of L -alanine by metabolically engineered *Escherichia coli*. Appl. Microbiol. Biotechnol. 77**,** 355-66.

Appendix 2.1. Effect of concentrations and assessment of transport mechanisms

$-\Delta_r G^{0'}$ can be estimated using the $\Delta_e G$ concept, as explained before, for different substrate-product couples (figure I). L-alanine production from glucose will be used as example. The so-called homoalanine fermentation has been well documented by different authors (Hols *et al.*, 1999; King and Feist, 2013; Ruhrmann *et al.*, 1994; Uhlenbusch *et al.*, 1991; Zhang *et al.*, 2007). When glucose is used as substrate under anaerobic conditions the overall reaction is:

$$0.5\times Glc_{(aq)} + NH^{+}_{4(aq)} \longrightarrow Alanine_{(aq)} + H^{+}_{(aq)} + H_2O_{(l)}$$

$$-\Delta_r G^{0'} = 106.83 \pm 3.23 \frac{kJ}{mol_P} \qquad \text{(A2.1.1)}$$

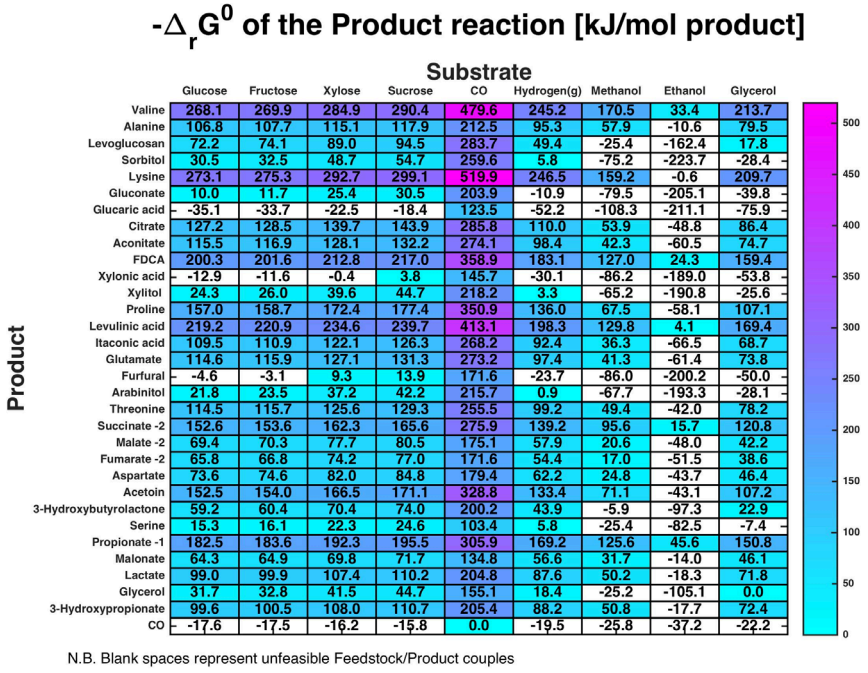

Appendix 2.1 figure I. $-\Delta_r G^{0'}$ in kJ/mol of product for each substrate/product pair, the color code is based on the $-\Delta_r G^{0'}$ value for each compound as shown in the scale at the right hand side of the figure. White squares indicate unfeasible substrate-product couples ($-\Delta_r G^{0'}<0$).

$-\Delta_rG$ at process conditions could be estimated assuming high product and low substrate concentration (Figure II). At these process conditions, $-\Delta_rG$ is higher than the minimum amount of free energy required for pmf production, and close to the thermodynamic limits proposed for ATP production using substrate-level phosphorylation, even at product concentrations of 1 mol/L. This indicates that anaerobic alanine production from glucose is feasible and high titers of L-alanine can be achieved under the correct process conditions, i.e. excess of ammonium.

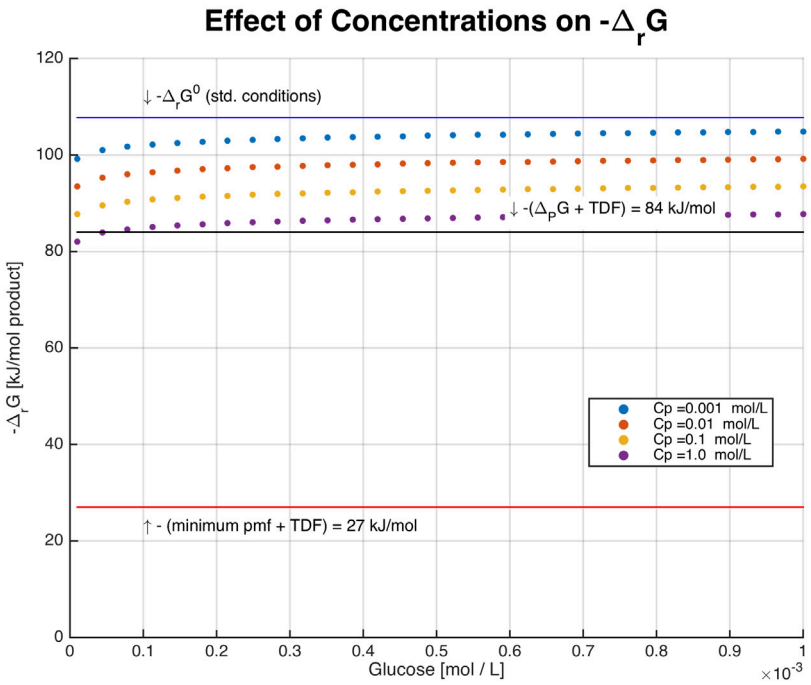

Appendix 2.1 figure II. Effect of product (L-alanine) and substrate (Glucose) concentrations on $-\Delta_rG$ for L-alanine production. In this sensitivity analysis, a product concentration between 10^{-3} mol/L (0.09 g/L) and 1 mol/L (89 g/L) is assumed. Glucose concentration (C_S) varies between 10^{-5} mol/L and 10^{-3} mol/L, temperature (T) of 298.15 K (25 °C), pH of 7 and ammonium concentration (C_{NH4+}) of 10^{-2} mol/L.

L-alanine has zero net charge between pH 3 and 9. Different studies (Ruhrmann *et al.*, 1994; Uhlenbusch *et al.*, 1991) point at diffusion or facilitated transport (of the neutral species) as the most likely

mechanisms for L-alanine excretion in a recombinant strain of *Zymomonas mobilis* growing under anaerobic conditions. Ruhrmann *et al.* (1994) reports intra- and extracellular concentrations of 200 $mmol/L_{Intracellular}$ and 6 $mmol/L_{Extracellular}$, respectively, which indeed suggests that diffusion or facilitated passive transport are the mechanisms for L-alanine excretion in this strain. The Gibbs free energy of these mechanisms can be expressed as (A2.1.2).

$$-\Delta_r G = -\Delta_f G^{0'}_{Alanine,out} + \Delta_f G^{0'}_{Alanine,in} + R \times T \times \ln\left(\frac{C_{Alanine,out}}{C_{Alanine,in}}\right) \quad \text{(A2.1.2)}$$

It is clear that the ratio out/in for alanine at equilibrium is one; which means that L-alanine in the extracellular space must be equal or lower than in the intracellular space. Although the transport mechanism is efficient in terms of ATP costs as no ATP is required for L-alanine excretion. Transport of L-alanine through a uniport/diffusion mechanism might lead to problematic situations under process conditions, i.e. product concentration of 1 $mol/L_{extracellular}$. At equilibrium, the intracellular concentration will be 1 $mol/L_{Intracellular}$ or higher. Assuming an intracellular volume of 2 $mL_{Intracellular}/g_{CellDryWeight}$, 2000 $\mu mol/g_{CellDryWeight}$ (or higher) are expected. A huge amount given the fact that intracellular metabolites range typically between 0.1 and 100 $\mu mol/g_{CellDryWeight}$ (Heijnen, 2010). Therefore, product export under process conditions will require an active transporter, e.g. ABC transport or proton antiport.

Appendix 2.2. Effect of temperature, dissociation and change of phase

a) Effect of temperature

The Production of fumarate, using methanol and CO_2 as substrates (A2.2.1), is an example of a reaction with a gaseous substrate.

$$2\times \text{Methanol}_{(aq)} + CO_{2(g)} \longrightarrow \text{Fumarate}^{-2}_{(aq)} + 2\times H^{+}_{(aq)} + 2\times H_2O_{(l)}$$

$$-\Delta_r G^{0'} = 17.19 \pm 3.44 \frac{kJ}{mol_P}$$

$$-\Delta_r H^{0'} = 68.80 \frac{kJ}{mol_P} \qquad \text{(A2.2.1)}$$

$$-\Delta_r S = 0.17 \frac{kJ}{mol_P \times K}$$

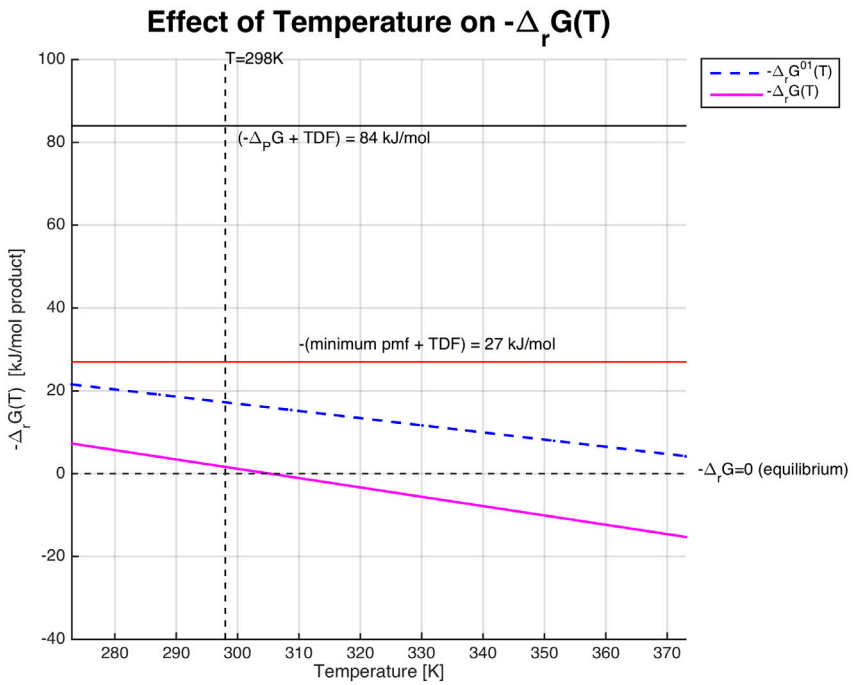

Appendix 2.2 figure I. Effect of T on $\Delta_r G$ for fumarate production using methanol as substrate. Dashed line (blue) represents values calculated considering standard conditions ($\Delta_r G^{0'}$); solid line (magenta) represents values calculated considering process conditions. In both cases, $-\Delta_r G$ decreases with temperature.

Assuming the following process conditions: methanol concentration of 10^{-2} mol/L (0.3 g/L), total fumarate concentration of 0.054 mol/L, temperature (T) between 0 ºC (273.15 K) and 100 ºC (373.15 K), pH of 7 and a CO_2 partial pressure of 1 bar, it can be observed that $-\Delta_r G$ is far below the energy requirements for ATP production at all temperatures (figure I). In this particular process, increasing T does not lead to a case in which the product-reaction is favorable ($-\Delta_r G > 0$); in addition decreasing pH to favor crystallization of fumaric acid (the solubility of the undissociated species is 0.054 mol/L at 25 ºC) will make the process even less favorable, similarly to the case of fumarate production from glucose (Taymaz-Nikerel *et al.*, 2013).

b) Effect of dissociation and change of phase

For the case of dissociation and change of phase, consider the production of L-valine$_{(aq)}$ (A2.2.2).

$$\mathrm{Glc_{(aq)} + NH^{+}_{4(aq)} \longrightarrow Valine^{0}_{(aq)} + CO_{2(g)} + 2 \times H_2O_{(l)} + H^{+}_{(aq)}}$$
$$-\Delta_r G^{0'} = 268.19 \pm 5.47 \frac{\mathrm{kJ}}{\mathrm{mol_P}} \qquad \text{(A2.2.2)}$$

L-valine has three dissociated species and low solubility. The equations for dissociation and change of phase are (A2.2.3), (A2.2.4) and (A2.2.5)

$$\mathrm{Val^{+1}_{(aq)} \xrightarrow{pK_{a1}=2.72} Val^{0}_{(aq)} + H^{+}} \qquad \text{(A2.2.3)}$$

$$\mathrm{Val^{0}_{(aq)} \xrightarrow{pK_{a2}=9.60} Val^{-1}_{(aq)} + H^{+}} \qquad \text{(A2.2.4)}$$

$$\mathrm{Val^{0}_{(aq)} \xrightarrow{K_{eq}=\frac{1}{C^{*}_{Val^{0}_{(aq)}}}=2.0161} Val_{(S)}} \qquad \text{(A2.2.5)}$$

$C^*_{Val^o(aq)}$ is the maximum solubility of L-valine (neutral species), which is 0.496 mol/L at 25 ºC (~58 g/L). The total concentration of L-valine when $C_{Val^o(aq)} < C^*_{Val^o(aq)}$ is calculated as shown in (A2.2.6).

$$C^{Total}_{Val} = C_{Val^{+1}(aq)} + C_{Val^{0}(aq)} + C_{Val^{-1}(aq)} \qquad \text{(A2.2.6)}$$

Whereas, when $C_{Val^o(aq)} \geq C^*_{Val^o(aq)}$ the total L-valine is calculated as (A2.2.7).

$$C^{Total}_{Val} = C_{Val^{+1}(aq)} + C^{*}_{Val^{0}(aq)} + C_{Val^{-1}(aq)} + C_{Val(S)} \qquad \text{(A2.2.7)}$$

Using these equations, it is possible to calculate the dissociation and crystallisation profile of L-valine (figure II).

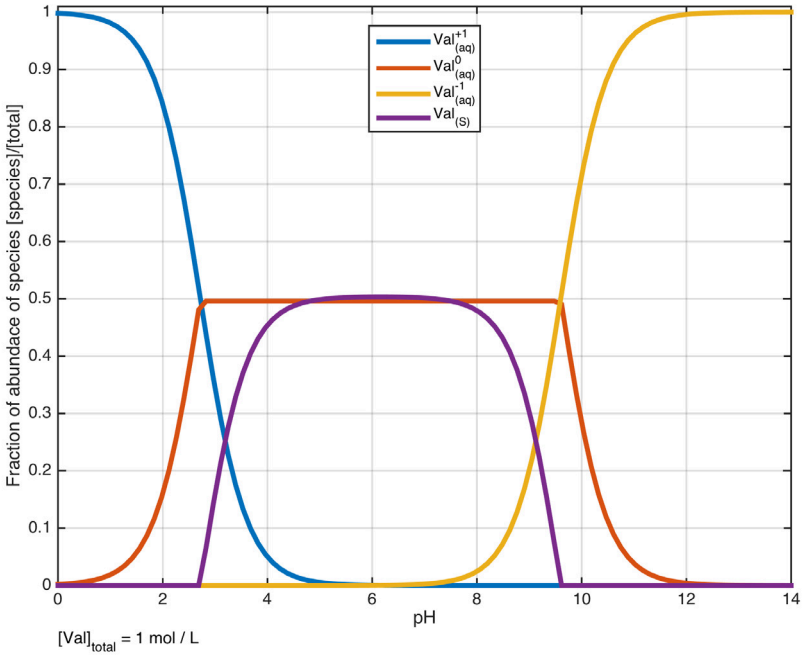

Appendix 2.2 figure II. Dissociation and crystallization profile of L-valine as function of pH. A total concentration of 1 mol L-valine/L is assumed.

The Gibbs free energy of the dissociated species and solid phase can be estimated as described in (Taymaz-Nikerel *et al.*, 2013). For example, $\Delta_f G^0$ for the solid phase can be estimated using (A2.2.8). $\Delta_f G^0$ values of all L-valine species were calculated for this example (table I).

$$\Delta_f G^0_{Valine_{(S)}} = \Delta_f G^0_{Valine^0_{(aq)}} - R \times T \times \ln\left(C^*_{Valine^0_{(aq)}}\right) \qquad \text{(A2.2.8)}$$

The product reaction expressed in terms of all the dissociated species becomes (A2.2.9).

$$\begin{aligned} Glc_{(aq)} + \chi_{NH^+_{4(aq)}} \times NH^+_{4(aq)} + \chi_{NH_{3(aq)}} \times NH_{3(aq)} \longrightarrow \chi_{Val^{-1}_{(aq)}} \times Val^{-1}_{(aq)} \\ + \chi_{Val^0_{(aq)}} \times Val^0_{(aq)} + \chi_{Val^{+1}_{(aq)}} \times Val^{+1}_{(aq)} + \chi_{Val_{(S)}} \times Val_{(S)} \\ + CO_{2(g)} + 2 \times H_2O_{(l)} + \upsilon_{H^+_{(aq)}} \times H^+_{(aq)} \end{aligned} \qquad \text{(A2.2.9)}$$

Appendix 2.2 Table I. $\Delta_f G^0$ of the compounds involved in L-valine production

Compound	$\Delta_f G^0$ (kJ / mol)
$Glucose_{(aq)}$	-917.33
Ammonium ($NH_4^+{}_{(aq)}$)	-80.43
Ammonia ($NH_{3(aq)}$)	-26.94
$Valine^{-1}{}_{(aq)}$	-300.62
$Valine^{0}{}_{(aq)}$	-356.20
$Valine^{+1}{}_{(aq)}$	-371.92
$Valine_{(S)}$	-357.97
$CO_{2(g)}$	-394.36
H_2O	-237.70
$H^+{}_{(aq)}$	0.0

And the stoichiometric coefficient of hydrogen ions and reaction quotient are calculated using (A2.2.10) and (A2.2.11).

$$\upsilon_{H^+_{(aq)}} = \chi_{NH^+_{4(aq)}} + \chi_{Val^{-1}_{(aq)}} - \chi_{Val^{+1}_{(aq)}} \quad \text{(A2.2.10)}$$

$$Q_r(pH) = \frac{\left(C_{Val^{+1}(aq)}\right)^{\chi_{Val^{+1}(aq)}} \times \left(C_{Val^{0}(aq)}\right)^{\chi_{Val^{0}(aq)}} \times \left(C_{Val^{-1}(aq)}\right)^{\chi_{Val^{-1}(aq)}} \times \left(P_{CO_{2(g)}}\right) \times \left(10^{-pH}\right)^{\upsilon_{H^+_{(aq)}}}}{\left(C_{Glc(aq)}\right) \times \left(C_{NH^+_4(aq)}\right)^{\chi_{NH^+_{4(aq)}}} \times \left(C_{NH_3(aq)}\right)^{\chi_{NH_{3(aq)}}}} \quad \text{(A2.2.11)}$$

For the pair glucose/L-valine, both dissociation and crystallisation have a positive impact on the Gibbs free energy available for the substrate-to-product conversion (Figure III). Recent efforts on L-valine production under anaerobic conditions can be found in the following references: (Hasegawa *et al.*, 2013; Oldiges *et al.*, 2014).

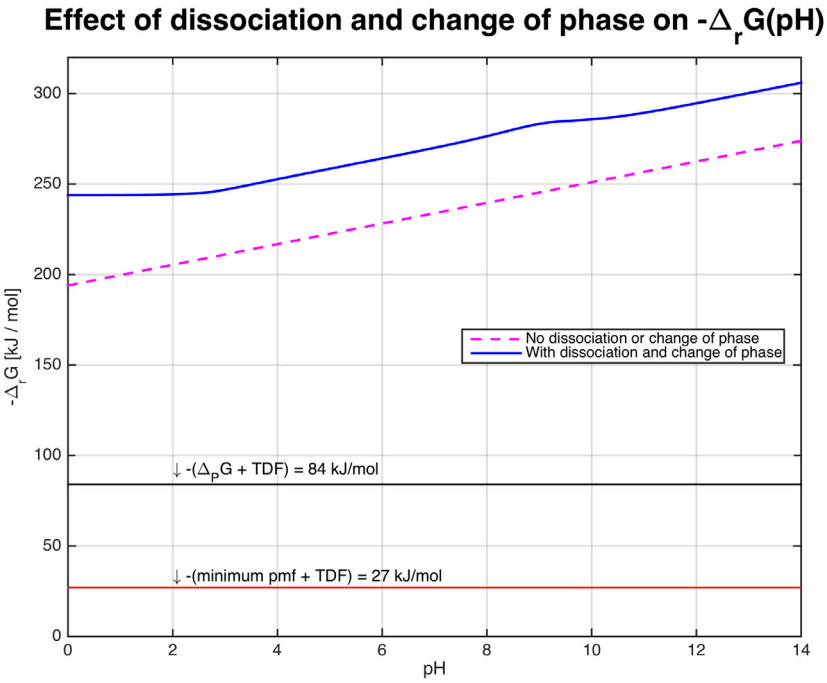

Appendix 2.2 figure III. Change in $-\Delta_r G$ with respect to pH, process conditions of T=298.15 K, $C_S=10^{-3}$ mol/L, $C_{NH4+}=10^{-3}$ mol/L, P_{CO2} = 1 bar and $C_{ValTotal}$ = 1 mol/L were assumed. Dashed line (magenta) represents values calculated without taking into account the dissociation and crystallization of L-Valine; solid line (blue) represents values calculated when both phenomena are considered. The difference is highest at low pH (high concentration of +1 species); at pH values between 3 and 8 there is a significant amount of product in the solid phase, creating a large chemical driving force for the reaction. On the other hand, at high pH the difference between NH_3 and ammonium ions as substrate becomes apparent.

Supplementary table S2.1. Standard Thermodynamic properties of various substrates and products

Compound	C	H	O	N	+/-	S	Fe	$\Delta_f G'^0$ [kJ/mol]	$\Delta_f H'^0$ [kJ/mol]	$\Delta S'^0$ [kJ/mol/K]	Solubility [M]	Phase	Ref
Glucose*	6	12	6	0	0	0	0	-917.3 ± 2.2	-1264.20	-1.16E+00	2.66E+00	aq	[1,2,8,13]
Fructose	6	12	6	0	0	0	0	-915.51	-1259.38	-1.15E+00	5.55E+00	aq	[1]
Xylose	5	10	5	0	0	0	0	-750.49	-1045.74	-9.90E-01	2.88E+00	aq	[1]
Sucrose	12	22	11	0	0	0	0	-1552.4	-2217.3	-2.23E+00	6.19E+00	aq	[2]
CO	1	0	1	0	0	0	0	-137.17	-110.53	8.94E-02	9.85E-04	g	[3]
Stearic	18	36	2	0	0	0	0	-282.5	-887.64	-2.03E+00	1.06E-04	l	[4,5]
Oleic	18	34	2	0	0	0	0	-201.8	-748.52	-1.83E+00	1.76E-04	l	[4,5]
Linoleic acid	18	32	2	0	0	0	0	-120.8	-674.04	-1.86E+00	1.43E-07	l	[4,6]
n-alkane	15	32	0	0	0	0	0	60	-439	-1.67E+00	1.35E-08	aq	[7]
Methanol	1	4	1	0	0	0	0	-175.39	-245.93	-2.37E-01	N.A.	aq	[2]
Ethanol	2	6	1	0	0	0	0	-181.6	-288.3	-3.58E-01	N.A.	aq	[2]
Glycerol	3	8	3	0	0	0	0	-488.5	-676	-6.29E-01	N.A.	aq	[2]
Acetate	2	3	2	0	-1	0	0	-369.4	-485.8	-3.90E-01	N.A.	aq	[2]
2-HB	4	7	3	0	-1	0	0	-506.3	N.A.	N.A.	4.65E+00	aq	[2]
Methane	1	4	0	0	0	0	0	-50.75	-74.81	-8.07E-02	1.25E-04	g	[2]
Fumarate^{-2}*	4	2	4	0	-2	0	0	-601.5 ± 3.0	-777.00	-5.80E-01	5.43E-02	aq	[2,8,13]
Malate^{-2}*	4	4	5	0	-2	0	0	-842.7 ± 2.3	-843.00	6.71E-03	4.16E+00	aq	[2,8,13]
Succinate^{-2}*	4	4	4	0	-2	0	0	-686.3 ± 6.9	-909.00	-7.34E-01	4.91E-01	aq	[2,8,13]
Propionate^{-1}*	3	5	2	0	-1	0	0	-361.7 ± 1.1	-510.74	-5.02E-01	5.00E+00	aq	[2,8,13]

Compound	C	H	O	N	+/-	S	Fe	$\Delta_f G^{0'}$ [kJ/mol]	$\Delta_f H^{0'}$ [kJ/mol]	$\Delta S^{0'}$ [kJ/mol/K]	Solubility [M]	Phase	Ref
Ethylene	2	4	0	0	0	0	0	68.358	52.4	-5.35E-02	4.80E-03	g	[3]
Alanine *	3	7	2	1	0	0	0	-368.3 ± 2.2	-563.58	-6.50E-01	1.86E+00	aq	[8,13]
Valine *	5	11	2	1	0	0	0	-356.2 ± 4.3	-611.99	-8.75E-01	4.96E-01	aq	[4,9,8,13]
Lysine *	6	15	2	2	1	0	0	-356.9 ± 1.5	N.A.	N.A.	N.A.	aq	[4,10,8,13]
Glutamate	5	8	4	1	-1	0	0	-643.9	-940.3	-9.94E-01	5.87E-02	aq	[2]
Tryptophan	11	12	2	2	0	0	0	-119.244	-415.05	-9.92E-01	6.66E-02	aq	[9]
Threonine	4	9	3	1	0	0	0	-528.9	-807.09	-9.33E-01	8.14E-01	aq	[4,9]
Methionine	5	11	2	1	0	1	0	-320.4	-758.14	-1.47E+00	3.77E-01	aq	[4,9]
Tyrosine	9	11	3	1	0	0	0	-370.7	-671.53	-1.01E+00	2.51E-03	aq	[4,9]
Cysteine	3	7	2	1	0	1	0	-343.9	-530.11	-6.25E-01	4.57E-04	aq	[4,9]
Lactate	3	5	3	0	-1	0	0	-517.81	-687	-5.67E-01	N.A.	aq	[2]
n-Butanol	4	10	1	0	0	0	0	-171.8	-327.4	-5.22E-01	9.85E-01	aq	[3,4]
Butanol	4	10	1	0	0	0	0	-162.5	-327.3	-5.53E-01	9.85E-01	l	[3]
Acetone	3	6	1	0	0	0	0	-159.7	-248.4	-2.98E-01	N.A.	aq	[3,4]
Farnesene	15	24	0	0	0	0	0	372	46.36	-1.09E+00	5.15E-08	l	[3,4]
Isoprene	5	8	0	0	0	0	0	159.7	75.5	-2.82E-01	1.30E-02	g	[2,3]
Ethylene glycol	2	6	2	0	0	0	0	-330.5	-460	-4.34E-01	N.A.	aq	[2,3]
Butanediol	4	10	2	0	0	0	0	-322	-523.6	-6.76E-01	N.A.	aq	[2]
n-propanol	3	8	1	0	0	0	0	-175.81	-331	-5.21E-01	3.08E+00	aq	[2]

Compound	C	H	O	N	+/-	S	Fe	$\Delta_f G^{0'}$ [kJ/mol]	$\Delta_f H^{0'}$ [kJ/mol]	$\Delta S^{0'}$ [kJ/mol/K]	Solubility [M]	Phase	Ref
2-propanol	3	8	1	0	0	0	0	-185.23	-330.83	-4.88E-01	2.28E+00	aq	[2]
propene	3	6	0	0	0	0	0	67.2	20	-1.58E-01	4.80E-03	g	[3,4]
Benzyl-penicillin	16	18	4	2	0	1	0	-338.9	-395.5	-1.90E-01	2.99E-01	aq	[2,11]
Itaconic acid*	5	6	4	0	0	0	0	-638.2 ± 1.4	N.A.	N.A.	6.41E-01	aq	[4,13]
Aspartate	4	6	4	1	-1	0	0	-689.7	-973.2	-9.51E-01	3.38E-02	aq	[4,9]
Caprolactam	6	11	1	1	0	0	0	-88.9	-329.4	-8.07E-01	4.03E+01	aq	[3,4]
Citrate	6	5	7	0	-3	0	0	-1168.3	-1515	-1.16E+00	3.80E+00	aq	[2]
Mevalonate	6	11	4	0	-1	0	0	-657.3	N.A.	N.A.	N.A.	c	[4]
FDCA	6	4	5	0	0	0	0	-885.6	-869.9	5.27E-02	N.A.	c	[12]
Diamino-butane	4	14	0	2	2	0	0	-36.2	N.A.	N.A.	N.A.	aq	[4]
Diamino-pentane	5	16	0	2	2	0	0	-29.6	N.A.	N.A.	N.A.	aq	[4]
Butadiene	4	6	0	0	0	0	0	160.6	110	-1.70E-01	1.36E-02	g	[3]
1,3 propanediol	3	8	2	0	0	0	0	-325.1	-480.8	-5.22E-01	N.A.	l	[3]
3-Hydroxy-propionate	3	5	3	0	-1	0	0	-518.4	N.A.	N.A.	N.A.	aq	[2]
Malonate *	3	2	4	0	-2	0	0	-684.7 ± 0.4	N.A.	N.A.	N.A.	aq	[4,13]
Serine *	3	7	3	1	0	0	0	-516.5 ± 7.9	N.A.	N.A.	N.A.	aq	[8,13]

Compound	C	H	O	N	+/-	S	Fe	$\Delta_f G^{0'}$ [kJ/mol]	$\Delta_f H^{0'}$ [kJ/mol]	$\Delta S^{0'}$ [kJ/mol/K]	Solubility [M]	Phase	Ref
Acetoin *	4	8	2	0	0	0	0	-284.9 ± 6.9	N.A.	N.A.	N.A.	aq	[2,13]
Arabinitol *	5	12	5	0	0	0	0	-784.4±11.8	N.A.	N.A.	N.A.	aq	[4,13]
Furfural *	5	4	2	0	0	0	0	-46.7 ± 4.5	N.A.	N.A.	N.A.	aq	[4,13]
Proline	5	9	2	1	0	0	0	-247	N.A.	N.A.	N.A.	aq	[4]
Xylitol *	5	12	5	0	0	0	0	-786.8 ± 5.1	N.A.	N.A.	N.A.	aq	[4,13,14]
Xylonic acid *	5	10	6	0	0	0	0	-991.1 ± 0.7	N.A.	N.A.	N.A.	aq	[4,13]
Aconitate *	6	3	6	0	-3	0	0	-919.0 ± 4.0	N.A.	N.A.	N.A.	aq	[4,8,13]
Glucaric acid*	6	9	8	0	-1	0	0	-1323.5±3.3	N.A.	N.A.	N.A.	aq	[8,13]
Gluconate *	6	11	7	0	-1	0	0	-1127.1±1.7	N.A.	N.A.	N.A.	aq	[8,13]
Sorbitol *	6	14	6	0	0	0	0	-946.0 ± 0.6	N.A.	N.A.	N.A.	aq	[8,13]
Levoglucosan	6	10	5	0	0	0	0	-751.86	N.A.	N.A.	N.A.	aq	C.G.C.
3-Hydroxy-butyrolactone	4	6	3	0	0	0	0	-433.044	N.A.	N.A.	N.A.	aq	C.G.C.
Levulinic acid	5	7	3	0	-1	0	0	-466.516	N.A.	N.A.	N.A.	aq	C.G.C.
Hydrogen (g)	0	2	0	0	0	0	0	0	0	0.00E+00	7.80E-04	g	[2]
Oxygen	0	0	2	0	0	0	0	0	0	0.00E+00	1.30E-03	g	[2]
Nitrate $^{-1}$	0	0	3	1	-1	0	0	-111.34	-173	-2.07E-01	N.A.	aq	[2]
Nitrite $^{-1}$	0	0	2	1	-1	0	0	-32.2	-107	-2.51E-01	N.A.	aq	[2]

Compound	C	H	O	N	+/-	S	Fe	$\Delta_f G^{0'}$ [kJ/mol]	$\Delta_f H^{0'}$ [kJ/mol]	$\Delta S^{0'}$ [kJ/mol/K]	Solubility [M]	Phase	Ref
CO	1	0	1	0	0	0	0	-119.9	-120.96	-3.56E-03	9.85E-04	aq	[2]
Hydrogen (aq)	0	2	0	0	0	0	0	17.6	-4.2	-7.31E-02	7.80E-04	aq	[2]
CO_2(g)	1	0	2	0	0	0	0	-394.4	-393.5	3.02E-03	3.41E-02	g	[2]
Water *	0	2	1	0	0	0	0	-237.7 ± 0.9	-285.33	-1.62E-01	N.A.	l	[2]
H^+ **	0	1	0	0	1	0	0	-39.87	0	0.00E+00	N.A.	aq	[2]
Ammonium^{+1} (aq) *	0	4	0	1	1	0	0	-80.4 ± 1.9	-133	-1.80E-01	N.A.	aq	[2]
Iron III (aq)	0	0	0	0	3	0	1	-4.6	-48.5	-1.47E-01	N.A.	aq	[2]
Sulphate^{-2} (aq) *	0	0	4	0	-2	1	0	-744.8 ± 0.4	-909.6	-5.53E-01	N.A.	aq	[2]
e -	0	0	0	0	-1	0	0	0	0	0.00E+00	N.A.	aq	[2]

N.A. = Data Not Available
C.G.C. = Calculated using Group Contribution

Phases:
g = gas(pure substance)
aq = aqueous
c = crystal (pure substance)
l = liquid (pure substance)

* $\Delta_f G^{0'}$ is reported as average ± standard deviation of data obtained from different sources. For compounds which we found a consistent $\Delta_f G^{0'}$ value between different data sources, the standard deviation was considered zero. $\Delta_r G$ values were calculated using values reported in this table and, when reported, the standard deviation is calculated using error propagation.

** Although the value of $\Delta_f G^0$ for H^+ is 0 kJ/mol; it is imperative to remind the reader that, the later value is obtained when the concentration of protons equals 1 mol/l. The value reported in the table is obtained from the definition of standard conditions, when pH=7.

Supplementary references.

[1] Amend J.P., Plyasunov A.V. (2001) *Geochimica et Cosmochimica Acta*, Vol.65 No. 21, pp. 3901-3917
[2] Kleerebezem R., van Loosdrecht M. C. M. (2010), Critical Reviews in Environmental Science and Technology, 40:1, pp. 1-54
[3] HCP on the web: CRC Handbook of Chemistry and Physics, 93rd Edition, 2012-2013. http://www.hbcpnetbase.com/ (Accessed November 21, 2012)
[4] Noor E., et al. (2012) Bioinformatics vol. 28 no. 15, pp. 2037-2044
[5] Domalski E.S. (1972), J. Phys. Chem. Ref. Data, Vol. 1, No. 2
[6] Vatani A., et al. (2007) Int. J. Mol. Sci., 8, pp. 407-432
[7] Heijnen J.J. (1999), Bioenergetics of microbial growthm, in Encyclopedia of bioprocess technology: Fermentation, biocatalysis, and bioseparation. John Wiley & sons, Inc., NY, USA Pages:267-291
[8] Alberty, R.A. (2003). Thermodynamics of biochemical reactions. Hoboken, NJ: Wiley Interscience.
[9] Hutchens, J.O., Heat of combustion, enthalpy and free energy of formation of amino acids and related compounds. In: Sober, Ed., Handbook of Biochemistry and Selected Data for Molecular Biology, 2nd ed., Chemical Rubber Co., Cleveland, US, 1970.
[10] HCP on the web: National Institute of Standards and Technology. http://www.nist.gov/public_affairs/nandyou.cfm (Accessed November 21, 2012)
[11] Venugopal, M., et al. (2012). International Journal of Research in Pharmaceutical and Biomedical Sciences, Vol. 3 (2) p. 824-830
[12] Verevkin S. P., et al. (2009) Biomass-derived platform chemicals: Thermodynamic studies on the conversion of 5-hydroxymethylfurfural into bulk intermediates. Ind. Eng. Chem. Res. 48 pp. 10087-10093
[13] Noor E., et al. (2013) PLoS Comput Biol, 9, e1003098
[14] Alberty, R.A. (2006). Biochemical Thermodynamics: Applications of Mathematica. Hoboken, NJ: John Wiley & Sons.

CHAPTER

3

Accurate measurement of the *in vivo* ammonium concentration in *Saccharomyces cerevisiae*

Inventar, es ver lo que todos han visto y pensar lo que nadie ha pensado.

Inventing, it is to see what everybody has seen and think what nobody else has thought.

Guillermo González Camarena

Abstract

Ammonium (NH_4^+) is the most common N-source for yeast fermentations, and N-limitation is frequently applied to reduce growth and increase product yields. While there is significant molecular knowledge on NH_4^+ transport and assimilation, there have been few attempts to measure the *in vivo* concentration of this metabolite. In this article, we present a sensitive and accurate analytical method to quantify the *in vivo* intracellular ammonium concentration in *Saccharomyces cerevisiae* based on standard rapid sampling and metabolomics techniques. The method validation experiments required the development of a proper sample processing protocol to minimize ammonium production/consumption during biomass extraction by assessing the impact of amino acid degradation —an element that is often overlooked. The resulting cold chloroform metabolite extraction method, together with quantification using ultra high performance liquid chromatography-isotope dilution mass spectrometry (UHPLC-IDMS), was not only more sensitive than most of the existing methods but also more accurate than methods that use electrodes, enzymatic reactions, or boiling-water or boiling ethanol biomass extraction because it minimized ammonium consumption/production during sampling processing and interference from other metabolites in the quantification of intracellular ammonium. Finally, our validation experiments showed that other metabolites like pyruvate or 2-oxoglutarate (αKG) need to be extracted with cold chloroform to avoid biased measurements due to degradation of other metabolites (*e.g.* amino acids).

Keywords

Intracellular ammonium, UHPLC-IDMS, metabolomics, *in vivo* quantification, rapid sampling

This Chapter is published as: Cueto-Rojas H. F., Maleki Seifar R., ten Pierick A., Heijnen J. J., Wahl S. A., Accurate measurement of the *in vivo* ammonium concentration in *Saccharomyces cerevisiae*, *Metabolites* 6(2), 12.
doi: 10.3390/metabo6020012

Introduction

One of the key challenges when studying nitrogen metabolism in different biological systems *in vivo* is measuring the intracellular ammonium concentration. Accurate data about the *in vivo* intracellular ammonium concentrations are needed to study the molecular mechanisms behind its transport, assimilation and regulation, as observed by Kim *et al.* (2012). Although the transporters and reactions by which ammonium is assimilated in cells are well known (Conrad *et al.*, 2014; Ljungdahl and Daignan-Fornier, 2012; Magasanik, 2003), little is known about the intracellular ammonium concentration and its regulatory mechanisms. In relation to *Saccharomyces cerevisiae*, many studies have described how central nitrogen metabolism is tightly regulated by the presence of ammonium, glutamate, glutamine and other nitrogenous compounds (Conrad *et al.*, 2014; Dikicioglu *et al.*, 2011; Magasanik and Kaiser, 2002).

Interestingly, in most of the studies related to ammonium transport, not NH_4^+, but analogous non-metabolizable molecules were used, such as methylamine (Kleiner, 1981; Roon *et al.*, 1975; Van Nuland *et al.*, 2006). In particular, the first attempts to describe ammonium transporter proteins involved the use of ^{14}C-labeled methylamine to determine the kinetics of the transporters (Roon *et al.*, 1975); Intracellular ammonium was not measured in these transport studies, to our knowledge. Other studies measured only the extracellular ammonium concentration and correlated this measurement with intracellular observations, or simply estimated the intracellular ammonium concentration based on certain assumptions, such as thermodynamic equilibrium of the reaction glutamate dehydrogenase (Kim *et al.*, 2012; Wang *et al.*, 2011). However, there is no experimental *in vivo* evidence for those assumptions.

In earlier studies, Van Nuland *et al.* (2006) measured intracellular ammonium in *S. cerevisiae* for resting cells using a water-based extraction method combined with an enzymatic method; Barreto *et al.* (2012) applied the same approach. On the other hand, Tate and Cooper (2003) used an ammonium-specific electrode to study the

relationship between intracellular ammonium and the genetic control mechanisms of the central nitrogen metabolism. Although the results obtained correlated with biological observations, it is debatable whether the N-metabolism was properly quenched and whether the leakage of intracellular ammonium was absent. For these reasons, it is not clear whether these methods for intracellular ammonium measurement are accurate when cells are growing with a high N-uptake rate as in N-limited chemostats.

Sampling and analytical protocols for quantitative analysis of intracellular ammonium must meet the following requirements (Canelas *et al.*, 2009):

i) Formation or consumption of NH_4^+ during sample processing must be avoided,
ii) Extensive leakage of NH_4^+ must be absent,
iii) Extraction of intracellular NH_4^+ from biomass must be fast and complete,
iv) Proper internal standards must be applied.

The aim of this article is to present an accurate and reliable analytical protocol for quantification of intracellular ammonium in *S. cerevisiae*. Our methods include conventional rapid sampling as well as new methods for biomass extraction and Isotope Dilution Mass Spectrometry (IDMS)-based analysis of ammonium. All biological samples were obtained from cultivations of *S. cerevisiae* in aerobic chemostats using glucose as C-source under N-source limitation at pH=5.

Materials and methods

Strain and culture conditions

The biological samples used for method validation experiments were obtained from available yeast cultivations. The strain used for validation of the intracellular ammonium method was *Saccharomyces cerevisiae* CEN.PK *ath1 nth1 nth2* mat **a** MAL2-8c *leu2 ath1Δ::kanMX4 nth1Δ::kanMX4 nth2Δ::LEU2* (Jules *et al.*, 2008), kindly provided by Dr. Jean-Luc Parrou from the Ingénierie des Systèmes Biologiques et des Procédés at INSA-Toulouse, France. Yeast cells from this strain were cultivated in aerobic ammonium-

limited chemostat conditions in a 2 L fermentor (Applikon, Schiedam, The Netherlands) with a working volume of 1 L. The dilution rate was maintained at 0.1 h^{-1}, the temperature was kept constant at 30º C and the pH was kept constant at a value of 5 with automatic additions of 4M KOH or 2M H_2SO_4. Dissolved oxygen tension (DOT) was monitored online using an oxygen probe (Mettler-Toledo, Tiel, The Netherlands). Stirring speed of 600 rpm, overpressure of 0.3 bar, and aeration rate of 0.25 vvm were used in order to keep the dissolved oxygen level above 40%.

The medium used was a modification of the N-limiting medium reported by Boer *et al.* (2003), with the following composition: glucose 130 g/L, $MgSO_4 \cdot 7H_2O$ 1.14 g/L, ethanol 25 g/L (supplemented to avoid oscillations), KH_2PO_4 6.9 g/L, trace elements 2 mL/L, vitamin solutions were added 2 mL/L and antifoam C 0.3 g/L; the N-source used was $NH_4H_2PO_4$ 3.48 g/L, equivalent to 30 mM of nitrogen, which is sufficient to produce about 8 g_{CDW}/L. All samples were taken at steady state, after stable values of DOT and off-gas CO_2 and O_2 were obtained, between three and eight volume changes after switching the medium.

Standards

Ammonium standards were prepared using serial dilutions of ammonium dihydrogen phosphate ($NH_4H_2PO_4$ 5 mM) in milli-Q water. The concentrations used for the calibration lines were between 1 to 500 µM. An additional standard of 250 µM of ammonium was prepared and used as spike solutions.

^{15}N- NH_4Cl 98% atom ^{15}N LOT# TA0525V (Sigma-Aldrich, Zwijndrecht, the Netherlands), was used to prepare a stock solution with a concentration of 500 µM dissolved in milli-Q water and used as internal standard in samples, as well as calibration standards.

Sampling and sample preparation

Samples for extracellular metabolites and ammonium analysis

Samples of approx. 1 mL broth were quenched using cold steel beads in a syringe, as described by Mashego *et al.* (2006), and rapidly

filtered using 0.45 µm disc filters (Millipore). 80 µL of filtrate were mixed with 20 µL of internal standard (500 µM ^{15}N-NH_4Cl) and derivatized according to the protocol used for ammonium quantification by LC-MS.

Rapid sampling and biomass extraction for intracellular metabolites and intracellular ammonium

Samples of approximately 1.2 g of broth were taken with a dedicated rapid-sampling setup (Lange *et al.*, 2001), quenched in 6 mL of -40º C methanol 100%, and after weighting they were centrifuged for 5 minutes at 10000G and -19ºC. For biomass washing, the pellet was recovered and re-suspended in 6 mL -40º C methanol 100%; centrifuged again for 5 minutes at 10000G and -19ºC. For the biomass pellet extraction four different protocols were used, because of possible production/consumption of N-containing compounds in the conventional (BE) extraction protocol.

BE: Boiling ethanol extraction of the biomass pellet

The biomass pellet obtained from *Rapid sampling for intracellular metabolites and intracellular ammonium* was recovered and re-suspended in 6 mL of ethanol-milli-Q 75%(v/v) pre-heated at 75ºC (*BE*), which is the conventional metabolite extraction for *S. cerevisiae* (Canelas *et al.*, 2009), or using 6 mL of ethanol 75%(v/v)-acetate buffer 10 mM (pH = 5) 25%(v/v) pre-heated at 75ºC (*BE5*) in order to extract intracellular metabolites and ammonium as described by Canelas *et al.* (2009). 120 µL of U-^{13}C- cell extract (intracellular metabolites samples) or 120 µL of ^{15}N- NH_4Cl 500 µM (intracellular ammonium samples) were added as internal standard prior the addition of the buffered ethanol (AQ in figure 3.1).

Some samples were spiked with 120 µL $NH_4H_2PO_4$ 250 µM; the spike solution was added at the same time with the internal standard. At this stage, all extraction mixtures were stored a couple of days at -80ºC until further processing.

The extraction mixture was dried using a rapidvap with cold trap (Labconco, USA) for 120 minutes, at a pressure lower than 5 mbar at 30ºC. The dry residue was re-suspended in 600 µL of milli-Q water and centrifuged for 5 min at 1ºC and 15 000 G to remove the cell

debris, the supernatant was recovered in screw-cap tubes and stored at -80º C until further processing. In some samples, 120 µL of U-^{13}C-cell extract was added to the dry residue after the rapidvap-drying step (BA in figure 3.1), without a previous addition of internal standard. The objective of this was to determine the extent of degradation during ethanol boiling of certain metabolites, which could lead to liberation of NH_4^+, such as glutamate conversion to αKG.

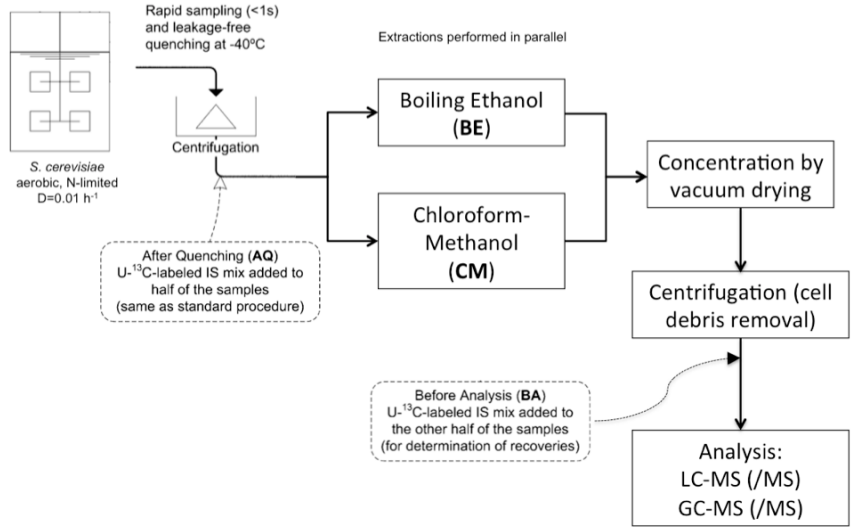

Figure 3.1. Experimental approach to quantify amino acid degradation (adapted from Canelas *et al.* (2009)).

CM5: Cold chloroform-methanol buffered at pH = 5 extraction of the biomass pellet

The biomass pellet obtained from *Rapid sampling for intracellular metabolites and intracellular ammonium* was suspended in 3.5 mL of methanol-acetate buffer 10 mM (pH of buffer solution without methanol was 5) 50%(v/v) pre-chilled at -40ºC. Afterwards, 3.5 mL of chloroform 100% pre-chilled at -40ºC was added followed by the addition of 120 µL of U-^{13}C- cell extract (intracellular metabolites samples) or 120 µL of ^{15}N- NH_4Cl 500 µM (intracellular ammonium samples) as internal standards (AQ in figure 3.1).

Selected samples were spiked with 120 µl of NH_4Cl 250 µM. The spike solution was added at the same time with the internal standard; during the holding times, the tubes were kept at -40ºC in a cryostat to avoid metabolic reactions. The chloroform and aqueous phases were homogenized (vortex) in order to create an emulsion (<3s), afterwards the tubes were kept at cold temperature (approx. -50ºC) for 45 minutes under constant vigorous agitation using an in-house built shaker.

After this first extraction, the tubes were centrifuged at 10000G and -20ºC for 5 minutes, with a rotor chilled at -50ºC; the supernatant (aqueous phase) was recovered, 3.5 mL of fresh Methanol-acetate buffer 10mM (pH = 5) 50%(v/v) pre-chilled at -40ºC were added; the samples were homogenized (<3s), afterwards the tubes were kept at cold temperature (approx. -50ºC) for 5 minutes under constant vigorous agitation using an in-house built shaker. After this second step of extraction, the samples were centrifuged at 10000G and -20ºC for 5 minutes, with a rotor chilled at -50ºC; the supernatant was again recovered and pooled together with the supernatant of the first extraction. All supernatants were stored at -80ºC until further processing.

The pooled supernatant was dried using a rapidvap with cold trap (Labconco, USA) for 180 minutes, at a pressure lower than 5 mbar at 30ºC. The dry residue was re-suspended in 600 µL of milli-Q water and centrifuged for 5 min at 1º C and 15000 G to remove the cell debris, the supernatant was recovered in screw-cap tubes and stored at -80º C until further processing. In some samples, 120 µL of U-^{13}C-cell extract was added to the dry residue after the rapidvap-drying step (BA in figure 3.1), without a previous addition of internal standard; the objective of this was to determine the extent of degradation of certain N-containing metabolites, as explained for the BE5 extraction protocol.

CM5: Cold non-buffered chloroform-methanol extraction of the biomass pellet

The biomass pellet obtained from *Rapid sampling for intracellular metabolites and intracellular ammonium* was recovered, 3.5 mL of Methanol-milli-Q water 50%(v/v) pre-chilled at -40ºC was added, and

then 120 µL of U-^{13}C- cell extract. Afterwards, 3.5 mL of Chloroform 100% pre-chilled at -40ºC was added in order to extract intracellular metabolites according to Canelas *et al.* (2009). This method was only used to extract acid unstable intracellular metabolites, *e.g.* NADH and NADPH; it was not used for extraction of intracellular ammonium. Also for total broth analysis, three different extraction protocols were used, for the same reasons as explained in the methods for biomass pellet extraction.

TBE5: Boiling buffered ethanol pH = 5 extraction of total broth

Approximately 1.2 g broth were taken from the reactor with a dedicated rapid-sampling setup (Lange *et al.*, 2001), quenched in 6 mL of -40º C methanol 100% and weighted to determine the exact mass of the sample.

3.5 mL of quenched broth solution were further processed; in all steps the sample was weighted to determine its exact mass. 120 µL of U-^{13}C- cell extract or 120 µL of ^{15}N- NH_4Cl 500 µM (intracellular ammonium samples) was added as internal standard. 3.5 mL of quenched broth/methanol solution were boiled in 30 mL of ethanol-acetate buffer 10mM (pH = 5) 75%(v/v) pre-heated at 75ºC as described by Canelas *et al.* (2009).

Subsequently the extraction mixture was dried using a rapidvap with coldtrap (Labconco, USA) for 240 minutes, at a pressure lower than 5 mbar at room temperature. The dry residue was re-suspended in 600 µL of milli-Q water, centrifuged for 5 min at 1º C and 15 000 G to remove the cell debris. The supernatant was recovered in screw-cap tubes and stored at -80º C until further processing.

TBE: Boiling non-buffered ethanol extraction of total broth

Approximately 1.2 g broth were taken from the reactor with a dedicated rapid-sampling setup (Lange *et al.*, 2001), quenched in 6 mL of -40º C methanol 100% and weighted to determine the exact mass of the sample.

3.5 mL of quenched broth solution were further processed; in all steps the sample was weighted to determine its exact mass. 120 µL of

U-^{13}C- cell extract or 120 µL of ^{15}N- NH_4Cl 500 µmol/L (intracellular ammonium samples) was added as internal standard. The sample was boiled in 30 mL of ethanol 75%(v/v) in milli-Q water pre-heated at 75ºC as described above.

TCM5: Cold chloroform-methanol buffered at pH = 5 extraction of total broth

Approximately 1.2 g were taken from the reactor with a dedicated rapid-sampling setup (Lange *et al.*, 2001), quenched in 6 mL of -40º C methanol-acetate buffer pH=5 60%(v/v) and weighted to determine the exact mass of the sample.

3.5 mL of quenched broth solution were further processed; in all steps the sample was weighted to determine its exact mass. 120 µL of U-^{13}C- cell extract or 120 µL of ^{15}N- NH_4Cl 500 µM (intracellular ammonium samples) was added as internal standard, followed by addition of chloroform 100% pre-chilled at -40ºC for extraction using the CM5 protocol for intracellular samples; the pooled supernatants were dried using a rapidvap with cold trap for 180 minutes, at a pressure lower than 5 mbar at 30ºC. The dry residue was re-suspended in 600 µL of milli-Q water and centrifuged for 5 min at 1º C and 15000 G to remove the cell debris, the supernatant was recovered in screw-cap tubes and stored at -80º C until further processing.

Analytical methods

Ammonium quantification

The ammonium in the samples was quantified using UHPLC-IDMS after derivatization of the sample with Diethyl Ethoxymethylenemalonate (DEEMM) as described by Redruello *et al.* (2013). Briefly, 100 µL of solution to be analyzed obtained from intracellular, extracellular or total broth samples were mixed with 175 µL of Na_3BO_3 buffer 1 M (pH=9), 75 µl of 100% methanol, 3 µL of DEEMM, in glass vials. The vials were incubated at 30ºC for 45 min to complete the derivatization reaction; excess DEEMM was degraded by incubation at 70 ºC for 2 h. All measurements were performed on an AcQuity ™UPLC system (Waters, Milford, MA, USA) coupled to a Quattro Premier XE mass spectrometer,

(Micromass MS Technologies-Waters, Milford, MA, USA) with an electrospray ion source. The MS was operated in negative mode. Masslynx 4.1 (Waters) used for data acquisition and peak integration. Metabolite detection was performed in selected ion monitoring mode (SIM). The general settings were as follows: the ESI capillary voltage was -2.8 kV, extractor voltage 5 V, RF lens voltage 0.5 V, and cone voltage 35 V. The desolvation gas (nitrogen) flow was 700 L/h at 360 °C, the cone gas (nitrogen) flow was 50 L/h, and the source block temperature was set at 120°C. For ^{14}N-aminoene the m/z of 186 and for ^{15}N-aminoene the m/z of 187 were monitored. The peak areas (heights) of internal standards were corrected considering blank injections and natural isotope contributions from carbon, nitrogen, hydrogen and oxygen atoms of the derivatization reagent. The chromatographic separation of ammonium was adopted using the protocol described by Maleki Seifar *et al.* (2013).

Metabolite quantification

Quantification of αKG, pyruvate and trehalose was performed using GC-MS as described by Niedenfuhr *et al.* (2015). Amino acids were measured using GC-MS according to de Jonge *et al.* (2011).

Data Reconciliation

Data reconciliation was performed using the total broth mass balance ([TB] = [IC] × gCDW/L_{TB} + [EC]) and the experimental measurements according to Verheijen (2010), under the constraint that mass conservation is satisfied.

Results and discussion

During the method development phase, we considered different analytical techniques, namely colorimetric and enzymatic assays. However, these techniques presented major drawbacks as they were either not specific enough (colorimetric), or the sample matrix decreased its effectiveness (enzymatic). In particular, the high glutamic acid content in the intracellular samples interfered with any enzymatic assay based on the glutamate dehydrogenase reaction, since we could observe an end-product inhibition of the reaction due

to thermodynamic equilibrium. Therefore, we used an UHPLC-IDMS-based method to overcome these challenges.

Reproducibility and linearity of the method using standards

We prepared different calibration lines in order to validate day-to-day reproducibility using the measured ^{15}N to ^{14}N ratio, corrected for the influence of natural isotopes (Niedenfuhr *et al.*, 2015). The slope was reproducible with 1.25% standard deviation, and the offset with 19% standard deviation. The correlation coefficient of the calibration line is r^2=0.9967, from these results it was concluded that the method is linear in the concentration range between 1 to 750 µmol/L.

Comparison between centrifugation and filtration for biomass separation

Initially, all biological samples were obtained using the filtration method described by Suarez-Mendez *et al.* (2014). After some preliminary tests using biological samples measured by UHPLC-IDMS, we observed a significant reduction (>90%) in the peak area of the internal standard (^{15}N-NH_4^+, m/z=187) between standards and biological samples. We determined the resolution of the MS to be 0.7 mass units, given that no interferences of other masses were detected at this mass difference. We therefore concluded that the instrument was not the source of such deviation between biological samples and standards. In order to isolate the cause of the reduction of peak intensities, we decided to test the extraction method using different conditions. The results and details of each set of samples are summarized in the appendix 3.1. From these tests, it was possible to infer the negative effect of 0.45 µm filters used in the filtration method during the ethanol-boiling step.

Although the filtration method did not work as it was expected, the results obtained using standards without filters were encouraging enough to continue the research using a processing method based on centrifugation for biomass separation. Indeed, further tests showed no significant changes in peak areas of labelled internal standards between standard calibration solutions and biological samples.

NH_3-evaporation during Rapid Vap drying

NH_4^+ is in equilibrium with NH_3, which is a hydrophilic gas that could escape from aqueous solution during the vacuum drying step. 120 µL of a 500 µmol/L ammonium dihydrogen phosphate solution was boiled together with 120 µL of internal standard (^{15}N-NH_4Cl 500 µmol/L) in 30 mL of ethanol 75%(v/v), and processed following the same procedure as the typical intracellular samples (Canelas *et al.*, 2009). After being dissolved in milli-Q water, the samples were derivatized and measured using LC-MS, as described above. The experimental results showed that NH_3 evaporation could be corrected by addition of ^{15}N-NH_4Cl as internal standard to the sample during the sample processing. Other experiments were carried out using extraction mixtures obtained from BE5 (buffered boiling ethanol), CM5 (cold-buffered chloroform-methanol extraction) and CM (cold non-buffered chloroform-methanol extraction) protocols, leading to similar results.

Absence of matrix effects

A known amount of ammonium was spiked to different samples, aiming to show that the amount measured in the spiked samples (intracellular, extracellular or total broth samples) is the sum of the amount present in the sample plus the added amount in order to demonstrate that no matrix effect takes place during the analysis. Table 3.1 presents the results of the spike experiments for samples obtained after CM5 extraction; all samples were spiked with the equivalent to 50 µmol/L NH_4^+. In all cases, the t-test ($p<0.05$, three independent observations) showed no significant difference between spiked samples and reference samples, confirming the absence of matrix effects in the NH_4^+ analysis.

Intracellular ammonium quantification requires extraction with cold-buffered chloroform-methanol

During quenching and extraction, leakage and/or chemical conversion of NH_4^+ could occur. Such reactions are more common with extreme pH, high temperature and high concentrations. Due to the different amounts of processed biomass, the resulting metabolite

concentrations in the extraction mixture for intracellular (IC) samples were approximately six-fold higher than for total broth (TB) samples.

Table 3.1. Results of the spike experiments using cold-buffered chloroform-methanol extraction (CM5) as extraction method. The estimated concentration when spiked amount (50 µmol/L) is subtracted from the measurement is shown in brackets. The results are displayed as µmol/L_{sample}. The results are single injections of independent triplicates.

Sample	Measured concentration µmol/L_{sample} (measurement - spike)	Average ± St. Dev. µmol/L_{sample}
Extracellular 1(Oct 14)	6.1	4.2 ± 2.8
Extracellular 2(Oct 14)	2.2	
Extracellular 3(Oct 14)	N.D.	
Spiked EC 1(Oct 14)	61.1 (11.1)	9.2 ± 2.1*
Spiked EC 2(Oct 14)	57.0 (7.0)	
Spiked EC 3(Oct 14)	59.5 (9.5)	
Intracellular 4 (Oct 14)	35.9	31.2 ± 4.1
Intracellular 5 (Oct 14)	28.7	
Intracellular 6 (Oct 14)	28.9	
Spiked IC4 (Oct 14)	94.4 (44.4)	34.3 ± 9.0*
Spiked IC5 (Oct 14)	81.3 (31.3)	
Spiked IC6 (Oct 14)	77.2 (27.2)	
Total broth 4(Oct 14)	21.8	22.7 ± 1.3
Total broth 5(Oct 14)	22.1	
Total broth 6(Oct 14)	24.2	
Spiked TB4 (Oct 14)	77.8 (27.8)	29.1 ± 6.5*
Spiked TB5 (Oct 14)	73.3 (23.3)	
Spiked TB6 (Oct 14)	86.2 (36.2)	

***** *Average of estimated concentration (measured concentration – spiked amount).*
EC: extracellular, TB: total broth, IC: intracellular

Table 3.2 shows a balance gap of +25% for the conventional BE method, which indicates ammonium formation from other metabolites during the boiling of the biomass pellet, or consumption of NH_4^+in the total broth by an unknown chemical reaction. For the buffered boiling ethanol protocol (BE5) there was a gap of -20%;

showing the opposite behavior. Only for the cold-buffered chloroform-methanol extraction (CM5) protocol was there no significant gap in the total ammonium balance, which required that data reconciliation be performed in order to calculate the best estimate of the real state (Table 3.2). An additional observation was that the CM5 method led to the best reproducibility.

Table 3.2. Results of total broth ammonium mass balance. Reconciled concentrations provide the best estimates of the measurements obtained by least square minimization of the differences between measurements and estimated amounts, weighted with respect to their measurement errors.

Type of sample	Concentration measured* ($\mu mol/L_{broth}$)	Recovery (%)	Reconciled concentration ($\mu mol/L_{broth}$)
Intracellular BE (Aug 14)	24.51 ± 2.15	124.50%	N.A.
Extracellular (Aug 14)	6.23 ± 1.15		
Total broth BE (Aug 14)	24.69 ± 5.25		
Intracellular BE5 (Oct 14)	10.04 ± 1.93	77.93%	N.A.
Extracellular (Oct 14)	1.05 ± 0.49		
Total broth BE5 (Oct 14)	14.23 ± 0.23		
Intracellular CM5 (Oct 14)	15.16 ± 1.24	96.66%	15.57 ± 0.64
Extracellular (Oct 14)	1.05 ± 0.49		1.12 ± 0.46
Total broth CM5 (Oct 14)	16.77 ± 0.57		16.68 ± 0.52

* *Average of three independent samples injected and quantified three times; N.A. = not applicable; BE: conventional boiling ethanol extraction; BE5: buffered boiling ethanol extraction; CM5: cold-buffered chloroform-methanol extraction.*

Finally, we were able to use (for the CM5 method) the constraint of the NH_4^+-balance to obtain the reconciled data (table 3.2). Note that of the total NH_4^+ present in the NH_4^+-limited fermentation broth, only 7% is found in the extracellular space. The remaining 93% is present in the intracellular space.

Amino acid degradation

We prepared different samples for the different extraction protocols with two-time points for adding U-^{13}C cell extract, as in Canelas *et al.*

(2009) (figure 3.1), in order to quantify the occurrence of amino acid degradation and NH_4^+ formation. Table 3.3 shows significant differences in BE5 after quenching and before analysis.
The experimental results show that reactions occur involving NH_4^+. For instance, glutamine is a labile amino acid that degrades spontaneously to ammonium and pyroglutamic acid (equation 3.1).

$$\text{L-glutamine} \longrightarrow NH_3 + \text{Pyroglutamic acid} \qquad \Delta_r G^{0'} = -30.9 \frac{kJ}{mol} \tag{3.1}$$

A range of factors such as temperature and pH affect the kinetics of this degradation process. Furthermore, it is known that also glutamic acid decays into pyroglutamic acid in a similar manner (equation 3.2), but this reaction is much slower than glutamine decay and does not produce NH_3. Moreover, due to the nature of the extraction methods (*e.g.* in the boiling ethanol method), it is likely that some amino acid degradation or pH shifts take place.

$$\text{L-glutamic acid} \longrightarrow H_2O + \text{Pyroglutamic acid} \qquad \Delta_r G^{0'} = -19.5 \frac{kJ}{mol} \tag{3.2}$$

Given the very large intracellular concentration of glutamine and glutamate (in the order of 100 µmol/g_{CDW}) the spontaneous decay of glutamine (which produces NH_4^+) can sensibly compromise the intracellular NH_4^+ concentration measured. L-glutamine is more stable in the pH range between pH=5 and 7, therefore we tested buffered extraction solutions (BE5 and CM5). We expected that the cold-chloroform-methanol-buffered CM5 extraction method would display the least amino acid conversion, which proved to be the case. From Table 3.3, we can see that there is a reduction of alanine of 1.23 µmol/gCDW, which explains the origin of the 1.75 µmol/gCDW (1.96 µmol/gCDW – 0.21 µmol/gCDW) increase in pyruvate. We found other metabolites such as PEP in lower concentrations than alanine and expect their contribution to increased pyruvate concentrations to be less significant. For glutamate there is a decrease of 1.74 µmol/gCDW and for glutamine a decrease of 0.95 µmol/gCDW. The decrease in glutamate and glutamine is accompanied by increase of αKG and pyroglutamate levels compared to CM5 extraction.

Table 3.3. Quantitative analysis of amino acid decay using different extraction methods. The results displayed are averages of three independent samples (in µmol/gCDW).

^{13}C addition	Extraction solution	Intracellular metabolite concentration (µmol/gCDW) (% recovery with respect to 13C addition after quenching)							
		Ala	Glu	Asp	Gln	PyrGlu	Pyruvate	αKG	NH_4^+
AQ	BE5	6.97 ± 0.21	52.79 ± 0.36	11.51 ± 0.14	10.77 ± 0.25	0.78 ± 0.02	1.96 ± 0.17	3.01 ± 0.05	3.46 ± 0.28
BA	BE5	5.73 ± 0.25 (82.3%)*	51.05 ± 0.75 -96.7%	10.80 ± 0.33 -93.9%	9.81 ± 0.19 -91.2%	1.11 ± 0.02 (141.9%)*	N.M.	N.M.	N.M.
AQ	CM5	6.50 ± 0.07	51.95 ± 0.65	9.03 ± 0.09**	10.85 ± 0.16	0.51 ± 0.02**	0.21 ± 0.01	0.50 ± 0.01	2.29 ± 0.44
BA	CM5	6.00 ± 0.05 (92.4%)*	49.95 ± 0.30 -96.2%	8.90 ± 0.07 -98.5%	10.68 ± 0.07 -98.4%	0.57 ± 0.06 -112.2%	N.M.	N.M.	N.M.
AQ	BE	7.86 ± 0.13	56.00 ± 0.95	11.54 ± 0.28	11.28 ± 0.14	N.M.	2.17 ± 0.24	2.81 ± 0.06	5.78 ± 0.20

gCDW= gram cell dry weight.

N.M.= not measured. In these cases the analysis was not performed, therefore no experimental data ara available.

** Statistically significant difference found between AQ and BA samples, according to a t-test at a significant level of 0.05.*

*** Statistically significant difference found between BE5 AQ and CM5 AQ samples, according to a t-test at a significant level of 0.05.*

This indicated that both glutamine and glutamate degrade to αKG and ammonium, which is particularly important since αKG concentrations are then overestimated six-fold and intracellular NH_4^+ is also significantly overestimated, which explains the NH_4^+-balance deviations observed, as discussed before.
Furthermore, we observed important differences in the levels of pyroglutamate; although small, this also suggest that glutamine or glutamate are converted into pyroglutamate during sample processing. These results show that extraction of ammonium from biomass must be carried out using the cold-buffered chloroform-methanol CM5 extraction method to avoid measurements being biased by the degradation of amino acids, given that the concentration ratio amino acid/precursor is usually very high.

Conclusions

Here, we introduce a sampling/analysis method for accurately measuring intracellular NH_4^+. Our experimental results demonstrated that intracellular ammonium measurements require biomass separation using a centrifugation method. They also demonstrated that the standard filtration method resulted in biased measurements originated by filters used. Centrifugation, on the other hand, enabled us to obtain reproducible samples, with no other matrix effect. We therefore selected centrifugation as the standard method. Furthermore, the experimental evidence firmly established that NH_3-evaporation could be corrected using ^{15}N-NH_4Cl as internal standard.
In addition, the various validation tests showed that cold-buffered chloroform-methanol CM5 was the best method for extracting intracellular ammonium because it prevented formation/consumption of ammonium during sample processing. However, caution is advised when using this method to extract pH-sensitive metabolites (*e.g.* coenzymes). Further experimental evidence also suggested that boiling ethanol extraction procedure degrades amino acids, particularly glutamate and glutamine, generating pyroglutamic acid. Therefore, amino acids should be extracted using cold methods, such as cold chloroform-methanol-water extraction.

Acknowledgements

This work was performed within the BE-Basic R&D program (http://www.be-basic.org), which was granted a FES subsidy from the Dutch Ministry of Economic Affairs, Agriculture and Innovation (EL&I). The author HFCR received a scholarship from CONACyT (Scholarship number: 212059). The founding sponsors had no role in the design of the study; in the collection, analyses, or interpretation of data; in the writing of the manuscript, and in the decision to publish the results.

The author HFCR thanks the entire CSE group for the help during rapid sampling experiments, particularly to Camilo Suárez-Méndez, Cristina Bernal, Mihir Shah, Mariana Velasco-Álvarez, Leonor Guedes da Silva and Francisca Lameiras for their invaluable help and collaboration.

References

Barreto, L., Canadell, D., Valverde-Saubi, D., Casamayor, A., Arino, J., 2012. The short-term response of yeast to potassium starvation. Environ. Microbiol. 14**,** 3026-42.

Boer, V. M., de Winde, J. H., Pronk, J. T., Piper, M. D., 2003. The genome-wide transcriptional responses of *Saccharomyces cerevisiae* grown on glucose in aerobic chemostat cultures limited for carbon, nitrogen, phosphorus, or sulfur. J. Biol. Chem. 278**,** 3265-74.

Canelas, A. B., ten Pierick, A., Ras, C., Maleki Seifar, R., van Dam, J. C., van Gulik, W. M., Heijnen, J. J., 2009. Quantitative evaluation of intracellular metabolite extraction techniques for yeast metabolomics. Anal. Chem. 81**,** 7379-89.

Conrad, M., Schothorst, J., Kankipati, H. N., Van Zeebroeck, G., Rubio-Texeira, M., Thevelein, J. M., 2014. Nutrient sensing and signaling in the yeast *Saccharomyces cerevisiae*. FEMS Microbiol. Rev. 38**,** 254-99.

de Jonge, L. P., Buijs, N. A., ten Pierick, A., Deshmukh, A., Zhao, Z., Kiel, J. A., Heijnen, J. J., van Gulik, W. M., 2011. Scale-down of penicillin production in *Penicillium chrysogenum*. Biotechnology journal. 6**,** 944-58.

Dikicioglu, D., Karabekmez, E., Rash, B., Pir, P., Kirdar, B., Oliver, S. G., 2011. How yeast re-programmes its transcriptional profile in response to different nutrient impulses. BMC Syst Biol. 5**,** 148.

Jules, M., Beltran, G., Francois, J., Parrou, J. L., 2008. New insights into trehalose metabolism by Saccharomyces cerevisiae: NTH2 encodes a functional cytosolic trehalase, and deletion of TPS1 reveals Ath1p-dependent trehalose mobilization. Appl. Environ. Microbiol. 74**,** 605-14.

Kim, M., Zhang, Z., Okano, H., Yan, D., Groisman, A., Hwa, T., 2012. Need-based activation of ammonium uptake in Escherichia coli. Mol. Syst. Biol. 8**,** 616.

Kleiner, D., 1981. The transport of NH_3 and HN_4^+ across biological membranes. Biochimica et Biophysica Acta (BBA) - Reviews on Bioenergetics. 639**,** 41-52.

Lange, H. C., Eman, M., van Zuijlen, G., Visser, D., van Dam, J. C., Frank, J., de Mattos, M. J., Heijnen, J. J., 2001. Improved rapid sampling for *in vivo* kinetics of intracellular metabolites in *Saccharomyces cerevisiae*. Biotechnol. Bioeng. 75**,** 406-15.

Ljungdahl, P. O., Daignan-Fornier, B., 2012. Regulation of amino acid, nucleotide, and phosphate metabolism in *Saccharomyces cerevisiae*. Genetics. 190**,** 885-929.

Magasanik, B., 2003. Ammonia Assimilation by *Saccharomyces cerevisiae*. Eukaryot. Cell. 2**,** 827-829.

Magasanik, B., Kaiser, C. A., 2002. Nitrogen regulation in *Saccharomyces cerevisiae*. Gene. 290**,** 1-18.

Maleki Seifar, R., Ras, C., Deshmukh, A. T., Bekers, K. M., Suarez-Mendez, C. A., da Cruz, A. L., van Gulik, W. M., Heijnen, J. J., 2013. Quantitative analysis of intracellular coenzymes in *Saccharomyces cerevisiae* using ion pair reversed phase ultra high performance liquid chromatography tandem mass spectrometry. J. Chromatogr. A. 1311**,** 115-20.

Mashego, M. R., van Gulik, W. M., Vinke, J. L., Visser, D., Heijnen, J. J., 2006. *In vivo* kinetics with rapid perturbation experiments in *Saccharomyces cerevisiae* using a second-generation BioScope. Metab. Eng. 8**,** 370-83.

Niedenfuhr, S., Pierick, A. T., van Dam, P. T., Suarez-Mendez, C. A., Noh, K., Wahl, S. A., 2015. Natural isotope correction of MS/MS measurements for metabolomics and C fluxomics. Biotechnol. Bioeng.

Redruello, B., Ladero, V., Cuesta, I., Alvarez-Buylla, J. R., Martin, M. C., Fernandez, M., Alvarez, M. A., 2013. A fast, reliable, ultra high performance liquid chromatography method for the simultaneous determination of amino acids, biogenic amines and ammonium ions in cheese, using diethyl ethoxymethylenemalonate as a derivatising agent. Food Chem. 139**,** 1029-35.

Roon, R. J., Even, H. L., Dunlop, P., Larimore, F. L., 1975. Methylamine and ammonia transport in Saccharomyces cerevisiae. J. Bacteriol. 122**,** 502-9.

Suarez-Mendez, C. A., Sousa, A., Heijnen, J. J., Wahl, A., 2014. Fast "Feast/Famine" Cycles for Studying Microbial Physiology Under Dynamic Conditions: A Case Study with Saccharomyces cerevisiae. Metabolites. 4**,** 347-72.

Tate, J. J., Cooper, T. G., 2003. Tor1/2 regulation of retrograde gene expression in *Saccharomyces cerevisiae* derives indirectly as a consequence of alterations in ammonia metabolism. J. Biol. Chem. 278**,** 36924-33.

Van Nuland, A., Vandormael, P., Donaton, M., Alenquer, M., Lourenco, A., Quintino, E., Versele, M., Thevelein, J. M., 2006. Ammonium permease-based sensing mechanism for rapid

ammonium activation of the protein kinase A pathway in yeast. Mol. Microbiol. 59**,** 1485-505.

Verheijen, P. J. T., 2010. Data Reconciliation and Error Detection. In: Smolke, C. D., (Ed.), The metabolic pathway engineering handbook. CRC Press, Boca Raton, pp. 8.1-8.13.

Wang, L., Lai, L., Ouyang, Q., Tang, C., 2011. Flux balance analysis of ammonia assimilation network in E. coli predicts preferred regulation point. PloS one. 6**,** e16362.

Appendix 3.1. Comparison between samples exposed to PVDF filters and samples not exposed to PVDF filters.

Sample set	Measured concentration* (µM)	Condition
Standard 100 µL	103.6 ± 4.9	Standard solution mixed with internal standard and derivatized with DEEMM.
Centrifugation "mock" sample	105.8 ± 4.2	120 µL standard solution 500 µM NH_4^+ mixed with 120 µL internal standard in 5 mL ethanol 75% (v/v), boiled for 3 minutes. Resuspended in 600 µL milli-Q after ethanol evaporation.
Standard 100 µL in 30 mL Ethanol	92.3 ± 14.7	120 µL standard solution 500 µM NH_4^+ mixed with 120 µL internal standard in 30 mL ethanol 75% (v/v), boiled for 3 minutes. Resuspended in 600 µL milli-Q after ethanol evaporation.
Filtration "mock" sample	120.6 ± 20.9	120 µL standard solution 500 µM NH_4^+ mixed with 120 µL internal standard in 30 mL ethanol 75% (v/v), boiled together with a 0.45µm PVDF filter for 3 minutes. Resuspended in 600 µL milli-Q after ethanol evaporation.
Filter + NaCl in ethanol	156.3 ± 15.7	120 µL standard solution 500 µM NH_4^+ mixed with 120 µL internal standard and 100 µL of NaCl 100 mg/mL in 30 mL ethanol 75% (v/v), boiled together with a PVDF filter for 3 minutes. Resuspended in 600 µL milli-Q after ethanol evaporation.
Filter + NaCl in quenching solution	117.0 ± 41.7	120 µL standard solution 500 µM NH_4^+ mixed with 120 µL internal standard in 30 mL ethanol 75% (v/v), boiled together with a PVDF filter for

Sample set	Measured concentration* (µM)	Condition
		3 minutes. The filter was previously exposed to 30 mL of methanol at -40 ºC and 100 µL NaCl 100 mg/mL. Resuspended in 600 µL milli-Q after ethanol evaporation.
Filter incubated in DBAA	107.7 ± 33.7	120 µL standard solution 500 µM NH_4^+ mixed with 120 µL internal standard and 100 µL of NaCl 100 mg/mL in 30 mL ethanol 75% (v/v), boiled together with a PVDF filter for 3 minutes. The filter was previously exposed to 30 mL of methanol at -40 ºC and incubated 5 minutes in DBAA 25 mM. Resuspended in 600 µL milli-Q after Ethanol evaporation.

* Average value ± Standard deviation of three injections of triplicate samples.

CHAPTER 4

In vivo analysis of NH_4^+ transport and central N-metabolism of *Saccharomyces cerevisiae* under N-limited conditions

Messieurs, c'est les microbes qui auront le dernier mot.

Gentlemen, it is the microbes who will have the last word.

Louis Pasteur

Abstract

Ammonium is the most common N-source for yeast fermentations. Although, its transport and assimilation mechanisms are well documented, there are only few attempts to measure *in vivo* the intracellular concentration of ammonium and assess its impact on gene expression. Using an isotope dilution mass spectrometry (IDMS)-based method it was possible to measure the intracellular ammonium concentration in N-limited aerobic chemostat cultivations in three different N-sources (ammonium, urea and glutamate) at the same growth rate (0.05 h^{-1}). The experimental results suggest that, at the same growth rate, there is a similar concentration of intracellular ammonium, about 3.6 mmol NH_4^+/L_{IC}, required to supply the reactions in the central N-metabolism independent of the N-source. Based on the experimental results and different assumptions, it was inferred the vacuolar and cytosolic ammonium concentrations. Furthermore, we identified a futile cycle caused by NH_3 leakage to the extracellular space, which can cost up to 30% of the ATP production of the cell in N-limited conditions, and a futile redox cycle between reactions Gdh1 and Gdh2. Finally, using a large proteomic survey it was possible to identify relative protein expression differences between the different environmental conditions tested and correlate those differences with previously identified N-compound sensing mechanisms.

Keywords

Metabolomics, proteomics, intracellular ammonium, ammonium transport, nitrogen metabolism, thermodynamics

This Chapter is submitted as: Cueto-Rojas H.F., Maleki Seifar R., ten Pierick A., van Helmond W., Pieterse M.M., Heijnen J.J., Wahl S.A., 2016. *In vivo* analysis of NH_4^+ transport and N-central metabolism in *Saccharomyces cerevisiae* under N-limited conditions, *Appl Environ Microbiol*.

Introduction

Saccharomyces cerevisiae is a versatile organism that can grow on a large variety of N-sources, namely ammonium (NH_4^+), urea, citrulline, ornithine, gamma aminobutyric acid (GABA), allatoin, allantoate, and all proteinogenic L-amino acids, with the exceptions of L-lysine, L-histidine and L-cysteine (Conrad *et al.*, 2014; Ljungdahl and Daignan-Fornier, 2012). Therefore, *S. cerevisiae* cells require a complex machinery to achieve metabolic regulation for efficient uptake, anabolic and catabolic processing of N-compounds.

Particularly, *S. cerevisiae* can differentiate between preferred and non-preferred N-sources using the Nitrogen Catabolite Repression (NCR) suprapathway. This system allows yeast cells to use first those N-sources, such as ammonium and glutamine, that promote a fast growth rate, over those compounds that sustain slow growth rates, such as isoleucine and methionine (Conrad *et al.*, 2014; Godard *et al.*, 2007; Ljungdahl and Daignan-Fornier, 2012). Although, nitrogen-sensing mechanisms are still not completely elucidated, several regulatory proteins including Ure2, Gln3, Gzf3, Tor1, Tor2 and Dal80 are known to influence the expression of NCR-sensitive genes.

One of the most relevant preferred N-sources for *S. cerevisiae* is ammonia/ammonium, which is the second most common N-compound on earth, and a well-known N-source of many organisms from the three kingdoms of life (Kleiner, 1981; Winkler, 2006). In aqueous solution ammonia is protonated producing the ammonium (NH_4^+) ion (equation 1).

$$NH_{4(aq)}^{+} \xleftrightarrow{pKa=9.25} NH_{3(aq)} + H_{(aq)}^{+} \quad (1)$$

It is widely accepted in the literature that NH_3 is transported via passive diffusion through cell membranes, with a permeability coefficient of 48×10^{-3} cm/s (1.73 m/h) in synthetic bilayer lipid membranes (Antonenko *et al.*, 1997) and 53×10^{-3} cm/s (1.91 m/h) in erythrocyte membranes (Labotka *et al.*, 1995). In contrast, there is an on-going debate about the particularities of the protein-mediated transport mechanism for NH_4^+ (Gruswitz *et al.*, 2010; Javelle *et al.*, 2007; Khademi *et al.*, 2004; Nakhoul and Lee Hamm, 2013). Particularly, in *S. cerevisiae*, Mep proteins (Methylamine and

ammonium permeases) are responsible for ammonium transport (Hess *et al.*, 2006) and sensing (Van Nuland *et al.*, 2006); the available experimental evidence (Boeckstaens *et al.*, 2008; Wood *et al.*, 2006) suggests that ammonium is transported against the chemical NH_3-gradient but in favour of an electrochemical gradient, therefore the mechanism must be membrane potential-driven (Ullmann *et al.*, 2012; Winkler, 2006). The three known Mep proteins are Mep1p, Mep2p and Mep3p with reported K_M values of 5-10 μM, 1-2 μM, and 1.4-2.1 mM, respectively (Marini *et al.*, 1997).

If we consider that ammonium is transported through a uniport mechanism dependent on the electrochemical gradient of ammonium ions across the cell membrane (Ullmann *et al.*, 2012), at thermodynamic equilibrium, the cytosol/extracellular ratio (from now on called in/out ratio) of total ammonium in both sides of the cell membrane can be calculated using equation 2 (a full derivation of this equation is found in **Appendix 4.1**).

$$\frac{\left[NH_3 + NH_4^+\right]_{total,Cyt}}{\left[NH_3 + NH_4^+\right]_{total,EC}} = \left(\frac{1+10^{pH_{in}\text{-}pKa}}{1+10^{pH_{out}\text{-}pKa}}\right) \times \exp\left(\frac{z \times F \times \Delta\psi_m}{R \times T}\right) \quad (2)$$

Under common cultivation conditions for *S. cerevisiae* (pH_{EC} = 5, T = 303 K, pH_{Cyt} = 6.5), the membrane potential equals $\Delta\psi_m$ = 110 mV (with the inside negative) and the proton motive force value is pmf = 200mV (inside negative); and the maximal in/out ratio of total ammonium equals 67, which indicates that the intracellular ammonium concentration will be higher than extracellular (Figure 4.1). Thus, it is clear that the electrochemically-driven Mep-dependent mechanism is advantageous for *S. cerevisiae* to accumulate intracellular ammonium, particularly when ammonium concentrations are low, which is typically the case in grape juices (Crepin *et al.*, 2014) and other ecologically relevant environments for *S. cerevisiae* such as fruit juices and fermentations musts, which are rich in fermentable sugars (Mortimer, 2000).

Urea is another industrially relevant nitrogen source for *S. cerevisiae* cultivations, particularly due to its safety, low cost and availability. Urea can be transported to the intracellular space using either i) passive diffusion/facilitated uniport uptake at urea concentrations

above 0.5 mmol urea/L (Cooper and Sumrada, 1975) or ii) using a H^+-symport protein (DUR3) with an apparent K_M= 14 µmol/L (Cooper and Sumrada, 1975) when extracellular concentrations of urea are lower than 0.25 mmol/L (Abreu *et al.*, 2010).

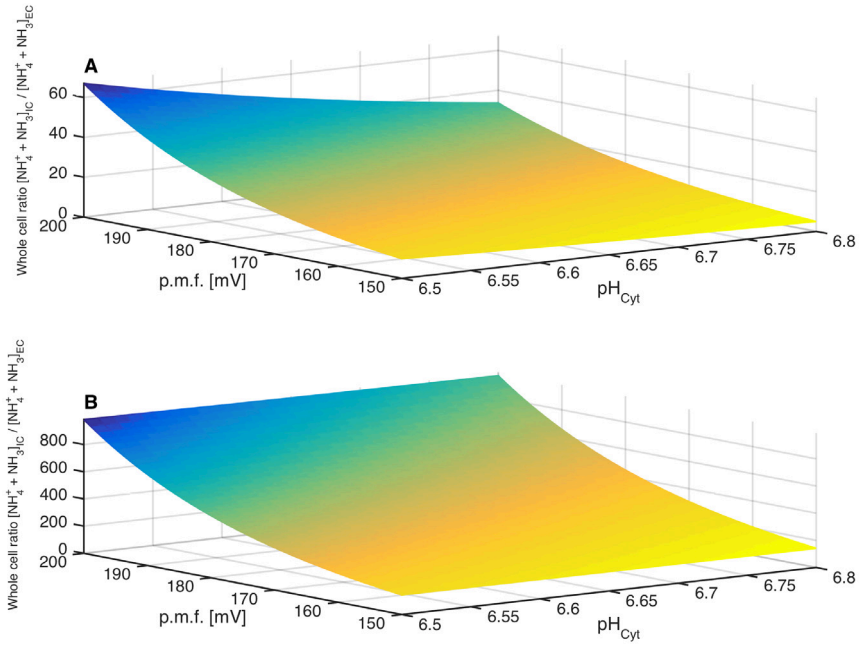

Figure 4.1. Thermodynamic equilibrium whole cell (IC) /extracellular (EC) ratios of the ammonium transporter -if a uniport mechanism is considered- at different values of cytosolic pH (pH_{Cyt}) and proton motive force (pmf). **(A)** Shows the values if it assumed that ammonium is evenly distributed in the whole cell (no compartmentalization), and **(B)** shows that NH_3-diffusion from the cytosol into an acidic compartment (vacuole) increases significantly the ratios. Whole cell concentrations are calculated using the intracellular mass balance for ammonium (eq. 9), NH_3-diffusion between cytosol and vacuole is considered to be an equilibrium process; the cytsol/vacuole ratio is calculated using eq. 10. The following assumptions were made: pH_{vac} = 4.5, V_{Cyt} = 0.7 V_{cell}, V_{vac} = 0.14 V_{cell}, and extracellular pH (pH_{EC}) = 5.

Once in the intracellular space, urea is further metabolized via ATP-dependent urea amidolyase (DUR1,2) (Milne *et al.*, 2015), which converts one molecule of urea into two molecules of ammonia and one molecule of CO_2 at the cost of the hydrolysis of 1 ATP molecule. Although, urea can sustain high growth rates (similar to ammonium)

it is known that major regulation systems such as NCR and SPS-mediated control do not operate when cells grow on urea (Godard *et al.*, 2007), which makes it one of the most interesting N-sources to study NCR-sensitive metabolic pathways.

Furthermore, glutamate is another preferred N-source like ammonium; this amino acid is taken up through a specific transporter. Several genome-scale stoichiometric models consider that the transport mechanism is a Glu^-/H^+ symport (Duarte *et al.*, 2004; Herrgard *et al.*, 2008; Nookaew *et al.*, 2008), the thermodynamic equilibrium in/out ratio of this mechanism, at pH = 5, can be calculated to be around 28 (see **Appendix 4.1**). It is known that amino acids promote the expression of their own specific transporters, for instance several amino acids trigger the response of the SPS-sensing mechanism which leads to the expression of certain amino acid permeases (Conrad *et al.*, 2014; Ljungdahl and Daignan-Fornier, 2012). Particularly glutamate being the central point of N-metabolism is expected to affect the expression of proteins related to C- and N-metabolism.

In the cytosol of *S. cerevisiae*, glutamate and glutamine are used to produce other amino acids. Nevertheless, all N-sources are converted into free ammonium, particularly for the production of glutamine if it is not present in the medium. Ammonium is assimilated using two main pathways to produce glutamate and glutamine. The first pathway involves the enzyme Glutamate Dehydrogenase (Gdh) NADPH-dependent (equation 3), which uses 2-Oxo-glutarate (αKG) as substrate.

Two enzymes catalyze the second pathway: Glutamine Synthase (eq. 4), and Glutamine 2-Oxo-glutarate Amino Transferase (eq. 5), this pathway is also called GS-GOGAT system (eq. 6). The amino group from glutamate is reported to be the source of 80% of the cellular nitrogen (Magasanik, 2003), and the amido group from glutamine is the source of the remaining 20% (Magasanik, 2003).

$$\begin{gathered} NH_4^+ + NADPH + \alpha KG \xrightarrow{Gdh} \text{L-glutamate} + H_2O + NADP \\ \Delta_r G^{0'} = -30.5 kJ/mol \end{gathered} \quad (3)$$

$$NH_4^+ + ATP + L\text{-}glutamate \xrightarrow{GS} L\text{-}glutamine + ADP + Pi + H^+ \quad \Delta_r G^{0'} = -5.6 kJ/mol \tag{4}$$

$$NADH + \alpha KG + L\text{-}glutamine + H^+ \xrightarrow{GOGAT} 2 \times L\text{-}glutamate + NAD^+ \quad \Delta_r G^{0'} = -56.2 kJ/mol \tag{5}$$

$$NH_4^+ + NADH + \alpha KG + ATP \xrightarrow{GS\text{–}GOGAT} L\text{-}glutamate + ADP + Pi + NAD^+ \quad \Delta_r G^{0'} = -61.8 kJ/mol \tag{6}$$

Comparing equation 6 and 3 shows that the GS-GOGAT system differs from Gdh by use of NADH instead of NADPH and concomitant consumption of 1 ATP. Although, the transporters and reactions by which ammonium and other N-sources are assimilated in the cell are well known, the impact of the intracellular ammonium concentration on the regulatory machinery of *S. cerevisiae* is still unclear. For *S. cerevisiae* many studies have described that central nitrogen metabolism is tightly regulated by the presence of ammonium, glutamate, glutamine and other nitrogenous compounds (Conrad *et al.*, 2014; Dikicioglu *et al.*, 2011; Fayyad-Kazan *et al.*, 2016; Magasanik and Kaiser, 2002). It was shown that a pulse of ammonium leads to significant changes in the expression of its own transporters, and genes related to N-assimilation and central carbon metabolism, among others (Dikicioglu *et al.*, 2011).

Aim of this work was to study *in vivo*, for different N-sources under aerobic N-limited conditions, the role of NH_4^+ in the transport and central N-metabolism of *S. cerevisiae*, particularly focusing on the effects of the N-source over the intracellular ammonium concentration and expression level of different proteins. The already available methods for quantification of glutamate and glutamine (de Jonge *et al.*, 2011) together with new IDMS-based methods for ammonium and urea were applied to study for three N-sources (NH_4^+, urea and glutamate), compartmentalization and the thermodynamic status of central N-metabolism; furthermore, a large proteomic survey was carried out to obtain data to elucidate the potential effects of these three N-sources on protein expression. The experiments were performed with *S. cerevisiae* in aerobic chemostats using glucose as C-source under N-source limitation to avoid

excessive extracellular N-source to facilitate the study of N-source transport and, more specifically, to increase the accuracy of the intracellular NH_4^+ quantification.

Materials and Methods

Strain and culture conditions

The prototrophic strain *Saccharomyces cerevisiae* CEN.PK 113-7D was obtained from the Centraalbureau voor Schimmelcultures (Fungal Biodiversity Center, Utrecht, The Netherlands) was cultivated in aerobic glucose-fed N-limited chemostats ($D \approx 0.05\ h^{-1}$) using three different nitrogen sources: ammonium, urea and L-glutamic acid. The media used for inoculum preparation, batch and chemostat experiments are modifications of the N-limiting medium reported by Boer *et al.* (2003). The media contained: Glucose monohydrate 130 g/L (656.56 mM), $MgSO_4 \cdot 7H_2O$ 1.14 g/L (4.62 mM), KH_2PO_4 6.9 g/L (50.7 mM), trace elements 2 mL/L (Postma *et al.*, 1989), vitamins solution 2 mL/L (Bruinenberg *et al.*, 1983) and antifoam C 0.3 g/L. At low dilution rate under aerobic N-limiting conditions metabolic oscillations (Silverman *et al.*, 2010) were observed, which are detrimental to steady state studies. It was found empirically that supplementation of the media with ethanol (as suggested by Suarez-Mendez *et al.* (2016)) to a final concentration of 25 g/L (543.48 mM) avoided these metabolic oscillations, thus all media contained that ethanol concentration. The N-sources used were $NH_4H_2PO_4$ (3.48 g/L), urea (0.9 g/L) and L-glutamic acid (4.44 g/L), all N-sources were added to a final concentration of 30.26 mmol-N/L, which is sufficient to produce about 8 g_{CDW}/L. All media were adjusted before use to a final pH of 5 using KOH as titrant.

To start the NH_4^+-limited culture, two 500 mL Erlenmeyer flasks containing 200 mL of ammonium-limited medium each were inoculated with 1-mL cryovials (glycerol, -80 ºC) of yeast cells, and incubated at 30 ºC, 200rpm for 12 h. After morphological inspection to check purity of the culture, one of the flasks was used to inoculate a 7 L bioreactor (Applikon, Schiedam, The Netherlands) with a working volume of 4 L. The reactor temperature was kept constant at

30 ºC; dissolved oxygen tension (DOT) was monitored in-line using an oxygen probe (Mettler-Toledo, Tiel, The Netherlands). A stirring speed of 500 rpm, overpressure of 0.3 bar, and aeration rate of 0.5 vvm were used to keep the dissolved oxygen level above 80%. The fractions of CO_2 and O_2 in the dry off-gas were measured on-line using a combined paramagnetic/infrared analyser (NGA 2000, Fisher-Rosemount, Hasselroth, Germany). The pH was kept at 5 with automatic additions of 4M KOH or 2M H_2SO_4.

Once the batch phase was finished, fresh ammonium-limited medium was fed to the reactor at a dilution rate of $D \approx 0.05\ h^{-1}$. After reaching steady state and taking the samples, the medium was switched to urea-limited medium keeping the dilution rate constant; the same operation was performed to switch the N-source from urea to L-glutamic acid.

All samples were taken at each steady state, after stable values of DOT and off-gas CO_2 and O_2 were obtained between three and seven volume changes after switching the medium. To obtain biomass specific uptake and production rates, extracellular concentration measurements, flow rates and volumes were used together with the appropriate fermenter balance equations for broth components: glucose, ammonium, biomass, ethanol, glycerol, acetate and for gas components: O_2, CO_2 and ethanol. Ethanol evaporation has a big impact over the ethanol balance and C-recovery; the ethanol evaporation constant (k_{evap}) was experimentally determined, as explained in **Appendix 4.2**.

Internal standards

Ammonium

Since our in-house prepared U-^{13}C-yeast cell extract (Wu *et al.*, 2005) contained a high concentration of ^{14}N-NH_4^+, samples for intracellular ammonium quantification were prepared separately using as internal standard a solution of ^{15}N- NH_4Cl 98% atom ^{15}N LOT# TA0525V (Sigma Aldrich) dissolved in milli-Q water to a concentration of 500 μmol/L.

Urea

^{13}C, $^{15}N_2$-Urea 99% atom ^{13}C, 98% atom ^{15}N LOT# SZ0618V (Sigma Aldrich) was dissolved in milli-Q water and added to the in-house prepared uniformly labeled ^{13}C-yeast cell extract (Wu *et al.*, 2005) to a final concentration in the sample of 20 µmol/L (concentration in the extract equals 100 µmol/L). Previously, it was experimentally observed that this cell extract did not contain any labeled or non-labeled urea; the mixture of U-^{13}C-yeast cell extract and ^{13}C, $^{15}N_2$-Urea was used as internal standard in samples selected for analysis of intracellular metabolites and urea.

Sampling and sample preparation

Samples for extracellular metabolites and ammonium analyis

Samples of approx. 1 mL_{broth} for quantification of extracellular metabolites and ammonium were quenched using cold steel beads in a syringe, as described by Mashego *et al.* (2006), and filtered using 0.45 µm disc filters (Milipore). 80 µL of filtrate were mixed with 20 µL of internal standard (500 µmol/L ^{15}N-NH_4Cl) and derivatized according to the protocol used for ammonium quantification by LC-MS. The rest of the filtrate was stored at -80 ºC until further analysis of the extracellular metabolites.

Rapid sampling and biomass extraction for intracellular metabolites and intracellular ammonium

Samples of approximately 1.2 g of broth were taken with a dedicated rapid-sampling setup (Lange *et al.*, 2001), quenched in 6 mL of -40 ºC methanol 100%, and after weighting to determine the mass of the sample they were centrifuged 5 minutes at 10000G and -19 ºC. For biomass washing, the pellet was recovered and resuspended in 6 mL -40 ºC methanol 100%; centrifuged again 5 minutes at 10000G and -19 ºC.

CM: Cold Non-buffered Chloroform-Methanol extraction of the biomass pellet

The biomass pellet obtained from *Rapid sampling for intracellular metabolites and intracellular ammonium* was recovered, 3.5 mL of Methanol-milli-Q water 50%(v/v) pre-chilled at -40 ºC was added, and

then 120 µL of U-^{13}C- cell extract with labeled urea. Afterwards, 3.5 mL of Chloroform 100% pre-chilled at -40 ºC was added in order to extract intracellular metabolites according to Canelas *et al.* (2009). This method was used to extract intracellular metabolites, excluding ammonium, particularly to protect acid unstable metabolites, *e.g.* NADH and NADPH.

CM5: Cold Chloroform-Methanol buffered at pH = 5 extraction of the biomass pellet

The biomass pellet obtained from *Rapid sampling for intracellular metabolites and intracellular ammonium* was recovered, 3.5 mL of Methanol-acetate buffer 10mM (pH = 5) 50%(v/v) pre-chilled at -40 ºC was added, and then 120 µL of U-^{13}C- cell extract with labeled urea (intracellular metabolites samples) or 120 µL of ^{15}N- NH_4Cl 500 µmol/L (intracellular ammonium samples) were added as internal standard. Afterwards, 3.5 mL of Chloroform 100% pre-chilled at -40 ºC was added in order to extract intracellular metabolites according to Cueto-Rojas *et al.* (2016). Samples for quantification of intracellular ammonium were extracted using exclusively this method.

Analytical methods

Dry weight, cell count, size distribution and average cell volume

Determination of cell dry weight was performed gravimetrically using pre-weighted 0.45 µm filters (Millipore). The broth was removed by filtration, and the cell pellet in the filter was washed with milli-Q water. The filters were dried at 70 ºC until constant weight (approx. 72h).

To calculate the intracellular concentrations (mmol/L_{IC}) from the intracellular amounts (µmol/g_{CDW}) the cell volume was measured as described by Bisschops *et al.* (2014) using a Coulter counter with a 50-µm orifice (Multisizer II, Beckman, Fullerton, CA), the average cell volume (in mL_{IC}/g_{CDW}) was estimated using equation 7.

$$V_{cell}\left(\frac{mL_{IC}}{g_{CDW}}\right)=\frac{\text{Average particle volume (fL)}\times\text{Average number of particles (particles/L)}}{\text{Dry weight }(g_{CDW}/L)}\times10^{-12} \quad (7)$$

Metabolite quantification

100 µL of extracellular samples were used to quantify glucose, ethanol, glycerol and acetate using HPLC as described by Cruz *et al.* (2012). Quantification of αKG, pyruvate and trehalose was performed using GC-MS/MS as described by Niedenfuhr *et al.* (2015). The concentrations of the coenzymes NAD, NADH, NADP, NADPH were measured using LC-MS/MS as described by Maleki Seifar *et al.* (2013) and nucleotides according to Maleki Seifar *et al.* (2009). Amino acids and urea were measured using GC-MS according to de Jonge *et al.* (2011). Finally, intra- and extracellular ammonium were quantified according to Cueto-Rojas *et al.* (2016).

Protein quantification

U-^{13}C-labelled *S. cerevisiae* biomass was prepared as described by Wu *et al.* (2005) and used as internal standard for relative protein quantification. Cell suspensions of the sample biomass and internal standard were mixed 1:1 based on the OD_{600}, washed with milli-Q and freeze-dried. Proteins were extracted by grinding the freeze-dried biomass with pestle and mortar, which were precooled with liquid nitrogen. After grinding, 2 mL of 50 mM PBS with 200 mM NaOH was added to extract proteins. The soluble protein fraction was separated from the cell debris by centrifugation at 13,300 rpm for 15 minutes. Proteins were precipitated overnight in cold acetone at -20 ºC by adding 4 parts of cold acetone to 1 part of protein solution. After washing and drying the protein pellet was dissolved in 400 µL of 100 mM ammonium bicarbonate (ABC) with 6 M urea. Of this solution, 20 µL was further processed; proteins were reduced by addition of tris(2-carboxyethil)phosphine (TCEP) to a final concentration of 10 mM and incubating for 60 minutes at room temperature.

Proteins were alkylated by addition of Iodoacetamide (IAM) to a final concentration of 10 mM and incubating for 60 minutes at room temperature. Prior to digestion the protein solution was 6 times diluted by addition of 100 µL of 100 mM ABC to dilute the urea concentration to 1 M. Proteins were digested by addition of trypsin (trypsin singles, proteomics grade, Sigma-Aldrich) in a 1:100 ratio and incubating at 37 ºC for 16 hours. The digested protein mixture

was purified and concentrated using an in-house made SPE pipette tip using 5 µm particles of Reprosil-Pur C_{18}-Aq reversed phase material (Dr. Maisch GmbH, Ammerbuch-Entringen, Germany).
Digested peptides were separated using nanoflow chromatography performed using a vented column system essentially as described by Meiring *et al.* (2002) and a 2-dimensional precolumn (RP-SCX-RP). Analytical columns of 50 µm id were prepared with a 1 mm Kasil frit and packed with 5 µm particles of Reprosil-Pur C_{18}-Aq reversed phase material to a length of 40 cm. The capillary RP-SCX-RP precolumn of 150 µm id was prepared with a 1 mm Kasil frit and packed with 5 µm particles of Reprosil-Pur C18-Aq reversed phase material to a length of 17 mm, 5 µm particles of PolySulfoethyl a strong cation exchange material for 60 mm and again 5 µm particles of Reprosil-Pur C_{18}-Aq reversed phase material for 17 mm (total length 94 mm). The different column materials were kept separated from each other by insertion of a piece of glass wool. The used LC equipment and solvents were similar to Finoulst *et al.* (2011).
Each sample analysis consisted of six fractionations. In the first fraction the peptides are injected and trapped on the precolumn by applying 100% solvent A for 10 min. Then a first linear gradient was applied from 4 to 35% B in 75 min. After this, a linear gradient to 80% B was followed for 6 min and then 3 min of 80% B. Finally the column was reconditioned for 26 min with 100% A. In the following 5 fractionations, peptides were eluted by 10 µL injections of respectively 5, 10, 50, 250 or 1000 mM ammonium formate pH 2.6 from the autosampler (followed by 100% A for 10 min). Again a first linear gradient was applied from 4 to 35% B in 75 min, followed by a second linear gradient to 80% B for 6 min and then 3 min of 80% B. After each fraction the column was reconditioned for 26 min with 100% A. This results in six fractionations per sample with a total run-time of 12 hours per sample. For each analysis ~10 µg of protein was injected.
Mass spectrometry was performed using a protocol derived from Finoulst *et al.* (2011). Full scan MS spectra (from m/z 400–1500, charge states 2 and higher) were acquired at a resolution of 30,000 at m/z 400 after accumulation to a target value of 10^6 ions (automatic

gain control). Nine data-dependent MS/MS scans (HCD spectra, resolution 7,500 at m/z 400) were acquired using the 9 most intense ions with a charge state of 2+ or higher and an ion count of 10,000 or higher. The maximum injection time was set to 500 ms for the MS scans and 200 ms for the MS/MS scan (accumulation for MS/MS was set to target value of 5×10^4). Dynamic exclusion was applied using a maximum exclusion list of 50, one repeat count, repeat duration of 10 s and exclusion duration of 45 s. The exclusion window was set from −10 to + 10 ppm relative to the selected precursor mass.

Data processing and analysis was performed similarly to Finoulst *et al.* (2011). Briefly, MS/MS spectra were converted to Mascot Generic Files (MGF) using Proteome Discoverer 1.4 (ThermoFisher Scientific) and DTASuperCharge version 2.0b1 (Mortensen *et al.*, 2010). MGF's from the 6 SCX fractions of the same sample were combined using MGFcombiner version 1.10 (Mortensen *et al.*, 2010). The samples were analyzed with Mascot v2.2.02 search engine (Matrix Science, Boston, MA, USA). As reference proteome the Uniprot (UniProt, 2015) proteome of *Saccharomyces cerevisiae* strain ATCC 204508 / 288c (ID: UP000002311; 6634 sequences) was used.

Carbamidomethyl cysteine was set as a fixed modification and oxidized methionine as a variable modification. Trypsin was specified as the proteolytic enzyme, and up to three missed cleavages were accepted. Mass tolerance for fragment ions was set at 0.05 Da and for precursor peptide ions at 10 ppm. Peptides with Mascot score <10 were removed and only the highest scoring peptide matches for each query listed under the highest scoring protein (bold red) were selected. Proteins were quantified using MSQuant version 2.0b7 (Mortensen *et al.*, 2010) by importing the Mascot results html file with the corresponding raw mass spectrometric data files. MSQuant automatically calculated peptide and protein ratios by using a ^{13}C quantitation method (in quantitationmodes.xml), containing 7 modifications based on the amount of carbon atoms each amino acid contains. The difference in mass between ^{12}C and ^{13}C is 1.00335 Da. Resulting in mass shifts of 2 (glycine), 3 (ASC), 4 (NDT), 5 (EQMPV), 6 (RHILK), 9 (FY) or 11 (W) carbon atoms. Quantification was restricted to peptides with Mascot score ≥25.

Results

Overview of the q-rates found under N-limited aerobic cultivations

Table 4.1 shows the experimental results of the N-limited cultures, q-rates are shown for the different N-sources. As expected they are very similar, because of the same growth rate used. The residual glucose concentration is much larger than in a glucose-limited chemostat, which is 0.07mM in the later case (Suarez-Mendez *et al.*, 2016), showing that N-source limitation is achieved.

Also there is a large production of ethanol and a large trehalose content (approx. 10% w/w), which is expected under N-source limitation (Boer *et al.*, 2010; Hazelwood *et al.*, 2009). Finally, the N-source limitation is confirmed by the low extracellular concentrations of the used N-sources. The uptake rate of N-source (in µmol $N/g_{CDW}/h$) is the same for each N-source and shows that the biomass for the 3 N-sources has an N-content ranging between 5.92% and 6.23%, which is also expected. Using the q-values it is possible to estimate the ATP production rate, assuming 1 mol ATP produced per mol ethanol and 1.90 mol ATP produced per mol O_2 consumed (Verduyn *et al.*, 1991), leads to nearly the same value of q_{ATP} (around 7.8 mmol $ATP/g_{CDW}/h$) for the 3 N-sources. Under aerobic glucose limited conditions it is known that 1 mol ATP allows the synthesis of 16 g_{CDW} (Verduyn *et al.*, 1990), which at $\mu = 0.05\ h^{-1}$ leads to q_{ATP} = 3.12 mmol $ATP/g_{CDW}/h$. This comparison shows that under N-limited conditions, independent of the N-source, there is an extra ATP dissipation of 4.7 mmol/$ATP/g_{CDW}/h$.

Intra- and extracellular concentrations of N-sources under N-limited conditions

The intra- and extracellular NH_4^+ analysis showed surprising results:

1) NH_4^+ is transported from inside to outside when urea or glutamate were used as N-source, as deduced from the presence of extracellular ammonium. A similar phenomenon was observed by Marini *et al.* (1997) and Boeckstaens *et al.* (2007).

Table 4.1. Overview of the main experimental results between different N-sources, values for experimentally measured concentrations and cell volume are average ± std. error of three independent samples from the same steady state. N-content and q-rates are reported as mean value ± std. error calculated assuming linear error propagation.

Experimental variable	N-source		
	NH_4^+	Urea	L-glutamate
Biomass concentration (C_X in g_{CDW}/L)	7.41 ± 0.05	7.60 ± 0.04	7.14 ± 0.02
Residual glucose (C_S in mmol/L)	117.46 ± 2.07	113.11 ± 2.81	144.70 ± 1.27
Residual N-source (C_N in mmol/L)	0.008 ± 0.001	0.024 ± 0.006	0.467 ± 0.012
μ (h^{-1})	0.0517 ± 0.0001	0.0525 ± 0.0001	0.0501 ± 0.0001
$-q_{N\text{-source}}$ (μmol N/g_{CDW}/h)	226 ± 7	222 ± 1	223 ± 1
$-q_{O2}$ (mmol/g_{CDW}/h)	1.518 ± 0.010	1.427 ± 0.008	0.978 ± 0.005
q_{CO2} (mmol/g_{CDW}/h)	7.160 ± 0.044	7.249 ± 0.038	7.211 ± 0.015
$-q_S$ (mmol/g_{CDW}/h)	3.697 ± 0.028	3.907 ± 0.033	4.027 ± 0.013
q_{EtOH} (mmol/g_{CDW}/h)	4.998 ± 0.058	5.149 ± 0.145	5.874 ± 0.027
q_{ATP}(mmol/g_{CDW}/h)*	7.883 ± 0.060	7.861 ± 0.146	7.732 ± 0.028
N-content (% w/w)**	6.11 ± 0.20	5.92 ± 0.14	6.23 ± 0.02
Average cell volume (mL_{IC}/g_{CDW})	2.13 ± 0.04	1.97 ± 0.02	1.88 ± 0.03
Intracellular Trehalose (μmol/g_{CDW})	266.1 ± 3.1	249.2 ± 21.8	252.9 ± 8.6
Intracellular Glutamate (μmol/g_{CDW})	83.81 ± 1.60	71.72 ± 4.74	151.23 ± 6.45
Intracellular ammonium (μmol/g_{CDW})	6.89 ± 1.35	7.40 ± 0.39	7.17 ± 1.29
Extracellular ammonium (μmol/L_{EC})	7.6 ± 0.3	7.6 ± 2.3	9.1 ± 0.8

* Calculated as the sum of ATP produced through alcoholic fermentation and complete substrate oxidation. Assuming: 1 mol ATP/mol ethanol and P/O ratio of 0.95 (Verduyn *et al.*, 1991), this leads to $q_{ATP} = q_{EtOH} + 2\times0.95\times(-q_{O2})$.

** Calculated from the values of q_N and μ reported hereby.

2) For the 3 N-sources both, intracellular and extracellular, NH_4^+ concentrations are very close; this suggests that the NH_4^+-

scavenging/uptake mechanisms have similar affinity and equilibrium constants in all cases, meaning a common NH_4^+ transport mechanism.

3) The intracellular NH_4^+ concentration for the 3 N-sources is nearly the same. Using the measured average cell volumes the intracellular NH_4^+ concentrations follows as 3.24, 3.76 and 3.82 mmol/L_{IC}. For the cases of urea -which is hydrolyzed to ammonium and CO_2- and ammonium it was expected a similar intracellular ammonium concentration; in contrast it was expected intuitively a lower intracellular ammonium concentration when L-glutamate is the N-source, given that nitrogen is already provided as an amino acid and ammonium is only required for L-glutamine synthesis. This nearly constant level points to an important role of intracellular NH_4^+ in the regulation of N-metabolism.

4) From the measured NH_4^+ concentrations it can be calculated that >85% of total broth ammonium is inside the cells and the remaining is found in the extracellular space.

5) The in/out concentration ratio of NH_4^+ is about 475 for the 3 N-sources. This is far higher than the equilibrium ratio of 67, expected for the assumed NH_4^+-uniporter. One hypothesis, elaborated below, is that there is a strong compartmentalization of NH_4^+ between cytosol and vacuole (Figures 4.2 to 4.4).

For the urea limited culture intra- and extracellular urea concentrations show that, in contrast to NH_4^+ as N-source, the majority (80%) of the total broth urea is found in the extracellular space. The intracellular urea concentration (151 ± 48 µmol/L_{IC}) is higher than the extracellular concentration (23 µmol/L_{EC}), the in/out ratio of 6 is against the expectation based on urea uniport, which sets a maximum in/out ratio of 1. From the glutamate limited culture it follows that around 70% of the glutamate is found in the intracellular space. The in/out ratio is calculated to be >200, which is also higher than the ratio of 28 expected from a Glu^-/H^+ symporter.

Intracellular metabolites and large proteomics survey

Next to the intracellular concentrations of the N-sources, different metabolites were measured (Table 4.2) to determine the thermodynamic status of the most relevant reactions involved in the central N-metabolism. Particularly, it is interesting to analyze the reaction glutamate dehydrogenase NAPDH-dependent (Gdh1), as it is the main N-assimilating reaction in *S. cerevisiae*. Table 4.3 shows the most relevant N-metabolism reactions under NH_4^+, urea and glutamate limiting conditions.

Table 4.2. Measured intracellular metabolite concentrations under N-limited chemostat cultivations of *S. cerevisiae* (D=0.05 h^{-1}). The results shown are average ± std. error of three independent samples from the same steady state.

Metabolite	NH_4^+ (mmol/L_{IC})	Urea (mmol/L_{IC})	Glutamate (mmol/L_{IC})
Ammonium	3.239 ± 0.634	3.755 ± 0.198	3.819 ± 0.686
Urea	B.Q.L.	0.151 ± 0.048	B.Q.L.
Glutamate	39.363 ± 0.780	36.416 ± 2.407	80.543 ± 3.437
Glutamine	14.106 ± 0.346	13.083 ± 0.919	15.293 ± 0.531
Alanine	18.756 ± 0.329	16.593 ± 1.344	21.413 ± 0.789
Pyruvate	3.552 ± 0.142	3.722 ± 0.423	2.902 ± 0.115
αKG	0.338 ± 0.004	0.524 ± 0.037	3.067 ± 0.027
NAD	0.816 ± 0.050	0.921 ± 0.049	1.178 ± 0.072
NADH	0.013 ± 0.008	0.015 ± 0.007	0.046 ± 0.018
NADP	0.208 ± 0.015	0.241 ± 0.008	0.224 ± 0.011
NADPH	0.018 ± 0.003	0.015 ± 0.001	0.020 ± 0.001
AMP	0.290 ± 0.019	0.330 ± 0.020	0.379 ± 0.022
ADP	0.686 ± 0.012	0.775 ± 0.022	0.967 ± 0.024
ATP	2.223 ± 0.038	2.345 ± 0.036	2.860 ± 0.052
Energy charge	0.802 ± 0.019	0.792 ± 0.020	0.795 ± 0.021

B.Q.L. = below quantification limit

Finally, the experimental design was such that the different N-sources would allow identifying the differences in expression of key proteins of the central nitrogen metabolism; particularly it was aimed at covering a large number of proteins from the proteome of *S. cerevisiae* to identify regulators, transcription factors and key

pathway enzymes; Figure 4.5a summarizes the main results of our proteomic survey showing that more than 500 proteins were identified with more than 3 confidence peptides, from this analysis only the main findings will be commented.

Discussion

NH_4^+ compartmentalization model of S. cerevisiae

From the NH_4^+ experimental results it appeared that the measured in/out ratio of 475 is far higher than the equilibrium value of 67 (Figure 4.2) calculated for the assumed uniport mechanism. Nevertheless, the in/out ratio also does point at a membrane potential-driven mechanism opposing the conclusions of Soupene *et al.* (2001), who suggested that MEP proteins transport NH_3. From the experimental results it is clear that MEP proteins transport NH_4^+/NH_3 against the concentration gradient of NH_3, but in favor of an electrochemical gradient. A possible explanation for such high in/out ratios is the presence of a NH_4^+/ H^+ symporter; it is highly unlikely that such a transporter is active in yeast. As discussed by many authors the MEP/Amt protein family transports ammonium probably by uniport of NH_4^+ (Hall and Yan, 2013; Kleiner, 1981; Ullmann *et al.*, 2012), or thermodynamically equivalent (Boeckstaens *et al.*, 2008), and at the moment there is no further evidence to support the hypothesis of a symporter mechanism; the only report to our knowledge of a NH_4^+ symport was reported by Ritchie (2013), this author described a Na^+/ NH_4^+ symport mechanism in cyanobacteria at extracellular pH=7.5.

It was discussed by Wood *et al.* (2006) that in the cytosol of plant cells ammonium (NH_4^+) deprotonates into ammonia (NH_3), and this uncharged species diffuses into the vacuole where it is protonated again due to the acidic pH of this compartment. It is probable, that in yeast a similar mechanism occurs. First, ammonia (NH_3) diffuses from the slightly acidic environment of the cytosol (pH_{Cyt}=6.5) into the much more acidic vacuolar space, pH_{Vac} between 4 to 5 (Brett *et al.*, 2011). If no other transporter removes ammonium from the

vacuole it is possible to achieve an equilibrium ratio of ammonium (NH_4^+) across the vacuolar membrane where $[NH_4^+]_{Vac}$>>$[NH_4^+]_{Cyt}$.

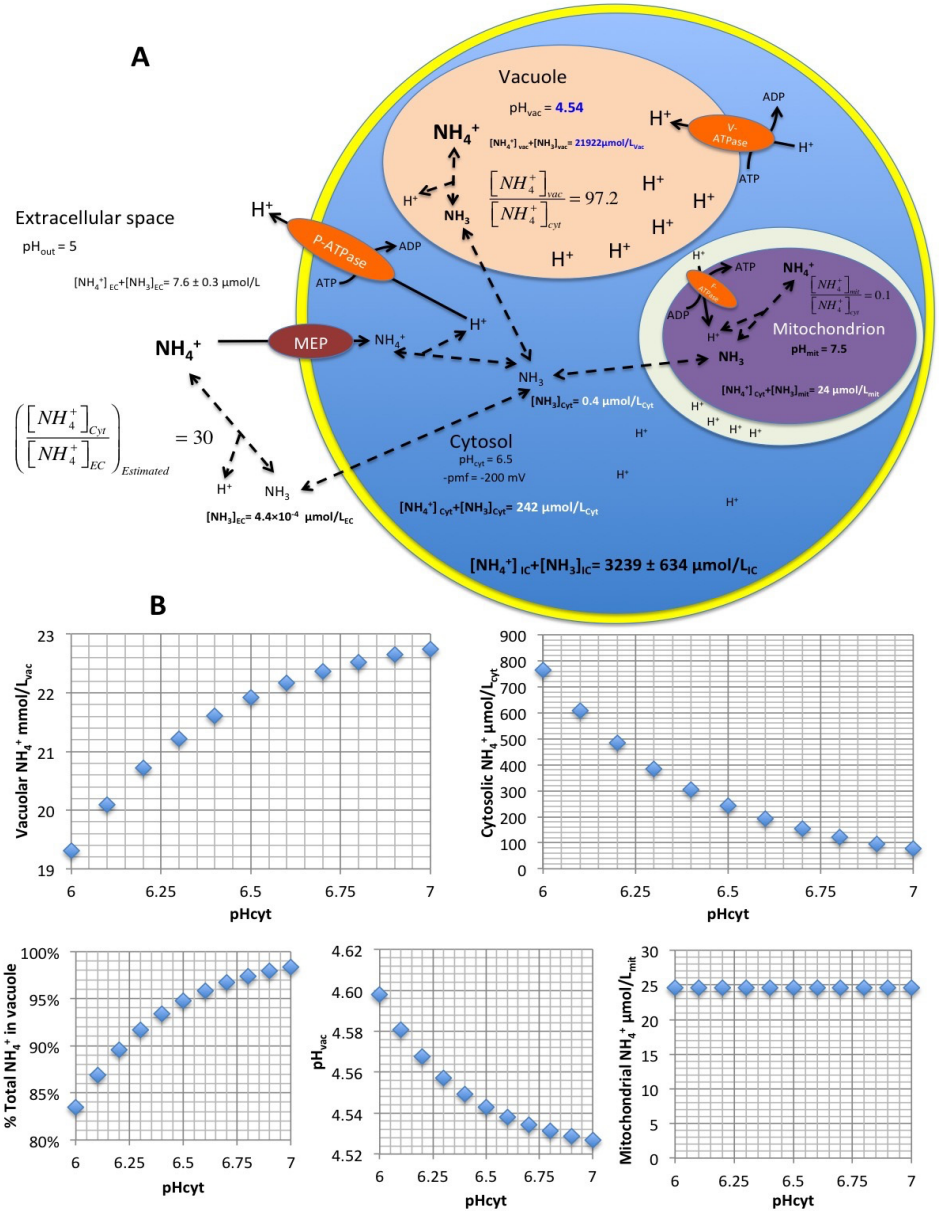

Figure 4.2. (A) Estimated intracellular ammonium distribution and pH_{Vac}. **(B)** Sensitivity analysis of $[NH_4^+]_{cyt}$, $[NH_4^+]_{vac}$, % total NH_4^+ in vacuole, pH_{vac} and $[NH_4^+]_{mit}$ values with respect to pH_{cyt}. The highest impact is observed in $[NH_4^+]_{cyt}$ and % total NH_4^+ in vacuole, whereas in pH_{vac} and $[NH_4^+]_{vac}$ the impact is lower than 10%; pH_{cyt} has no impact over $[NH_4^+]_{mit}$.

It has been estimated that the vacuolar volume is close to 14% of the total cell volume. On the other hand mitochondrial volume is around 1% and cytosol accounts for 70% of the whole cell volume (Uchida *et al.*, 2011). Using these compartment volumes, it is possible to estimate a feasible ammonium distribution (cytosol, mitochondria and vacuole) inside the cell using:

1) The balance of intracellular ammonium and compartment volumes relative to the whole cell (equation 9).

$$\left[NH_3+NH_4^+\right]_{IC} = 0.7\times\left[NH_3+NH_4^+\right]_{cyt} + 0.14\times\left[NH_3+NH_4^+\right]_{vac} + 0.01\times\left[NH_3+NH_4^+\right]_{mit} \quad (9)$$

2) The ammonium equilibrium ratios vacuole/cytosol and mitochondria/cytosol can be calculated assuming that NH_3 diffusion is the only transport mechanism between these compartments; these equilibrium ratios are dependent on the pH difference between compartments (*e.g.* pH_{cyt}=6.5, pH_{mit}=7.5 and pH_{vac}=4.5). The vacuole is the most relevant NH_4^+-storage compartment and the equilibration assumption of NH_3 is relevant to discuss. To calculate the NH_3-flux to the vacuole, its area is needed, assuming a large spherical vacuole per cell with a diameter of 0.77 µm (a sphere that occupies 14% of the cell volume, in average 34 fL/cell as measured in this study) leads to a vacuolar area (a_{vac}) of 0.11 m^2/g_{CDW}. From the measured intracellular NH_4^+ concentration (3.24 $mmol/L_{IC}$, Table 4.1), it is possible to estimate the intracellular NH_3 at cytosolic pH (pH_{cyt}=6.5), which is 0.006 mol/m^3_{IC}. Assuming that all intracellular ammonium is cytosolic leads to a maximal NH_3-flux into the vacuole of 1.2 mmol $NH_3/g_{CDW}/h$ ($NH_3\text{-}flux_{vac}$ = $P_{1a}\times a_{vac}\times[NH_3]_{cyt}$); considering a permeability of 1.73 m/h (Antonenko *et al.*, 1997).

This illustrates that the maximal flux over the membrane could be more than 5 times higher than the N-uptake rate (0.226 $mmol/g_{CDW}/h$, Table 4.1) and shows that the cytosol/vacuole equilibrium assumption is realistic due to the potentially high NH_3 diffusion rate between these compartments. In contrast, NH_3 diffusion over the cell membrane into the cytosol is much slower due to the low extracellular pH (pH_{EC} = 5) and total ammonium concentration (7.6 $\mu mol/L_{EC}$), which lead to very low $(NH_3)_{EC}$

concentrations and therewith very low NH_3 diffusion fluxes into the cytosol.

3) The vacuolar and mitochondrial pH are variables needed in the system of algebraic equations, but it is assumed that the cytosolic and mitochondrial pH remain the same as previously measured in exponentially growing cells, being 6.5 (Kresnowati *et al.*, 2007) and 7.5 (Orij *et al.*, 2009), respectively. The equilibrium ratios are (10) and (11):

$$\frac{\left[NH_3+NH_4^+\right]_{vac}}{\left[NH_3+NH_4^+\right]_{cyt}}=\left(\frac{1+10^{pKa-pH_{vac}}}{1+10^{pKa-pH_{cyt}}}\right)=97.2 \tag{10}$$

$$\frac{\left[NH_3+NH_4^+\right]_{mit}}{\left[NH_3+NH_4^+\right]_{cyt}}=\left(\frac{1+10^{pKa-pH_{mit}}}{1+10^{pKa-pH_{cyt}}}\right)=0.1 \tag{11}$$

Using pKa=9.25 and pH_{vac}=4.5, it is observed that the vacuole can indeed store a substantial amount of ammonium, but the mitochondrion does not function as NH_4^+ storage compartment, given its small volume and high pH.

4) Finally, the kinetic parameters (V_{max} and K_M) for the different transmembrane ammonium transporters were estimated by Marini and coworkers (Marini *et al.*, 2006; Marini *et al.*, 1997), particularly it is assumed that only MEP2 is relevant as the main ammonium transporter, as suggested by previous transcriptomics data obtained from N-limited cultivations (Hazelwood *et al.*, 2009). Values found are V_{max} = 600 µmol/gCDW/h (equivalent to 20 nmol/min/$mg_{Protein}$ (Marini *et al.*, 1997), assuming 0.5 $g_{Protein}/g_{CDW}$) and K_M = 2 µmol/L (Marini *et al.*, 1997) and the kinetic expression (Canelas *et al.*, 2011) that describes ammonium uptake under N-limiting conditions is equation 12.

$$-q_N=-V_{max}\times\left(\frac{\left[NH_3+NH_4^+\right]_{EC}}{\left[NH_3+NH_4^+\right]_{EC}+K_M}\right)\times\left(1-\frac{\frac{\left[NH_3+NH_4^+\right]_{cyt}}{\left[NH_3+NH_4^+\right]_{EC}}}{K_{eq}}\right) \tag{12}$$

Equation 12 is a q-linear expression (Canelas *et al.*, 2011) that can be used to model the specific rate of ammonium uptake ($-q_N$) based on the maximum ammonium uptake rate (V_{max}), the thermodynamic driving force ($1-Q/K_{eq} = 1-([NH_3+NH_4^+]_{cyt}/[NH_3+NH_4^+]_{EC})/K_{eq}$) and the mechanism specific non-linear function of concentrations and affinities ($[NH_3+NH_4^+]_{EC}/([NH_3+NH_4^+]_{EC}+K_M)$), being K_M the affinity constant of the main transporter (Mep2).

Given that –qN, total intra- and extracellular ammonium are experimentally measured, the system of 4 algebraic equations (eq. 9-12) can be solved using any conventional solver (for instance *fsolve* in Matlab®) to calculate pH_{vac}, $[NH_4^+]_{cyt}$, $[NH_4^+]_{mit}$ and $[NH_4^+]_{vac}$. These calculations (Figure 4.2a) indeed show that most of the intracellular ammonium is compartmentalized in the vacuole (around 95% of the total intracellular pool), and the cytosolic NH_4^+ concentration is very low. This result is in agreement with the experimental observations using the analogue molecule methylamine, which suggested that most of the methylamine is compartmentalized (Soupene *et al.*, 2001; Wood *et al.*, 2006). Figure 4.2a also shows that, with the very low $[NH_4^+]_{Cyt}$ concentration, the ratio $[NH_4^+]_{Cyt}/[NH_4^+]_{EC} = 30$, which is about 50% of the thermodynamic equilibrium value for the uniport mechanism. This shows that the NH_4^+-transporter operates not far from thermodynamic equilibrium, if it is an NH_4^+-uniporter or thermodynamically equivalent.

The results of figure 4.2a depend on the assumption of pH_{Cyt}. Experimental evidence shows that pH_{Vac} could take values between 4 and 5, and pH_{Cyt} = 6 to 7. Figure 4.2b shows a sensitivity analysis for the effect of pH_{cyt} on the intracellular ammonium distribution. It is seen that the previous result, where the majority of NH_4^+ is present in the vacuole, is not very sensitive to the assumed pH_{cyt}.

Our results show that the cytosolic pool of ammonium has a high turnover rate; given the measured ammonium consumption in this experiment ($-q_N$) of 226 µmol/g_{CDW}/h and calculated cytosolic ammonium content of 0.345 µmol/g_{CDW}, it is possible to calculate the turnover time of the cytosolic ammonium, which will be in the order of 5.5 seconds. The turnover time of the entire intracellular ammonium pool will be 20 times longer, 110 seconds. This short

turnover time shows that for reliable intracellular NH_4^+ measurements indeed rapid sampling is required.

NH_3/NH_4^+ futile cycling under N-limitation in S. cerevisiae

From the calculated intracellular ammonium distribution (Figure 4.2a) one observes an outwards concentration gradient for the non-dissociated species NH_3. This gradient leads to leakage of NH_3 from the intracellular space to the extracellular environment.

Combined with the uptake of NH_4^+, which dissociates to intracellular NH_3 (species that leaks out the cell) and H^+, this requires H^+ export by H^+-ATPase leading to a futile cycle where for each mole of NH_3 leaked out there is a dissipation of 1 mol ATP. The NH_3 futile cycling rate follows from the permeability of NH_3 (P_{1a}= 1.73 m/h (Antonenko *et al.*, 1997)), the specific cell membrane area (a_m in m^2/g_{CDW}) and the NH_3 concentration difference ($[NH_3]_{cyt}$-$[NH_3]_{EC}$; check Figure 4.2a) as equation 13.

$$-q_{N_{efflux}} = P_{1a} \times a_m \times \left(\left[NH_3\right]_{cyt} - \left[NH_3\right]_{EC} \right) = \left(1.73 \frac{m}{h}\right) \times \left(3.22 \frac{m^2}{g_{CDW}}\right) \times \left(402 \frac{\mu mol}{m^3} - 0.3 \frac{\mu mol}{m^3}\right)$$
$$-q_{N_{efflux}} = 2236 \frac{\mu mol}{g_{CDW} \times h} \quad (13)$$

This means that the total MEP-based ammonium influx should equal $-(q_N + q_{Nefflux})$= -2462 µmol/g_{CDW}/h. Most of the studies of NH_4^+ and methylamine transport measured a V_{max} for Mep transporters between 600 and 2100 µmol/gCDW/h (equivalent to 20 and 70 nmol/min/$mg_{Protein}$ (Marini *et al.*, 1997), respectively, assuming 0.5 $g_{Protein}/g_{CDW}$). However, we must comment that the value measured in previous studies is the net flux to the cell, which is the sum of the leaked NH_3 plus the real NH_4^+-uptake rate; this means that Mep-faciliated transport velocity maybe underestimated at least 2-fold. Every mole of NH_3 leaked out requires a mole of ATP to excrete one H^+ for maintaining constant the intracellular charge and pH leading to an ATP dissipation of about 2.24 mmol ATP/g_{CDW}/h (check calculation and eq. 13).

We showed above that in the N-limited cultures there is an unexplained ATP dissipation rate of 4.7 mmol ATP/g_{CDW}/h, the occurrence of NH_3 futile cycle can explain largely this energy loss.

Moreover, NH_3 leaking out from the cell explains the evolution of vacuolar membranes permeable to NH_3, leading to accumulation of high amounts of NH_4^+ in this acidic compartment without the need of specific transporters. In absence of compartmentalization, the cytosolic NH_4^+/NH_3 concentration could be much higher leading to a larger NH_3-diffusion rate (futile cycling) and higher ATP demand to keep the cytosolic NH_4^+/NH_3 homeostasis, similar observations were pointed out by Wood *et al.* (2006) studying *vma*-deficient yeasts incubated with methylamine. However, it is important to mention that under glucose limitation and when $[NH_4^+]_{EC}$ is far larger than the cytosolic (intracellular) concentration, such futile cycling does not occur.

Urea transport in S. cerevisiae

In contrast to the experimental observations for ammonium, the extracellular urea represents a bigger fraction (>80%) of the total broth urea than the intracellular urea. The concentration is higher in the intracellular (151.3 ± 48.3 μmol/L_{IC}) than in the extracellular space (23.7 ± 5.7 μmol/L), which indicates active urea transport (Figure 4.3).

It was suggested by ElBerry *et al.* (1993) that at low urea concentrations a special urea transporter (DUR3) is expressed; according to Sanguinetti *et al.* (2014) this urea transporter uses a proton symport mechanism to take up urea, and it is expressed when the extracellular concentrations of urea are below 0.25 mM (ElBerry *et al.*, 1993). The expected equilibrium in/out ratio of urea for this type of transporter is expressed mathematically as equation 14.

$$\frac{[\text{Urea}]_{cyt}}{[\text{Urea}]_{EC}} = \exp\left(\frac{z \times F \times pmf}{R \times T}\right) = 2117 \qquad (14)$$

In this case, z = +1 (symport of urea plus one proton) and pmf = 200 mV. Thus, the equilibrium in/out (cytosol/extracellular) ratio is 2117. There are no reports of urea being compartmentalized in *S. cerevisiae* therefore it is considered that all intracellular urea is found in the cytosol. Experimentally, the urea cytosolic/extracellular concentration ratio found is 6, and $[urea]_{Cyt}/[urea]_{EC}$ = 6/0.7 = 9; in

contrast with the ammonium transporter, the urea symporter is working at far from equilibrium conditions (Q/Keq≈0.004). The cytosolic urea concentration (0.15/0.7 = 0.21 mM) is close to the reported K_M value for urea amidolyase reaction (0.1 and 0.39 mM (Schomburg *et al.*, 2004)) and allophanate hydrolase reactions. The large thermodynamic driving force for the urea transporter is probably maintained by high activity of the enzyme urea amidolyase, which quickly metabolizes the intracellular urea.

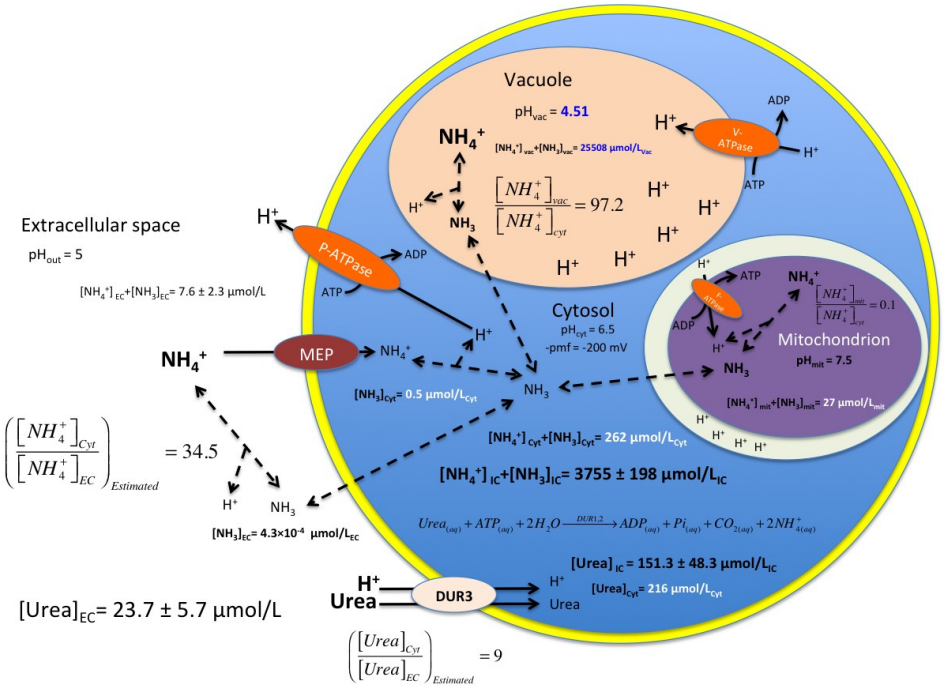

Figure 4.3. Estimated intracellular ammonium and urea distributions for *S. cerevisiae* growing at aerobic urea-limited conditions (D = 0.05h^{-1}).

L-glutamate transport in S. cerevisiae

Glutamate and glutamine are the central metabolites of the Nitrogen metabolism in yeast. Any other amino acid can be synthesized from these two by means of different reactions, usually transaminases (Hofman-Bang, 1999). Amino acids control the expression of their specific transporters, for the case of glutamate there are specific dicarboxylic acid permeases (Hofman-Bang, 1999), particularly Dip5 (Regenberg *et al.*, 1998). However, in the presence of poor nitrogen

sources or nitrogen limitation most of these specific permeases are replaced by general amino acid permeases (Conrad *et al.*, 2014), for instance Gap1 is derepressed in nitrogen-limited conditions (Chiva *et al.*, 2009; Hazelwood *et al.*, 2009). There is a general consensus that amino acid permeases work using an electrochemical gradient, by means of H^+-symport (Horák, 1997; Ljungdahl and Daignan-Fornier, 2012). Different widely used genome-scale stoichiometric models (Duarte *et al.*, 2004; Herrgard *et al.*, 2008; Nookaew *et al.*, 2008) assume that the amino acid species co-transported is the zero charged species in the case of neutral amino acids, -1 species for acidic amino acids, and +1 species for basic amino acids; however, for the particular case of glutamate early experimental evidence from Cockburn *et al.* (1975) showed that glutamate uptake requires co-transport of 2 moles of H^+ per mole glutamate.

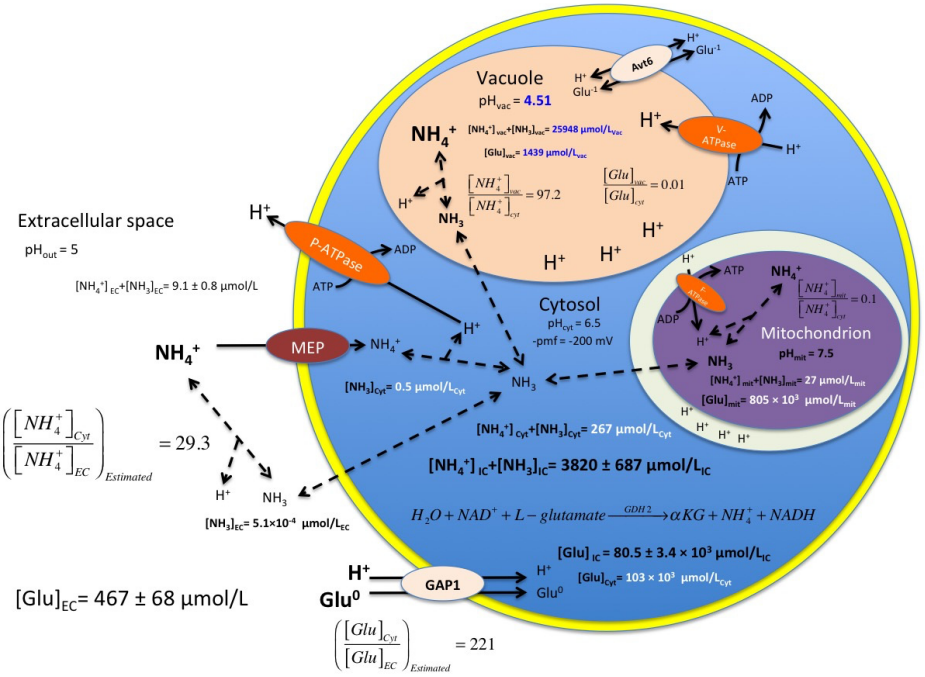

Figure 4.4. Estimated intracellular ammonium and L-glutamate distributions for *S. cerevisiae* growing at aerobic L-glutamate-limited conditions (D = 0.05h^{-1}).

From our experimental results, the in/out ratio equals 180 (Figure 4.4). Because glutamate is reported not to be strongly compartmentalized and expected to be mainly cytosolic (Ishimoto *et*

al., 2012), the cyt/out ratio follows as 180/0.7=221. This ratio agrees with a Glu^0/H^+ symport, which has an equilibrium in/out ratio of 6017 (**Appendix 4.1**) in agreement with the experimental findings of Cockburn *et al.* (1975), but does not agree with the generally assumed Glu^-/H^+ symport (in/out ratio = 28) (Duarte *et al.*, 2004; Herrgard *et al.*, 2008; Nookaew *et al.*, 2008). This suggests that under glutamate limitation, a different more active transport is present.

Thermodynamic state of N-central metabolism reactions

The thermodynamic analysis of the central N-metabolism also reinforces the hypothesis of NH_4^+ compartmentalization; when the whole cell metabolite amounts are used to calculate Δ_rG' for the reaction Glutamate dehydrogenase NADH-dependent (Gdh2), the values (Table 4.3) indicate that the reaction is unfeasible towards glutamate conversion into NH_4^+, even when glutamate is used as N-source. Given the fact that Gdh2 is arguably the main source of intracellular NH_4^+ when the cells grow using L-glutamate as N-source, the estimation of Δ_rG' using whole cell amounts is in conflict with experimental evidence. On the other hand, when metabolite compartmentalization is considered, Δ_rG' for Gdh2 becomes negative therefore the reaction is feasible, in this case it is assumed that NH_4^+, glutamate, αKG (this study), NADP/NADPH (Zhang *et al.*, 2015a) and NAD/NADH (Canelas *et al.*, 2008) are compartmentalized.

Additionally, the GS-GOGAT system is overall far from equilibrium in the direction of glutamate production. Our thermodynamic analysis of the central N-metabolism points at the possible presence of some futile redox cycles generating unnecessary waste of ATP, for instance glutamate synthesis by the NADPH-dependent enzyme Gdh1 (K_M for ammonium 10 mM (Schomburg *et al.*, 2004)) and concomitant glutamate degradation by Gdh2 (NAD-dependent); because both enzymes expressed under ammonium limited conditions (Hazelwood *et al.*, 2009), as observed in the proteomics results (**Appendix 4.3**); this evidence also supports previous reports of a necessary tight control of the expression of the enzymes involved in the central N-metabolism (Hofman-Bang, 1999).

Table 4.3. Experimental Gibbs free energy of reaction (Δ_rG')[a] of selected N-central metabolism reactions in *S. cerevisiae* using whole cell concentrations.

Reaction	NH_4^+ Δ_rG' (kJ/mol)	Urea Δ_rG' (kJ/mol)	Glutamate Δ_rG' (kJ/mol)	Considerations
Glutamate dehydrogenase Gdh1 (cytosolic, NADPH-dependent) Direction: L-glutamate synthesis	-7.4	-8.3	-11.6	Whole cell
	-13.9	-15.6	-18.0	Excluding NH_4^+ compartmentalization*
	-7.3	-9.0	-11.5	Compartmentalization (including NH_4^+)
Glutamate dehydrogenase Gdh2 (cytosolic, NADH-dependent) Direction: L-glutamate degradation	+3.0	+4.8	+9.3	Whole cell
	-8.2	-6.5	-4.1	Excluding NH_4^+ compartmentalization*
	-14.8	-13.1	-10.7	Compartmentalization (including NH_4^+)
Glutamine Synthetase (cytosolic) Direction: L-glutamine synthesis	-11.1	-11.3	-12.8	Whole cell**
	-19.8	-20.0	-21.6	Compartmentalization (including NH_4^+)**
GOGAT (cytosolic, NADH-dependent) Direction: L-glutamate synthesis	-26.4	-27.9	-30.8	Whole cell
	-10.6	-11.9	-12.7	Compartmentalization (including NH_4^+)
Alanine aminotransferase Direction: L-Alanine synthesis	-7.8	-7.0	-3.3	Whole cell

[a] *Calculations were performed using the online tool eQuilibrator (Noor et al., 2012; Noor et al., 2013), in all cases, pH_{cyt} = 6.5, I = 0.25 M.*

** In these cases, all metabolites except ammonium are considered compartmentalized as follows: 5% of the total αKG is considered as cytosolic ($\alpha KG_{cyt}=0.05\times\alpha KG_{IC}/0.7$), similarly to other eukaryotic systems (Lu et al., 2008), 90% of the glutamate is cytosolic ($Glu_{cyt}=0.90\times Glu_{IC}/0.7$) (Lu et al., 2008), 13.6% of the intracellular glutamine is assumed to be cytosolic based on thermodynamic equilibrium of the known Gln/H^+ vacuolar antiporters (Sekito et al., 2008). A cytosolic NADPH/NADP ratio of 22 was used, as estimated by Zhang et al. (2015a); cytosolic NAD/NADH ratio of 320 was used, as estimated by Canelas et al. (2008),*
*** Intracellular phosphate content was assumed to be 106.22 $\mu mol/g_{CDW}$ as reported by Zhang et al. (2015b) for phosphate excess conditions. Cytosolic phosphate was assumed to be 25.02 $\mu mol/g_{CDW}$ (Zhang et al., 2015b), which is the value reported for phosphate excess conditions. The energy of phosphorylation assumed is -45 kJ/mol_{ATP} (de Kok et al., 2012).*

Protein expression under different N-sources in S. cerevisiae

With the help of our large proteomic survey we observed a major rearrangement of the proteome in *S. cerevisiae* when urea is the sole N-source, more than 150 proteins were exclusively identified (>3 confidence peptides) in this condition, among the proteins exclusively found in the urea steady state were Crh1, Dur1,2, Dur3, Dal5 and Dal3 (Figure 4.5a). In the particular case of Crh1, previous transcriptome data (Godard *et al.*, 2007) showed significantly higher expression on urea compared to glutamate and ammonium. On the other hand, Dur and Dal genes are related to urea and allantoate metabolism, sensitive to NCR, and induced by the presence of urea (Cherry *et al.*, 2012). In addition, proteins such as Gap1, Car2 and Glt1 were found overexpressed (>50%) with respect to the ammonium steady state (Figure 4.5b).

When glutamate was used as N-source we found exclusive expression of proteins Agp1 and Vba4 (Figure 4.5a); Agp1 is a low affinity broad substrate range amino acid permease under the control of the SPS amino acid sensing mechanism (Liu *et al.*, 2008; Schreve *et al.*, 1998) and transcriptomics data suggests that when glutamate is the sole N-source its expression is higher than when urea or ammonium are N-sources (Godard *et al.*, 2007). Little is known about the function and regulation of Vba4 (Cherry *et al.*, 2012); it is hypothesized that works as a vacuolar basic amino acid transporter (Shimazu *et al.*, 2005).

Additionally, we observed overexpression of Gln1 (Figure 4.5c) - which is also expected because glutamate induces the expression of

this protein (Minehart and Magasanik, 1992)- and repression of Gap1 -the expression of this gene is sensitive to the N-source (Stanbrough and Magasanik, 1995).

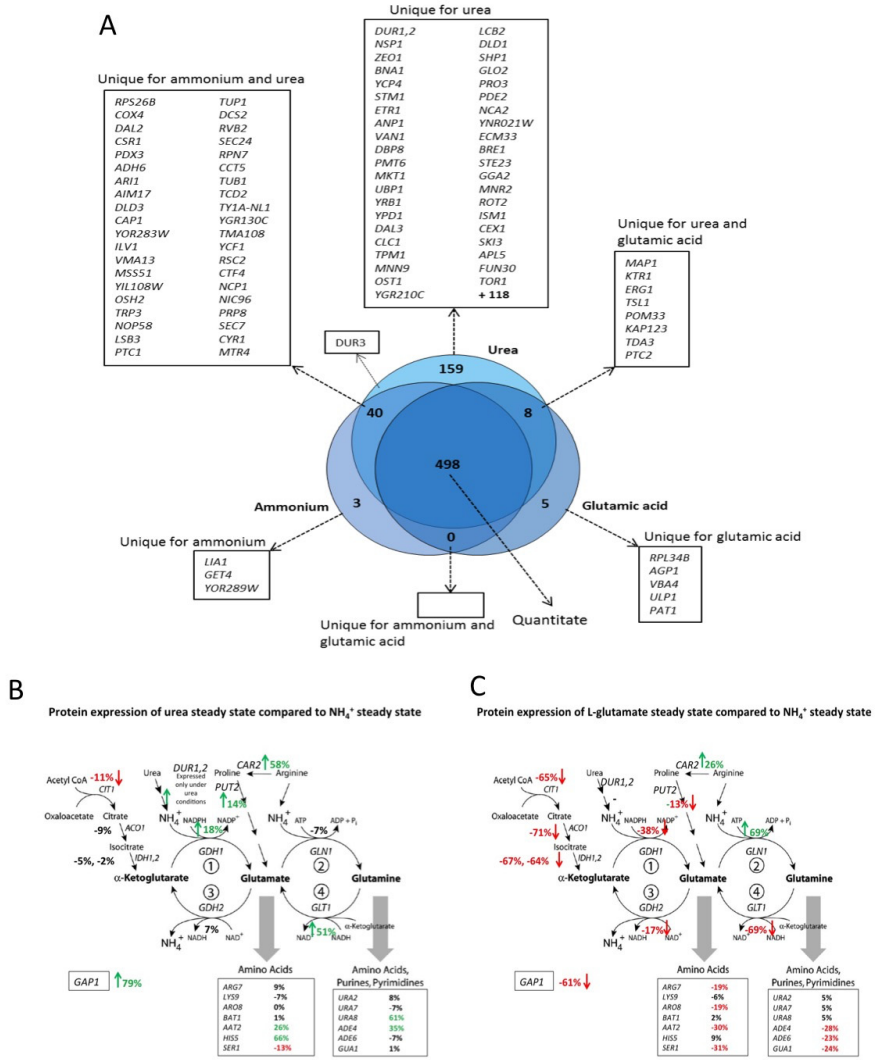

Figure 4.5. (a) Summary of the large proteomic survey for *S. cerevisiae* at steady state (D = 0.05h^{-1}) under aerobic N-limiting conditions using different N-sources. In this study, it is considered that unique proteins are those proteins that have an expression high enough to be identified with 3 or more confidence peptides, but not identified in other environmental conditions. Additionally, it is shown a comparison of protein expression patterns between (b) urea and ammonium steady states and (c) glutamate and ammonium steady states; overexpressed proteins are highlighted in green, repressed proteins are shown in red, proteins with no changes in expression

pattern are displayed in black (<10% differences with respect the reference steady state).

We also observed a major rearrangement of the C-metabolism (Figure 4.5c), probably related to the fact that additional Carbon is consumed by the cell in the form of glutamic acid, in agreement with previous experimental observations (Godard *et al.*, 2007; Tate and Cooper, 2003) we found that several proteins related to TCA such as Cit1, Aco1, and Idh1,2 were repressed. On top of that, the key enzymes of the central nitrogen metabolism Gdh2 and Glt1 were repressed (Figure 4.5c), in the case of Glt1 it is known that the expression of this protein is negatively regulated by the presence of glutamate (Valenzuela *et al.*, 1998), which is expected as glutamate does not need to be synthesized *de novo* as it is supplied in the medium.

When glutamate is the sole N-source the rest of the amino acids are synthesized using transamination reactions, and ammonium is only needed for glutamine synthesis, therefore Gdh2 is necessary as the main intracellular ammonium producing reaction; the expression of Gdh2 is regulated by many factors including intracellular ammonium concentration and NCR (Godard *et al.*, 2007; Tate and Cooper, 2003), particularly it is sensitive to the presence of ammonium in batch conditions (Tate and Cooper, 2003) but up-regulated under N-limitation (Barbosa *et al.*, 2015). It is expected then that overexpression of Gdh2 would mean higher enzymatic activity, thus higher intracellular ammonium concentrations when glutamate is the N-source, therefore we hypothesize that the repression of Gdh2 is related to intracellular ammonium homeostasis to avoid accumulation of large quantities of intracellular ammonium, maybe by means of a feedback inhibition mechanism.

Interestingly, other proteins exclusively found in the urea steady state were, Tor1, Npr1 and Ure2 (Figure 4.5a), known regulators of NCR (Conrad *et al.*, 2014; Ljungdahl and Daignan-Fornier, 2012; Tate and Cooper, 2003). Under urea-limited condition it is expected that Npr1, and Ure2 are not (hyper-)phosphorylated (Conrad *et al.*, 2014; Feller *et al.*, 2013; Schmidt *et al.*, 1998), and Tor1 is in its inactive conformational state (Conrad *et al.*, 2014; Crespo and Hall,

2002). Our experimental procedure allows quantification of proteins without post-translational modifications; we hypothesize that our protocol identified more confidence peptides of these proteins because phosphorylation interfered with their identification; therefore, Npr1 and Ure2 are found -according to our criterion of >3 confidence peptides- exclusively in the urea-limited condition when they are dephosphorylated. A different protocol/experimental setup will be required to identify and quantify accurately proteins with post-translational modifications, for instance the use of TiO_2-based separation of phosphoproteins (Pinkse *et al.*, 2008).

Conclusion

The experimental measurements suggest that, in aerobic NH_4^+ limited cultivations, most of the ammonium is found in the intracellular space (around 85%). This result fits with the hypothesis of ammonium transport by means of MEP-proteins using a uniport mechanism or with an equivalent thermodynamic equilibrium constant, which leads to the accumulation of ammonium in the intracellular space even at low ammonium concentrations in the extracellular space. Furthermore, the experimentally measured extracellular concentrations are in agreement with previous reports about the capacity and affinity of ammonium transporters (Mep-proteins) (Marini *et al.*, 1997), which indicates that at low ammonium concentrations the most active transporter is Mep2, with an affinity constant between 1 µmol/L and 2 µmol/L; under the experimental conditions, it is expected that Mep1 and Mep3 are also present, nevertheless their contribution to total ammonium uptake will be lower compared to Mep2 given their kinetic properties (Marini *et al.*, 1997) and optimal pH (Boeckstaens *et al.*, 2008). The experimental evidence also suggests that, under aerobic N-source limitation, urea and glutamate are transported using a proton-symport mechanism, in the case of glutamate the experimental data suggest that the transported species is Glu^0 (uncharged form), our observations are in agreement with previous experimental findings

from Cockburn *et al.* (1975), who suggested that glutamate is co-transported with two moles of H^+ per mole of glutamate taken up.
For the three different N-sources intracellular and extracellular ammonium was found at nearly the same levels, the mean total intracellular concentration was around ~3.6 mmol/L_{IC} and the extracellular concentration was ~8 µmol/L_{EC} in all cases. These results indicate that there is a minimum amount of ammonium required to regulate the important reactions related to the N-metabolism and this concentration has a major effect on expression of key proteins of central nitrogen metabolism, as observed in the case of Gdh2 repression during the glutamate steady state.
The experimental results also suggest that there is a very significant vacuolar/cytosol compartmentalization of NH_4^+ in *S. cerevisiae*, consistently observed for the 3 N-sources used. Furthermore, the extracellular ammonium concentration suggests, under aerobic N-limited conditions, the presence of a futile cycle due to NH_3 leakage. According to our estimations, this futile cycle could cost the cells as much as 30% of the total ATP produced.
Finally, it was observed that most of the main central N-metabolism reactions were found to be far from equilibrium, which suggests that thermodynamic assumptions such as equilibrium of glutamate dehydrogenase NADPH-dependent cannot be used to study NH_4^+ metabolism in *S. cerevisiae*.

Acknowledgements

The authors would like to thank Pascale Daran-Lapujade, Marijke Luttik and Tim Vos for the use of the Coulter counter equipment for cell volume and particle size distribution measurements; and Nick Milne, Jean-Marc Daran and A.J.A. van Maris for their valuable collaboration and fruitful discussions. This project is sponsored by the BE-BASIC Foundation. The author HFCR thanks CONACyT for the scholarship granted and the entire CSE group for the help during rapid sampling experiments, particularly to Camilo Suárez-Méndez, Cristina Bernal, Mihir Shah, Leonor Guedes da Silva, Mariana Velasco-Álvarez and Francisca Lameiras for their invaluable help and collaboration.

References

Abreu, C., Sanguinetti, M., Amillis, S., Ramon, A., 2010. UreA, the major urea/H^+ symporter in *Aspergillus nidulans*. Fungal Genet. Biol. 47**,** 1023-33.

Antonenko, Y. N., Pohl, P., Denisov, G. A., 1997. Permeation of ammonia across bilayer lipid membranes studied by ammonium ion selective microelectrodes. Biophys. J. 72**,** 2187-95.

Barbosa, C., Garcia-Martinez, J., Perez-Ortin, J. E., Mendes-Ferreira, A., 2015. Comparative transcriptomic analysis reveals similarities and dissimilarities in Saccharomyces cerevisiae wine strains response to nitrogen availability. PloS one. 10**,** e0122709.

Bisschops, M. M., Zwartjens, P., Keuter, S. G., Pronk, J. T., Daran-Lapujade, P., 2014. To divide or not to divide: a key role of *Rim15* in calorie-restricted yeast cultures. Biochim. Biophys. Acta. 1843**,** 1020-30.

Boeckstaens, M., Andre, B., Marini, A. M., 2007. The yeast ammonium transport protein Mep2 and its positive regulator, the Npr1 kinase, play an important role in normal and pseudohyphal growth on various nitrogen media through retrieval of excreted ammonium. Mol. Microbiol. 64**,** 534-46.

Boeckstaens, M., Andre, B., Marini, A. M., 2008. Distinct transport mechanisms in yeast ammonium transport/sensor proteins of the Mep/Amt/Rh family and impact on filamentation. J. Biol. Chem. 283**,** 21362-70.

Boer, V. M., Crutchfield, C. A., Bradley, P. H., Botstein, D., Rabinowitz, J. D., 2010. Growth-limiting intracellular metabolites in yeast growing under diverse nutrient limitations. Molecular biology of the cell. 21**,** 198-211.

Boer, V. M., de Winde, J. H., Pronk, J. T., Piper, M. D., 2003. The genome-wide transcriptional responses of *Saccharomyces cerevisiae* grown on glucose in aerobic chemostat cultures limited for carbon, nitrogen, phosphorus, or sulfur. J. Biol. Chem. 278**,** 3265-74.

Brett, C. L., Kallay, L., Hua, Z., Green, R., Chyou, A., Zhang, Y., Graham, T. R., Donowitz, M., Rao, R., 2011. Genome-wide analysis reveals the vacuolar pH-stat of *Saccharomyces cerevisiae*. PloS one. 6**,** e17619.

Bruinenberg, P. M., van Dijken, J. P., Scheffers, W. A., 1983. An enzymic analysis of NADPH production and consumption in Candida utilis. J. Gen. Microbiol. 129**,** 965-71.

Canelas, A. B., Ras, C., ten Pierick, A., van Gulik, W. M., Heijnen, J. J., 2011. An *in vivo* data-driven framework for classification and quantification of enzyme kinetics and determination of apparent thermodynamic data. Metab. Eng. 13**,** 294-306.

Canelas, A. B., ten Pierick, A., Ras, C., Maleki Seifar, R., van Dam, J. C., van Gulik, W. M., Heijnen, J. J., 2009. Quantitative evaluation of intracellular metabolite extraction techniques for yeast metabolomics. Anal. Chem. 81**,** 7379-89.

Canelas, A. B., van Gulik, W. M., Heijnen, J. J., 2008. Determination of the cytosolic free NAD/NADH ratio in *Saccharomyces cerevisiae* under steady-state and highly dynamic conditions. Biotechnol. Bioeng. 100**,** 734-43.

Cherry, J. M., Hong, E. L., Amundsen, C., Balakrishnan, R., Binkley, G., Chan, E. T., Christie, K. R., Costanzo, M. C., Dwight, S. S., Engel, S. R., Fisk, D. G., Hirschman, J. E., Hitz, B. C., Karra, K., Krieger, C. J., Miyasato, S. R., Nash, R. S., Park, J., Skrzypek, M. S., Simison, M., Weng, S., Wong, E. D., 2012. Saccharomyces Genome Database: the genomics resource of budding yeast. Nucleic Acids Res. 40**,** D700-5.

Chiva, R., Baiges, I., Mas, A., Guillamon, J. M., 2009. The role of GAP1gene in the nitrogen metabolism of *Saccharomyces cerevisiae* during wine fermentation. J. Appl. Microbiol. 107**,** 235-244.

Cockburn, M., Earnshaw, P., Eddy, A. A., 1975. The stoicheiometry of the absorption of protons with phosphate and L-glutamate by yeasts of the genus Saccharomyces. Biochem. J. 146**,** 705-12.

Conrad, M., Schothorst, J., Kankipati, H. N., Van Zeebroeck, G., Rubio-Texeira, M., Thevelein, J. M., 2014. Nutrient sensing and signaling in the yeast *Saccharomyces cerevisiae*. FEMS Microbiol. Rev. 38**,** 254-99.

Cooper, T. G., Sumrada, R., 1975. Urea Transport in *Saccharomyces cerevisiae*. J. Bacteriol. 121**,** 571-576.

Crepin, L., Sanchez, I., Nidelet, T., Dequin, S., Camarasa, C., 2014. Efficient ammonium uptake and mobilization of vacuolar arginine by *Saccharomyces cerevisiae* wine strains during wine fermentation. Microbial cell factories. 13**,** 109.

Crespo, J. L., Hall, M. N., 2002. Elucidating TOR Signaling and Rapamycin Action: Lessons from Saccharomyces cerevisiae. Microbiol. Mol. Biol. Rev. 66**,** 579-591.

Cruz, A. L., Verbon, A. J., Geurink, L. J., Verheijen, P. J., Heijnen, J. J., van Gulik, W. M., 2012. Use of sequential-batch fermentations to characterize the impact of mild hypothermic temperatures on the anaerobic stoichiometry and kinetics of *Saccharomyces cerevisiae*. Biotechnol. Bioeng. 109**,** 1735-44.

Cueto-Rojas, H., Maleki Seifar, R., ten Pierick, A., Heijnen, S., Wahl, A., 2016. Accurate Measurement of the in vivo Ammonium Concentration in Saccharomyces cerevisiae. Metabolites. 6**,** 12.

de Jonge, L. P., Buijs, N. A., ten Pierick, A., Deshmukh, A., Zhao, Z., Kiel, J. A., Heijnen, J. J., van Gulik, W. M., 2011. Scale-down of penicillin production in *Penicillium chrysogenum*. Biotechnology journal. 6**,** 944-58.

de Kok, S., Kozak, B. U., Pronk, J. T., van Maris, A. J., 2012. Energy coupling in *Saccharomyces cerevisiae*: selected opportunities for metabolic engineering. FEMS Yeast Res. 12**,** 387-97.

Dikicioglu, D., Karabekmez, E., Rash, B., Pir, P., Kirdar, B., Oliver, S. G., 2011. How yeast re-programmes its transcriptional profile in response to different nutrient impulses. BMC Syst Biol. 5**,** 148.

Duarte, N. C., Herrgard, M. J., Palsson, B. O., 2004. Reconstruction and validation of Saccharomyces cerevisiae iND750, a fully compartmentalized genome-scale metabolic model. Genome Res. 14**,** 1298-309.

ElBerry, H. M., Majumdar, M. L., Cunningham, T. S., Sumrada, R. A., Cooper, T. G., 1993. Regulation of the urea active transporter gene (DUR3) in *Saccharomyces cerevisiae*. J. Bacteriol. 175**,** 4688-98.

Fayyad-Kazan, M., Feller, A., Bodo, E., Boeckstaens, M., Marini, A. M., Dubois, E., Georis, I., 2016. Yeast nitrogen catabolite repression is sustained by signals distinct from glutamine and glutamate reservoirs. Mol. Microbiol. 99**,** 360-79.

Feller, A., Georis, I., Tate, J. J., Cooper, T. G., Dubois, E., 2013. Alterations in the Ure2 alphaCap domain elicit different GATA factor responses to rapamycin treatment and nitrogen limitation. J. Biol. Chem. 288**,** 1841-55.

Finoulst, I., Vink, P., Rovers, E., Pieterse, M., Pinkse, M., Bos, E., Verhaert, P., 2011. Identification of low abundant secreted proteins and peptides from primary culture supernatants of human T-cells. J Proteomics. 75**,** 23-33.

Godard, P., Urrestarazu, A., Vissers, S., Kontos, K., Bontempi, G., van Helden, J., Andre, B., 2007. Effect of 21 different nitrogen

sources on global gene expression in the yeast Saccharomyces cerevisiae. Mol. Cell. Biol. 27**,** 3065-86.

Gruswitz, F., Chaudhary, S., Ho, J. D., Schlessinger, A., Pezeshki, B., Ho, C. M., Sali, A., Westhoff, C. M., Stroud, R. M., 2010. Function of human Rh based on structure of RhCG at 2.1 A. Proceedings of the National Academy of Sciences of the United States of America. 107**,** 9638-43.

Hall, J. A., Yan, D., 2013. The molecular basis of K^+ exclusion by the *Escherichia coli* ammonium channel *AmtB*. J. Biol. Chem. 288**,** 14080-6.

Hazelwood, L. A., Walsh, M. C., Luttik, M. A., Daran-Lapujade, P., Pronk, J. T., Daran, J. M., 2009. Identity of the growth-limiting nutrient strongly affects storage carbohydrate accumulation in anaerobic chemostat cultures of *Saccharomyces cerevisiae*. Appl. Environ. Microbiol. 75**,** 6876-85.

Herrgard, M. J., Swainston, N., Dobson, P., Dunn, W. B., Arga, K. Y., Arvas, M., Bluthgen, N., Borger, S., Costenoble, R., Heinemann, M., Hucka, M., Le Novere, N., Li, P., Liebermeister, W., Mo, M. L., Oliveira, A. P., Petranovic, D., Pettifer, S., Simeonidis, E., Smallbone, K., Spasic, I., Weichart, D., Brent, R., Broomhead, D. S., Westerhoff, H. V., Kirdar, B., Penttila, M., Klipp, E., Palsson, B. O., Sauer, U., Oliver, S. G., Mendes, P., Nielsen, J., Kell, D. B., 2008. A consensus yeast metabolic network reconstruction obtained from a community approach to systems biology. Nat. Biotechnol. 26**,** 1155-60.

Hess, D. C., Lu, W., Rabinowitz, J. D., Botstein, D., 2006. Ammonium toxicity and potassium limitation in yeast. PLoS Biol. 4**,** e351.

Hofman-Bang, J., 1999. Nitrogen catabolite repression in *Saccharomyces cerevisiae*. Mol. Biotechnol. 12**,** 35-73.

Horák, J., 1997. Yeast nutrient transporters. Biochimica et Biophysica Acta (BBA) - Reviews on Biomembranes. 1331**,** 41-79.

Ishimoto, M., Sugimoto, N., Sekito, T., Kawano-Kawada, M., Kakinuma, Y., 2012. ATP-dependent export of neutral amino acids by vacuolar membrane vesicles of *Saccharomyces cerevisiae*. Biosci Biotechnol Biochem. 76**,** 1802-4.

Javelle, A., Lupo, D., Li, X.-D., Merrick, M., Chami, M., Ripoche, P., Winkler, F. K., 2007. Reprint of "Structural and mechanistic aspects of Amt/Rh proteins" [J. Struct. Biol. 158 (2007) 472–481]☆. Journal of Structural Biology. 159**,** 243-252.

Khademi, S., O'Connell, J., Remis, J., Robles-Colmenares, Y., Miericke, L. J. W., Stroud, R. M., 2004. Mechanism of ammonia transport by Amt/MEP/Rh: Structure of *AmtB* at 1.3.5 angstrom. Science. 305**,** 1587-1594.

Kleiner, D., 1981. The transport of NH_3 and HN_4^+ across biological membranes. Biochimica et Biophysica Acta (BBA) - Reviews on Bioenergetics. 639**,** 41-52.

Kresnowati, M. T., Suarez-Mendez, C., Groothuizen, M. K., van Winden, W. A., Heijnen, J. J., 2007. Measurement of fast dynamic intracellular pH in *Saccharomyces cerevisiae* using benzoic acid pulse. Biotechnol. Bioeng. 97**,** 86-98.

Labotka, R. J., Lundberg, P., Kuchel, P. W., 1995. Ammonia permeability of erythrocyte membrane studied by ^{14}N and ^{15}N saturation transfer NMR spectroscopy. Am J Physiol. 268**,** C686-99.

Lange, H. C., Eman, M., van Zuijlen, G., Visser, D., van Dam, J. C., Frank, J., de Mattos, M. J., Heijnen, J. J., 2001. Improved rapid sampling for *in vivo* kinetics of intracellular metabolites in *Saccharomyces cerevisiae*. Biotechnol. Bioeng. 75**,** 406-15.

Liu, Z., Thornton, J., Spirek, M., Butow, R. A., 2008. Activation of the SPS amino acid-sensing pathway in Saccharomyces cerevisiae correlates with the phosphorylation state of a sensor component, Ptr3. Mol. Cell. Biol. 28**,** 551-63.

Ljungdahl, P. O., Daignan-Fornier, B., 2012. Regulation of amino acid, nucleotide, and phosphate metabolism in *Saccharomyces cerevisiae*. Genetics. 190**,** 885-929.

Lu, M., Zhou, L., Stanley, W. C., Cabrera, M. E., Saidel, G. M., Yu, X., 2008. Role of the malate-aspartate shuttle on the metabolic response to myocardial ischemia. J. Theor. Biol. 254**,** 466-75.

Magasanik, B., 2003. Ammonia Assimilation by *Saccharomyces cerevisiae*. Eukaryot. Cell. 2**,** 827-829.

Magasanik, B., Kaiser, C. A., 2002. Nitrogen regulation in *Saccharomyces cerevisiae*. Gene. 290**,** 1-18.

Maleki Seifar, R., Ras, C., Deshmukh, A. T., Bekers, K. M., Suarez-Mendez, C. A., da Cruz, A. L., van Gulik, W. M., Heijnen, J. J., 2013. Quantitative analysis of intracellular coenzymes in *Saccharomyces cerevisiae* using ion pair reversed phase ultra high performance liquid chromatography tandem mass spectrometry. J. Chromatogr. A. 1311**,** 115-20.

Maleki Seifar, R., Ras, C., van Dam, J. C., van Gulik, W. M., Heijnen, J. J., van Winden, W. A., 2009. Simultaneous quantification of

free nucleotides in complex biological samples using ion pair reversed phase liquid chromatography isotope dilution tandem mass spectrometry. Anal. Biochem. 388**,** 213-9.

Marini, A. M., Boeckstaens, M., Andre, B., 2006. From yeast ammonium transporters to Rhesus proteins, isolation and functional characterization. Transfusion clinique et biologique : journal de la Societe francaise de transfusion sanguine. 13**,** 95-6.

Marini, A. M., Soussi-Boudekou, S., Vissers, S., Andre, B., 1997. A family of ammonium transporters in *Saccharomyces cerevisiae*. Mol. Cell. Biol. 17**,** 4282-93.

Mashego, M. R., van Gulik, W. M., Vinke, J. L., Visser, D., Heijnen, J. J., 2006. *In vivo* kinetics with rapid perturbation experiments in *Saccharomyces cerevisiae* using a second-generation BioScope. Metab. Eng. 8**,** 370-83.

Meiring, H. D., van der Heeft, E., ten Hove, G. J., de Jong, A. P. J. M., 2002. Nanoscale LC-MS(n): technical design and applications to peptide and protein analysis. J. Sep. Sci. 25**,** 557-568.

Milne, N., Luttik, M. A., Cueto Rojas, H. F., Wahl, A., van Maris, A. J., Pronk, J. T., Daran, J. M., 2015. Functional expression of a heterologous nickel-dependent, ATP-independent urease in *Saccharomyces cerevisiae*. Metab. Eng. 30**,** 130-140.

Minehart, P. L., Magasanik, B., 1992. Sequence of the *GLN1* gene of *Saccharomyces cerevisiae*: role of the upstream region in regulation of glutamine synthetase expression. J. Bacteriol. 174**,** 1828-36.

Mortensen, P., Gouw, J. W., Olsen, J. V., Ong, S. E., Rigbolt, K. T., Bunkenborg, J., Cox, J., Foster, L. J., Heck, A. J., Blagoev, B., Andersen, J. S., Mann, M., 2010. MSQuant, an open source platform for mass spectrometry-based quantitative proteomics. J Proteome Res. 9**,** 393-403.

Mortimer, R. K., 2000. Evolution and Variation of the Yeast (Saccharomyces) Genome. Genome Res. 10**,** 403-409.

Nakhoul, N. L., Lee Hamm, L., 2013. Characteristics of mammalian Rh glycoproteins (SLC42 transporters) and their role in acid-base transport. Mol Aspects Med. 34**,** 629-37.

Niedenfuhr, S., Pierick, A. T., van Dam, P. T., Suarez-Mendez, C. A., Noh, K., Wahl, S. A., 2015. Natural isotope correction of MS/MS measurements for metabolomics and C fluxomics. Biotechnol. Bioeng.

Nookaew, I., Jewett, M. C., Meechai, A., Thammarongtham, C., Laoteng, K., Cheevadhanarak, S., Nielsen, J., Bhumiratana, S., 2008. The genome-scale metabolic model iIN800 of Saccharomyces cerevisiae and its validation: a scaffold to query lipid metabolism. BMC Syst Biol. 2**,** 71.

Noor, E., Bar-Even, A., Flamholz, A., Lubling, Y., Davidi, D., Milo, R., 2012. An integrated open framework for thermodynamics of reactions that combines accuracy and coverage. Bioinformatics. 28**,** 2037-2044.

Noor, E., Haraldsdottir, H. S., Milo, R., Fleming, R. M., 2013. Consistent estimation of Gibbs energy using component contributions. PLoS Comput Biol. 9**,** e1003098.

Orij, R., Postmus, J., Ter Beek, A., Brul, S., Smits, G. J., 2009. *In vivo* measurement of cytosolic and mitochondrial pH using a pH-sensitive GFP derivative in *Saccharomyces cerevisiae* reveals a relation between intracellular pH and growth. Microbiology. 155**,** 268-78.

Pinkse, M. W., Mohammed, S., Gouw, J. W., van Breukelen, B., Vos, H. R., Heck, A. J., 2008. Highly robust, automated, and sensitive online TiO2-based phosphoproteomics applied to study endogenous phosphorylation in Drosophila melanogaster. J Proteome Res. 7**,** 687-97.

Postma, E., Verduyn, C., Scheffers, W. A., Van Dijken, J. P., 1989. Enzymic analysis of the crabtree effect in glucose-limited chemostat cultures of Saccharomyces cerevisiae. Appl. Environ. Microbiol. 55**,** 468-77.

Regenberg, B., Holmberg, S., Olsen, L. D., Kielland-Brandt, M. C., 1998. Dip5p mediates high-affinity and high-capacity transport of L-glutamate and L-aspartate in *Saccharomyces cerevisiae*. Curr. Genet. 33**,** 171-7.

Ritchie, R. J., 2013. The ammonia transport, retention and futile cycling problem in cyanobacteria. Microb. Ecol. 65**,** 180-96.

Sanguinetti, M., Amillis, S., Pantano, S., Scazzocchio, C., Ramon, A., 2014. Modelling and mutational analysis of *Aspergillus nidulans* UreA, a member of the subfamily of urea/H^+ transporters in fungi and plants. Open biology. 4**,** 140070.

Schmidt, A., Beck, T., Koller, A., Kunz, J., Hall, M. N., 1998. The TOR nutrient signalling pathway phosphorylates NPR1 and inhibits turnover of the tryptophan permease. EMBO J. 17**,** 6924-31.

Schomburg, I., Chang, A., Ebeling, C., Gremse, M., Heldt, C., Huhn, G., Schomburg, D., 2004. BRENDA, the enzyme database:

updates and major new developments. Nucleic Acids Res. 32**,** D431-3.

Schreve, J. L., Sin, J. K., Garrett, J. M., 1998. The *Saccharomyces cerevisiae YCC5*(*YCL025c*) Gene Encodes an Amino Acid Permease, *Agp1*, Which Transports Asparagine and Glutamine. J Bacteriol. 180**,** 2556-2559.

Sekito, T., Fujiki, Y., Ohsumi, Y., Kakinuma, Y., 2008. Novel families of vacuolar amino acid transporters. IUBMB Life. 60**,** 519-25.

Shimazu, M., Sekito, T., Akiyama, K., Ohsumi, Y., Kakinuma, Y., 2005. A family of basic amino acid transporters of the vacuolar membrane from *Saccharomyces cerevisiae*. J. Biol. Chem. 280**,** 4851-7.

Silverman, S. J., Petti, A. A., Slavov, N., Parsons, L., Briehof, R., Thiberge, S. Y., Zenklusen, D., Gandhi, S. J., Larson, D. R., Singer, R. H., Botstein, D., 2010. Metabolic cycling in single yeast cells from unsynchronized steady-state populations limited on glucose or phosphate. Proceedings of the National Academy of Sciences of the United States of America. 107**,** 6946-51.

Soupene, E., Ramirez, R. M., Kustu, S., 2001. Evidence that Fungal MEP Proteins Mediate Diffusion of the Uncharged Species NH_3 across the Cytoplasmic Membrane. Mol. Cell. Biol. 21**,** 5733-5741.

Stanbrough, M., Magasanik, B., 1995. Transcriptional and posttranslational regulation of the general amino acid permease of *Saccharomyces cerevisiae*. J. Bacteriol. 177**,** 94-102.

Suarez-Mendez, C. A., Hanemaaijer, M., ten Pierick, A., Wolters, J. C., Heijnen, J. J., Wahl, S. A., 2016. Interaction of storage carbohydrates and other cyclic fluxes with central metabolism: A quantitative approach by non-stationary 13C metabolic flux analysis. Metabolic Engineering Communications. 3**,** 52-63.

Tate, J. J., Cooper, T. G., 2003. Tor1/2 regulation of retrograde gene expression in *Saccharomyces cerevisiae* derives indirectly as a consequence of alterations in ammonia metabolism. J. Biol. Chem. 278**,** 36924-33.

Uchida, M., Sun, Y., McDermott, G., Knoechel, C., Le Gros, M. A., Parkinson, D., Drubin, D. G., Larabell, C. A., 2011. Quantitative analysis of yeast internal architecture using soft X-ray tomography. Yeast. 28**,** 227-36.

Ullmann, R. T., Andrade, S. L., Ullmann, G. M., 2012. Thermodynamics of transport through the ammonium transporter *Amt-1* investigated with free energy calculations. J. Phys. Chem. B. 116**,** 9690-703.

UniProt, C., 2015. UniProt: a hub for protein information. Nucleic Acids Res. 43**,** D204-12.

Valenzuela, L., Ballario, P., Aranda, C., Filetici, P., Gonzalez, A., 1998. Regulation of expression of *GLT1*, the gene encoding glutamate synthase in *Saccharomyces cerevisiae*. J. Bacteriol. 180**,** 3533-40.

Van Nuland, A., Vandormael, P., Donaton, M., Alenquer, M., Lourenco, A., Quintino, E., Versele, M., Thevelein, J. M., 2006. Ammonium permease-based sensing mechanism for rapid ammonium activation of the protein kinase A pathway in yeast. Mol. Microbiol. 59**,** 1485-505.

Verduyn, C., Postma, E., Scheffers, W. A., van Dijken, J. P., 1990. Energetics of *Saccharomyces cerevisiae* in anaerobic glucose-limited chemostat cultures. J. Gen. Microbiol. 136**,** 405-12.

Verduyn, C., Stouthamer, A. H., Scheffers, W. A., van Dijken, J. P., 1991. A theoretical evaluation of growth yields of yeasts. Antonie Van Leeuwenhoek. 59**,** 49-63.

Winkler, F. K., 2006. Amt/MEP/Rh proteins conduct ammonia. Pflugers Archiv : European journal of physiology. 451**,** 701-7.

Wood, C. C., Poree, F., Dreyer, I., Koehler, G. J., Udvardi, M. K., 2006. Mechanisms of ammonium transport, accumulation, and retention in ooyctes and yeast cells expressing *Arabidopsis AtAMT1;1*. FEBS Lett. 580**,** 3931-6.

Wu, L., Mashego, M. R., van Dam, J. C., Proell, A. M., Vinke, J. L., Ras, C., van Winden, W. A., van Gulik, W. M., Heijnen, J. J., 2005. Quantitative analysis of the microbial metabolome by isotope dilution mass spectrometry using uniformly ^{13}C-labeled cell extracts as internal standards. Anal. Biochem. 336**,** 164-71.

Zhang, J., Pierick, A. T., van Rossum, H. M., Maleki Seifar, R., Ras, C., Daran, J. M., Heijnen, J. J., Aljoscha Wahl, S., 2015a. Determination of the Cytosolic NADPH/NADP Ratio in *Saccharomyces cerevisiae* using Shikimate Dehydrogenase as Sensor Reaction. Sci Rep. 5**,** 12846.

Zhang, J., Sassen, T., ten Pierick, A., Ras, C., Heijnen, J. J., Wahl, S. A., 2015b. A fast sensor for *in vivo* quantification of cytosolic phosphate in *Saccharomyces cerevisiae*. Biotechnol. Bioeng. 112**,** 1033-46.

Appendix 4.1 Thermodynamic calculations of uptake mechanisms

Derivation of the in/out equilibrium ratio for the NH_4^+-uniport uptake mechanism in Saccharomyces cerevisiae

In *S. cerevisiae* three different genes are reported to encode for NH_4^+ transporters, namely Mep1, Mep2 and Mep3. These proteins are highly similar in terms of protein structure, but are differently regulated as a result of extracellular ammonium concentrations and their affinity and capacity. Mep2 has the highest affinity (K_M between 1 – 2 μM), followed by Mep1 (K_M between 5 – 10 μM) and Mep3 (K_M between 1.2 – 2.4 mM) (Marini *et al.*, 1997). Experimental evidence found in the homologous Amt-proteins from *Escherichia coli* suggests that NH_4^+ (cation, +1) is the species that is conducted through the Mep transporters, and not NH_3 (uncharged/gas) (Hall and Yan, 2013), the high degree of homology among the Amt- and Mep-family allows to hypothesize that the transport mechanism in both *E. coli* and *S. cerevisiae* are similar; thus, NH_4^+ it is likely to be the species transported by the Mep-proteins. The NH_4^+ uptake mechanism is sketched in figure A4.1.1.

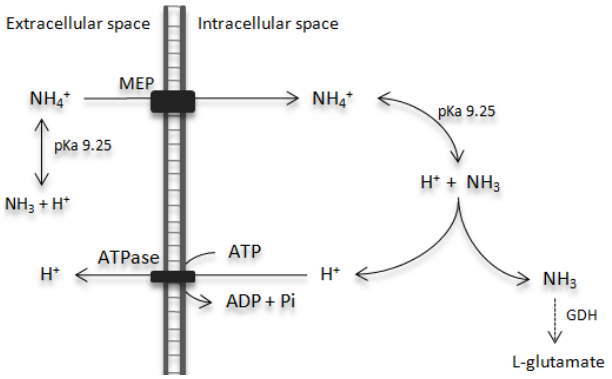

Figure A4.1.1. Ammonium transport through Mep proteins and assimilation into L-glutamic acid

Given that NH_4^+ is the species transported across the cell membrane, the Gibbs free energy of the transport process is given by the following equation A4.1.1.

$$\Delta_f G = \Delta_f G_{NH_{4,in}^+} - \Delta_f G_{NH_{4,out}^+} + R \times T \times \ln\left(\frac{\left[NH_4^+\right]_{in}}{\left[NH_4^+\right]_{out}}\right) + z \times F \times \Delta\psi_m \qquad (A4.1.1)$$

Where $\Delta_t G$ is the Gibbs free energy of the transport process, $\Delta_f G_{NH4+,in}$ and $\Delta_f G_{NH4+,out}$ are the Gibbs free energy of formation of ammonium in the intracellular space and extracellular space, respectively; because their value is exactly the same they cancel each other in the equation. R is the ideal gas constant, T the temperature at which the process is carried out (303 K), $[NH_4^+]_{in}$ and $[NH_4^+]_{out}$ are the concentrations of ammonium inside and outside the cell, respectively; z the charge of the species being transported inside the cell (+1 in this case), F the Faraday's constant and $\Delta\psi_m$ is the membrane potential. The membrane potential is defined as a function of the proton motive force (pmf) and difference of pH (ΔpH) across the cell membrane as shown in A4.1.2

$$pmf = \Delta\psi_m - 2.303 \times \frac{R \times T}{F} \times \left(pH_{out} - pH_{in}\right) \qquad (A4.1.2)$$

If the condition of thermodynamic equilibrium is applied ($\Delta_t G = 0$), equation A4.1.1 is reduced to A4.1.3.

$$\frac{\left[NH_4^+\right]_{in}}{\left[NH_4^+\right]_{out}} = \exp\left(\frac{z \times F \times \Delta\psi_m}{R \times T}\right) \qquad (A4.1.3)$$

Given that NH_4^+ is a weak dissociable species (pK_a = 9.25), its concentration depends on the local pH. It is possible to express the in/out equilibrium ratio in terms of total ammonium (sum of NH_4^+ and NH_3), by substitution of A4.1.4 in A4.1.3, being equation A4.1.4 the mathematical expression used to calculate the concentration of NH_4^+ as function of total ammonium and pH.

$$\left[NH_4^+\right] = \frac{\left[NH_3 + NH_4^+\right]}{1 + 10^{pH-pKa}} \qquad (A4.1.4)$$

The final result is equation A4.1.5, which can be found in the main.

$$\frac{\left[NH_3+NH_4^+\right]_{total,IC}}{\left[NH_3+NH_4^+\right]_{total,EC}}=\left(\frac{1+10^{pH_{in}-pKa}}{1+10^{pH_{out}-pKa}}\right)\times\exp\left(\frac{z\times F\times\Delta\psi_m}{R\times T}\right) \quad \text{(A4.1.5)}$$

Derivation of the in/out equilibrium ratio for Glu^0/H^+ symport uptake mechanism in Saccharomyces cerevisiae

The proposed transport mechanism is a symport of glutamate (Glu^0 uncharged species) plus one proton as sketched in figure A4.1.2.

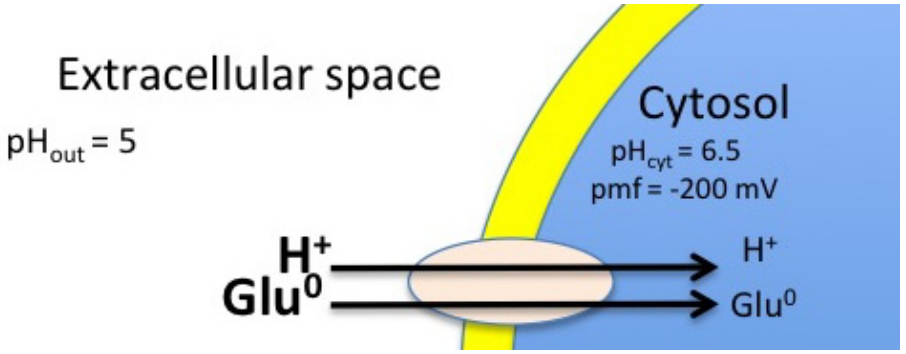

Figure A4.1.2. Ammonium transport through Mep proteins and assimilation into L-glutamic acid

The in/out equilibrium ratio is equation A4.1.6.

$$\frac{\left[Glu\right]_{In}\times\left[H^+\right]_{In}}{\left[Glu\right]_{Out}\times\left[H^+\right]_{Out}}=\exp\left(\frac{-z\times F\times\Delta\psi_m}{R\times T}\right) \quad \text{(A4.1.6)}$$

Glutamate is a weak acid with 3 dissociation constants; therefore, glutamate exists in 4 different dissociated species (figure A4.1.3)

$$Glu^{+1}_{(aq)}\overset{pKa_1=2.1}{\rightleftharpoons}Glu^{0}_{(aq)}+H^+_{(aq)} \quad \text{(A4.1.7)}$$

$$Glu^{0}_{(aq)}\overset{pKa_2=4.07}{\rightleftharpoons}Glu^{-1}_{(aq)}+H^+_{(aq)} \quad \text{(A4.1.8)}$$

$$Glu^{-1}_{(aq)}\overset{pKa_3=9.47}{\rightleftharpoons}Glu^{-2}_{(aq)}+H^+_{(aq)} \quad \text{(A4.1.9)}$$

The total glutamate concentration can be estimated using the following equation, which is expressed in terms of Glu^0.

$$[Glu]_{TOTAL}=\left(\frac{1}{10^{pH-pKa_1}}+1+10^{pH-pKa_2}+\left(10^{pH-pKa_2}\right)\times\left(10^{pH-pKa_3}\right)\right)\times\left[Glu^0\right] \quad \text{(A4.1.10)}$$

Proper substitution of A4.1.10 in A1.6; yields the in/out equilibrium ratio of total glutamate for the Glu^0/H^+ symport (figure A4.1.4).

$$\frac{[Glu_{TOTAL}]_{In}}{[Glu_{TOTAL}]_{Out}} = \exp\left(\frac{-z\times F\times \Delta\psi_m}{R\times T}\right)\times\left(10^{pH_{in}-pH_{out}}\right)\times\frac{\left(1+\frac{1}{10^{pH_{in}-pKa_1}}+10^{pH_{in}-pKa_2}+\left(10^{pH_{in}-pKa_2}\right)\times\left(10^{pH_{in}-pKa_3}\right)\right)}{\left(1+\frac{1}{10^{pH_{out}-pKa_1}}+10^{pH_{out}-pKa_2}+\left(10^{pH_{out}-pKa_2}\right)\times\left(10^{pH_{out}-pKa_3}\right)\right)} \quad \text{(A4.1.11)}$$

$$\frac{[Glu_{TOTAL}]_{In}}{[Glu_{TOTAL}]_{Out}} = 60171$$

On the other hand, if the mechanism is Glu^{-1}/H^+ symport, then the in/out equilibrium ratio will be described by equation A4.1.12 (figure A4.1.5). In this case,

$$\frac{[Glu_{TOTAL}]_{In}}{[Glu_{TOTAL}]_{Out}} = \left(10^{pH_{in}-pH_{out}}\right)\times\frac{\left(1+\frac{1}{\left(10^{pH_{in}-pKa_1}\right)\times\left(10^{pH_{in}-pKa_2}\right)}+\frac{1}{\left(10^{pH_{in}-pKa_2}\right)}+10^{pH_{in}-pKa_3}\right)}{\left(1+\frac{1}{\left(10^{pH_{out}-pKa_1}\right)\times\left(10^{pH_{out}-pKa_2}\right)}+\frac{1}{\left(10^{pH_{out}-pKa_2}\right)}+10^{pH_{out}-pKa_3}\right)} \quad \text{(A4.1.12)}$$

$$\frac{[Glu_{TOTAL}]_{In}}{[Glu_{TOTAL}]_{Out}} = 28.4$$

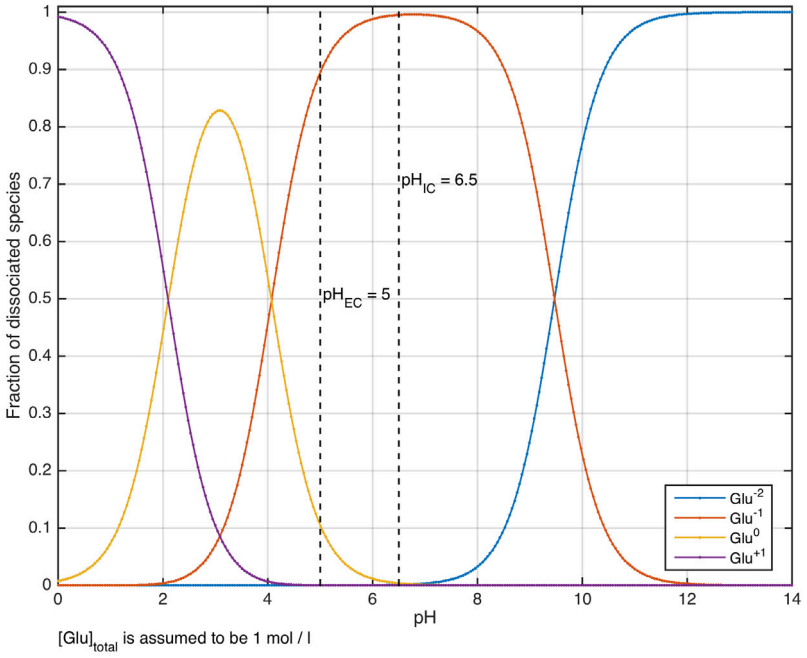

Figure A4.1.3. L-glutamate dissociation at different pH

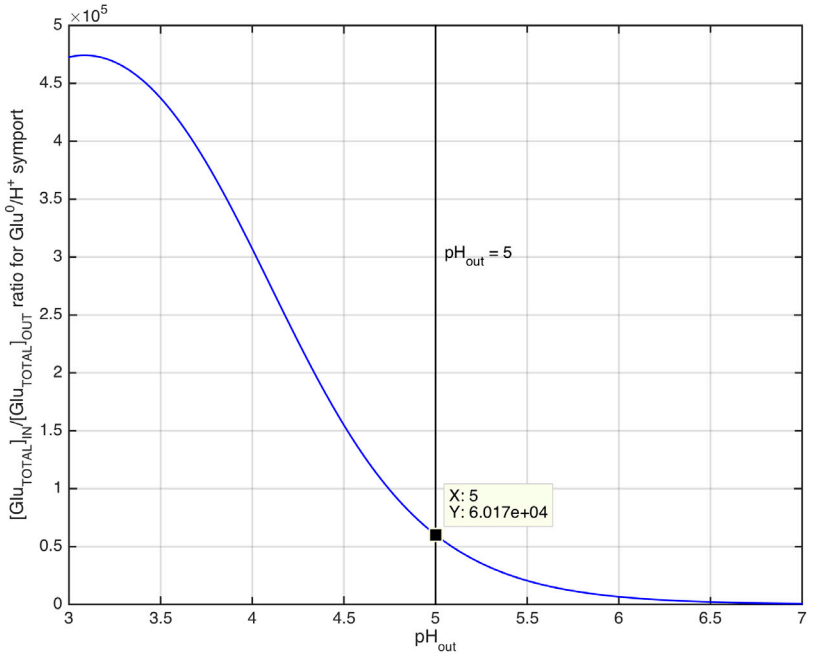

Figure A4.1.4. In/out ratios for a Glu^0/H^+ symport mechanism at different extracellular pH. Intracellular pH is assumed to be 6.5.

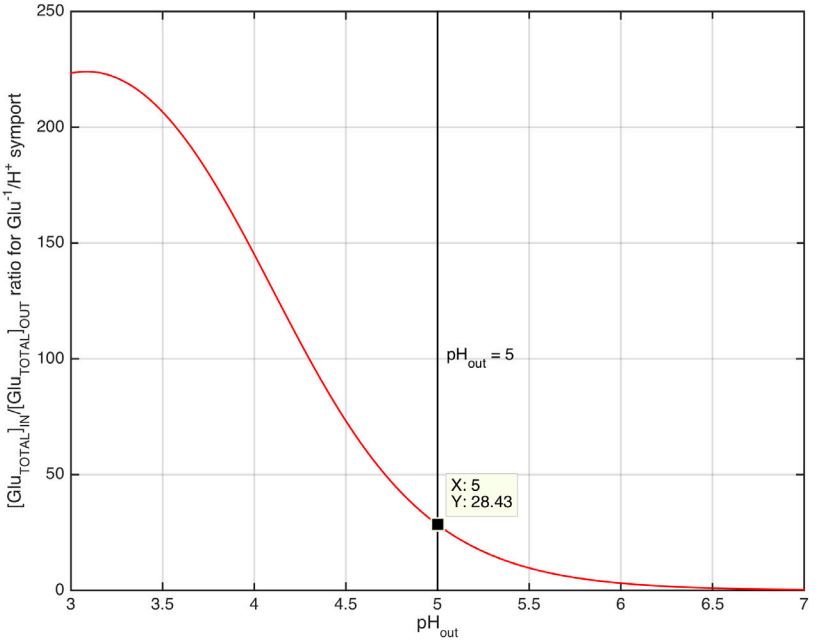

Figure A4.1.5. In/out ratios for a Glu^{-1}/H^+ symport mechanism at different extracellular pH. Intracellular pH is assumed to be 6.5.

Appendix 4.2 Determination of the ethanol evaporation constant in 7-L bioreactor under normal operation conditions

One of the key parameters to close the ethanol and total mass balances in *S. cerevisiae* cultivations is the ethanol evaporation constant. This constant was determined experimentally in a 7-L bioreactor with 4-L working volume using the solution described in table A4.2.1, this solution resembles the fermentation broth during the aerobic N-limited chemostat cultivation. The air sparging rate, stirring speed and temperature were the same as used in the cultivation experiments.

Table A4.2.1. Synthetic broth used in the evaporation experiment

Compound	g/L (mM)
Glucose·H2O	24.75 (125)
$MgSO_4 \cdot 7H_2O$	0.57 (2.31)
Ethanol	23 (500)
KH_2PO_4	3.45 (25.35)
Antifoam C	0.3 g/L
pH (adjusted with KOH 4M)	5

During a period of 11 days, the mass in the reactor was constantly monitored online. Samples of 5 mL broth were taken at the following time points: 0, 1, 11, 23, 27, 48, 52, 72, 96, 222 and 247 h. The experimental measurements were used to calculate: a) Evaporation constant of the broth (r_{evap}) and, b) evaporation constant of ethanol (k_{evap}) using the total broth (A4.2.1) and ethanol mass balances (A4.2.2).

$$\frac{d(M)}{dt} = -r_{evap} \times M \qquad \text{(A4.2.1)}$$

$$\frac{d(M \times C_{Ethanol})}{dt} = -k_{evap} \times M \times C_{Ethanol} \qquad \text{(A4.2.2)}$$

By means of the minimization of the weighted squared errors. The results of the parameter estimation routine are shown in table A4.2.2. The estimated parameters were used to solve the system of

ODE's to check for consistency with the experimental data, the results are shown in figure A4.2.1.

Table A4.2.2. Synthetic broth used in the evaporation experiment

Parameter	Estimated value	Error	Units
k_{evap}	6.887 x 10^{-3}	4.886 x 10^{-5}	$mol_{ethanol\ evaporated}$ / $mol_{ethanol\ in\ solution}$ /h
r_{evap}	2.284 x 10^{-4}	7.092 x 10^{-6}	$kg_{liquid\ evaporated}$ /$kg_{broth\ in\ vessel}$ /h

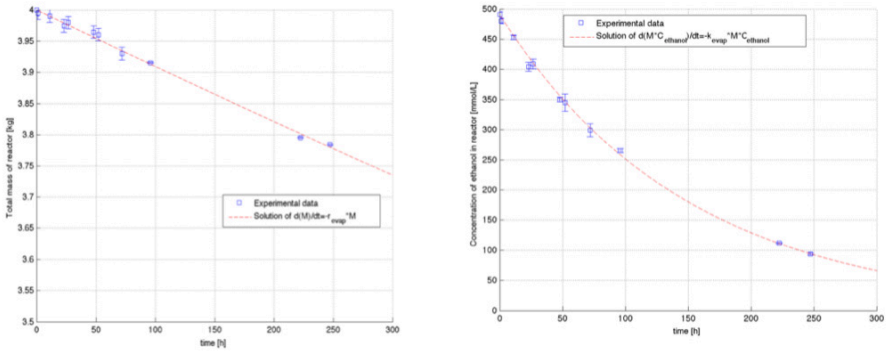

Figure A4.2.1. Experimental data obtained in the evaporation experiment (blue), and simulation using the estimated parameters (red) r_{evap} and k_{evap}

CHAPTER 5

Membrane-potential independent transport of NH_3 in absence of ammonium permeases in *Saccharomyces cerevisiae*

"...When you have eliminated the impossible, whatever remains, however improbable, must be the truth..."

Sherlock Holmes (Sir Arthur Conan Doyle, 1890) *The Sign of the Four*, Ch. 6

Abstract

Microbial production of nitrogen containing compounds requires a high flux of uptake and assimilation of the N-source, such as for instance ammonium, which is generally coupled to ATP consumption and negatively influences the product yield. In the industrial workhorse *Saccharomyces cerevisiae* ammonium (NH_4^+) uptake is facilitated by ammonium permeases (Mep1, 2 and 3), which transport the NH_4^+-ion, resulting in ATP expenditure to remove the corresponding proton using the plasma membrane bound H^+-ATPase to maintain cellular homeostasis. To decrease ATP costs for nitrogen assimilation Mep-genes were removed resulting in a strain unable to uptake the NH_4^+-ion. Subsequent analysis revealed that growth of this Δ*mep1,2,3* strain was influenced by the extracellular NH_3 concentrations, suggesting that the uncharged species was able to diffuse into the cell. Further determination of the intracellular/extracellular NH_X ratio under aerobic nitrogen-limiting conditions was also consistent with this hypothesis. Metabolomic analysis revealed a significantly 3.3-fold higher intracellular NH_X concentration in the Δ*mep1,2,3* strain compared to the reference strain. Further proteomic analysis revealed significant up-regulation of vacuolar proteases and genes involved in various stress responses potentially indicating a higher turnover of biomass components due to a more severe N-limitation state in the Δ*mep1,2,3* strain compared to the reference strain.

Keywords

Intracellular ammonium, metabolomics, ammonium transport, central nitrogen metabolism, ammonia passive diffusion, thermodynamics

This Chapter is submitted as: Cueto-Rojas H.F., Milne N., van Helmond W., Pieterse M.M., van Maris A.J.A., Daran J.M., Wahl S.A, 2016. Membrane-potential independent transport of NH_3 in absence of ammonium permeases in *Saccharomyces cerevisiae*. *BMC Syst Biol*.

Introduction

A significant number of fuels and commodity chemicals have the potential to be produced in bio-refineries using microbial fermentation (Choi *et al.*, 2015), which represents a more sustainable alternative to current oil-based production (Choi *et al.*, 2015). The increasing interest in microbial-based production is best exemplified by the intensive research efforts to improve the productivity and yield of a vast range of different compounds produced by *Saccharomyces cerevisiae* (Hong and Nielsen, 2012; Nielsen *et al.*, 2013) and other industrial workhorses. Nevertheless, while the number of compounds produced at industrial scale by *S. cerevisiae* is increasing, the production of nitrogen containing compounds by this organism is significantly under-represented with heterologous protein production being the only known example (Hong and Nielsen, 2012).

Nitrogen containing compounds represent an economically relevant class of commodity chemicals that includes amino acids such as L-lysine and L-glutamate, as well as diamines such as 1,5-diaminopentane (cadaverine) and 1,4-diaminobutane (putrescine), and relevant synthesis precursors such as caprolactam. Their microbial production is currently performed under aerobic conditions using bacteria, most commonly *Corynebacterium glutamicum* and *Escherichia coli* (Oldiges *et al.*, 2014; Qian *et al.*, 2011; Turk *et al.*, 2015). *S. cerevisiae* is seen as an attractive host organism for industrial fermentation due to its fast anaerobic conversion of sugar to product, its resistance to phage attack and robustness under common industrial conditions (van Maris *et al.*, 2007). When using *S. cerevisiae* for the production of nitrogen containing compounds, if permitted by the thermodynamics and biochemistry of the product pathway, the process should preferably occur under anaerobic conditions (de Kok *et al.*, 2012a), which is favorable not only in terms of the resulting fermentation costs, but also in terms of the product yield, which is typically higher under anaerobic conditions (Weusthuis *et al.*, 2011). However, under anaerobic conditions energy supply in *S. cerevisiae* cells relies solely on substrate-level phosphorylation, which limits the amount of ATP available for

growth and maintenance. Therefore, to enable a viable process, the anaerobic production of nitrogen-containing compounds should result in net ATP formation. Therefore, it is essential that the N-source is transported and assimilated using ATP-independent mechanisms. Urea and ammonium are the most common N-sources used industrially in *S. cerevisiae* fermentations; previously we presented a novel strategy for achieving ATP-independent urea assimilation in *S. cerevisiae* (Milne *et al.*, 2015).

On the other hand, ammonium is often used in industrial fermentation and is also present in plant hydrolysates used for second generation chemical production (Franden *et al.*, 2013; Kumar *et al.*, 2009), thus mechanisms of ATP-neutral ammonium transport and assimilation would have significant relevance for anaerobic production of nitrogen containing compounds. Ammonium exists in two forms in aqueous solutions: the solubilized gas ammonia (NH_3) and ammonium ion (NH_4^+). The sum of both species, NH_3 and NH_4^+, will be described onwards as NH_X. With a *pKa* of 9.25, under biologically relevant conditions (between pH 3 and 7), the ratio NH_3/NH_4^+ equals $10^{pH-9.25}$, which means that at these conditions the vast majority of NH_X is present as the charged ammonium species (NH_4^+).

In *S. cerevisiae* NH_4^+ is taken up by the ammonium permeases Mep1, Mep2 and Mep3, which belong to the Amt-class of proteins that use the negative membrane potential as thermodynamic driving force (Ullmann *et al.*, 2012). The evolutionary advantage of this transport mechanism compared to passive diffusion is that the transport rate is higher, and due to the negative cytosolic membrane potential, accumulation of NH_X is favored in the intracellular space even at low extracellular concentrations. However, one H^+ must be exported from the cytosol by the plasma-membrane-bound H^+-ATPase Pma1 (Magasanik, 2003) to recover the proton motive force (pmf) and charge homeostasis after taken up NH_4^+, and subsequent assimilation of NH_3 (de Kok *et al.*, 2012a). The deletion of the ammonium permease genes *MEP1, MEP2* and *MEP3* results in a viable strain able to grow on ammonium concentrations above 5 mM; which was hypothesized to be due to the presence of additional ammonium transporters (Marini *et al.*, 1997). Another proposed

hypothesis is that NH_4^+ is able to enter the cell through potassium channels due to the similarity in charge and ionic radii of both, K^+ and NH_4^+ (Hess *et al.*, 2006). However, an alternative hypothesis presented here is that the uncharged NH_3 species is able to diffuse into the cell, which if correct would result in ATP-independent NH_X-uptake and consequently reduces the ATP demand, which is of high relevance to industry. Previous experimental observations in synthetic bilayer lipid membranes suggest that the NH_3 apparent permeability coefficient is P_{1a} = 1.728 m/h (48×10^{-3} cm/s) (Antonenko *et al.*, 1997), which indicates that cell membranes are indeed permeable to NH_3.

The aim of this study was to elucidate the NH_X-uptake mechanism in a Δ*mep1,2,3 S. cerevisiae* strain, and assess the impact of the deletion of *MEP1, 2 and 3* on the physiology of *S. cerevisiae*. Furthermore, proteomic and metabolomic measurements were used to investigate the global impact of the changed NH_X-uptake mechanism on cellular physiology.

Materials and Methods

Table 5.1. Strains used in this study

Name	Relevent genotype	Origin
CEN.PK113-3B	*MATalpha ura3-52 his3-D1 LEU2 TRP1 MAL2-8c SUC2*	(Entian and Kotter, 2007)
CEN.PK113-3B-Δmep1	*MATalpha ura3-52 his3-D1 LEU2 TRP1 MAL2-8c SUC2 mep1::loxP*-KanMX4-loxP	This study
CEN.PK113-3B-Δmep1,2	*MATalpha ura3-52 his3-D1 LEU2 TRP1 MAL2-8c SUC2 mep1::loxP*-KanMX4-*loxP mep2::loxP*-NatNT2-*loxP*	This study
CEN.PK113-3B-Δmep1,2,3	MATalpha ura3-52 his3-D1 LEU2 TRP1 MAL2-8c SUC2 *mep1::loxP*-KanMX4-*loxP mep2::loxP*-NatNT2-loxP *mep3::loxP-Ura3-loxP*	This study
CEN.PK113-3B-Δmep1,2,3-Cure	*MATalpha ura3-52 his3-D1 LEU2 TRP1 MAL2-8c SUC2 mep1::loxP-loxP mep2::loxP-loxP mep3::loxP-loxP*	This study
IMZ351	*MATalpha ura3-52 his3-D1 LEU2 TRP1 MAL2-8c SUC2 mep1::loxP-loxP mep2::loxP-loxP mep3::loxP-loxP* pUDE199 (*HIS3 URA3*)	This study
IME169	*MATalpha ura3-52 his3-D1 LEU2 TRP1 MAL2-8c SUC2* pUDE199 (*HIS3 URA3*)	This study

Strains and maintenance

All *Saccharomyces cerevisiae* strains used in this study (table 5.1) were derived from the CEN.PK strain family background (Entian

and Kotter, 2007; Nijkamp *et al.*, 2012). Frozen stocks of *E. coli* and *S. cerevisiae* were prepared by addition of glycerol (30% (v/v)) to exponentially growing cells followed by aseptic storage of 1 mL aliquots at -80 °C. Cultures were grown at 30 °C either in synthetic medium (Verduyn *et al.*, 1992) with 20 g/L glucose as carbon source and appropriate growth factors (Pronk, 2002), or complex medium containing 20 g/L glucose, 10 g/L Bacto yeast extract and 20 g/L Bacto peptone. If required for anaerobic growth Tween-80 (420 mg/L) and ergosterol (10 mg/L) were added. Agar plates were prepared as described above but with the addition of 20 g/L agar (Becton Dickinson B.V. Breda, The Netherlands).

Plasmid and strain construction

S. cerevisiae strains were transformed using the lithium acetate method according to Gietz and Woods (2002). The plasmid pUDE199 (*HIS3 URA3*) (table 5.2) was constructed by amplifying the HIS3 gene cassette from pSH62 using primers flanked by the restriction sites SacI and NaeI (SacI-HIS3 Fwd / Nae-HIS3 Rev) (table 5.3).

Table 5.2. Plasmids used in this study

Name	Characteristics	Origin
pUDE199	2µm ori *URA3 HIS3*	This study
pSH62	*CEN6-ARS4* ori *HIS3 GAL1$_p$-Cre-CYC1$_t$*	(Gueldener *et al.*, 2002)
pUG6	PCR template for *loxP*-KanMX4-*loxP* cassette	(Gueldener *et al.*, 2002)
pUG72	PCR template for *loxP-KlURA3*3-*loxP* cassette	(Gueldener *et al.*, 2002)
pUG-natNT2	PCR template for *loxP*-NatNT-*loxP* cassette	(de Kok *et al.*, 2012b)

Both the amplified *HIS3* cassette and the vector pSH47 (containing the *URA3* gene cassette) were digested with SacI and NaeI (Thermo Scientific) following the manufacturer's instructions thereby creating complimentary ends. Both linear DNA fragments were dephosphorylated using FastAP Thermosensitive Alkaline Phosphotase (Thermo Scientific) following the manufacturer's instructions then ligated using T4 DNA ligase (Thermo Scientific) following the manufacturer's instructions.

The ligation mixture was then transformed into chemically competent *E. coli* DH5α, a correctly assembled plasmid was

confirmed by Sanger DNA sequencing (BaseClear, Leiden, The Netherlands) and stocked in the *E. coli* host.

The strain IMZ351 was constructed by sequential deletion of each *MEP* gene and marker removal using the Cre/loxP recombination system (Sauer, 1987). *MEP1* was deleted from CEN.PK113-3B by replacement with a *loxP*-KanMX4-*loxP* cassette yielding strain CEN.PK113-3B-Δmep1. The *MEP1* deletion cassette was constructed by amplifying the KanMX cassette from vector pUG6 (Guldener *et al.*, 1996) using primers with added homology to the upstream and downstream regions of *MEP1* (*MEP1* KO Fwd / *MEP1* KO Rev) (table 5.3). Transformants were selected on complex medium agar with 200 mg/L G418 (Sigma Aldrich).

MEP2 was deleted from CEN.PK113-3B-Δmep1 by replacement with a *loxP*-NatNT2-*loxP* cassette yielding strain CEN.PK113-3B-Δmep1,2. The *MEP2* deletion cassette was constructed by amplifying the NatNT2 cassette from pUG-natNT2 (de Kok *et al.*, 2012b) using primers with added homology to the upstream and downstream regions of *MEP2* (*MEP2* KO Fwd / *MEP2* KO Rev) (table 5.3). Transformants were selected on complex medium agar with 200 mg/L G418 and 100 mg/L nourseothricin (Jena Bioscience, Jena, Germany). *MEP3* was deleted from CEN.PK113-3B-Δmep1,2 by replacement with a *loxP-KlURA3-loxP* cassette yielding strain CEN.PK113-3B-Δmep1,2,3.

The *MEP3* deletion cassette was constructed by amplifying the *KlURA3* cassette from pUG72 (Gueldener *et al.*, 2002) using primers with added homology to the upstream and downstream regions of *MEP3* (*MEP3* KO Fwd / *MEP3* KO Rev) (table 5.3). Transformants were selected on synthetic medium agar with 200 mg/L G418, 100 mg/L nourseothricin and 125 mg/L histidine. The KanMX4, NatNT2 and *KlURA3* markers were removed using the Cre/loxP system with pSH62 (Gueldener *et al.*, 2002) yielding strain CEN.PK113-3B-Δmep1,2,3-Cure. Finally, pUDE199 (*HIS3 URA3*) was transformed into CEN.PK113-3B-Δmep1,2,3-Cure yielding strain IMZ351.

In all cases PCR amplification of the deletion cassettes and plasmid expression cassettes was performed using Phusion® Hot Start II High Fidelity Polymerase (Thermo scientific, Waltham, MA)

according to the manufactures instructions using HPLC or PAGE purified, custom synthesized oligonucleotide primers (Sigma Aldrich, Zwijndrecht, The Netherlands) in a Biometra TGradient Thermocycler (Biometra, Gottingen, Germany). IME169 was constructed by transforming pUDE199 (*HIS3 URA3*) into CEN.PK113-3B.

Table 6. Primers used in this study

Name	Sequence (5'→3')
Primers for knockout cassette	
MEP1 KO Fwd	TCAGAGATTGCGATAACGATAAGATTCACAATTGCTACAGACACCCTTGTGTGACCA GCTGAAGCTTCGTACGC
MEP1 KO Rev	TTAAGGCGTGCGACTGTTAATCGCAAGATCGTGAGTTCAACCCTCACTGGGGTCGGC ATAGGCCACTAGTGGATCTG
MEP2 KO Fwd	CTGCACCATATATAAGCAGTAGTTACACATGTGCTAACCAAACATCAGTGGGTAGCA GCTGAAGCTTCGTACGC
MEP2 KO Rev	CATAAGACAAGAGAAGTAATACTAACGTCTCCCCTCATCATTCGGAGTTATCAAAGC ATAGGCCACTAGTGGATCTG
MEP3 KO Fwd	ATATGCTGATATGCAGCACGGACTTTCCCTCTCCTTGTCTTATCGCATCTTATCGCAG CTGAAGCTTCGTACGC
MEP3 KO Rev	CCCAATTCATCATTATTTGCGACTCCATGGCCAAGTTGGTTAAGGCGTGCGACTGGC ATAGGCCACTAGTGGATCTG
Primers for verification of knockout cassettes	
MEP1 Upstream Fwd	TTGCTTATCTCTGCGGACACGCGCC
MEP1 Downstream Rev	GAAATCGAGGTAAAGGCCCGAGCAA
MEP2 Upstream Fwd	TATAGGCTGCCTGGTCACCGATTAC
MEP2 Downstream Rev	TCTTGCTATCATGCTCTGGAGATGC
MEP3 Upstream Fwd	TAGATGTGCCCGTTTCTGTCACTCC
MEP3 Downstream Rev	GAAGCACAGGCGCTACCATGAGAAA
Primers for plasmid construction	
SacI-HIS3 Fwd	GAGCTCGGCGTATCACGAGGCCCTTTC
NaeI-HIS3 Rev	GCCGGCTTTCCCCGTCAAGC

In all cases conformation of cassette integration, subsequent Cre/loxP excision, and correct plasmid insertion was confirmed by PCR on

genomic or plasmid DNA preparations using the diagnostic primers listed in table 5.3. Diagnostic PCR was performed using DreamTaq (Thermo scientific) and desalted primers (Sigma Aldrich) in a Biometra TGradient Thermocycler (Biometra). In all cases genomic DNA was prepared using a YeaStar Genomic DNA kit (Zymo Research, Orange, CA) while plasmid DNA was prepared using a GenEluteTM Plasmid Miniprep Kit (Sigma Aldrich).

Strain Cultivation

Shake flask cultivation

S. cerevisiae strains were grown in synthetic medium (Verduyn *et al.*, 1990). Cultures were grown in either 500 mL or 250 mL shake flasks containing 100 mL or 50 mL of medium, respectively, and incubated at 30 °C in an Innova incubator shaker (New Brunswick Scientific, Edison, NJ) at 200 rpm.

Aerobic nitrogen-limited chemostat cultivation

Controlled aerobic, nitrogen limited chemostat cultivations were carried out at 30 °C in 7 L bioreactors (Applikon, Schiedam, the Netherlands) with a working volume of 4 L. Chemostat cultivations were preceded by a batch phase using the same synthetic medium as the continuous phase. Continuous cultivation was initiated at a dilution rate of 0.05 h^{-1}; synthetic nitrogen-limited medium was used modified from Boer *et al.* (2010), which contained: 130 g/L glucose, 25 g/L ethanol, 3.48 g/L $NH_4H_2PO_4$, 1.14 g/L $MgSO_4 \cdot 7H_2O$, 6.9 g/L KH_2PO_4, 0.3 g/L Antifoam C, with the appropriate growth factors added accordingly (Pronk, 2002) (vitamin solution 2 mL/L and trace element solution 2 mL/L), ethanol was added to the medium to avoid potential oscillations. The medium was designed to sustain a biomass concentration of up to 8 g/L in nitrogen-limited anaerobic conditions for the wild type (CEN.PK113-7D) strain.

The temperature and stirring speed were kept constant at 30 ºC and 500 rpm, respectively; overpressure of 0.3 bar, and aeration rate of 0.5 vvm were used to keep the dissolved oxygen level above 80%. Dissolved oxygen tension (DOT) was monitored in-line using an oxygen probe (Mettler-Toledo, Tiel, The Netherlands), and a

combined paramagnetic/infrared analyser (NGA 2000, Fisher-Rosemount, Hasselroth, Germany) was used to measure on-line the fractions of CO_2 and O_2 in the dry off-gas. During the batch phase and the first steady state the pH was kept constant at a value of 5 with automatic additions of 4M KOH or 2M H_2SO_4; after reaching steady state and taking all samples, the pH control was changed to maintain a constant value of 6, while keeping the dilution rate constant; the same operation was performed to switch pH from 6 to 7. All samples were taken at steady state between three and seven volume changes after switching on the medium addition or pH changes.

Sampling and sample preparation

Extracellular sampling

For aerobic nitrogen limited chemostats, samples of approx. 2 mL were quenched using cold steel beads (Mashego *et al.*, 2006), and filtered using 0.45 µm disc filters (Milipore). Samples for residual ammonium determination were prepared by mixing 80 µL of sample with 20 µL of internal standard (500 µmol/L ^{15}N-NH_4Cl). All samples were stored at -80ºC until further analysis.

Intracellular sampling

Samples containing approximately 1.2 g broth were obtained using a dedicated setup, as described by Lange *et al.* (2001), quenched in 6 mL of -40 ºC methanol 100%, and after weighing to accurately determining the mass of each sample, these were centrifuged for 5 minutes at 10000 g and -19 ºC. The pellet was recovered and resuspended in 6 mL -40 ºC methanol 100%; then centrifuged again for 5 minutes at 10000 g and -19 ºC (Canelas *et al.*, 2009).

Intracellular ammonium extraction

The biomass pellet obtained from *Intracellular sampling* was recovered, 3.5 mL of Methanol-acetate buffer 10mM (pH = 5) 50%(v/v) pre-chilled at -40 ºC was added, and then 120 µL of U-^{13}C-cell extract with labeled urea (intracellular metabolites samples) or 120 µL of ^{15}N- NH_4Cl 500 µmol/L (intracellular ammonium samples) were added as internal standard. Afterwards, 3.5 mL of Chloroform

100% pre-chilled at -40 ºC was added in order to extract intracellular metabolites according to Cueto-Rojas *et al.* (2016). Samples for quantification of intracellular ammonium were extracted using exclusively this method.

Intracellular metabolite extraction

The biomass pellet obtained in *Intracellular sampling* was recovered by addition of 3.5 mL Methanol-MilliQ water 50% (v/v) pre-chilled at -40 ºC and 120 µL of U-^{13}C- cell extract. 3.5 mL of chloroform 100% pre-chilled at -40 ºC was added in order to extract intracellular metabolites as described by Canelas *et al.* (2009).

Analytical methods

Micro-titer plate assays

96 well plate assays were prepared by adding 100uL of synthetic medium with 20 g/L glucose, Tween-80 (420 mg/L) and ergosterol (10 mg/L). The initial pH of the medium was adjusted using 2 M HCl and 2 M KOH. $(NH_4)_2SO_4$ was used as the nitrogen source and the SO_4^{2-} concentration was kept constant at 38 mM by addition of K_2SO_4 to compensate for the decrease in SO_4^{2-} from $(NH_4)_2SO_4$. Cells were inoculated in each well to a starting OD_{660} of 0.1. Plates were covered with Nunc™ sealing tape (Thermo Scientific) and incubated at 30 ºC with constant shaking at 200 rpm. OD660 was measured regularly in a GENios pro plate reader (Tecan Benelux, Giessen, The Netherlands).

Metabolite quantification

Quantification of intracellular trehalose, glycolytic, TCA cycle and PPP intermediates was performed as described by Niedenfuhr *et al.* (2015); amino acids were quantified according to de Jonge *et al.* (2011), nucleotides as described in Maleki Seifar *et al.* (2009) and coenzymes were measured using LC-MS/MS as reported by Maleki Seifar *et al.* (2013). Intra- and extracellular ammonium was quantified using UPLC-IDMS as described by Cueto-Rojas *et al.* (2016). Quantification of extracellular metabolites was performed using HPLC as described in Cruz *et al.* (2012). Cellular

concentrations were estimated using the metabolite content per g_{CDW} ($\mu mol/g_{CDW}$) and the average cell volume including dry matter (mL_{WC}/g_{CDW}), which was determined using a Z2 Coulter counter (50 µm aperture, Beckman, Fullerton, CA) (Bisschops *et al.*, 2014).

Proteomic analysis

U-^{13}C-labelled *S. cerevisiae* biomass was prepared as described by (Wu *et al.*, 2005) and used as internal standard for relative protein quantification. Cell suspensions of the sample biomass and internal standard were mixed 1:1 based on the OD_{600}, washed with milli-Q and freeze-dried. Proteins were extracted by grinding the freeze-dried biomass with pestle and mortar, which were precooled with liquid nitrogen. After grinding, 2 mL of 50 mM PBS with 200 mM NaOH was added to extract proteins. The soluble protein fraction was separated from the cell debris by centrifugation at 13,300 rpm for 15 minutes. Proteins were precipitated overnight in cold acetone at -20 ºC by adding 4 parts of cold acetone to 1 part of protein solution. After washing and drying the protein pellet was dissolved in 400 µL of 100 mM ammonium bicarbonate (ABC) with 6 M urea. Of this solution, 20 µL was further processed; proteins were reduced by addition of tris(2-carboxyethil)phosphine (TCEP) to a final concentration of 10 mM and incubating for 60 minutes at room temperature. Proteins were alkylated by addition of Iodoacetamide (IAM) to a final concentration of 10 mM and incubating for 60 minutes at room temperature. Prior to digestion the protein solution was 6 times diluted by addition of 100 µL of 100 mM ABC to dilute the urea concentration to 1 M. Proteins were digested by addition of trypsin (trypsin singles, proteomics grade, Sigma-Aldrich) in a 1:100 ratio and incubating at 37 ºC for 16 hours. The digested protein mixture was purified and concentrated using an in-house made SPE pipette tip using 5 µm particles of Reprosil-Pur C_{18}-Aq reversed phase material (Dr. Maisch GmbH, Ammerbuch-Entringen, Germany).

Digested peptides were separated using nanoflow chromatography performed using a vented column system essentially as described by Meiring *et al.* (2002) and a 2-dimensional precolumn (RP-SCX-RP). Analytical columns of 50 µm id were prepared with a 1 mm Kasil frit

and packed with 5 µm particles of Reprosil-Pur C_{18}-Aq reversed phase material to a length of 40 cm. The capillary RP-SCX-RP precolumn of 150 µm id was prepared with a 1 mm Kasil frit and packed with 5 µm particles of Reprosil-Pur C18-Aq reversed phase material to a length of 17 mm, 5 µm particles of PolySulfoethyl a strong cation exchange material for 60 mm and again 5 µm particles of Reprosil-Pur C_{18}-Aq reversed phase material for 17 mm (total length 94 mm). The different column materials were kept separated from each other by insertion of a piece of glass wool. The used LC equipment and solvents were similar to Finoulst *et al.* (2011). Each sample analysis consisted of six fractionations. In the first fraction the peptides are injected and trapped on the precolumn by applying 100% solvent A for 10 min. Then a first linear gradient was applied from 4 to 35% B in 75 min. After this, a linear gradient to 80% B was followed for 6 min and then 3 min of 80% B. Finally the column was reconditioned for 26 min with 100% A. In the following 5 fractionations, peptides were eluted by 10 µL injections of respectively 5, 10, 50, 250 or 1000 mM ammonium formate pH 2.6 from the autosampler (followed by 100% A for 10 min). Again a first linear gradient was applied from 4 to 35% B in 75 min, followed by a second linear gradient to 80% B for 6 min and then 3 min of 80% B. After each fraction the column was reconditioned for 26 min with 100% A. This results in six fractionations per sample with a total run-time of 12 hours per sample. For each analysis ~10 µg of protein was injected.

Mass spectrometry was performed using a protocol derived from Finoulst *et al.* (2011). Full scan MS spectra (from m/z 400–1500, charge states 2 and higher) were acquired at a resolution of 30,000 at m/z 400 after accumulation to a target value of 10^6 ions (automatic gain control). Nine data-dependent MS/MS scans (HCD spectra, resolution 7,500 at m/z 400) were acquired using the 9 most intense ions with a charge state of 2+ or higher and an ion count of 10,000 or higher. The maximum injection time was set to 500 ms for the MS scans and 200 ms for the MS/MS scan (accumulation for MS/MS was set to target value of 5×10^4). Dynamic exclusion was applied using a maximum exclusion list of 50, one repeat count, repeat duration of 10

s and exclusion duration of 45 s. The exclusion window was set from −10 to + 10 ppm relative to the selected precursor mass.

Data processing and analysis was performed similarly to Finoulst *et al.* (2011). Briefly, MS/MS spectra were converted to Mascot Generic Files (MGF) using Proteome Discoverer 1.4 (ThermoFisher Scientific) and DTASuperCharge version 2.0b1(Mortensen *et al.*, 2010). MGF's from the 6 SCX fractions of the same sample were combined using MGFcombiner version 1.10 (Mortensen *et al.*, 2010). The samples were analyzed with Mascot v2.2.02 search engine (Matrix Science, Boston, MA, USA). As reference proteome the Uniprot (UniProt, 2015) proteome of *Saccharomyces cerevisiae* strain ATCC 204508 / 288c (ID: UP000002311; 6634 sequences) was used.

Carbamidomethyl cysteine was set as a fixed modification and oxidized methionine as a variable modification. Trypsin was specified as the proteolytic enzyme, and up to three missed cleavages were accepted. Mass tolerance for fragment ions was set at 0.05 Da and for precursor peptide ions at 10 ppm. Peptides with Mascot score <10 were removed and only the highest scoring peptide matches for each query listed under the highest scoring protein (bold red) were selected. Proteins were quantified using MSQuant version 2.0b7 (Mortensen *et al.*, 2010) by importing the Mascot results html file with the corresponding raw mass spectrometric data files. MSQuant automatically calculated peptide and protein ratios by using a ^{13}C quantitation method (in quantitationmodes.xml), containing 7 modifications based on the amount of carbon atoms each amino acid contains. The difference in mass between ^{12}C and ^{13}C is 1.00335 Da. Resulting in mass shifts of 2 (glycine), 3 (ASC), 4 (NDT), 5 (EQMPV), 6 (RHILK), 9 (FY) or 11 (W) carbon atoms. Quantification was restricted to peptides with Mascot score ≥25, it is considered that a protein is up regulated when the concentration of protein is at least 50% higher in one strain compared to the other, growing at the same environmental condition. On the other hand, proteins identified with 2 or more confidence peptides with Mascot score ≥25 in one strain but not in the other are considered "unique proteins".

Results and Discussion

Effect of extracellular NH_3 concentration on growth rate

In order to test the hypothesis that removal of ammonium permeases would eliminate NH_4^+-uptake resulting in NH_3 diffusion as the sole mechanism of transport, *MEP1, MEP2* and *MEP3* were removed resulting in strain IMZ351 (Appendix 5.1). Relative specific aerobic growth rates in micro-titer plate (μ_{MTP}) of IMZ351 (*mep1Δ, mep2Δ, mep3Δ*) and the control strain IME169 (*MEP1*, *MEP2*, *MEP3*) were compared at varying initial pH values and $(NH_4)_2SO_4$ concentrations under aerobic conditions (Figure 5.1). The concentration of NH_3 at a given $(NH_4)_2SO_4$ concentration is dependent on the extracellular pH. Increasing the pH increases the NH_3 concentration, however because the *pKa* strongly favors the charged form (*pKa* = 9.25), the NH_4^+ concentration remains relatively unchanged between pH 3 and 7.

Growth of IME169 reached a maximum at approximately 20 mM NH_X; however, it was negatively affected by increasing pH values (figure 5.1.A), an expected effect caused by the deviation from the optimum pH for growth of *S. cerevisiae* (pH = 5). On the other hand, it was observed that the strain IMZ351 increased its growth rate with increasing pH values (figure 5.1.B). Consequently, plotting the specific growth rate as a function of the NH_3 concentration revealed a clear correlation between both variables (Figure 5.1.C), indicating that growth of IMZ351 was dependent on NH_3 concentration whereas IME169 growth was dependent on NH_4^+ concentrations, supporting the hypothesis that deletion of Mep-proteins leads to a change of transport mechanism from NH_4^+-uniport to NH_3-diffusion.

If the Δ*mep1,2,3* strain (IMZ351) indeed relied on diffusion of NH_3 to supply nitrogen to the cell, then the specific rate of N-uptake ($-q_N$, in mol N/g_{CDW}/h) is dependent on the NH_3 concentration gradient between extracellular space and cytosol ($[NH_3]_{EC}$-$[NH_3]_{cyt}$, in mmol/L); the ability of NH_3 to permeate the cell membrane, as represented by the apparent permeability coefficient (P_{1a}, in m/h); and specific mass transfer area of the cell (a_m, in this study 3.22 m^2/g_{CDW}); and therefore $-q_N = P_{1a} \times a_m \times ([NH_3]_{EC}-[NH_3]_{cyt})$.

Consequently, the growth rate of this strain (μ, in h^{-1}) should be dependent on the extracellular NH_3 concentration, as $\mu = 1/\chi_N \times -q_N$,

being χ_N the biomass N-content (usually 0.148 mol N/C-mol biomass or 5.60 $\times 10^{-3}$ mol N/g_{CDW} (Lange and Heijnen, 2001)).

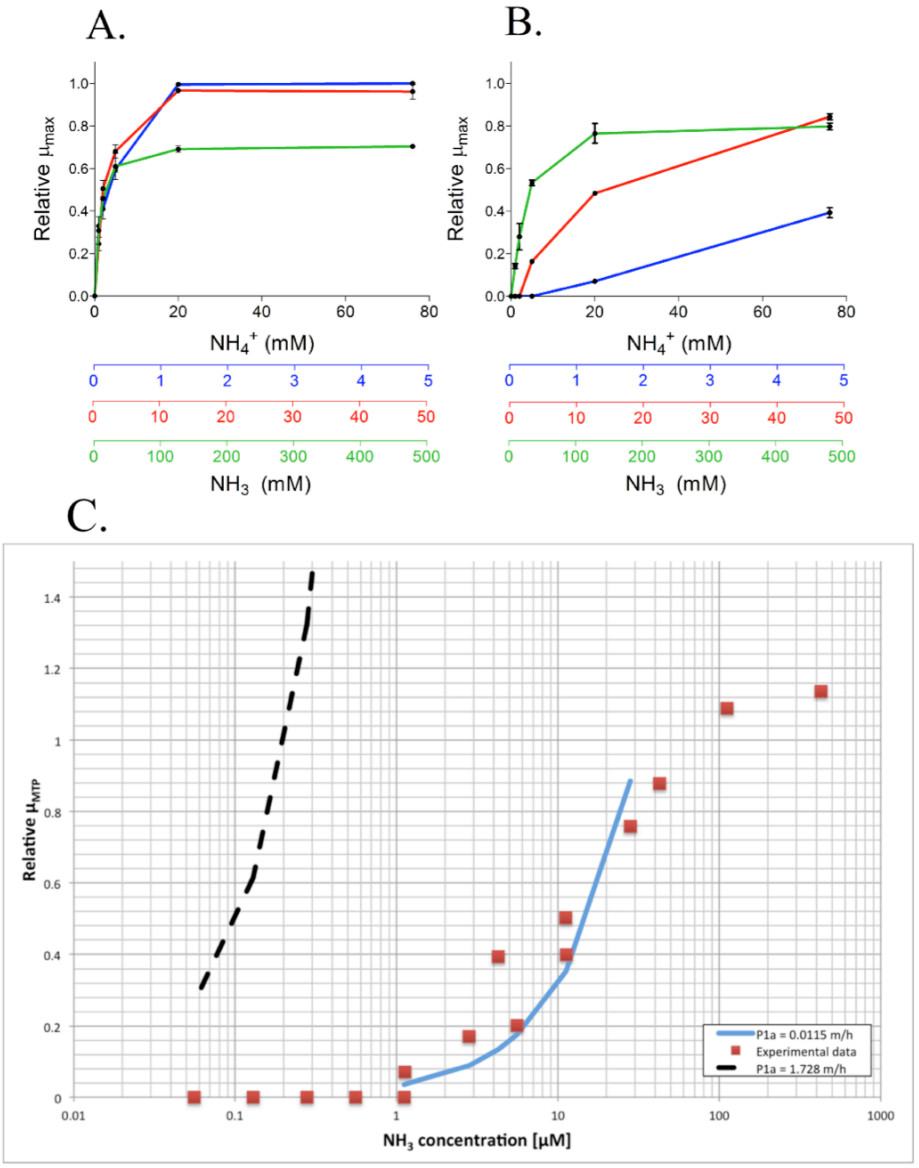

Figure 5.1. Relative specific growth rate in micro-titer plate (μ_{MTP}) of (A) IME169 (*MEP1*, *MEP2*, *MEP3*) and (B) IMZ351 (*mep1Δ, mep2Δ, mep3Δ*) at different pH and extracellular NH_X-concentrations, pH = 5 (blue), pH = 6 (red) and pH = 7 (green) in synthetic medium with glucose supplemented with Tween-80 (420 mg/L) and

ergosterol (10 mg/L). (C) Relative specific growth rates in micro-titer plate (μ_{MTP}) of IMZ351 at different NH_3-concentrations irrespective of extracellular pH. Growth rates were determined from exponentially growing cells cultured in 100 µL synthetic medium in 96 well plates with OD_{660} measurements taken every 15 minutes. The SO_4 concentration was kept constant at 38 mM by supplementation with K_2SO_4. Data are presented as averages and standard deviations of duplicate experiments, relative to the average growth rate of IME169 at pH = 5, with 76 mM NH_4^+ (μ_{max} = 0.21 h^{-1}). The continuous blue line represents an apparent permeability coefficient of 0.0115 m/h (0.32 $\times 10^{-3}$ cm/s), calculated using least squares in the linear region of the experimental data (R^2 = 0.73); the discontinuous black line shows the trend of the growth rate if an apparent permeability coefficient of 1.728 m/h (48×10^{-3} cm/s) is assumed (Antonenko *et al.*, 1997).

To estimate the NH_3 permeability coefficient for batch conditions, we assumed that the NH_3 extracellular concentration is much higher than the cytosolic concentration, therefore the growth rate is linearly dependent on the NH_3 extracellular concentration ($\mu = 1/\chi_N \times P_{1a} \times a_m \times [NH_3]_{EC}$). Based on these assumptions and the measurements of μ_{MTP} as a function of the initial NH_3 concentration (Figure 5.1.C), a rough estimation of the NH_3 permeability coefficient resulted in a P_{1a} value of around 0.01 m/h, which is two orders of magnitude below values reported in literature. These experiments did however show that near wild-type growth rates could be sustained by NH_3-diffusion.

Intracellular and extracellular NH_X ratios under N-limiting conditions

While the previous micro-titer assay showed a clear link between the extracellular NH_3 concentration and the growth rate of IMZ351, the results cannot provide insights into the intracellular metabolism, and the absence of pH control and monitoring of dissolved oxygen concentration could potentially bias these results. In order to perform a detailed analysis of the resulting strain physiology in response to different mechanisms of NH_X assimilation, aerobic N-limited chemostat cultures were carried out at varying pH values (pH = 5, pH = 6, pH = 7) and a range of extracellular and intracellular samples taken at each steady state condition.

Strain	pH_{EC}	Average cell volume (mL_{IC}/g_{CDW})	Biomass concentration (g_{CDW}/L_{Broth})	Intracellular NH_X ($mmol/L_{IC}$)	Extracellular NH_X ($mmol/L_{EC}$)	Measured IC/EC ratio	Predicted IC/EC equilibrium ratio range	
							Minimum	Maximum
IME169 Uniport NH_4^+	5	2.59 ± 0.04	7.00 ± 0.02	1.74 ± 0.14	0.008 ± 0.001	219 ± 39	108	5.44×10^3
	6	2.43 ± 0.04	7.45 ± 0.01	3.16 ± 0.16	0.011 0.003	302 ± 40	1.09×10^3	5.44×10^4
	7	2.62 ± 0.02	7.73 ± 0.03	3.33 ± 0.09	0.013 ± 0.001	254 ± 10	1.09×10^4	5.44×10^5
IMZ351 Diffusion NH_3	5	2.01 ± 0.08	6.44 ± 0.01	10.5 ± 0.7	6.99 ± 0.28	1.5 ± 0.1	0.05	2.57
	6	2.00 ± 0.04	7.37 ± 0.04	10.9 ± 0.6	2.61 ± 0.09	4.2 ± 0.3	0.5	25.7
	7	2.31 ± 0.09	7.73 ± 0.01	7.48 ± 0.7	0.57 ± 0.02	13.2 ± 1.3	5	255

Table 5.4. Intracellular and extracellular NH_X concentrations of IME169 (*MEP1*, *MEP2*, *MEP3*) and IMZ351 (*mep1Δ, mep2Δ, mep3Δ*) measured at steady state at varying pH values from aerobic N-limited chemostats in synthetic medium with glucose at a dilution rate of 0.05 h^{-1} and the corresponding NH_X IC/EC ratios. For calculation of predicted intracellular/extracellular ratios with compartmentalization three compartments were considered: cytosol, mitochondria and vacuole. The ratios were calculated as the maxima and minima of a sensitivity analysis where the following critical variables were considered: vacuolar volumes (between 25% and 14% intracellular volume), cytosolic pH (between 6 and 7) and vacuolar pH (between 4 and 5.5). The data represent average and mean deviation of triplicates.

Aerobic N-limited conditions were selected to observe the energetic effect of NH_3-diffusion based on differences in specific oxygen consumption rates ($-q_{O2}$) between strains; additionally, the use of N-limited conditions avoided an excess of residual NH_X, thus increasing the accuracy of the intracellular NH_X measurements.To ensure that the differential effect of pH and NH_X concentration between the two strains were indeed based on differences in transport mechanisms, the cytosolic/extracellular NH_X ratio was determined for both strains. If NH_4^+ was the only species being transported into the cell then the uptake rate and the cytosolic/extracellular NH_X ratio at steady state under N-limiting conditions depend on the membrane potential. In contrast, if NH_3 was the only species being transported into the cell, the NH_X-uptake rate and cytosolic/extracellular NH_X ratio depend only on the NH_3 concentration gradient across the cell membrane (appendix 5.2). Thus, both transport mechanisms can be discriminated on the basis of their different cytosolic/extracellular NH_X ratios (Table 5.4). Furthermore, because the growth rate is similar for all cultivations and NH_X is the limiting substrate, the cytosolic concentration of this compound was expected to be similar (if not the same) independently of the transport mechanism.

However, the cytosolic NH_X concentration cannot be measured directly, metabolomics approaches only allow for whole-cell quantifications, which from now on will be called intracellular (IC). In the case of NH_X, previous works (Soupene *et al.*, 2001; Wood *et al.*, 2006) suggest significant accumulation and storage of NH_X in the vacuole, which would impact the cytosolic and measured intracellular concentration. To account for vacuolar storage, the measured NH_X ratios were compared to expected maximum and minimum ratios (IC/EC) based on assumptions for vacuolar diffusion (appendix 5.2). Interestingly, the expected difference in ratios still allows for a clear separation of mechanisms in the presence of vacuolar storage.

Estimation of the NH3 permeability coefficient at steady state N-limiting conditions

Under N-limiting conditions it can be assumed that transport of the N-source is the limiting factor for growth in both strains. In IMZ351

the diffusion rate is determined, as explained before, by the NH_3 permeability and the concentration gradient across the plasma membrane ($([NH_3]_{EC}-[NH_3]_{cyt}$). While the concentration in the extracellular space ($[NH_3]_{EC}$) is directly measured, the cytosolic concentration ($[NH_3]_{cyt}$) needs to be estimated from the whole-cell measurement (IC) and assumptions regarding the intracellular NH_X distribution. Here it is assumed that the cytosol volume represents 70% of the cell volume, the vacuolar volume is 14% of the cellular volume and the mitochondrial volume is about 1% of the total cell volume (Uchida *et al.*, 2011).
Additionally NH_3 transport processes between different compartments are assumed to be at thermodynamic equilibrium, and, since no transport proteins (besides *MEP* proteins) are described in literature that could translocate NH_X between compartments, passive diffusion of NH_3 between vacuole and cytosol, and cytosol and mitochondria was assumed.

Table 5.5. Estimation of the apparent permeability coefficient of ammonium for IMZ351 (*mep1Δ, mep2Δ, mep3Δ*) into the plasma membrane.

Strain	pH_{EC}	pH_{vac}	Cytosolic NH_3 ($\mu mol/L_{Cyt}$)	Extracellular NH_3 ($\mu mol/L_{EC}$)	Estimated Cyt/EC ratio	Apparent permeability coefficient (m/h)
IMZ351	5.0*	4.2*	0.37	0.39	0.030	2.73*
	6.0	4.5	1.31	1.47	0.283	0.37
	7.0	4.5	0.90	3.16	0.902	0.03

* In this particular case, a numerical solution to the system of algebraic equations that estimates P_{1a} (appendix 5.2) is achieved only if the vacuolar pH was 4.2 and the vacuolar volume considered was 25% of the total cell volume.

Solving the system of linear equations obtained from these assumptions (appendix 5.2) results in values for the apparent permeability coefficient between 0.03 m/h and 2.73 m/h (Table 5.5), which decreases with pH as observed in other biological systems (Ritchie, 2013). It has to be mentioned that for an extracellular pH of

5, the assumptions for vacuolar size and pH had to be adjusted to 25% of the cell volume and 4.2, respectively, to justify a positive NH_3 concentration gradient between extracellular space and cytosol.

Impact of NH3-diffusion on the physiology and metabolic fluxes of S. cerevisiae under aerobic N-limiting conditions

Effect of diffusion on the specific consumption and production rates

Having previously confirmed a NH_3-dependent mechanism of nitrogen uptake, the metabolic effect of such modification was investigated by determining the impact on ATP consumption. The ATP production rate was calculated based on the oxygen consumption rate (1.9 mol ATP/mol O_2) and the rate of alcoholic fermentation (1 mol ATP/mol ethanol) under respirofermentative conditions, which was observed under N-limiting conditions (Boer *et al.*, 2003). Contrary to the expectation of a reduced ATP cost per N-mole assimilated, IMZ351 consumed more ATP per mole of N-assimilated than IME169 (table 5.6), indicating a stronger nitrogen limitation compared to the reference strain, this is further supported by a decreased N-content and higher C/N consumption, related to higher production of reserve carbohydrates (*i.e.* trehalose and glycogen).

Intracellular metabolite concentrations

IMZ351 showed decreased biomass N-content when compared to IME169, suggesting that deletion of *MEP* genes resulted in a significantly altered cellular response in nitrogen-limited chemostat cultures. To investigate physiological effects caused by the decreased specific NH_X uptake rates, the concentrations of intracellular metabolites involved in carbon and nitrogen metabolism were measured (appendix 5.3).

While the intracellular NH_X concentration was significantly higher in IMZ351, surprisingly, the intracellular concentration of the product of the most prominent entry route for NH_X assimilation, L-glutamate (Glu), was comparable in both strains at each pH. The L-glutamine

concentration, which is the end product of the alternative route of NH_X assimilation via the GS-GOGAT system, was lower for IMZ351 compared to the reference strain but increased with pH. Downstream, the concentration of amino acids synthesized in the mitochondria: L-alanine, L-valine and L-lysine were significantly lower in IMZ351, and finally the intracellular trehalose concentration, which is an indicator of cellular stress and/or nitrogen limitation (Hazelwood *et al.*, 2009), was significantly higher in IMZ351 at all pH conditions.

Effects of NH_3 diffusion on protein expression

Alteration of the NH_X transport mechanism resulted in changes in cellular metabolism, which was additionally related to changes in the proteome (Kleijn *et al.*, 2010; Kotte *et al.*, 2010). From the proteome of *S. cerevisiae* it was possible to identify more than 300 different proteins; from those proteins, the relative changes in protein abundance were measured in both strains at all pH conditions in order to link the changes in the metabolome with changes in protein expression.

Furthermore, it was found that the expression levels of certain proteins were extremely low to be identified and measured in one strain, but not in the other; those proteins are called from now on "unique proteins", the term "unique" does not imply that in one case they were truly absent, but simply that their concentration was below the detection limit in one case but not in the other and they can be considered an especial subset of up regulated proteins.

From the different proteins measured, eleven proteins were consistently found as unique in IMZ351 but not in the reference strain (IME169) at all pH conditions, indicating that these proteins were expressed in high and measurable levels in IMZ351 compared to IME169 (appendix 5.4). Of these 11 proteins, of particular interest were Rav1; involved in regulation of the activity of the vacuolar ATPase, Hog1; a global regulator of stress responses, and Mck1 a Threonine/Serine protein kinase that regulates DNA replication (Ikui *et al.*, 2012), C-metabolism and protein kinase A activity (Quan *et al.*, 2015).

Strain	pH_{EC}	μ	$-q_S$	$-q_{O2}$	q_{CO2}	$q_{Ethanol}$	$-q_N$	N-content	Y_{XS}	C/N cons.	q_{ATP}	$q_{ATP}/-q_N$
IME169	5	0.053 ± 0.001	3.86 ± 0.05	1.64 ± 0.01	7.03 ± 0.02	4.60 ± 0.22	0.25 ± 0.01	4.7 ± 0.1	0.077 ± 0.001	92.3 ± 1.3	7.7 ± 0.2	30.8 ± 0.9
	6	0.052 ± 0.001	3.40 ± 0.01	1.47 ± 0.01	6.16 ± 0.01	4.44 ± 0.06	0.22 ± 0.01	4.3 ± 0.1	0.085 ± 0.001	91.4 ± 1.7	7.2 ± 0.1	32.4 ± 0.6
	7	0.051 ± 0.001	2.95 ± 0.01	1.27 ± 0.01	5.22 ± 0.02	3.61 ± 0.04	0.21 ± 0.01	4.1 ± 0.1	0.096 ± 0.001	104.1 ± 2.3	6.0 ± 0.1	28.9 ± 0.6
IMZ351	5	0.047 ± 0.001	3.49 ± 0.03	1.39 ± 0.01	6.62 ± 0.01	4.74 ± 0.04	0.19 ± 0.01	4.0 ± 0.2	0.081 ± 0.001	110.1 ± 4.7	7.4 ± 0.1	38.9 ± 1.6
	6	0.047 ± 0.001	3.07 ± 0.02	1.22 ± 0.01	5.83 ± 0.03	4.40 ± 0.05	0.18 ± 0.01	3.9 ± 0.1	0.085 ± 0.001	100.8 ± 1.7	6.7 ± 0.1	36.7 ± 0.6
	7	0.048 ± 0.001	2.83 ± 0.03	1.24 ± 0.01	5.08 ± 0.01	3.64 ± 0.05	0.19 ± 0.01	3.9 ± 0.1	0.095 ± 0.001	90.7 ± 1.8	6.0 ± 0.1	32.0 ± 0.5

Table 5.6. Overview of measured extracellular fluxes and N-content of IME169 (*MEP1*, *MEP2*, *MEP3*) and IMZ351 (*mep1Δ, mep2Δ, mep3Δ*) during N-limited aerobic chemostats in synthetic medium with glucose at a dilution rate of 0.05 h^{-1} at different extracellular pH.

Units:

-q_S in mmol glucose/g_{CDW}/h
q_{O2} in mmol O_2/gCDW/h
q_{CO2} in mmol CO_2/g_{CDW}/h
$q_{Ethanol}$ in mmol ethanol/g_{CDW}/h
-q_N in mmol NH_X/g_{CDW}/h
N-content in mmol N/g_{CDW}
Y_{XS} in g_{CDW}/g_{Glc}
C/N consumption in C-mol/N-mol
q_{ATP} in mmol ATP/g_{CDW}/h
q_{ATP}/-q_N in mol ATP/mol N

Further GO-term cluster analysis revealed that among the 31 proteins with at least a 40% increase in expression in IMZ351, most of them were related to stress-response terms, in particular several were associated with DNA replication stress, *i.e.* inefficient DNA replication (Burhans and Weinberger, 2012) and the cellular processes of autophagy and decreased protein production (Onodera and Ohsumi, 2005), (Rtp6 and Cps1) which correlates with a severe N-limitation state. While a significant up-regulation of proteins involved in various stress responses was observed, no significant differences in proteins involved in nitrogen catabolite repression (NCR) and central nitrogen metabolism were observed.

Mep proteins are essential for NH_4^+-sensing and are involved in signaling cascades related to N-starvation

The metabolic profile in both strains presented clear differences, in particular the significantly higher concentration of intracellular NH_X and trehalose in the strain IMZ351. While the cause of the increased intracellular NH_X concentration in strain IMZ351 remains unanswered, it does raise questions about how this strain senses N-limitation. Currently, the exact mechanisms of N-sensing are unknown; our experimental results suggest that intracellular NH_X is not involved in signaling.

Proteomic analysis revealed a significant up regulation of proteins related to recycling of N-compounds (protein, amino acids) and general cellular stress responses, overall suggesting a significantly altered cellular response to N-limitation. However in view of the higher intracellular NH_X concentration (table 5.4), and the generally comparable concentrations of most intracellular N-based metabolites (appendix 5.3), this appears to be unrelated to any particular signaling metabolite in the intracellular space. Mep1 and Mep2 have been described as NH_4^+ transceptors, responsible not only for transport across the cell membrane, but also as cAMP-independent activators of the protein kinase A (PKA) signaling cascade; this signal is triggered due to conformational changes in Mep1 and Mep2 after binding with ammonium (Van Nuland *et al.*, 2006).

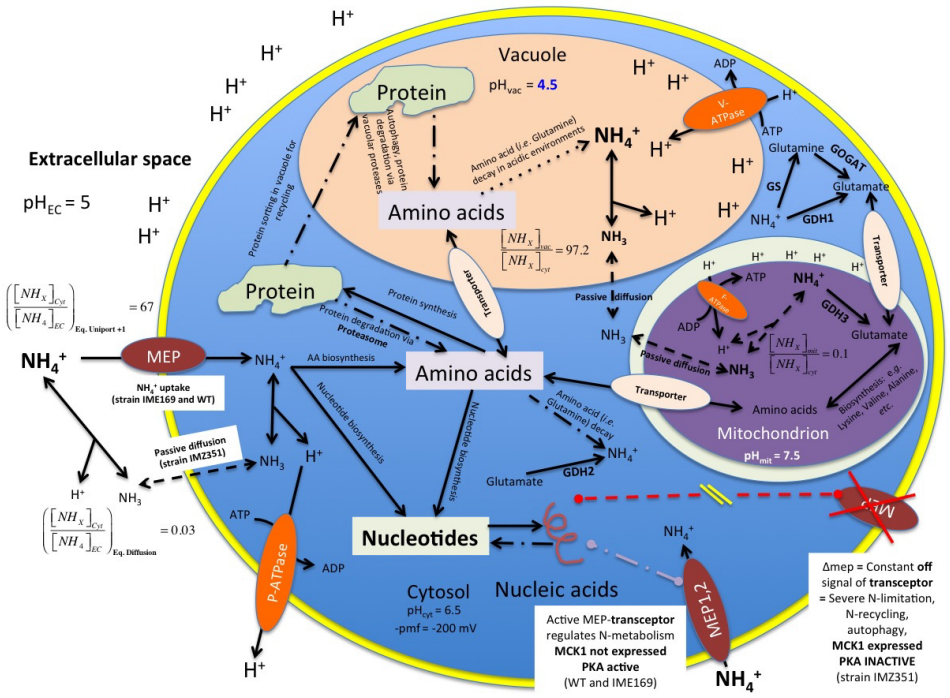

Figure 5.2. Proposed hypotheses of NHx transport mechanisms in IME169 (*MEP1*, *MEP2*, *MEP3*) and IMZ351 (*mep1Δ, mep2Δ, mep3Δ*), and the cellular response to the absence of MEP-proteins in IMZ351. The main reactions of N-central metabolism (GS-GOGAT, Gdh1, Gdh2 and Gdh3) and relevant macromolecule biosynthesis and degradation pathways are sketched together with the hypotheses presented hereby. Mep1 and Mep2 work as transceptors, signaling the presence of ammonium, and activate a yet unidentified signaling cascade (Conrad *et al.*, 2014) (light purple discontinuous line), possibly protein kinase A (PKA) as described in previous works (Conrad *et al.*, 2014; Van Nuland *et al.*, 2006). In the absence of MEP-proteins there is a constitutive down-regulation/repression of PKA (maybe via *Mck1* as suggested by the proteomics survey) and up-regulation/activation (broken red line) of genes associated with autophagy and DNA replication stress, potentially related to STRE- (stress response element) mediated cellular stress response. DNA replication stress and autophagy signals decrease DNA replication and protein biosynthesis, and an increasing protein turnover (vacuolar or proteasome mediated leading to production of amino acids and/or higher NHx concentrations), amino acid recycling and trehalose overproduction.

In the absence of extracellular NH_4^+ no ammonium permease mediated signal is sent to the PKA complex leading to its inactivation and subsequent repression of glycolytic genes, genes

involved in cellular growth and proliferation and in particular, an up-regulation of genes responsible for the cellular stress response mediated by STRE (stress response element) (Thevelein and de Winde, 1999). This hypothesis is reinforced indirectly by the presence of Mck1, which was one of the proteins only found in IMZ351 but not in the reference strain. As Mck1 is a known transcriptional regulator, PKA inhibitor and modulator of other cellular processes such as DNA replication and protein degradation.

Thus, we speculate that upon deletion of the genes encoding the ammonium permeases a constitutive up-regulation of the cellular stress response is generated leading to the expression of genes involved in various stress responses, in particular DNA replication stress, decreasing protein synthesis, increasing protein turnover, and increased cell-wall protective agents (trehalose, cell wall repair systems) (MartinezPastor *et al.*, 1996), a phenotype observed in the proteomic analysis of IMZ351 (Figure 5.2). However whether this fully explains the metabolite profile of IMZ351, in particular the increase in intracellular NH_X and the decrease in mitochondrial amino acids, or whether additional responses are also involved is yet to be ascertained.

Unspecific NH_4^+-transport through K^+-channels

The results presented previously support NH_3 diffusion as the sole mode of NH_X transport in Mep-deficient strain IMZ351 over transport through K^+-channels or alternative transport mechanisms. Aerobic micro-titer experiments clearly showed that the relative specific growth rate was dependent on extracellular NH_3 concentration. The determination of the cytosolic/extracellular ratio of NH_X for IMZ351 under aerobic N-limiting conditions was consistent with the ratio predicted for NH_3 diffusion, but not with any transport mechanism dependent on the cell membrane potential or pmf.

The hypothesis that ammonium enters the cells through K^+-channels is further falsified by the lack of differences in competitive inhibition at different K^+ levels. In the chemostat experiments, 2 M KOH was used as pH titrant, which in the case of strain IMZ351 resulted in residual K^+ concentrations of 21 mM, 38 mM and 84 mM at

respectively pH = 5, 6 and 7. If K^+-channels were used as alternative transporters for NH_X, as suggested by Hess *et al.* (2006), the process should be competitively inhibited at higher K^+ (Hess *et al.*, 2006). At higher pH, and consequently at higher K^+ concentrations, a higher biomass concentration was obtained indicating that K^+ was not inhibiting biomass production in IMZ351. While the measured IC/EC ratio for IMZ351 matched with our predictions, the observed ratios for IME169 remained relatively constant and at least one order of magnitude higher than the ratios observed in IMZ351 across all pH values.

Nevertheless, the experimental ratios did not match the predicted ratios at pH 6 and pH 7 suggesting that the NH_X uptake rate is potentially limited by the affinity (K_M) of the Mep proteins rather than exclusively by the thermodynamic driving force. Notwithstanding, our results for IME169 at different pH values clearly show that NH_4^+ is the transported species, opposing previous studies suggesting that Mep proteins and other Amt-class transporters transport uncharged NH_3 across the membrane (Soupene *et al.*, 2002; Soupene *et al.*, 2001).

Conclusions

The underlying goal of this study was to engineer membrane potential-decoupled NH_X assimilation for use in bulk N-containing chemical production. Although NH_3 uptake through passive diffusion should in theory conserve one ATP per N-assimilated, the experimental results presented hereby were unable to show such effect, most likely the different degrees of N-limitation in both strains led to an uncoupling between ATP generation and biomass production, as observed from the experimental N-biomass content, trehalose concentration and $-q_N/q_{ATP}$.

While the resultant NH_X assimilation was indeed membrane potential-decoupled, the genetic modifications performed in IMZ351 resulted in a significant alteration of nitrogen metabolism under the tested conditions, potentially due to constitutive activation of cellular stress responses. Overall, this suggests that in order to be applicable for industrial applications, elucidation and subsequent engineering of

this response as well as the mechanisms behind NH_x sensing are required.

Acknowledgements

This work was performed within the BE-Basic R&D program (http://www.be-basic.org), which was granted a FES subsidy from the Dutch Ministry of Economic Affairs, Agriculture and Innovation (EL&I). The author HFCR received a scholarship from CONACyT (Scholarship number: 212059). The funders had no role in study design, data collection and interpretation, or the decision to submit the work for publication. The authors wish to thank Martijn Pinkse, Sebastiaan de Bruin, Erik de Hulster, Reza Maleki Seifar, Angela ten Pierick, Marijke Luttik, Tim Vos and Pascale Daran-Lapujade for their valuable contribution to this work; special thanks to Prof. Dr. Ir. Sef Heijnen and Prof. Dr. Jack Pronk for their valuable feedback and critical revision of this manuscript. The author HFCR wishes to thank with particular emphasis the rapid sampling team from the CSE group: Camilo Suárez-Méndez, Cristina Bernal, Angel Sevilla, Francisca Lameiras, Leonor Guedes da Silva, Mariana Velasco-Alvarez and Mihir Shah.

References

Antonenko, Y. N., Pohl, P., Denisov, G. A., 1997. Permeation of ammonia across bilayer lipid membranes studied by ammonium ion selective microelectrodes. Biophys. J. 72**,** 2187-95.

Bisschops, M. M., Zwartjens, P., Keuter, S. G., Pronk, J. T., Daran-Lapujade, P., 2014. To divide or not to divide: a key role of *Rim15* in calorie-restricted yeast cultures. Biochim. Biophys. Acta. 1843**,** 1020-30.

Boer, V. M., Crutchfield, C. A., Bradley, P. H., Botstein, D., Rabinowitz, J. D., 2010. Growth-limiting intracellular metabolites in yeast growing under diverse nutrient limitations. Molecular biology of the cell. 21**,** 198-211.

Boer, V. M., de Winde, J. H., Pronk, J. T., Piper, M. D., 2003. The genome-wide transcriptional responses of *Saccharomyces cerevisiae* grown on glucose in aerobic chemostat cultures limited for carbon, nitrogen, phosphorus, or sulfur. J. Biol. Chem. 278**,** 3265-74.

Burhans, W. C., Weinberger, M., 2012. DNA damage and DNA replication stress in yeast models of aging. Subcell Biochem. 57**,** 187-206.

Canelas, A. B., ten Pierick, A., Ras, C., Maleki Seifar, R., van Dam, J. C., van Gulik, W. M., Heijnen, J. J., 2009. Quantitative evaluation of intracellular metabolite extraction techniques for yeast metabolomics. Anal. Chem. 81**,** 7379-89.

Choi, S., Song, C. W., Shin, J. H., Lee, S. Y., 2015. Biorefineries for the production of top building block chemicals and their derivatives. Metab. Eng. 28**,** 223-39.

Conrad, M., Schothorst, J., Kankipati, H. N., Van Zeebroeck, G., Rubio-Texeira, M., Thevelein, J. M., 2014. Nutrient sensing and signaling in the yeast *Saccharomyces cerevisiae*. FEMS Microbiol. Rev. 38**,** 254-99.

Cruz, A. L., Verbon, A. J., Geurink, L. J., Verheijen, P. J., Heijnen, J. J., van Gulik, W. M., 2012. Use of sequential-batch fermentations to characterize the impact of mild hypothermic temperatures on the anaerobic stoichiometry and kinetics of *Saccharomyces cerevisiae*. Biotechnol. Bioeng. 109**,** 1735-44.

Cueto-Rojas, H., Maleki Seifar, R., ten Pierick, A., Heijnen, S., Wahl, A., 2016. Accurate Measurement of the in vivo Ammonium

Concentration in Saccharomyces cerevisiae. Metabolites. 6**,** 12.

de Jonge, L. P., Buijs, N. A., ten Pierick, A., Deshmukh, A., Zhao, Z., Kiel, J. A., Heijnen, J. J., van Gulik, W. M., 2011. Scale-down of penicillin production in *Penicillium chrysogenum*. Biotechnology journal. 6**,** 944-58.

de Kok, S., Kozak, B. U., Pronk, J. T., van Maris, A. J., 2012a. Energy coupling in *Saccharomyces cerevisiae*: selected opportunities for metabolic engineering. FEMS Yeast Res. 12**,** 387-97.

de Kok, S., Nijkamp, J. F., Oud, B., Roque, F. C., de Ridder, D., Daran, J. M., Pronk, J. T., van Maris, A. J. A., 2012b. Laboratory evolution of new lactate transporter genes in a *jen1* Delta mutant of *Saccharomyces cerevisiae* and their identification as *ADY2* alleles by whole-genome resequencing and transcriptome analysis. FEMS Yeast Res. 12**,** 359-374.

Entian, K. D., Kotter, P., 2007. Yeast genetic strain and plasmid collections. Yeast Gene Analysis, Second Edition. 36**,** 629-666.

Finoulst, I., Vink, P., Rovers, E., Pieterse, M., Pinkse, M., Bos, E., Verhaert, P., 2011. Identification of low abundant secreted proteins and peptides from primary culture supernatants of human T-cells. J Proteomics. 75**,** 23-33.

Franden, M. A., Pilath, H. M., Mohagheghi, A., Pienkos, P. T., Zhang, M., 2013. Inhibition of growth of *Zymomonas mobilis* by model compounds found in lignocellulosic hydrolysates. Biotechnol Biofuels. 6**,** 99.

Gietz, R. D., Woods, R. A., 2002. Transformation of yeast by lithium acetate/single-stranded carrier DNA/polyethylene glycol method. Methods Enzymol. 350**,** 87-96.

Gueldener, U., Heinisch, J., Koehler, G. J., Voss, D., Hegemann, J. H., 2002. A second set of *loxP* marker cassettes for Cre-mediated multiple gene knockouts in budding yeast. Nucleic Acids Res. 30**,** e23.

Guldener, U., Heck, S., Fiedler, T., Beinhauer, J., Hegemann, J. H., 1996. A new efficient gene disruption cassette for repeated use in budding yeast. Nucleic Acids Res. 24**,** 2519-2524.

Hazelwood, L. A., Walsh, M. C., Luttik, M. A., Daran-Lapujade, P., Pronk, J. T., Daran, J. M., 2009. Identity of the growth-limiting nutrient strongly affects storage carbohydrate accumulation in anaerobic chemostat cultures of *Saccharomyces cerevisiae*. Appl. Environ. Microbiol. 75**,** 6876-85.

Hess, D. C., Lu, W., Rabinowitz, J. D., Botstein, D., 2006. Ammonium toxicity and potassium limitation in yeast. PLoS Biol. 4**,** e351.

Hong, K. K., Nielsen, J., 2012. Metabolic engineering of *Saccharomyces cerevisiae*: a key cell factory platform for future biorefineries. Cell. Mol. Life Sci. 69**,** 2671-90.

Ikui, A. E., Rossio, V., Schroeder, L., Yoshida, S., 2012. A yeast GSK-3 kinase *Mck1* promotes *Cdc6* degradation to inhibit DNA re-replication. PLoS Genet. 8**,** e1003099.

Kleijn, R., Fendt, S. M., Schuetz, R., Heinemann, M., Zamboni, N., Sauer, U., 2010. Transcriptional control of metabolic fluxes and computational identification of the governing principles. FEBS J. 277**,** 27-27.

Kleiner, D., 1981. The transport of NH_3 and HN_4^+ across biological membranes. Biochimica et Biophysica Acta (BBA) - Reviews on Bioenergetics. 639**,** 41-52.

Kotte, O., Zaugg, J. B., Heinemann, M., 2010. Bacterial adaptation through distributed sensing of metabolic fluxes. Mol. Syst. Biol. 6**,** 355.

Kresnowati, M. T., Suarez-Mendez, C., Groothuizen, M. K., van Winden, W. A., Heijnen, J. J., 2007. Measurement of fast dynamic intracellular pH in *Saccharomyces cerevisiae* using benzoic acid pulse. Biotechnol. Bioeng. 97**,** 86-98.

Kumar, P., Barrett, D. M., Delwiche, M. J., Stroeve, P., 2009. Methods for Pretreatment of Lignocellulosic Biomass for Efficient Hydrolysis and Biofuel Production. Industrial & Engineering Chemistry Research. 48**,** 3713-3729.

Labotka, R. J., Lundberg, P., Kuchel, P. W., 1995. Ammonia permeability of erythrocyte membrane studied by ^{14}N and ^{15}N saturation transfer NMR spectroscopy. Am J Physiol. 268**,** C686-99.

Lange, H. C., Eman, M., van Zuijlen, G., Visser, D., van Dam, J. C., Frank, J., de Mattos, M. J., Heijnen, J. J., 2001. Improved rapid sampling for *in vivo* kinetics of intracellular metabolites in *Saccharomyces cerevisiae*. Biotechnol. Bioeng. 75**,** 406-15.

Lange, H. C., Heijnen, J. J., 2001. Statistical reconciliation of the elemental and molecular biomass composition of *Saccharomyces cerevisiae*. Biotechnol. Bioeng. 75**,** 334-44.

Magasanik, B., 2003. Ammonia Assimilation by *Saccharomyces cerevisiae*. Eukaryot. Cell. 2**,** 827-829.

Maleki Seifar, R., Ras, C., Deshmukh, A. T., Bekers, K. M., Suarez-Mendez, C. A., da Cruz, A. L., van Gulik, W. M., Heijnen, J. J., 2013. Quantitative analysis of intracellular coenzymes in

Saccharomyces cerevisiae using ion pair reversed phase ultra high performance liquid chromatography tandem mass spectrometry. J. Chromatogr. A. 1311**,** 115-20.

Maleki Seifar, R., Ras, C., van Dam, J. C., van Gulik, W. M., Heijnen, J. J., van Winden, W. A., 2009. Simultaneous quantification of free nucleotides in complex biological samples using ion pair reversed phase liquid chromatography isotope dilution tandem mass spectrometry. Anal. Biochem. 388**,** 213-9.

Marini, A. M., Soussi-Boudekou, S., Vissers, S., Andre, B., 1997. A family of ammonium transporters in *Saccharomyces cerevisiae*. Mol. Cell. Biol. 17**,** 4282-93.

MartinezPastor, M. T., Marchler, G., Schuller, C., MarchlerBauer, A., Ruis, H., Estruch, F., 1996. The *Saccharomyces cerevisiae* zinc finger proteins *Msn2p* and *Msn4p* are required for transcriptional induction through the stress-response element (STRE). EMBO J. 15**,** 2227-2235.

Mashego, M. R., van Gulik, W. M., Vinke, J. L., Visser, D., Heijnen, J. J., 2006. *In vivo* kinetics with rapid perturbation experiments in *Saccharomyces cerevisiae* using a second-generation BioScope. Metab. Eng. 8**,** 370-83.

Meiring, H. D., van der Heeft, E., ten Hove, G. J., de Jong, A. P. J. M., 2002. Nanoscale LC-MS(n): technical design and applications to peptide and protein analysis. J. Sep. Sci. 25**,** 557-568.

Milne, N., Luttik, M. A., Cueto Rojas, H. F., Wahl, A., van Maris, A. J., Pronk, J. T., Daran, J. M., 2015. Functional expression of a heterologous nickel-dependent, ATP-independent urease in *Saccharomyces cerevisiae*. Metab. Eng. 30**,** 130-140.

Mortensen, P., Gouw, J. W., Olsen, J. V., Ong, S. E., Rigbolt, K. T., Bunkenborg, J., Cox, J., Foster, L. J., Heck, A. J., Blagoev, B., Andersen, J. S., Mann, M., 2010. MSQuant, an open source platform for mass spectrometry-based quantitative proteomics. J Proteome Res. 9**,** 393-403.

Niedenfuhr, S., Pierick, A. T., van Dam, P. T., Suarez-Mendez, C. A., Noh, K., Wahl, S. A., 2015. Natural isotope correction of MS/MS measurements for metabolomics and C fluxomics. Biotechnol. Bioeng.

Nielsen, J., Larsson, C., van Maris, A., Pronk, J., 2013. Metabolic engineering of yeast for production of fuels and chemicals. Curr. Opin. Biotechnol. 24**,** 398-404.

Nijkamp, J. F., van den Broek, M., Datema, E., de Kok, S., Bosman, L., Luttik, M. A., Daran-Lapujade, P., Vongsangnak, W.,

Nielsen, J., Heijne, W. H., Klaassen, P., Paddon, C. J., Platt, D., Kotter, P., van Ham, R. C., Reinders, M. J., Pronk, J. T., de Ridder, D., Daran, J. M., 2012. *De novo* sequencing, assembly and analysis of the genome of the laboratory strain *Saccharomyces cerevisiae* CEN.PK113-7D, a model for modern industrial biotechnology. Microbial cell factories. 11**,** 36.

Oldiges, M., Eikmanns, B. J., Blombach, B., 2014. Application of metabolic engineering for the biotechnological production of L-valine. Appl. Microbiol. Biotechnol. 98**,** 5859-70.

Onodera, J., Ohsumi, Y., 2005. Autophagy is required for maintenance of amino acid levels and protein synthesis under nitrogen starvation. J. Biol. Chem. 280**,** 31582-6.

Perktold, A., Zechmann, B., Daum, G., Zellnig, G., 2007. Organelle association visualized by three-dimensional ultrastructural imaging of the yeast cell. FEMS Yeast Res. 7**,** 629-38.

Pronk, J. T., 2002. Auxotrophic yeast strains in fundamental and applied research. Appl. Environ. Microbiol. 68**,** 2095-100.

Qian, Z. G., Xia, X. X., Lee, S. Y., 2011. Metabolic engineering of *Escherichia coli* for the production of cadaverine: a five carbon diamine. Biotechnol. Bioeng. 108**,** 93-103.

Quan, Z., Cao, L., Tang, Y., Yan, Y., Oliver, S. G., Zhang, N., 2015. The Yeast GSK-3 Homologue *Mck1* Is a Key Controller of Quiescence Entry and Chronological Lifespan. PLoS Genet. 11**,** e1005282.

Ritchie, R. J., 2013. The ammonia transport, retention and futile cycling problem in cyanobacteria. Microb. Ecol. 65**,** 180-96.

Sauer, B., 1987. Functional expression of the cre-lox site-specific recombination system in the yeast *Saccharomyces cerevisiae*. Mol. Cell. Biol. 7**,** 2087-96.

Soupene, E., Lee, H., Kustu, S., 2002. Ammonium/methylammonium transport (Amt) proteins facilitate diffusion of NH3 bidirectionally. Proceedings of the National Academy of Sciences of the United States of America. 99**,** 3926-31.

Soupene, E., Ramirez, R. M., Kustu, S., 2001. Evidence that Fungal MEP Proteins Mediate Diffusion of the Uncharged Species NH_3 across the Cytoplasmic Membrane. Mol. Cell. Biol. 21**,** 5733-5741.

Thevelein, J. M., de Winde, J. H., 1999. Novel sensing mechanisms and targets for the cAMP-protein kinase A pathway in the yeast Saccharomyces cerevisiae. Mol. Microbiol. 33**,** 904-918.

Turk, S. C., Kloosterman, W. P., Ninaber, D. K., Kolen, K. P., Knutova, J., Suir, E., Schurmann, M., Raemakers-Franken, P.

C., Muller, M., de Wildeman, S. M., Raamsdonk, L. M., van der Pol, R., Wu, L., Temudo, M. F., van der Hoeven, R. A., Akeroyd, M., van der Stoel, R. E., Noorman, H. J., Bovenberg, R. A., Trefzer, A. C., 2015. Metabolic Engineering toward Sustainable Production of Nylon-6. ACS Synth Biol.

Uchida, M., Sun, Y., McDermott, G., Knoechel, C., Le Gros, M. A., Parkinson, D., Drubin, D. G., Larabell, C. A., 2011. Quantitative analysis of yeast internal architecture using soft X-ray tomography. Yeast. 28**,** 227-36.

Ullmann, R. T., Andrade, S. L., Ullmann, G. M., 2012. Thermodynamics of transport through the ammonium transporter *Amt-1* investigated with free energy calculations. J. Phys. Chem. B. 116**,** 9690-703.

UniProt, C., 2015. UniProt: a hub for protein information. Nucleic Acids Res. 43**,** D204-12.

van Maris, A. J., Winkler, A. A., Kuyper, M., de Laat, W. T., van Dijken, J. P., Pronk, J. T., 2007. Development of efficient xylose fermentation in *Saccharomyces cerevisiae*: xylose isomerase as a key component. Advances in biochemical engineering/biotechnology. 108**,** 179-204.

Van Nuland, A., Vandormael, P., Donaton, M., Alenquer, M., Lourenco, A., Quintino, E., Versele, M., Thevelein, J. M., 2006. Ammonium permease-based sensing mechanism for rapid ammonium activation of the protein kinase A pathway in yeast. Mol. Microbiol. 59**,** 1485-505.

Verduyn, C., Postma, E., Scheffers, W. A., van Dijken, J. P., 1990. Physiology of *Saccharomyces cerevisiae* in anaerobic glucose-limited chemostat cultures. J. Gen. Microbiol. 136**,** 395-403.

Verduyn, C., Postma, E., Scheffers, W. A., Van Dijken, J. P., 1992. Effect of benzoic acid on metabolic fluxes in yeasts: a continuous-culture study on the regulation of respiration and alcoholic fermentation. Yeast. 8**,** 501-17.

Weusthuis, R. A., Lamot, I., van der Oost, J., Sanders, J. P., 2011. Microbial production of bulk chemicals: development of anaerobic processes. Trends Biotechnol. 29**,** 153-8.

Wood, C. C., Poree, F., Dreyer, I., Koehler, G. J., Udvardi, M. K., 2006. Mechanisms of ammonium transport, accumulation, and retention in ooyctes and yeast cells expressing *Arabidopsis AtAMT1;1*. FEBS Lett. 580**,** 3931-6.

Wu, L., Mashego, M. R., van Dam, J. C., Proell, A. M., Vinke, J. L., Ras, C., van Winden, W. A., van Gulik, W. M., Heijnen, J. J., 2005. Quantitative analysis of the microbial metabolome by

isotope dilution mass spectrometry using uniformly ^{13}C-labeled cell extracts as internal standards. Anal. Biochem. 336**,** 164-71.

Zhang, J., Pierick, A. T., van Rossum, H. M., Maleki Seifar, R., Ras, C., Daran, J. M., Heijnen, J. J., Aljoscha Wahl, S., 2015. Determination of the Cytosolic NADPH/NADP Ratio in *Saccharomyces cerevisiae* using Shikimate Dehydrogenase as Sensor Reaction. Sci Rep. 5**,** 12846.

Appendix 5.1. Construction and confirmation of *mep1,2,3*Δ in *S. cerevisiae*

To investigate the role of *MEP1*, *MEP2* and *MEP3* in ammonium assimilation and the effects of deletion on cell physiology, *MEP1*, *MEP2* and *MEP3* were sequentially deleted using the Cre/loxP recombinase system from CEN.PK113-3B. The genotype of the resulting prototrophic strain IMZ351 (*ura3-52, his3-D1, mep1*Δ, *mep2*Δ, *mep3*Δ pUDE199) and the corresponding prototrophic *MEP1*, *MEP2*, *MEP3* positive control strain IME169 (*ura3-52, his3-D1*, *MEP1, MEP2, MEP3* pUDE199) were confirmed by diagnostic PCR (figure I) then used for further analysis.

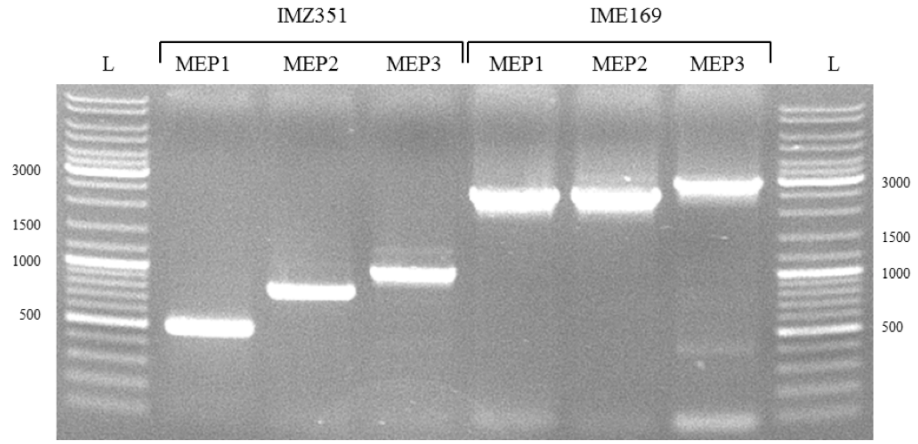

Appendix 5.1 Figure I. PCR analysis of the MEP1, MEP2 and MEP3 regions of IMZ351 and IME169. PCR bands were generated using primers which bound in the upstream and downstream region of each gene with different sized bands between IMZ351 and IME169 confirming the deletion of each gene. L: DNA ladder.

Appendix 5.2 Theoretical calculations

Cytosol/Extracellular ammonium equilibrium ratios

Thermodynamic equilibrium NH_4^+ uniport transport (no compartmentalization)

If ammonium is transported as single positively charged species using an electrochemical gradient as driving force, and it is assumed that it is evenly distributed in the intracellular space, the in/out equilibrium ratio of ammonium is described by equation A5.2.1.

$$\frac{\left[NH_X\right]_{IC}}{\left[NH_X\right]_{EC}} = \left(\frac{1+10^{pH_{cyt}-pKa}}{1+10^{pH_{EC}-pKa}}\right) \times \exp\left(-\frac{F \times \Delta\psi_m}{R \times T}\right) \qquad \text{(A5.2.1)}$$

With,

$$\Delta\psi_m = -pmf + 2.303 \times \frac{R \times T}{F} \times \left(pH_{in} - pH_{out}\right) \qquad \text{(A5.2.2)}$$

Where F is the Faraday's constant, pmf is the proton motive force (assumed -pmf = -200 mV), R the universal gas constant, T the absolute temperature in K, pH_{cyt} and pH_{EC} are the cytosolic and extracellular pH, respectively; the pKa for ammonium is 9.25. When pH_{cyt} and pH_{EC} are assumed to be 6.5 (Kresnowati et al., 2007) and 5, respectively; the in/out ratio is 67 at an absolute temperature of 303.15K; this indicates that at equilibrium most of the ammonium will be found in the intracellular space.

Equilibrium of NH_3 diffusion (no compartmentalization)

On the other hand, if diffusion is the main transport mechanism the in/out equilibrium ratio of NH_X is dependent on the concentration of ammonia (NH_3) in both sides of the membrane, as it is the only species that can cross the cytosolic membrane without transporter. The in/out equilibrium of ammonia is dependent on the cytosolic (pH_{cyt}) and the extracellular pH (pH_{EC}), if there is no compartmentalization of ammonium, equation A5.2.3 describes the equilibrium between $[NH_X]_{IC}$ and $[NH_X]_{EC}$.

$$\frac{\left[NH_X\right]_{IC}}{\left[NH_X\right]_{EC}} = \left(\frac{1+10^{pKa-pH_{cyt}}}{1+10^{pKa-pH_{EC}}}\right) \qquad \text{(A5.2.3)}$$

Assuming similar conditions as in the case of *Equilbrium of NH_4^+ uniport transport*, the in/out ratio is 0.03, in this case at equilibrium most of the ammonium will be present in the extracellular space.

Effect of compartmentalization

In previous sections, it was considered that ammonium would be evenly distributed in the cell. However, previous studies (Wood *et al.*, 2006) suggest large accumulation of NHX in the intracellular space that do not correspond with a NH_4^+-uniport transport mechanism.

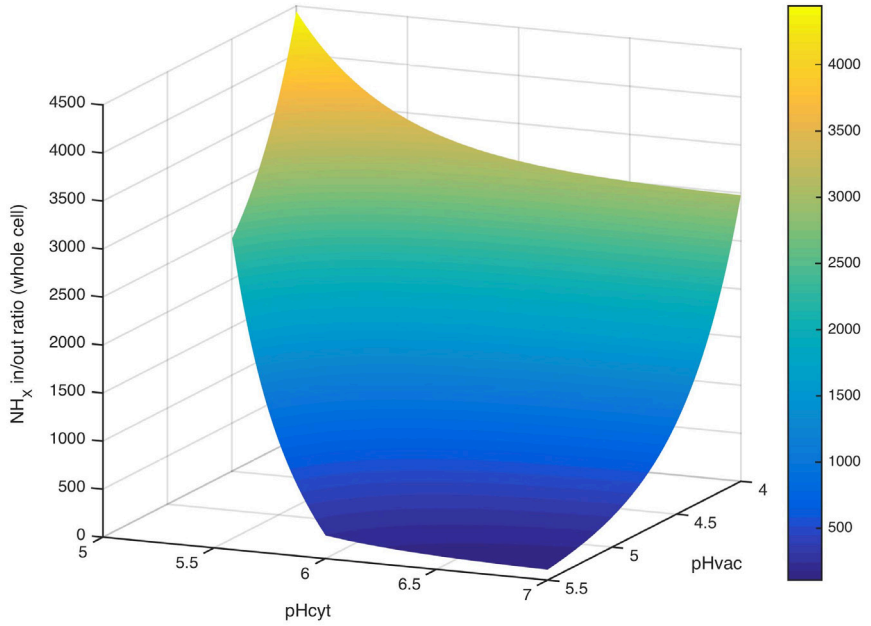

Appendix 5.2 Figure I. In/out NHX equilibrium ratios at pH_{out} = 5. It is considered that NH_4^+-uniport is the transport mechanism for NHX, and compartmentalization of the molecule into the vacuole. Only in/out ratios for the case $pH_{cyt} > (pH_{vac}+0.5)$ are plotted. Color code is based on the NHX in/out ratios (z-axis).

It was shown (Wood *et al.*, 2006) that *S. cerevisiae* cells defective on V-ATPase activity accumulate significantly lower concentrations of ammonium compared to strains with functional V-ATPase; which is good evidence to hypothesize that NHX is transported into the vacuole as NH_3 and due to the acid environment in that compartment is protonated again into NH_4^+ creating significant

accumulation of NH_X in the vacuole (appendix 5.2 Figure I); due to the basic pH in the mitochondrion, it is unlikely that NH_X is accumulated in large quantities in that compartment. Compartmentalization of ammonium is critical, as it will change the expected intracellular/extracellular ratios significantly.

Vacuoles could occupy as much as 25% of the cell volume (Perktold *et al.*, 2007). The most recent measurements suggest that an average of 14% can be assumed (Uchida *et al.*, 2011) and the cytosolic volume corresponds to 70% of the cell volume (Uchida *et al.*, 2011). Additionally, V-ATPase can sustain a pH difference between cytosol and vacuole of 1-2 pH units, typically pH_{cyt} = 6.5 and pH_{vac} = 4.5; therefore, vacuolar compartmentalization could significantly affect the in/out equilibrium ratio of NH_3-diffusion (appendix 5.2 Figure II).

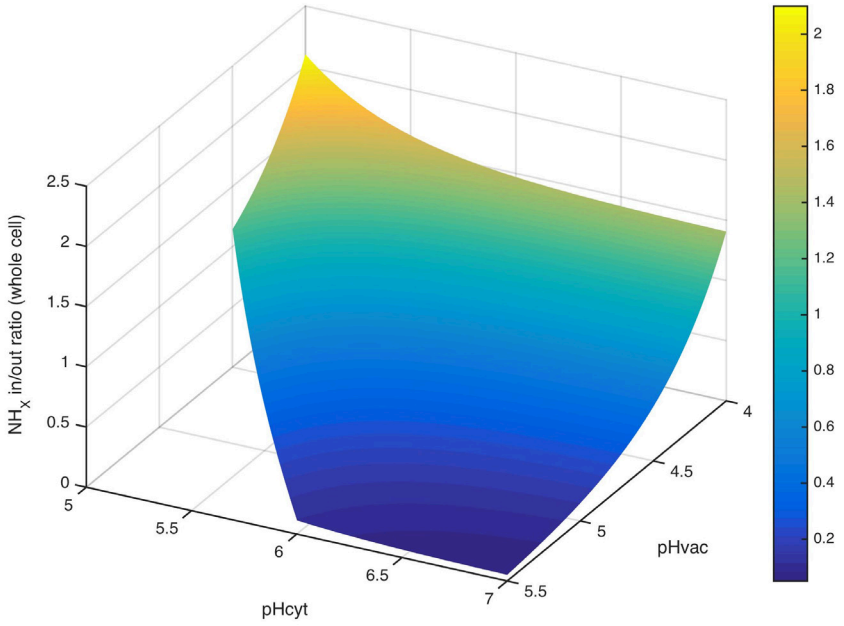

Appendix 5.2 Figure II. In/out NH_X equilibrium ratios at pH_{out} = 5. It is considered that NH_3-diffusion is the transport mechanism for NH_X, compartmentalization into the vacuole is assumed. In/out ratios for the condition $pH_{cyt} > (pH_{vac}+0.5)$ are shown. Color code is based on the NH_X in/out ratios (z-axis).

Theoretical calculation of permeability coefficient of ammonium in Saccharomyces cerevisiae

Ammonia (NH_3) is transported across cell membranes using passive diffusion (Kleiner, 1981), different works measured the apparent permeability coefficient of ammonia in synthetic bilayer lipid membranes (48×10^{-3} cm/s) (Antonenko *et al.*, 1997) and erythrocyte membranes (53×10^{-3} cm/s) (Labotka *et al.*, 1995). The theoretical permeability coefficient could be calculated with the $-q_N = P_{1a} \times a_m \times ([NH_3]_{EC}-[NH_3]_{cyt})$ and the maximum growth rate in *S. cerevisiae*, when NH_4^+ is used as N-source and glucose as C- and energy source at pH_{EC}=5, μ^{max} is around 0.35 h^{-1}. The N content in biomass is 0.148 mol/CmolX (Lange and Heijnen, 2001), which is equivalent to 5.60 $\times10^{-3}$ mol N/g_{CDW}; this leads to a $-q_{NH4+}^{max}$ = 1.96 $\times10^3$ µmol N/g_{CDW}. Assuming that $[NH_3]_{cyt} << [NH_3]_{EC}$, a_m=3.22 m^2/g_{CDW} and a typical NH_X concentration of 75 mmol/L ($[NH_3]_{EC}$ = 4.21 µmol/L); the estimated apparent permeability coefficient of NH_3 for *S. cerevisiae* will be 0.144 m/h (4.02×10^{-3} cm/s).

Although, many reactions would require a minimal amount of ammonium, therefore $[NH_X]_{cyt}$ will never be zero. The assumption of negligible $[NH_3]_{cyt}$ is realistic, based on the equilibrium of the reaction glutamate dehydrogenase NADPH-dependent (GDH1) at cytosolic pH (pH_{cyt} = 6.5), typical intracellular glutamate concentration of 35 $mmol/L_{IC}$, AKG concentration of 0.6 $mmol/L_{IC}$, and NADPH/NADP ratio of 22 (Zhang *et al.*, 2015). We estimated a minimal NH_X concentration in the intracellular space of 0.33 $\mu mol/L_{IC}$ (5.0×10^{-4} $\mu mol/L_{IC}$), which is much lower than the extracellular NH_3. This calculation shows that even an apparent permeability coefficient for NH_3 10 times lower than the reported for other systems should be sufficient to sustain fast growth rates in *Saccharomyces cerevisiae*, if NH_3-diffusion is the nitrogen uptake mechanism.

Estimation of cytosolic NH_X concentration and P_{1a} using experimental results

As explained in the main text, estimation of the cytosolic NH_X concentration requires the whole cell NH_X content, compartment pH

and volumes. The first equation used to obtain the intracellular NH_X distribution is the total intracellular NH_X balance (equation A5.2.4), in A5.2.4 the ratios V_{cyt}/V_{cell}, V_{vac}/V_{cell}, and V_{mit}/V_{cell} express the volume fraction that each compartment represents with respect to the total cell volume; the values used in the text are 0.7, 0.14 and 0.01, respectively.

$$\frac{V_{cyt}}{V_{cell}} \times \left[NH_X\right]_{cyt} + \frac{V_{vac}}{V_{cell}} \times \left[NH_X\right]_{vac} + \frac{V_{mit}}{V_{cell}} \times \left[NH_X\right]_{mit} - \left[NH_X\right]_{IC} = 0 \quad \text{(A5.2.4)}$$

Additionally, it is necessary to assume that NH_3 diffusion is the transport mechanism between compartments, and this process is so fast that can be considered at thermodynamic equilibrium; equation A5.2.5 expresses the equilibrium for the transport between cytosol and vacuole, and equation A5.2.6 expresses the equilibrium for the transport process between cytosol and mitochondria.

$$\frac{1+10^{pKa-pH_{vac}}}{1+10^{pKa-pH_{cyt}}} \times \left[NH_X\right]_{cyt} - \left[NH_X\right]_{vac} = 0 \quad \text{(A5.2.5)}$$

$$\frac{1+10^{pKa-pH_{mit}}}{1+10^{pKa-pH_{cyt}}} \times \left[NH_X\right]_{cyt} - \left[NH_X\right]_{mit} = 0 \quad \text{(A5.2.6)}$$

Finally, the kinetic expression of $-q_N$, which is the mathematical expression for NH_3 diffusion from the extracellular space to the cytosol (A5.2.7), completes a system of 4 algebraic equations.

$$-q_N + P_{1a} \times a_m \times \left(\left[NH_X\right]_{EC} - \left[NH_X\right]_{cyt}\right) = 0 \quad \text{(A5.2.7)}$$

This system of equations can be solved numerically using the experimentally measured variables $[NH_X]_{EC}$, $[NH_X]_{IC}$, and $-q_N$; assumptions about compartment volumes and pH (pH_{cyt}, pH_{vac} and pH_{mit}); being the four variables to determine $[NH_X]_{cyt}$, $[NH_X]_{mit}$, $[NH_X]_{vac}$ and P_{1a}.

Appendix 5.3 Metabolomic analysis of IMZ351 and IME169

Appendix 5.3 Table I. Metabolite concentrations measured in strains IMZ351 and IME169 under aerobic N-limited chemostat conditions (D = 0.05 h^{-1}).

Metabolite	Whole cell concentration (mmol/L_{IC})					
	IMZ351			IME169		
	pH = 5	pH = 6	pH = 7	pH = 5	pH = 6	pH = 7
Glutamate	33.075 ± 1.337	40.889 ± 0.750	41.098 ± 1.513	35.667 ± 0.520	39.681 ± 0.576	45.336 ± 0.350
Glutamine	8.776 ± 0.355	8.812 ± 0.162	7.877 ± 0.290	11.253 ± 0.164	9.333 ± 0.136	6.090 ± 0.047
Aspartate	5.363 ± 0.217	6.001 ± 0.110	6.454 ± 0.238	5.922 ± 0.086	5.757 ± 0.084	6.738 ± 0.052
Lysine	5.041 ± 0.204	5.172 ± 0.095	2.959 ± 0.109	7.063 ± 0.103	6.806 ± 0.099	5.530 ± 0.043
Alanine	11.810 ± 0.477	11.387 ± 0.209	8.073 ± 0.297	16.963 ± 0.247	14.584 ± 0.212	11.558 ± 0.089
Valine	2.320 ± 0.094	2.552 ± 0.047	1.857 ± 0.068	2.764 ± 0.040	2.815 ± 0.041	2.492 ± 0.019
Arginine	8.403 ± 0.340	12.702 ± 0.226	6.706 ± 0.247	9.677 ± 0.141	12.479 ± 0.182	13.466 ± 0.094
AKG	0.388 ± 0.016	0.648 ± 0.012	0.831 ± 0.031	0.604 ± 0.009	0.864 ± 0.013	1.389 ± 0.011
Trehalose	147.79 ± 5.97	180.19 ± 3.30	175.17 ± 6.45	95.72 ± 1.40	115.64 ± 1.68	131.06 ± 1.01
NAD	1.220 ± 0.070	1.042 ± 0.026	0.709 ± 0.037	0.874 ± 0.018	0.760 ± 0.016	0.656 ± 0.006
NADH	0.013 ± 0.001	0.027 ± 0.001	0.017 ± 0.001	0.027 ± 0.001	0.041 ± 0.001	Not detected
NADP	0.299 ± 0.017	0.304 ± 0.008	0.197 ± 0.010	0.219 ± 0.004	0.225 ± 0.005	0.244 ± 0.002
NADPH	0.026 ± 0.002	0.021 ± 0.001	0.017 ± 0.001	0.025 ± 0.001	0.021 ± 0.001	0.017 ± 0.001
ADP	0.879 ± 0.036	0.936 ± 0.017	0.536 ± 0.020	0.704 ± 0.010	0.733 ± 0.011	0.677 ± 0.005
ATP	2.810 ± 0.114	2.711 ± 0.050	1.614 ± 0.059	2.188 ± 0.032	2.047 ± 0.030	1.908 ± 0.015
Energy charge	0.799 ± 0.041	0.790 ± 0.018	0.780 ± 0.036	0.793 ± 0.015	0.775 ± 0.014	0.795 ± 0.008

Appendix 5.4 Thermodynamic calculations of uptake mechanisms

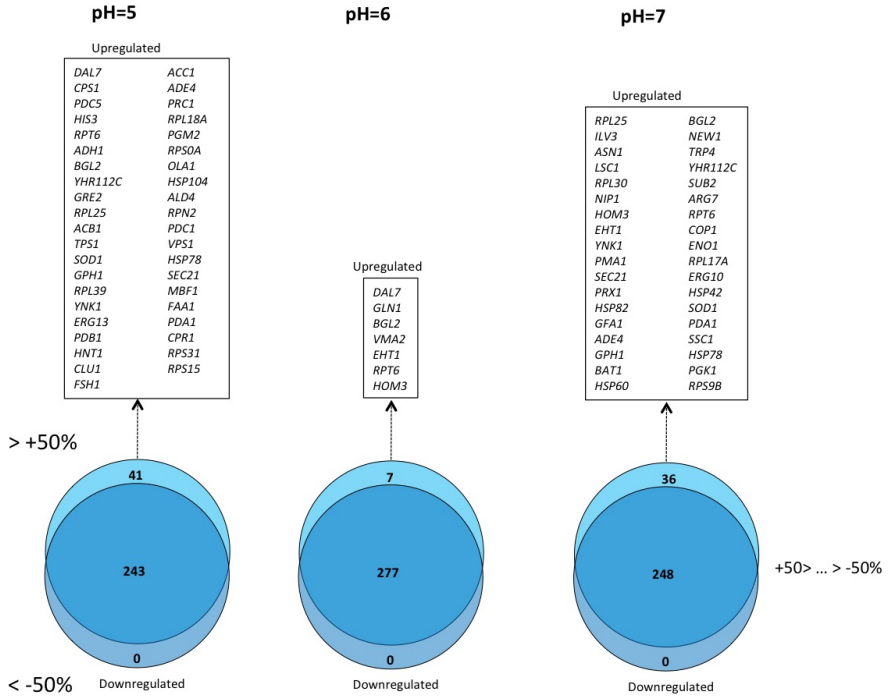

Appendix 5.4 Figure I. Changes in protein expression found in strain IMZ351 compared to IME169 under aerobic N-limited chemostat conditions (D = 0.05 h^{-1}) at individual pH conditions. Protein expression is considered up regulated when the relative change in protein content is 50% or higher with respect to the reference strain (IME169), at the same environmental condition. Bgl2 and Rpt6 are consistently found up regulated in all cases.

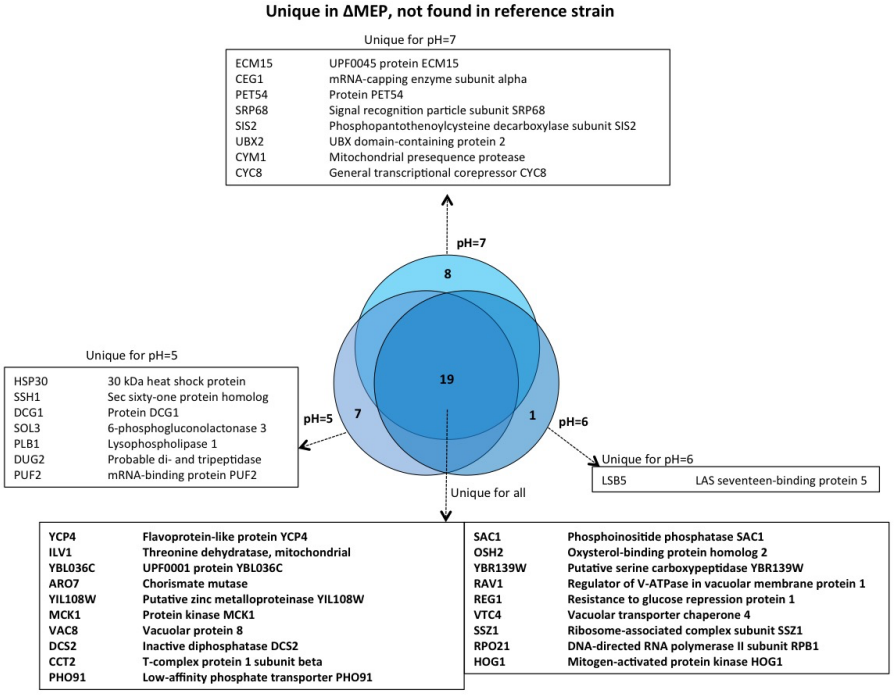

Appendix 5.4 Figure II. Proteins identified with two or more confidence peptides in the strain IMZ351, but not found in IME169 growing under aerobic N-limited chemostat conditions (D = 0.05 h^{-1}) at every pH condition are considered "unique proteins". Unique proteins are in a sense a especial type of up regulated proteins, as their concentration was high enough to be found in IMZ351 extracts but not in IME169; this does not necessarily imply that they are absent in IME169.

CHAPTER

6

Concluding remarks and outlook

It is common sense to take a method and try it. If it fails, admit it frankly and try another. But above all, try something.

Franklin D. Roosevelt, Looking Forward (1933)

Concluding Remarks: *Where do we stand?*

Acknowledging the power of thermodynamic calculations as a tool to describe biological processes, we developed a general method to assess substrate-to-product reactions, which allowed us to recognize the potential of bio-based processes for anaerobic amino acid production. However, the practical implementation of metabolic engineering strategies that conserve free energy in the form of ATP or pmf remains challenging.

Metabolic engineering approaches require a thorough understanding of the cellular metabolism to predict changes that will lead to optimal product formation (Stephanopoulos, 2012). Different transport, assimilation, sensing, and molecular regulation mechanisms of the N-metabolism are described in literature for the industrial workhorse *S. cerevisiae* (Conrad *et al.*, 2014; Ljungdahl and Daignan-Fornier, 2012; Magasanik, 2003). Early descriptions of the N-metabolism resulted in the first kinetic model for yeast's central N-metabolism (van Riel *et al.*, 1998), but to our knowledge no further improvements to that model have been made.

N-metabolism in *S. cerevisiae* is quantitatively less understood than C-metabolism, which led us to recognize earlier in this project that anaerobic amino acid production would require us to first fill gaps in our understanding of yeast's physiology. Therefore, the main objectives of our project shifted to developing tools to achieve a better quantitative description of the central N-metabolism and NH_4^+-transport in yeast.

An important step forward was the elucidation of NH_4^+ and NH_3 transport processes in yeast using *in vivo* intracellular ammonium measurements. Furthermore, our experimental approaches allowed us to gather valuable information that reinforces the hypothesis of NH_4^+-compartmentalization into the vacuole of *S. cerevisiae*, as proposed earlier by Wood *et al.* (2006). Additionally, transport mechanisms for urea and L-glutamic acid were discussed based on our *in vivo* intracellular urea and amino acid measurements, finding a potentially new mechanism for transport of glutamic acid in yeast.

Furthermore, the introduced protocols for *in vivo* intracellular ammonium and amino acid measurements were useful to obtain

better estimates of the thermodynamic driving forces of the main reactions in the central N-metabolism, showing that assuming near-equilibrium reactions in yeast's N-metabolism will lead to erroneous conclusions. In addition, *in vivo* extra- and intracellular ammonium measurements allowed us to recognize a potential futile cycling between NH_4^+ uptake and NH_3-diffusion under aerobic N-limiting conditions, when Mep-proteins are present.

Interestingly, a potential redox futile cycle between glutamate synthesis via *gdh1* (NADPH-dependent) and degradation via *gdh2* (NADH-dependent) was identified using metabolomics and proteomics measurements. The semi-quantitative proteomics approach used in this work also allowed us to observe important rearrangements in the proteome of *S. cerevisiae* when different N-sources are present, showing the relevance of such proteomics surveys to study metabolic pathways quantitatively. However, key challenges are absolute protein quantification and the identification of signaling cascades related to NH_4^+-sensing under N-limitation in *S. cerevisiae*.

We foresee that these protocols will one day also be used to obtain more accurate parameters in kinetic models of N-metabolism in yeast. Moreover, the application of similar protocols in other organisms such as *E. coli* or *C. glutamicum* will be critical for designing better pathways for the production of N-containing metabolites (*e.g.*, valine, lysine, cadaverine, caprolactam, *etc.*), and developing kinetic models of the metabolism in these organisms, which are better known since the lack of compartments makes them easier to study.

Finally, the next step in the overall project will be the direct application of the concepts and experimental methods developed in this work to anaerobic cultures of *S. cerevisiae*, and to candidate strains for the anaerobic production of amino acids.

Outlook: *Where could we go from here?*

In previous chapters we discussed various approaches and tools we developed explicitly to demonstrate the feasibility of anaerobic amino acid production in *Saccharomyces cerevisiae*. Through that process, we learnt valuable lessons about the N-metabolism in yeast, and we came across other particularities that previously were not taken into account. From this research on yeast's metabolism, we recognize that future metabolic engineering strategies for amino acid production should focus on the following key items:

1. **Compartmentalization.** One of the most interesting findings of this work is that the N-metabolism is highly compartmentalized. So far, few studies have focused on developing protocols for measuring compartmentalized metabolites (Ohsumi *et al.*, 1988; Sekito *et al.*, 2008), and the available protocols are quite laborious. Such relevant items as the degradation of metabolites, transport between compartments, and appropriate quenching of the metabolism are not fully demonstrated in the available protocols. Therefore, new and thoroughly validated methods are required to study the dynamics of the metabolites between compartments.

2. ***In vivo* measurement of pmf values.** A key challenge for metabolic engineering is the study of transport processes across cell membranes. In the case of charged molecules, the transport is dependent on the proton motive force of the cytosolic membrane. Biological systems have different mechanisms to achieve ionic homeostasis across the cell membrane; however, these mechanisms cause energy losses, which lead to the depolarization of the cell membrane. Therefore, it is clear that pmf is often incorrectly assumed to be constant under dynamic conditions. The lack of experimental protocols to measure *in vivo* the pmf value severely limits our understanding of transport processes across the cell membrane.

   In a first attempt (data not published), our group proposed to measure pmf using the sensor reaction concept. Although

encouraging, the preliminary experimental results did not indicate whether we are likely to find a strain of *S. cerevisiae* with appropriate genotype that we can use to estimate *in vivo* the pmf. Nevertheless, follow-up experiments are expected and encouraged.

3. **Intracellular and intracompartment pH.** Another important assumption used in this work, is a constant value for intracellular pH and the vacuolar pH. Various techniques are used in literature to estimate these parameters. In particular, we tried to use the method reported by Kresnowati *et al.* (2007). Unfortunately, benzoic acid uptake was not observed. Other methods (Orij *et al.*, 2009) are recommended to quantify this important cellular parameter when studying NH_4^+ cuptake.

4. **Quantification of futile cycles.** An important assumption made in this work is the NH_3-permeability coefficient; this parameter determines the value for the efflux of NH_3 in the futile cycle NH_4^+-uptake/NH_3-excretion. In order to estimate accurately the flux, and therefore the energetic requirements for this futile cycle, it is necessary to estimate the NH_3-uptake flux. Potentially, the use of ^{15}N-NH_4^+ could help to determine the amount of NH_3-leaking to the extracellular space, based on the enrichment dynamics of the extracellular total NH_4^+.
   Furthermore, the intracellular enrichment dynamics will provide valuable information about the amount of compartmentalized NH_4^+ in the vacuole. Additionally, ^{15}N-labelling could help to unravel quantitative information about the redox-futile cycle between *gdh2* and *gdh1*, as the fluxes of these reactions could be quantified.

5. **Tools for transport engineering.** One of the key processes in amino acid metabolism and industrial production is the transport across the cell membrane. Several proteins are in charge of amino acid trafficking (Barnett, 2008). One of the most relevant is the protein GAP1 (general amino acid permease), which imports

amino acids using active transport (H^+ symport) (Chen and Kaiser, 2002; Herrgard *et al.*, 2008; Magasanik and Kaiser, 2002). In the case of L-alanine, it appears that the excretion mechanism in yeast is the reversible proton symport of alanine.

By knowing the transport mechanism (symport of amino acid with one H^+; figure 6.1), it is possible to calculate the maximum cytosolic/extracellular (from now on, "in/out") concentration ratios for amino acids assuming thermodynamic equilibrium of the transport process (equation 6.1).

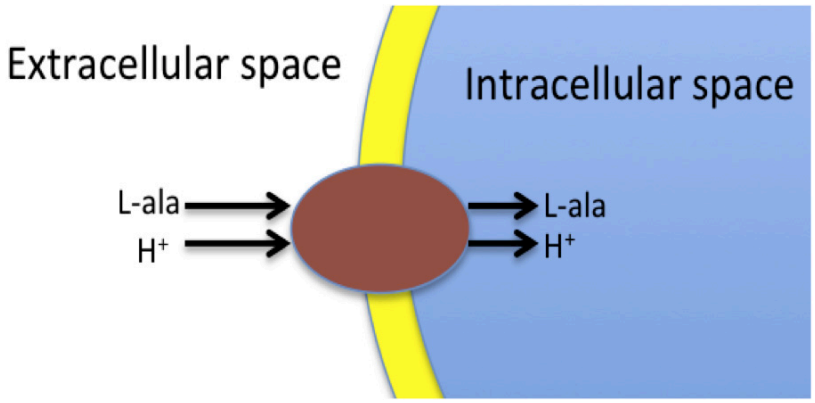

Figure 6.1. Sketch of the L-alanine uptake mechanism in *S. cerevisiae*.

$$\frac{[\mathrm{Ala}]_{\mathrm{In}}}{[\mathrm{Ala}]_{\mathrm{Out}}} = \exp\left(\frac{-z \times F \times \Delta\psi_m}{R \times T}\right) \times 10^{pH_{in} - pH_{out}} \qquad (6.1)$$

In this equation R is the ideal gas constant, T is the temperature at which the process occurs, [AA] and $[H^+]$ are the concentrations of amino acid and protons (the subscript indicates the side of the membrane), z is the overall charge of the species being transported across the membrane, F is the Faraday's constant (96.5 kJ/mol/V), and $\Delta\psi_m$ is the membrane potential in V (equation 6.2).

$$\Delta\psi_m = -\mathrm{pmf} + 2.303 \times \frac{R \times T}{F} \times \left(pH_{in} - pH_{out}\right) \qquad (6.2)$$

Although it is clear that the thermodynamic equilibrium of the H^+-symport mechanism of amino acids leads to the accumulation of these compounds in the intracellular space (table 6.1), it is also clear that amino acid excretion via a reversible H^+-symport would be difficult.

Table 6.1. Typical in/out equilibrium ratios for amino acids using an H^+-symport mechanism. At typical physiological conditions for *S. cerevisiae*, *i.e.*, $pH_{out} = 5$, T = 303.15 K, pmf = -200 mV and $pH_{in} = 6.5$ (Kresnowati *et al.*, 2007).

Overall charge transported across the cell membrane (z)	**Amino acid charge at physiological conditions**	**Examples of amino acids**	**Cyt/EC concentration ratio**
0	-1	Glutamate & aspartate	31
+1	0	Alanine, valine & all other neutral amino acids	2116
+2	+1	Lysine, asparagine, & arginine	1.42E5

It can be inferred from this calculation that amino acids accumulate in the intracellular space due to the nature of the uptake mechanism. Therefore, the excretion of amino acids in *S. cerevisiae* requires different and energetically more efficient transporters. Various protein engineering approaches could be used to change the type of transporter to a more favorable mechanism (*e.g.*, uniport).

6. **Evolutionary selection for energy efficient strains.** The main advantage of developing an anaerobic process for the production of metabolites, is that the product pathway produces the thermodynamic driving force for growth. Therefore, the selective pressure will push evolution in the direction of obtaining the strain that produces the desired metabolite faster and in larger amounts. Once the various issues of energy conservation, redox neutrality in the production pathway, and efficient product transport are overcome, evolutionary engineering can be applied to maximize the anaerobic production of amino acids.

We envision that the research on these topics will result in discoveries that are sufficiently novel and exciting to attract funds and drive forward the research on anaerobic amino acid production in yeast.

Recommended references

Barnett, J. A., 2008. A history of research on yeasts 13. Active transport and the uptake of various metabolites. Yeast. 25**,** 689-731.

Chen, E. J., Kaiser, C. A., 2002. Amino acids regulate the intracellular trafficking of the general amino acid permease of Saccharomycescerevisiae. Proceedings of the National Academy of Sciences of the United States of America. 99**,** 14837-42.

Conrad, M., Schothorst, J., Kankipati, H. N., Van Zeebroeck, G., Rubio-Texeira, M., Thevelein, J. M., 2014. Nutrient sensing and signaling in the yeast *Saccharomyces cerevisiae*. FEMS Microbiol. Rev. 38**,** 254-99.

Herrgard, M. J., Swainston, N., Dobson, P., Dunn, W. B., Arga, K. Y., Arvas, M., Bluthgen, N., Borger, S., Costenoble, R., Heinemann, M., Hucka, M., Le Novere, N., Li, P., Liebermeister, W., Mo, M. L., Oliveira, A. P., Petranovic, D., Pettifer, S., Simeonidis, E., Smallbone, K., Spasic, I., Weichart, D., Brent, R., Broomhead, D. S., Westerhoff, H. V., Kirdar, B., Penttila, M., Klipp, E., Palsson, B. O., Sauer, U., Oliver, S. G., Mendes, P., Nielsen, J., Kell, D. B., 2008. A consensus yeast metabolic network reconstruction obtained from a community approach to systems biology. Nat. Biotechnol. 26**,** 1155-60.

Kresnowati, M. T., Suarez-Mendez, C., Groothuizen, M. K., van Winden, W. A., Heijnen, J. J., 2007. Measurement of fast dynamic intracellular pH in *Saccharomyces cerevisiae* using benzoic acid pulse. Biotechnol. Bioeng. 97**,** 86-98.

Ljungdahl, P. O., Daignan-Fornier, B., 2012. Regulation of amino acid, nucleotide, and phosphate metabolism in *Saccharomyces cerevisiae*. Genetics. 190**,** 885-929.

Magasanik, B., 2003. Ammonia Assimilation by *Saccharomyces cerevisiae*. Eukaryot. Cell. 2**,** 827-829.

Magasanik, B., Kaiser, C. A., 2002. Nitrogen regulation in *Saccharomyces cerevisiae*. Gene. 290**,** 1-18.

Ohsumi, Y., Kitamoto, K., Anraku, Y., 1988. Changes induced in the permeability barrier of the yeast plasma membrane by cupric ion. J. Bacteriol. 170**,** 2676-82.

Orij, R., Postmus, J., Ter Beek, A., Brul, S., Smits, G. J., 2009. *In vivo* measurement of cytosolic and mitochondrial pH using a

pH-sensitive GFP derivative in *Saccharomyces cerevisiae* reveals a relation between intracellular pH and growth. Microbiology. 155**,** 268-78.

Sekito, T., Fujiki, Y., Ohsumi, Y., Kakinuma, Y., 2008. Novel families of vacuolar amino acid transporters. IUBMB Life. 60**,** 519-25.

Stephanopoulos, G., 2012. Synthetic biology and metabolic engineering. ACS Synth Biol. 1**,** 514-25.

van Riel, N. A. W., Giuseppin, M. L. F., TerSchure, E. G., Verrips, C. T., 1998. A Structured, Minimal parameter Model of the Central Nitrogen Metabolism inSaccharomyces cerevisiae: the Prediction of the Behaviour of Mutants. J. Theor. Biol. 191**,** 397-414.

Wood, C. C., Poree, F., Dreyer, I., Koehler, G. J., Udvardi, M. K., 2006. Mechanisms of ammonium transport, accumulation, and retention in ooyctes and yeast cells expressing *Arabidopsis AtAMT1;1*. FEBS Lett. 580**,** 3931-6.

Curriculum vitae

By the time of the defense of this thesis (some time around the first semester of 2016), Hugo Federico Cueto Rojas is a Guest Researcher in the Cell Systems Engineering group at (his beloved *alma mater*) Delft University of Technology, in the Netherlands. Previously, he was enrolled in the same group as Ph.D. student in a 4-year project, finishing officially his research in September 2015.

He took the decision of pursuing a Ph.D. degree after concluding his MSc. Degree at TU Delft in 2011. During his MSc. studies, he was part of the TU Delft iGEM team 2010, an experience that profoundly changed his view about science and academic research. In order to pursue his MSc. degree he was granted a HSP Huygens scholarship by the Dutch government, and a CONACyT scholarship by the Mexican government, the later was extended to continue with his Ph.D. studies.

Before staring his studies in the Netherlands, he worked in Mexico at Probiomed S.A. de C.V. (Tengancingo, Edo. Mex.), after finishing his BSc. in Biotechnology Engineering at the Instituto Politécnico Nacional (Mexico), the institution that nurtured his curiosity and gave him the tools to pursue the truth.

He had the extraordinary luck of being born on January 16th, 1987 in Teziutlan, Puebla, Mexico as the firstborn son of Víctor Hugo Cueto Cárdenas and Silvia Rojas Arroyo.

List of publications

Cueto-Rojas H. F., Maleki Seifar R., ten Pierick A., Heijnen J.J., Wahl S.A. (2015) "Accurate measurement of the *in vivo* ammonium concentration in *Saccharomyces cerevisiae*". Metabolites 23: 6(12) DOI: 10.3390/metabo6020012

Ortiz-Enriquez C., Romero-Diaz A.J., Hernández-Moreno A.V., **Cueto-Rojas H.F.**, Miranda-Hernández M.P., López-Morales C.A., Pérez N.O., Salazar-Ceballos R., Cruz-García N., Flores-Ortiz L.F.,

Medina-Rivero E., "Optimization of a rhGH Purification Process Using Quality by Design". Preparative Biochemistry & Biotechnology. Accepted (01-Feb-2016).
DOI: 10.1080/10826068.2015.1135467

Cueto-Rojas H. F., van Maris A.J.A., Wahl S.A., Heijnen J.J. (2015) "Thermodynamics-based design of microbial cell factories for anaerobic product formation". Trends in Biotechnology 33 (9) : pp. 534-46
DOI: 10.1016/j.tibtech.2015.06.010

Milne N., Luttik M.A., **Cueto-Rojas H.**, Wahl S.A., van Maris A.J.A., Pronk J.T., Daran J.M. (2015) "Functional expression of a heterologous nickel-dependent, ATP-independent urease in Saccharomyces cerevisiae". Metabolic Engineering 30: pp. 130-140
DOI: 10.1016/j.ymben.2015.05.003

Jordá J., **Cueto-Rojas H.F.**, Carnicer M., Wahl A., Ferrer P., Albiol J., (2014) "Quantitative Metabolomics and Instationary 13C-Meabolic Flux Analysis Reveals Impact of Recombinant Protein Production on Trehalose and Energy Metabolism in *Pichia pastoris*". Metabolites 4: p. 281-299

Cueto-Rojas H.F., Pérez N.O., Pérez-Sánchez G., Ocampo-Juárez I., Medina-Rivero E., (2010). "Interferon α 2b quantification in inclusion bodies using RP-UPLC". Journal of Chromatography B, 878:13-14 p. 1019-1023

Acknowledgements

Once more, I have to thank CONACyT for the scholarship granted (No. 212059), and the BE-BASIC foundation for the grant to perform all experiments and make possible my research.
-After that brief announcement from our sponsors-
Now, I must admit that I've been ruminating this section in my head for quite some time. I decided to crystalize it on paper at my mother's house in my birthplace, this was the place where I felt the required inspiration to write it with the necessary care, in order to choose the appropriate words. Nevertheless, I shall ask for forgiveness, whether there are important omissions or in case my words do not make the adequate justice to any particular recipient, after all "*manners maketh the man*". However, please remember that what I say hereby, it is pure sincerity that comes from the bottom of my heart.
Above all, I must be grateful with the wonderful gifts that I've been granted, therefore the honor position in this section and my heart is already reserved (1-Chron 29:11; Jos 24:15), and there is no force on this planet capable of changing that. One of those gifts is the love of my parents, to whom I owe more than I can give back in this life.
To my mother, Silvia, the woman that has loved me even before I existed, I owe the passion and endless persistence that inhabits my mind, she nurtured in me a love for science and human kind that no other living being will be able to do, and taught me the skills necessary to survive, not only to this world, but also to a Ph.D. project. To my father, Víctor Hugo, I owe that beautiful curiosity, amazing creativity and wonderful ungovernability that you see in me today. He taught me that assumptions are useless, that I should not be happy until I have found the truth, and that all men were created equal, therefore all of us are wrong until proven the contrary. I deeply thank those two marvelous human beings for loving, supporting, teaching, tolerating and taking care of me through time; Mom and Dad, the man that you see today is a result of all your effort. I've been trying to follow your teachings, even though I could and I have failed, for which I also apologize in case you've been disappointed.

Next to my parents, the other living soul that has accompanied me all these years is my brother, Víctor. Vic thanks for all your support and love; I'm deeply grateful for your company and complicity all these years. My grandfather, Don Antonio de Rojas Ramos, deserves an especial mention; he is the person that inspired in me the love for all living things, and with his life as example, I've seen how the hard work and love for our family can become true sources of progress and well-being.

Thanks to my uncle Heriberto (*Gracias por el Triptofanito*) who is to blame for my affinity towards life and medical sciences; my aunt Sara for all her spells (that I may not approve), and my aunts Amparo and Guadalupe for being here for me. From my mom's side, I thank my uncle Gilberto for his loyalty and support, uncle Othón for his kindness and aunt Minerva for spoiling me. To all aunts, uncles, cousins, nieces and nephews thank you all for your love and support in the past six years. To end with this section, which is dedicated to my relatives, I thank my angels: Vicenta, Heriberto and Zeferina; they know that I couldn't make it without them. I thank them for those beautiful memories, their example, love, and protection that helped me to achieve this.

I have an especial place reserved for my paranymphs: Francisca and Ileana. I thank Francisca, for her friendship, support and help through the last three years of my Ph.D., she was critical to conclude successfully this. Particularly because she took a lot of samples for me, it was a truly Herculean job; and I thank her, especially, for all the cows and wonderful memories.

And, THANK YOU (yes, with capital letters) to Ileana, who I have the luck to call friend; her example allowed me to keep going on in spite of the difficult times, and her counseling help me to find the solutions to many problems. Dear Ileana, I'm having a hard time to express all my gratitude for these five wonderful years of good memories -I'm counting the time from the first time that we spoke to each other until today, I must admit that we truly became friends later in this story. Our friendship has experienced amazing and rough times, for which I'm grateful, I've learnt a lot from you. Trust

me, your presence made the difference, if we are in this point is thanks to you.
To Antonio "*el Bofo*" Ramos Maurer Salido, his constancy as friend is admirable. I'm truly grateful for all his life lessons, economy lectures (*you betta gimme ma 17 dollars!*), jokes, shared sadness, and friendship. Dear Toño, I'm sorry that you were not a paranymph, and probably I will be in eternal debt with you because of that, just keep in mind that you are extremely important to me, and that your friendship has incommensurable value *Bofo*. To Bartje (*Frieslan boppe!*), thanks for his support without constraints, I must admit that he saved my *ss several times, for which I'm extremely grateful.
I want to make an especial mention to the members of the Delftse gang: Bea, Camilo Medina, Flavia, Rosa, Simeon and all the Solis-Escalante siblings, I am not the friend that you guys deserved, but definitively you were the friends that I needed. I appreciate that you let me be part of your life; certainly you made mine different, for the good. And I also thank a bunch of (ex-)members of the Mexican community in Delft: Alondra (+ Tiemo), Mar (+ Steph), Omar and Diana (+ Caro), Marcelo Huet and Runa (+ Satoshi and Makoto), Ander, Emilio, Luis, Adonis (Bro, we made it), Antonio Jarquin (and his maximum age of 27 y.o.), Jorge Maxil and Paula (+ babies), Zeus, Hilda and Edmundo (actually, I should only include Hilda), Perla, Fabian, David Calvillo (+ Marcela), Gaby Ascencio, Gabriel and Merel (again, probably I should only include Merel), Wilson (*El Maestro*), Amauri (*awanta*) and Aline (once more, I should only include Aline), Gaby Sánchez (my roommate for 2 weeks) and Carlos Guerra (I'll meet you on the battlefield), Dalya (+ Rik)… forgive me if I missed someone, thank you all for being part of my extended family, and for the amazing moments together.
Thank you to Victor Cruz, for a lifetime of friendship; to Eva Juarez for her valuable presence and friendship; Lupita Reyes, Fabian Orendain, Jaime, Bet, and Antonieta thanks for all your support in the distance; my good friends Sonia (+ Beto), Allison, Ulises, Laura, Cristian Mata, Bazan, Gheorghe and Denisse for all the years of adventures; and to Karina Zazueta and Carolina Ortiz for making this trip more interesting.

Camilo Suárez, my great associate in crime. Thanks for putting your faith on me -Yes, we could! I also need to apologize for not including you as paranymph, the geopolitical situation didn't make it possible. But, I'm sure you'll make me suffer once more in due time. You are responsible for giving me those long sought experimental results, I cannot recall how many times you help me sampling, but I'm sure the number of samples is in the order of hundreds, possibly thousands. Your patience while listening to my complaints was truly amazing -sometimes I wonder if you truly were hearing anything but a bunch of crickets… You are a great friend and no matter the distance you know how to summon my presence if you need it. I owe Joel Jorda the opportunity to know you better. And, together with Mihir Shah, we certainly had great adventures. I don't know about you Camilo, but I cannot wait for either presenting embarrassing videos about Mihir on his defence or paying to see Mihir riding that mythical elephant very soon. By the way, Mihir, you're the next in line, we have a lot of faith on your writing skills (*you're a machine man*!). Cristina and Angel, you were also important part of this Mexican soap opera, speaking about adventures you gave me some of the best… they included sushi, ducks, cows, tears, laughter and valuable life lessons, right *Sensei*?

Leonor, my favorite landlady, best flat mate, personal editor and highly treasured friend. Thanks for all your help *kiddo*, especially for rescuing me from street, checking most of my research papers, and for the amazing months we shared together in *the ranch*; it was quite an adventure, and I piled up a bunch of great memories with you. Mariana, thanks for listening to me, you are great human being, patience is a virtue, and you have a lot of it… You'll see how things go in the right direction in due time. Luisa da Cruz, one of my great mentors, what could I possibly do without your help some years ago? I did survive thanks to you. Your example and teachings were amazing. Once more, thank you.

Thank you Amit! And thank you Don Sushil, Jin Rui, Eleni (*Trip-Master*), Yaya, Walter, Robin, Katelijne, Paulina, Karel, Li Weiwei, Manas, Mathias, Ramon, Kira *et al*., for the coffee, the cake and the great experiences; it was amazing to work with you all.

To my friends from the BPE section: Alex, David Méndez, Susana, Joana (+Douglas), Carlos, Silvia Pirrung… well, I only have one thing to say: *So long, and thanks for all the fish!* And, María Cuellar, your coaching was decisive. You found the right words in the worst times. To my good friends from IMB: Wesley and Pilar, thank you for the moral support and good times guys. An important acknowledgment deserves Tamara Bacsik for helping me to start my little adventure at TU Delft.

I must thank, as well, those people that marked me positively in my professional life: Peter Verheijen, my greatest mentor and the role model that I looked for many years. I appreciate your wisdom, feedback and teachings; I treasure them all with great respect. And, Emilio Medina, the person that showed me how to be a good scientist, whom I had the honor to work with and called leader. Sometimes a person needs someone to believe in his or her capacities. You, Emilio, gave me the lifeline necessary to hold on until the end. Thank you Ton van Maris and Jean Marc Daran, I wish I had the opportunity to share a bit more academic experiences with you, but the meetings and your feedback were good enough for the time being, I hope the future brings other collaborations together. And Francisco Javier Sánchez Galicia, your acting lessons put me on the spot and today's success is thanks to those moments.

I have not forgotten about the people that made technically and literally possible this work: the analysis section of the CSE group. Thanks to Angie for her valuable contribution to my work and all the wonderful scientific discussions that made possible to measure the impossible. And thank you Reza, sometimes crazy people need of someone to believe in their arguments to prove that they are sane or at least not so crazy; you know perfectly that I owe your tenacity *ca.* 75% of this work. Cor and Patricia, you also made possible to conclude this; it was great to work with you. Yi Song, Dirk and Rob, sometimes we underestimate the dark magic that you do behind that window, certainly the CSE group (including me) owes you a lot.

Jenifer, what would we do without you?! Your organization skills made possible to survive many meetings, and you bravely defended me against my old foe, bureaucracy, countless times. I am extremely

grateful for your collaboration and help. Not to mention that little help with the *Vancouver incident* (right Peter?)…
I also have an especial place in this section for my students: Lisanne van Wijngaarden, Lore Keijzers, Sieze Duowenga, Michel Mulders (for a while), Sebastiaan de Bruin, and Nikita de Keijzer. You all gave me more lessons than I gave to you, thanks for your hard work. You really inspired me to become a better supervisor, and I hope I was up to the task.
Sef, you also became in some point a great role model to me, I have learnt a lot from you, and your feedback was always invaluable to me, even in the last months when I really surpassed my patience limit with the revisions. I appreciate your guidance, patience, teachings, and calling me *stubborn* several times -*oh yes, they were quite a lot!* From time to time you needed to pull my leash, which I also appreciate, because by now you are aware that I tend to bite quite hard. If you didn't know, here's the truth: you were the reason why I decided to do this. I respect and admire your work, and I hope I performed well the role of being your student. Thank you for trusting me and doubting about my results; being wrong (according to you) until proven the contrary, truly made my work better.
Aljoscha, thank you for the patience and for giving that process-oriented perspective to all this; it was quite a ride, but we managed to survive it together. Like I said some time ago, I did appreciate your effort to get out the best of me, I regret if sometimes I was not up to the challenge. This thesis reflects the hard work that Sef, you, and I put on it -and yes! I feel proud about the result.
Finally, thanks to *Sophia*, I have not forgotten about you darling, you are still the major driving force that makes all these processes favorable; we shall meet in the near future.
Being all that said; it's high time for me to move on to the next chapter…

Thank you all!
Dank je wel!
¡Gracias, totales!